Towards the directed evolution of an L-aspartate oxidase from *Pseudomonas putida*

Charlotte Leese

PhD

University of York

Chemistry

July 2012

Abstract

Amino acid oxidases (AAOs) are enantioselective flavoenzymes that catalyse the oxidation of amino acids into imino acids, which spontaneously hydrolyse in water to form keto acids. AAOs have several potential applications, most notably as biocatalysts in the production of enantiomerically pure amino acids and keto acids, or in enzymatic biosensors. Therefore, there is a demand for a range of AAOs with specific activity against various substrates, encouraging the characterisation of less well understood oxidases.

Seven putative oxidases were cloned into the pET-YSBLIC-3C expression vector, expressed in *E. coli*-DE3 expression strains and assayed for activity against all proteinogenic amino acids. Of these seven targets, the L-amino acid oxidase from *Pseudomonas putida* (PpLAAO) was found to be highly soluble, had detectable activity against L-aspartate and L-asparagine and had not been investigated in depth previously.

The purified PpLAAO protein showed high substrate specificity against L-aspartate and lower activity with substrate inhibition against L-asparagine. Very low activity was also detected against L-glutamate. The purified protein had optimal activity around pH 7.5 and at temperatures between 4°C and 30°C.

To investigate the role of residues in the active site area of the PpLAAO protein thirteen active site residues, determined by comparison with the structure of the L-aspartate oxidase from *E. coli* (L-AspO), were mutated to alanine. Eleven of these mutants were purified and assayed against L-aspartate, L-asparagine and L-glutamate. Results were largely consistent with knowledge of L-AspO.

Ingenza Ltd. has an interest in potential applications of L-tyrosine and L-alanine oxidases. Because of this iterative combinatorial active site saturation testing, using the active structure of L-AspO was performed alongside a small scale epPCR mutagenesis in an attempt to introduce activity against L-alanine and L-tyrosine. L-homoserine was also targeted as part of a substrate walking approach towards L-alanine; however no novel activity was detected in any transformants.

Contents

Figures and Tables

List of Abbreviations

$(NH_4)_2SO_4$	Ammonium sulfate
4-AAP	4-aminoantipyrine
6-APA	6-amino penicillic acid
AA	Amino acid
AAO	Amino acid oxidase
ACE	Angiotensin-converting enzyme
AEBSF	4-(2-Aminoethyl) benzenesulfonyl fluoride hydrochloride
AO	Amine oxidase
AIM	Auto induction media
Alitame	L-alpha-aspartyl-N-(2,2,4,4-tetramethyl-3-thietanyl)-D-alaninamide
AMBA	α-methylbenzylamine
APS	Ammonium persulfate
AS	Ammonium sulphate
AsAAO	L-amino acid oxidase from *Anabaena* sp. strain PCC 7120
Aspartame	α-L-aspartyl-L-phenylalanine-methyl ester
ATC	2-amino-Δ^2-thiazoline-4-carboxylic acid
β-OG	β-n-octyl-β-D-glucopyranoside
BaAO	Amine oxidase from *Bacillus anthracis*
BHI	Brain-heart infusion
BLAST	Basic local alignment search tool
BSA	Bovine serum albumin
BsGO	Glycine oxidase from *Bacillus subtilis*
CASTing	Combinatorial active site saturation testing
$CaCl_2$	Calcium chloride
CHAPS	3[(3-Cholamidopropyl)dimethylammonio]-propanesulfonic acid
CO_2	Carbon dioxide
$CoCl_2$-$6H_2O$	Cobalt chloride hexahydride
$CuCl_2$-$2H_2O$	Copper chloride dihydrate
DAB	3,3'-diaminobenzidine
dATP	Deoxyadenosine triphosphate
dNTP	Deoxynucleotidetriphosphate
ddNTP	Dideoxynucleotidetriphosphate
DHAP	Dihydroxyacetone phosphate
DLS	Dynamic light scattering

DMSO	Dimethyl sulfoxide
DNA	Deoxyribonucleic acid
dNTP	Dinucleotide triphosphate
dsDNA	Double stranded deoxyribonucleic acid
DTT	Dithiothreitol
dTTP	Deoxythymidine triphosphate
EDTA	Ethylenediaminetetraacetic acid
epPCR	Error prone polymerase chain reaction
FAD	Flavin adenine dinucleotide
FDA	US Food and Drug Administration
$FeCl_3$-$6H_2O$	Iron chloride hexahydride
Fluvalinate	Cyano-(3-phenoxyphenyl)methyl] 2-[2-chloro-4-(trifluoromethyl)anilino]-3-methylbutanoate
G. HCl	Guanidine hydrochloride
GMP	Good manufacturing practice
GnRH	Gonadotropin-releasing hormone
H_2O	Water
H_2O_2	Hydrogen peroxide
H_3BO_3	Boric acid
HCl	Hydrogen chloride
HEPES	4-(2-hydroxyethyl)-1-piperazineethanesulfonic acid
His_6	Hexa-histidine
HRP	Horseradish peroxidase
IPTG	Isopropyl β-D-1-thiogalactopyranoside
I.V.	Intravenous
K_2HPO_4	Dipotassium phosphate
k_{cat}	Catalytic constant
KCL	Potassium chloride
KH_2PO_4	Monopotassium phosphate
K_i	Dissociation constant
K_M	Substrate concentration at which the reaction rate is half of V_{max}
L-AspO	L-aspartate oxidase from *E. coli*
LB-agar	Luria-Bertani agar
LB-media	Luria-Bertani media
LDAO	Lauryldimethylamine-oxide
LIC	Ligation independent cloning

LiCl	Lithium chloride
MAP	Mycolic acid & arabinogalactan-peptidoglycan
MAO	Monoamine oxidase
MAO-N	Monoamine oxidase from *Aspergillus niger*
MES	2-(N-morpholino)ethanesulfonic acid
$MgCl_2$	Magnesium chloride
$MgSO_4$	Magnesium sulfate
$MnCl_2$	Manganese chloride
MRSA	Methicillin-resistant *Staphylococcus aureus*
MSG	Monosodium glutamate
MWCO	Molecular weight cut-off
Na_2HPO_4	Sodium phosphate dibasic
Na_2MoO_4-$5H_2O$	Sodium molybdate pentahydride
Na_2SeO_3	Sodium selenite
NaCl	Sodium chloride
NAD	Nicotinamide adenine dinucleotide
NADH	Nicotinamide adenine dinucleotide + hydrogen
NDSB-201	Non detergent sulphobetaines-201
NEP	Neutral endopeptidase
NfOR	Oxidoreductase from *Nocardia farcinica*
$NiCl_2$-$6H_2O$	Nickel chloride hexahydrate
NiNTA	Nickel-nitriloacetic acid
$NiSO_4$	Nickel sulfate
NMDA	*N*-methyl-D-aspartate
OD	Optical density
P-CHO	Wang aldehyde resin
P-TEA	Polymer-supported triethylamine
PAGE	Polyacrylamide gel electrophoresis
PCR	Polymerase chain reaction
Pd-C	Palladium on carbon
PEG	Polyethylene glycol
PheOMe	Phenylalanine-methyl ester
PpLAAO	L-AAO from *Pseudomonas putida*
PNDT	NDT mutants of PpLAAO
r.p.m	Revolutions per minute
RoLAAO	L-AAO from *Rhodococcus opacus*

(*S*)-MOIPA	(*S*)-1-methoxy-2-aminopropane
SDS	Sodium dodecyl sulfate
SDS-PAGE	Sodium dodecyl sulfate polyacrylamide gel electrophoresis
SDM	Site directed mutagenesis
SDSM	Site directed saturation mutagenesis
SHMT	Serine hydroxymethyltransferase
SLAAO	L-AAO from *Synechococcus* sp. strain ATCC 27144
SOC media	Super optimal broth with catabolite repression
TAE	Tris/acetate buffer
TBHBA	2-hydroxy-2,4,6-tribromobenzoic acid
TEMED	Tetramethylethylenediamine
THF	Tetrahydrofuran
TMAO	Trimethylamine N-oxide
Tris	Tris(hydroxymethyl)aminomethane
UV	Ultraviolet
$V_{component}$	Volume of component
V_{max}	Maximum velocity
V_{total}	Total Volume
WT	Wild type
YSBL	York structural biology laboratory
Z-Asp	N-protected benzoyloxycarbonyl-L-aspartate
$ZnSO_4$-$7H_2O$	Zinc sulfate heptahydrate

Acknowledgements

I would like to thank my supervisor, Dr Gideon Grogan, for the opportunity to take part in this project, and for all of his help, support and encouragement over the course of my PhD, as well as Dr Ian Fotheringham, Dr Franck Escalettes, Dr Ian Archer and Dr Robert Speight of Ingenza Ltd. for their helpful input into my project. I would also like to thank Dr Marek Brzozowski for his suggestions and for acting as my Internal Panel Member.

I am grateful for the funding provided by Ingenza Ltd. and the EPSRC that made this work possible and for the support and interest in my project from the members of the YSBL. Finally I would like to thank my family for their emotional and financial support over the years.

Author's Declaration

The non recombinant pET-YSBLIC-3C vector was provided by members of the YSBL, and the non recombinant pEKEX2 shuttle vector was provided by Prof. Sun-Yang Park. The pET-YSBLIC-3C-SLAAO, pET-YSBLIC-3C-RoLAAO and pET-YSBLIC-3C-PpLAAO were cloned previously by Dr Gideon Grogan. Figure 1.29 was also created by Dr Gideon Grogan.

All other work was completed by the author.

Chapter 1 Introduction

1.1 Uses of enantiomerically pure amino acids and amines

Enantiomerically pure amino acids and amines are important products for the chemical industry as special intermediates for chiral compounds produced by pharmaceutical and agrochemical companies, as enantiomerically pure chiral products often require lower doses and have improved efficiency over their racemic counterparts.[1] Having enantiomerically pure products also means that there is no risk of the other enantiomer of the compound having an unwanted effect, as happened the case of the thalidomide drug, where the *(S)*-form of the drug had a teratogenic effect that the *(R)*-form did not.[2]

The importance of the market for enantiomerically pure chiral intermediates was increased in 1992, when both the US Food and Drug Administration (FDA) and the European Committee for Proprietary Medicinal Products both insisted that the physiological effects of each enantiomer of a pharmaceutical product must be characterised individually, resulting in longer testing periods for racemic chiral compounds. Since 1997, the FDA has also allowed single isomer products to be registered in a shorter amount of time, also encouraging the production of enantiomerically pure products.

Several proteinogenic amino acids are also used in human and animal nutrition, either as additives to foodstuffs that would otherwise be deficient in essential amino acids, e.g. modern animal feeds[1] or intravenous nutrition solutions[3] or as flavourings for food.[1]

1.1.1 Uses of enantiomerically pure L-amino acids

Enantiomerically pure L-amino acids have many industrial uses, and consequently a large market for their production- in 1999 the total market for proteinogenic L-amino acids was around 1.5 million tons, estimated to be worth €3.5 billion. The majority of these amino acids are used in human and animal nutrition, with the estimated worldwide consumption of amino acids being around 2 million tons in 2001.[3]

Animal nutrition accounts for around 55% of the market, with L-lysine, LD-methionine, L-threonine and L-tryptophan being added to modern animal feed, as it is usually deficient in these essential amino acids.[1] According to an estimate by Ajinomoto Co. Inc. (http://www.fao.org/docrep/007/y5019e/y5019e0a.htm accessed 26/04/12), in 2000 between

500,000-600,000 tons of both L-lysine and methionine were produced for this purpose. Roughly 30,000 tons of L-threonine and 1,000 tons of L-tryptophan were also produced for the same reason.

The racemate of methionine can be used in animal feed as D-methionine is converted in animals into L-methionine through oxidation of the D-form into α-keto-γ-methiolbutyric acid, followed by a transaminase reaction into L-methionine, although some of the α-keto-γ-methiolbutyric acid is lost through the spontaneous decarboxylation into β-methylthiopropanoic acid (**Figure 1.1**).[4]

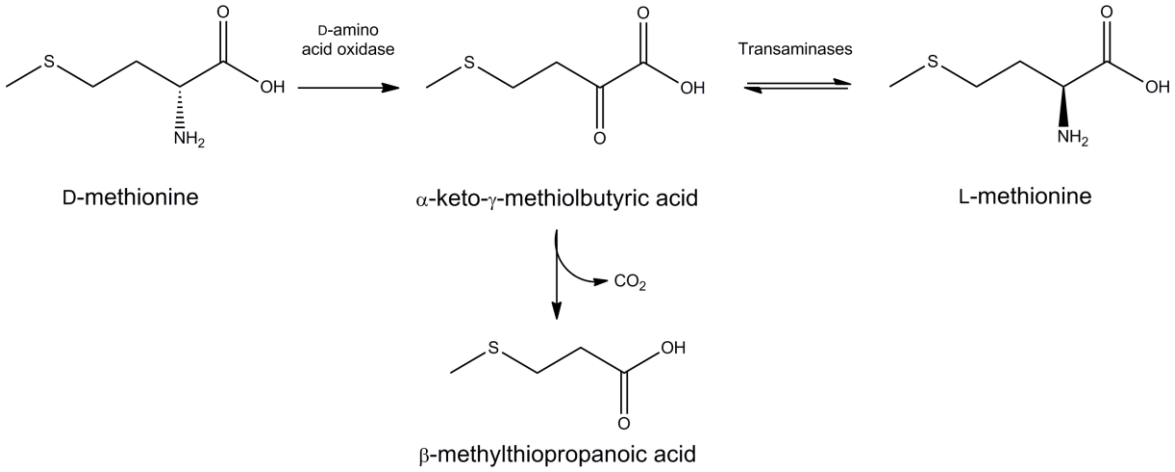

Figure 1.1 Reaction scheme for the natural conversion of D-methionine into L-methionine by animal and adult humans.[4]

Human nutrition and health accounts for a further 40% of the market for proteinogenic amino acids. L-glutamate, L-phenylalanine, L-aspartate and glycine are all used as food additives. L-glutamate is mostly used as the flavouring monosodium glutamate (MSG) and more than 650,000 tons are produced every year.

Several enantiomerically pure L-amino acids are used as intermediates for chemical synthesis of other compounds. L-phenylalanine and L-aspartate are used as the initial substrates in both the chemical and chemoenzymatic synthesis of the sweetener aspartame (α-L-aspartyl-L-phenylalanine-methyl ester). [5]

In the chemical reaction L-phenylalanine is reacted with methanol to form L-phenylalanine-methyl ester (L-PheOMe), which is then reacted with an *N*-protected anhydride form of L-aspartate to form *N*-protected αβ-L-aspartyl-L-PheOMe. The *N*-protected αβ-L-aspartyl-L-PheOMe is then treated with acid to form a αβ-aspartame. HCl salt, allowing the α-form to be separated by precipitation as the α-salt is less soluble in aqueous solution than the β-salt. The α-aspartame. HCl salt is then neutralised with a base allowing α-aspartame to be recovered by crystallisation (**Figure 1.2a**).[5, 6]

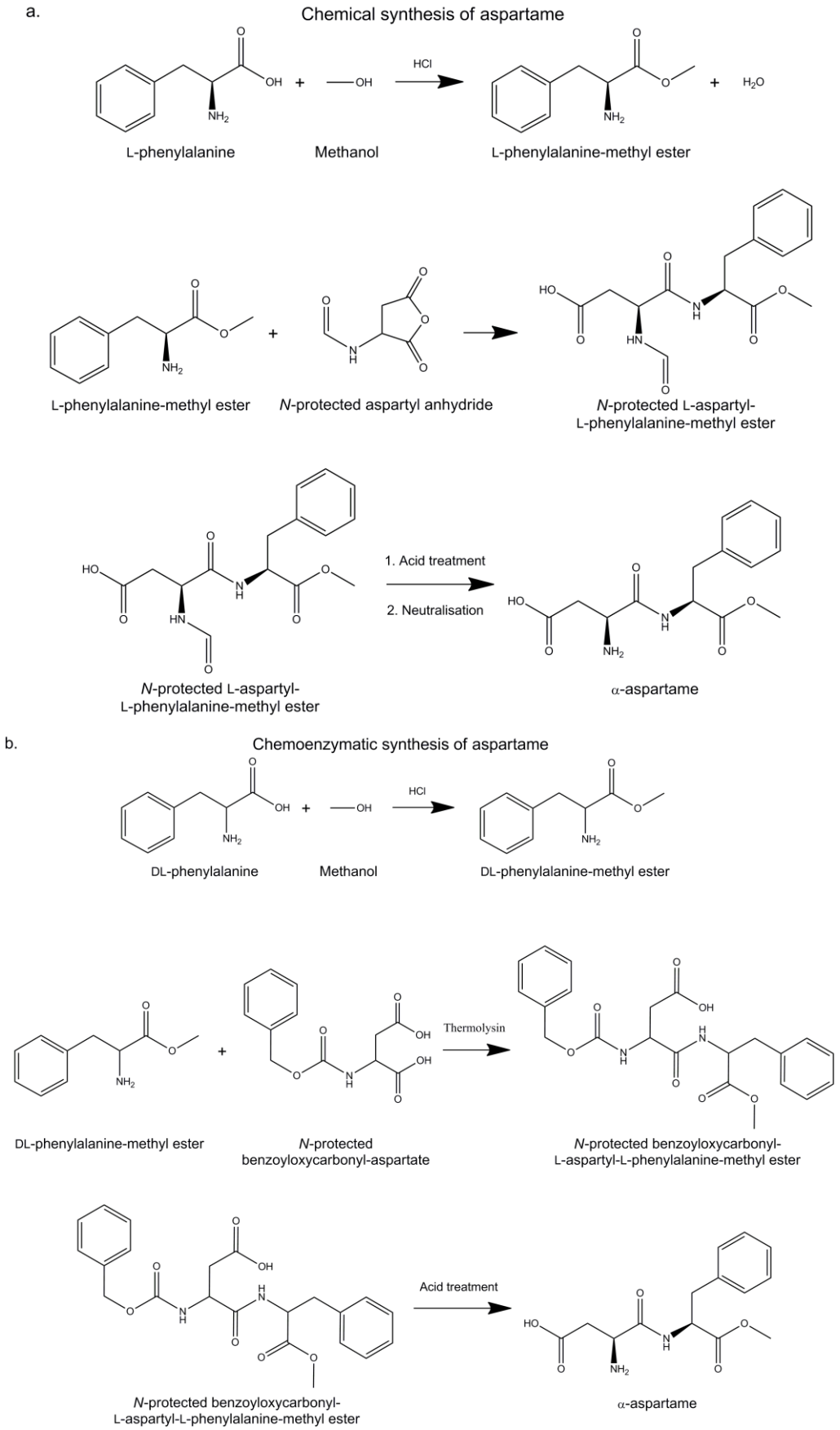

Figure 1.2 Commercial methods for the synthesis of aspartame. **a.** Chemical synthesis method. **b.** chemoenzymatic synthesis method.

The chemoenzymatic reaction is similar, but is catalysed by the enantioselective thermolysin enzyme from *Bacillus thermoproteolyticus*. This enantioselectivity means that DL-phenylalanine can be used as a starting substrate. In this case the DL-phenylalanine-methyl ester (DL-PheOMe) is reacted with *N*-protected benzoyloxycarbonyl-L-aspartate (Z-Asp) to form *N*-Z-Asp-L-PheOMe (**Figure 1.2b**), which then reacts with the remaining D-PheOMe to form an insoluble salt, allowing more efficient production of *N*-Z-Asp-L-PheOMe (not shown), with yields of 95% being described. After the reaction the *N*-Z-Asp-L-PheOMe is separated from the D-PheOMe (which can be racemized and reused) and is converted to aspartame through hydrogenolysis (**Figure 1.2b**).[5]

L-aspartate is also one of the starting substrates of the dipeptide sweetener alitame (L-alpha-aspartyl-*N*-(2,2,4,4-tetramethyl-3-thietanyl)-D-alaninamide)[7] and L-valine is one of the precursors in the fermentation of the immune suppressant drug cyclosporin A, which is used in transplant surgeries.[1, 8] The ethyl ester of the synthetic L-homophenylalanine is also used as an intermediate in the production of several angiotensin-converting enzyme (ACE) inhibitors, which are used to prevent hypertension and congestive heart failure (**Figure 1.3**).[9] L-homophenylalanine can also be used as an intermediate in the production of β-lactam antibiotics, acetylcholinesterase inhibitor (used for treatment of Alzheimer's disease) and neutral endopeptidase (NEP) inhibitor (which complement the effects of ACE inhibitors when used simultaneously).[10]

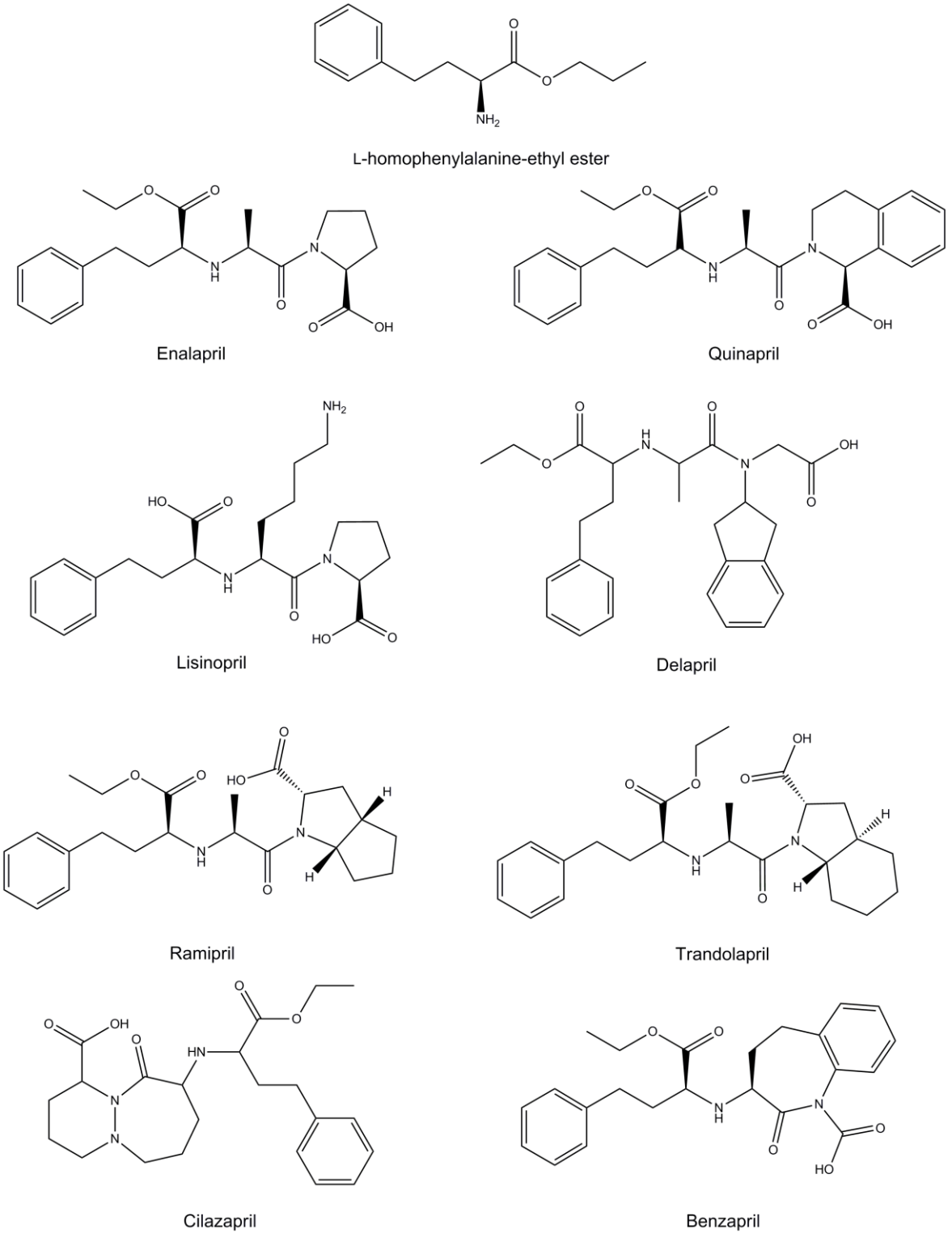

Figure 1.3 L-homophenylalanine-ethyl ester and ACE inhibitor derivatives.[9, 10]

1.1.2 Uses of enantiomerically pure D-amino acids

Enantiomerically pure, synthetic D-amino acids can also be used as intermediates in the production of other pharmaceutical and nutritional compounds. The most well known example is the use of D-phenylglycine and D-parahydroxyphenylglycine (D-p-hydroxyphenylglycine) in the production of the semisynthetic β-lactam antibiotics ampicillin and amoxicillin, respectively. This is performed commercially by reacting the D-amino acid with 6-amino penicillic acid (6-APA), catalysed by penicillin acylase enzyme from *Escherichia coli* (**Figure 1.4**),[11] although work is still being performed to increase the activity[12] and stereoselectivity[13] of the enzyme.

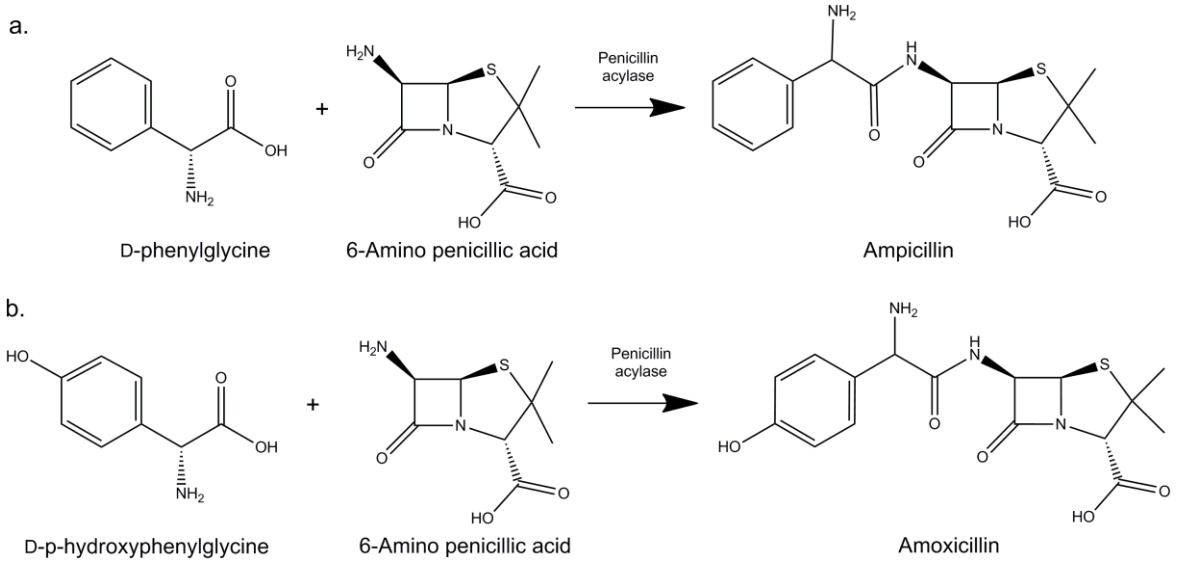

Figure 1.4 Synthesis of β-lactam antibiotics from synthetic D-amino acids and 6-APA.[11] **a.** Synthesis of Ampicillin from D-phenylglycine. **b.** Synthesis of amoxicillin from D-*p*-hydroxyphenylglycine.

D-alanine is used as another starting point in the synthesis of the sweetener alitame. One possible reaction scheme for this starts with a reaction between a *N*-protected form of D-alanine and 3-amino-2,2,4,4-tetramethylthietane to form an *N*-protected *N*-(2,2,4,4-tetramethyl-3-thietanyl)-D-alaninamide. This is then deprotected by hydrogenolysis and the resulting *N*-(2,2,4,4-tetramethyl-3-thietanyl)-D-alaninamide is reacted with L-aspartate *N*-thiocarboxyanhydride (**Figure 1.5**).[14]

Another unnatural amino acid, D-valine, is used in the synthesis of the pyrethroid insecticide fluvalinate (Cyano-(3-phenoxyphenyl)methyl] 2-[2-chloro-4-(trifluoromethyl)anilino]-3-methylbutanoate), which is used to control the population of varroa mites in beehives (http://www.biosecurity.govt.nz/pests-diseases/animals/varroa/paper/varroa-treatment-options.htm#4, accessed 25/09/12) (**Figure 1.6**).[8]

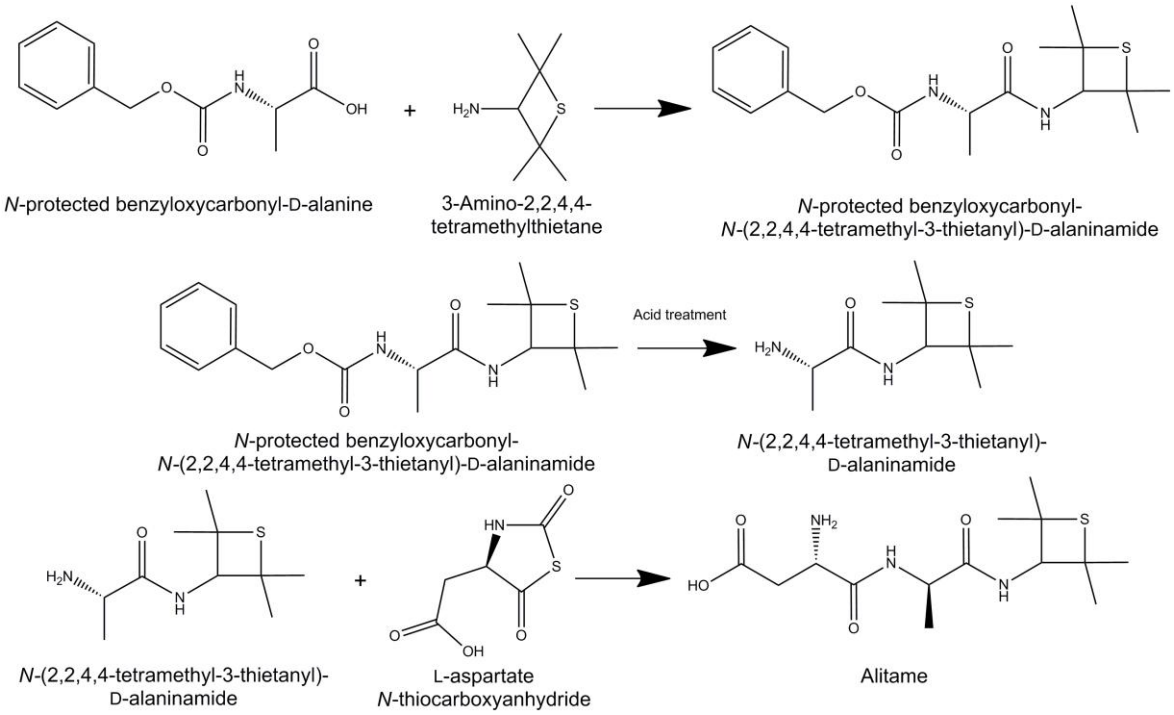

Figure 1.5 Possible reaction scheme for the production of sweetener Alitame starting from a *N*-protected form of D-alanine.[14]

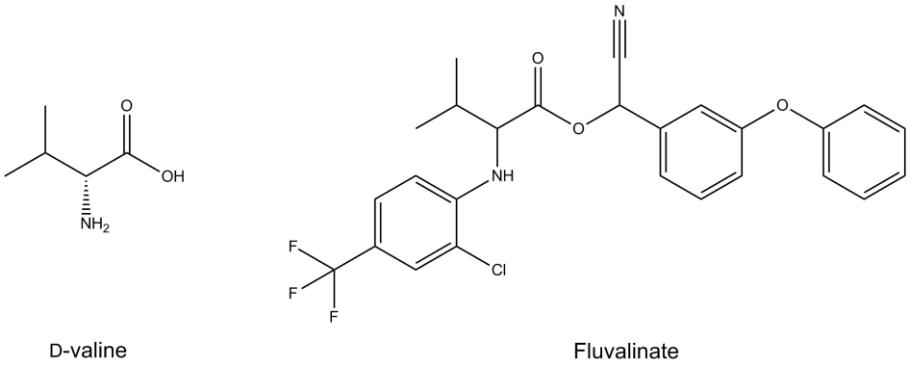

Figure 1.6 Comparison of pyrethroid insecticide Fluvalinate and its amino acid substrate, D-valine.

Similarly to its L-form, D-homophenylalanine can also be used as a precursor to several ACE inhibitors, including benazepril (**Figure 1.3**), as the D-homophenylalanine is converted to ***(R)***-2-nosyloxy-4-phenylbutyric acid ethyl ester over a three step reaction, and (*R*)-2-nosyloxy-4-phenylbutyric acid ethyl ester reacts with a corresponding chiral amine to produce the ACE inhibitor.[15]

1.1.3 Uses of enantiomerically pure amines

Enantiomerically pure amines are of use as resolving agents for chiral carboxylic acids, as amines and carboxylic acids form diastereoisomeric salts, so adding two molar equivalents of an enantiomerically pure amine to a racemate of a carboxylic acid will result in one form of the carboxylic acid forming a crystal with the amine, and the other staying in solution, allowing the two enantiomers of the carboxylic acid to be separated, and the diastereoisomeric salt crystal to be separated into the carboxylic acid and the amine using an acid treatment.[1]

The commercial production of (*R*)-mandelic acid uses (*R*)-phenylethylamine to resolve the racemic form of mandelic acid using this method,[1] and a method for the synthesis of a cardioprotective calcium antagonist, SP-060-S, involves resolving the racemate form of the substrate thiazolidinone carboxylic acid into the S-form through crystallisation with (*S*)-*N*-benzyl-1-phenylethylamine (**Figure 1.7**).[16] In this case the amine can be recycled by treatment with NaOH followed by extraction and distillation, making it a more environmentally friendly resolving agent.

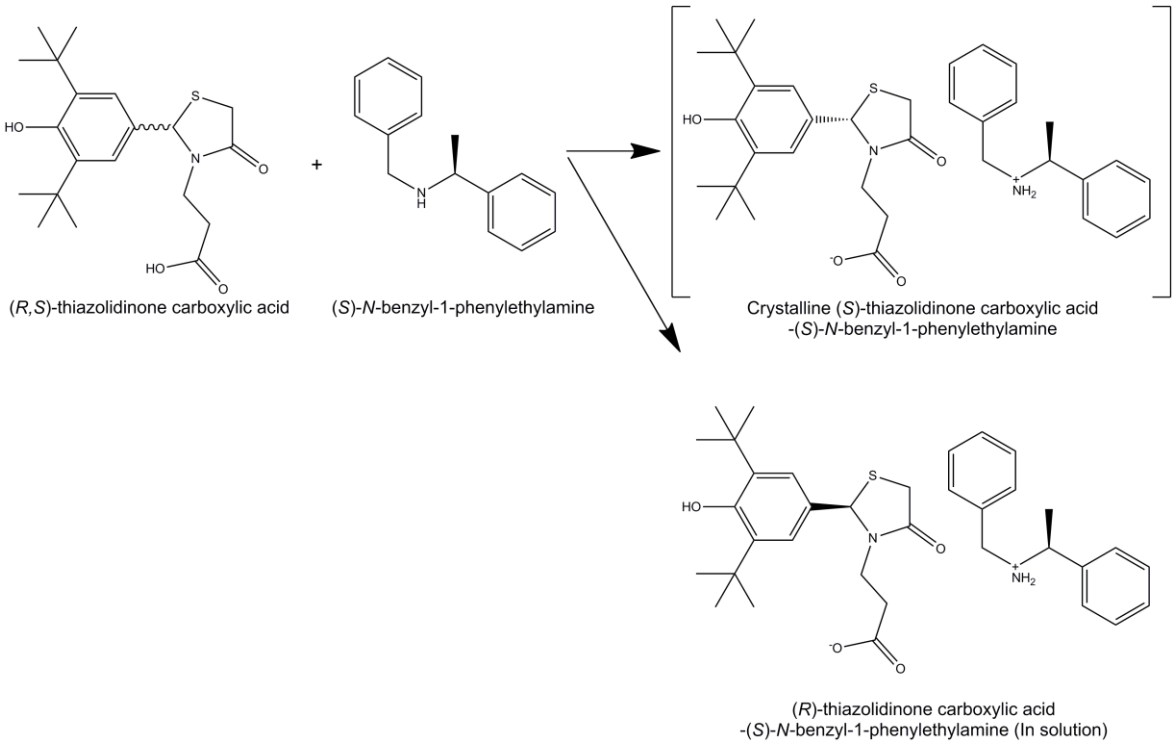

Figure 1.7 Racemate resolution of (*R,S*)-thiazolidinone carboxylic acid by crystallisation with enantiomerically pure (*S*)-*N*-benzyl-1-phenylethylamine for use in synthesis of calcium antagonist SP-060-SP.[16]

As finding a single, optimal amine to crystallise each carboxylic acid can be quite time consuming, a variant of racemic resolution by crystallisation has been developed by Vries *et al.*, which involves using a mixture of similar enantiomerically pure amines to form crystals with the carboxylic acid.

This "Dutch resolution" has the advantage that the effects of several amines on crystallisation can be investigated at the same time, and the enantiomeric excess of the crystallised carboxylic acids can be higher when using several amines than with the classical single amine resolution.[17]

Enantiomerically pure amines are also of importance as chiral auxiliaries or bases, such as lithium amide bases, which can be used for a wide range of enantioselective reactions, including the deprotonation of ketones (**Figure 1.8**), rearrangement of epoxides to allylic alcohols (**Figure 1.9**) and reactions of tricarbonyl (η^6-arene)-chromium complexes.[18] Magnesium amide bases may also be used for similar purposes, as shown by Henderson *et al.* using them to deprotonate conformationally locked ketones.[19]

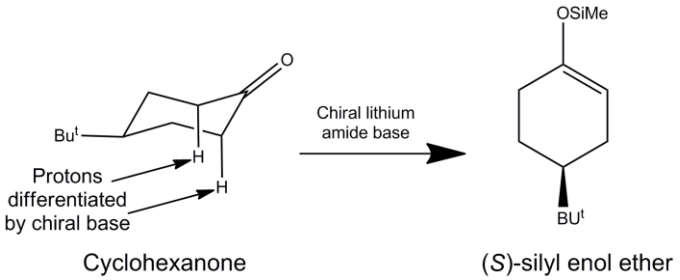

Figure 1.8 Example of enantioselective ketone deprotonation using a chiral lithium amide.[18]

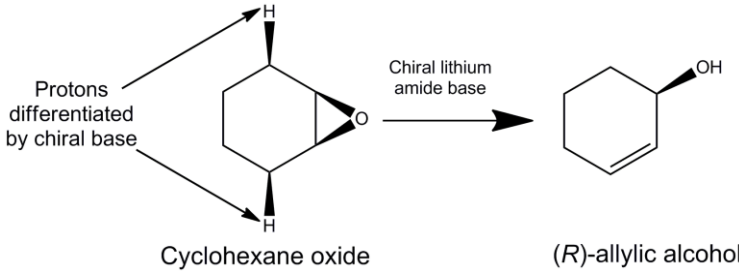

Figure 1.9 Example of enantioselective epoxide rearrangement using a chiral lithium amide.[18]

Chiral amines can also act as enantioselective catalysts for certain reactions, such as the enantioselective epoxidation of alkenes using potassium peroxymonosulfate (Oxone®), which can be catalysed by (*S*)-2-(diphenylmethyl)pyrrolidine.[20]

As chiral amines are chemically active, they are also often used as enantiomerically pure intermediates in reactions to produce pharmaceutical compounds. One example is the (*S*)-4-(1-phenylethylamino)quinazolines, which are inhibitors of Immunoglobulin E (IgE) synthesis and were made by Berger *et al.*[21] by reacting 4-chloroquinazoline with two molar equivalents of a (*S*)-form primary amine, such as (*S*)-1-phenylethylamine, in tetrahydrofuran (THF) and polymer-supported triethylamine (P-TEA) to form a mix of the (*S*)-4-(1-phenylethylamino)quinazoline and the primary amine, which was then separated in THF containing 1% acetic acid and Wang aldehyde resin (P-CHO) (**Figure 1.10**).[21]

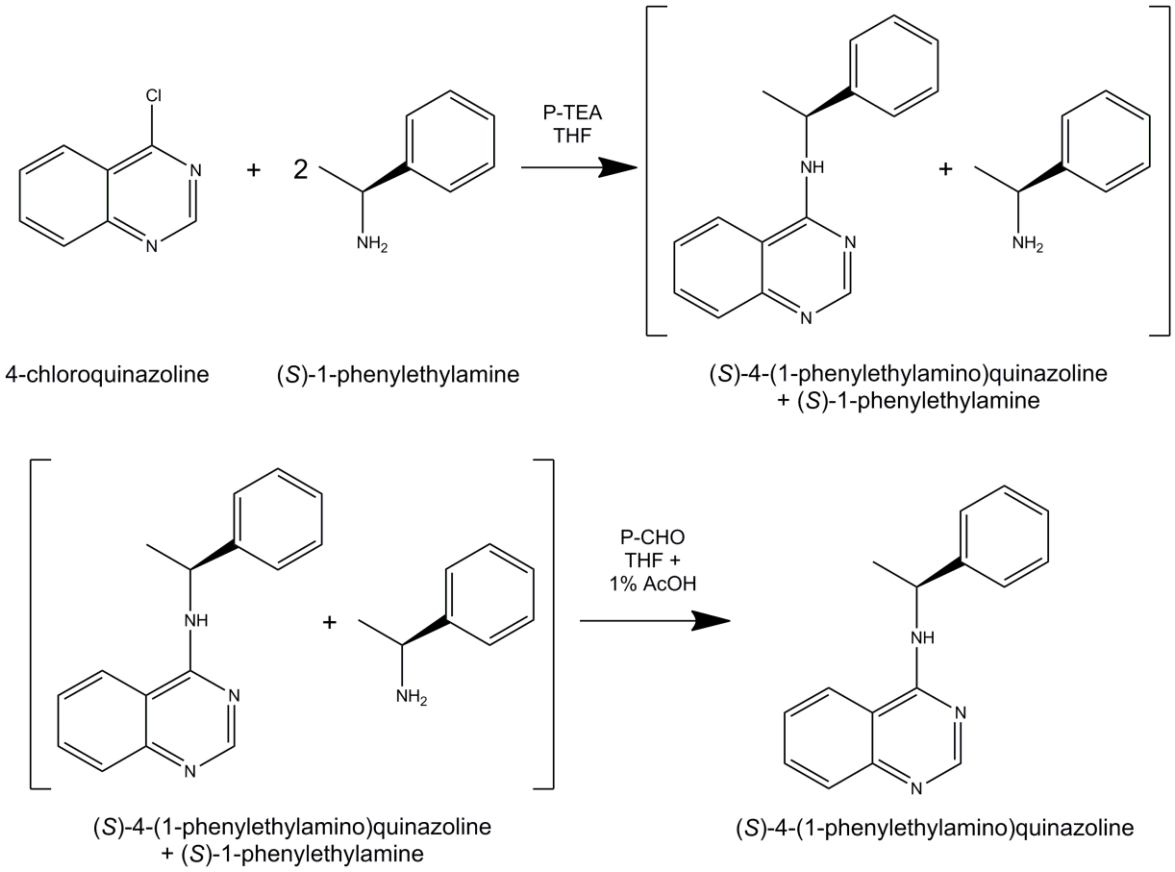

Figure 1.10 Example of production of a (*S*)-4-(1-phenylethylamino)quinazoline using (*S*)-1-phenylethylamine as the amine.[21]

Also, the herbicide FRONTIER X2 ® is commercially synthesized from (*S*)-1-methoxy-2-aminopropane ((*S*)-MOIPA), as only the (*S*)-enantiomer is biologically active (**Figure 1.11**).[22]

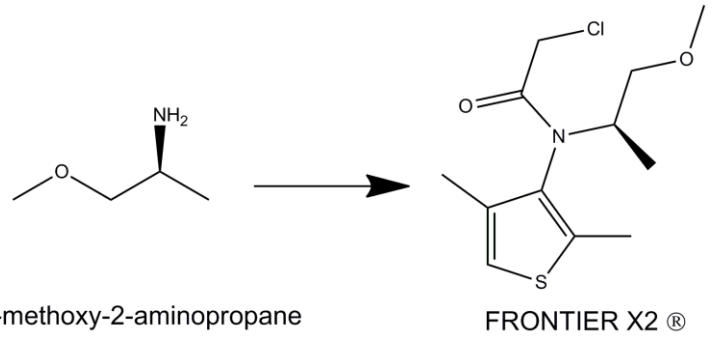

Figure 1.11 (*S*)-1-methoxy-2-aminopropane and its derivative herbicide FRONTIER X2®.[22]

1.2 Production of enantiomerically pure amino acids

1.2.1 Extraction of L-amino acids

As proteins naturally contain L-amino acids, one of the oldest used ways of producing pure amino acids is to extract them from protein-rich materials, preferably ones that are produced in large quantities and not useful for other reasons, such as hair, meat extracts, plant hydrolysates[1] and feathers.[23] The most commonly extracted L-amino acid is cysteine, which is present in the keratin found in hair and feathers (cysteine accounts for 14% of the amino acid content of hair keratin),[24] although L-amino acids serine and proline can also be extracted from keratin.[23]

As keratin has a high degree of cross linking disulphide and hydrogen bonds, as well lots of hydrophobic interactions, it is a highly stable protein structure that is resistant to traditionally used proteases, such as trypsin and pepsin.[25] Due to this stability, the traditional way of extracting amino acids from protein-rich materials involves hydrolysing the keratin with strong acids and consequently neutralizing the acid with alkalis or buffering it with sodium acetate, which results in the amino acids being difficult to separate and leads to the production of unwanted salts as by-products,[24] which are damaging to the environment.[1]

Due to these disadvantages, more recent biocatalytic methods use keratinases to extract the cysteine from keratin. Keratinase-like enzymes were traditionally found in mesophilic fungi and actinomycetes, however more recently thermophillic bacteria species, which are capable of growing on feathers as the only food source, have been discovered. The enzymes responsible for the keratin degradation in two of these species; *Fervidobacterium pennavorans*[23] and *Thermoanaerobacter keratinophilus* sp. nov.,[23] have been purified, in both cases the enzyme is a serine-type protease with a molecular mass of 130 kDa and 135 kDa respectively.[23, 25] It is hoped that these enzymes can be used to extract amino acids from feathers and other keratin-rich materials without producing unnecessary salt as a by-product.

1.2.2 Chemical synthesis of amino acids

Racemic amino acids synthesized for industry can be produced chemically using the Strecker synthesis method, first described in 1850, where the respective aldehyde is reacted with ammonia and hydrogen cyanide to form an α-amino nitrile. The α-amino nitrile can then be hydrolysed to the respective amino acid (**Figure 1.12**).[26]

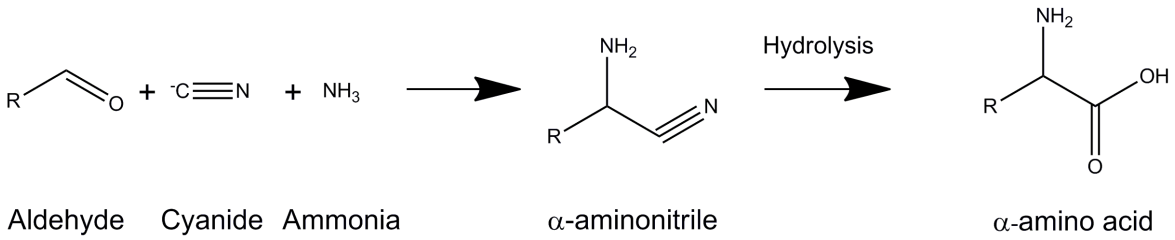

Figure 1.12 Strecker synthesis method of producing racemic amino acids.[26]

Another chemical method for the production of racemic amino acids is amidocarbonylation, where an aldehyde, an amide and carbon monoxide are combined in a single step reaction to form a *N*-acyl α-amino acid(**Figure 1.13**).[27]

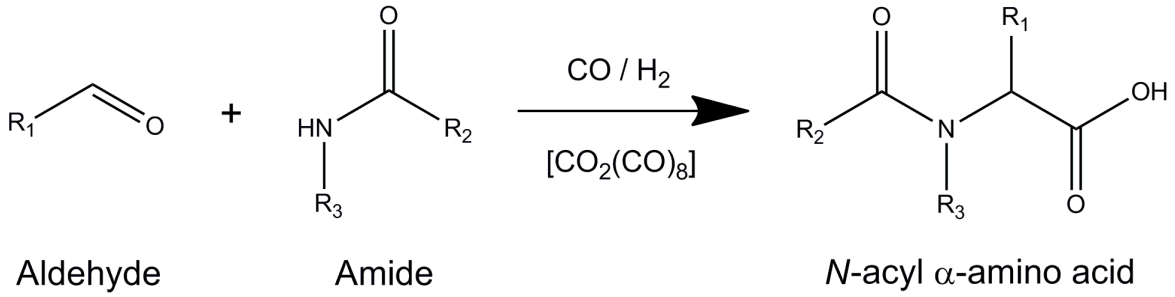

Figure 1.13 Amidocarbonylation method for production of racemic *N*-acyl α-amino acids.[27]

These asymmetric amino acid synthesis methods can be useful in the production of enantiomerically pure amino acids as the products can be racemized afterwards using biocatalytic methods. There are also two amino acids that can be synthesized asymmetrically for use in industry; glycine, due to it being achiral, and methionine, which is converted from its D-form into its L-form through a transaminase reaction in animals and human adults, although enantiomerically pure L-methionine is still needed when used as a baby food additive.[1]

As large-scale synthesis of racemic methionine is commerically viable, Degussa (now Evonik Industries) developed a synthesis method that would avoid the formation of large quantities of salts. Acrolein and methanethiol are reacted to form 3-methylmercaptopropionaldehyde, which is then combined with ammonium hydrogen carbonate and hydrogen cyanide to form 5-(2-methylthioethyl)hydantoin. The 5-(2-methylthioethyl)hydantoin is then hydrolysed at 170°C with an excess of potassium carbonate to form potassium methioninate, which is then acidified under CO_2 pressure to produce methionine (**Figure 1.14**).[1]

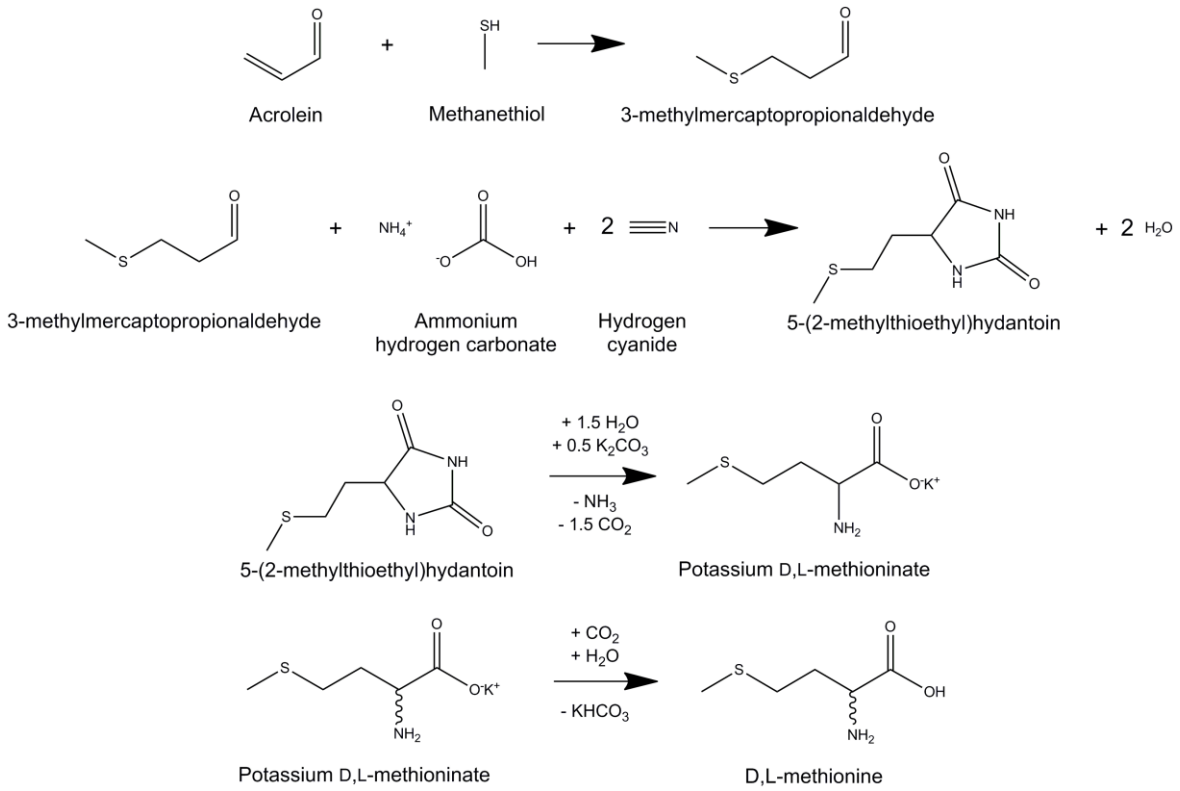

Figure 1.14 Methionine synthesis method developed by Degussa.[1]

Modified versions of the Strecker synthesis method can be used to asymmetrically synthesize amino acids, although none are economical enough to be used in an industry scale.[1] One example uses a chiral zirconium catalyst to introduce the asymmetrical aspect. This method involves reacting an aldehyde with 2-hydroxy-6-methylaniline and ammonia in the presence of a chiral zirconium catalyst to form an α-aminonitrile (**Figure 1.15**). This α-aminonitrile can then be converted into a α-amino acid by methylation of the phenolic hydroxyl group, followed by acid or base hydrolysis and oxidative cleavage with cerium ammonium nitrate.[28]

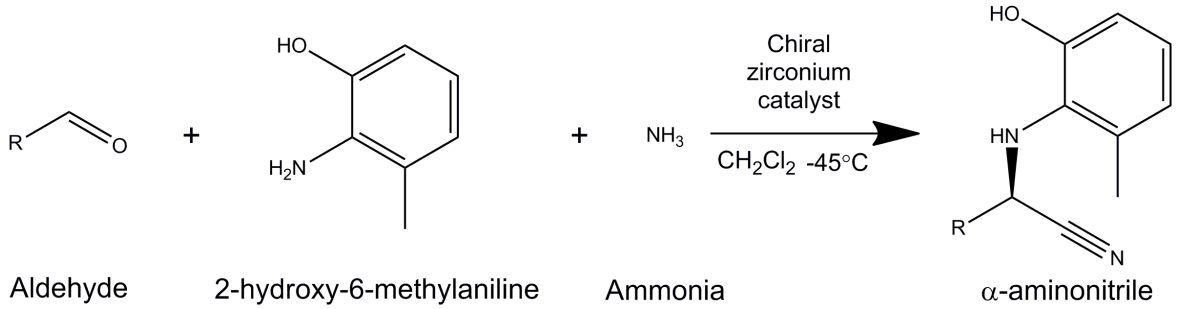

Figure 1.15 Asymmetric Strecker synthesis of a α-aminonitrile.[28]

1.2.3 Biocatalytic production and racemization of amino acids

There are several biocatalytic methods of producing enantiomerically pure amino acids, either using fermentation, chemoenzymatic methods or biotransformations to synthesize the pure amino acids, or using biotransformations to resolve racemates that have already been produced by chemical synthesis or other means.

Corynebacterium glutamicum was isolated in 1957 and was discovered to produce and secrete a large amount of L-glutamate, making it useful for the production of L-glutamate by fermentation.[1] *C. glutamicum* can also produce other amino acids, including L-lysine, L-threonine, L-aspartate and L-alanine. However, L-glutamate and L-lysine are the amino acids produced in the greatest quantities in industry, due to their large markets[29] and strains of *C. glutamicum* that increase the production efficiency of lysine by overproducing dihydropicolinate synthase, which results in more L-lysine production at the expense of L-threonine.[1]

L-threonine can also be produced by fermentation of modified strains of *E. coli* or *Serratia marcescens*. The *E. coli* strain KY10935 has a deregulated L-threonine biosynthetic pathway and blocked L-threonine degradation pathways, allowing it to produce up to 100 g L^{-1} L-threonine after 77 h fermentation.[30] The *S. marcescens* strain T-2000 contains a plasmid with deregulated versions of aspartokinase and homoserine dehydrogenase, involved in L-threonine production, and defective L-threonine degradation enzymes, this strain can produce 100 g L^{-1} after 96 h.[31] The *E. coli* strain is the most commonly used for industrial production of L-threonine,[32] with its high growth rate and well-researched physiology being advantages compared to other production species.[33]

These advantages of *E. coli* were also an important factor in the optimisation of *E. coli* for producing L-phenylalanine by fermentation by Backman *et al*.,[34] which is now used as the method for producing L-phenylalanine on an industrial scale.[1]

Monsanto Co. developed a strain of *E coli* K12 that produces D-phenylalanine by fermentation. The strain uses the 3-deoxy-D-arabinoheptulosonate 7-phosphate (DAHP) synthase and the chorismate mutase-prephenate dehydratase enzymes from *E. coli* to overproduce L-phenylalanine, and an alanine racemase from *Salmonella typhimurium* to convert L-alanine to D-alanine. The L-phenylalanine is converted to phenylpyruvate by a L-amino acid deaminase from *Proteus myxofaciens* before a D-amino acid aminotransferase from *Bacillus sphaericus* is used to transfer the D-amino group from the D-alanine to the phenylpyruvate, resulting in D-phenylalanine and a carboxylic acid. The carboxylic acid is then degraded by natural metabolic pathways from *E. coli*,

which encourages the reaction to work in the direction of D-phenylalanine production (**Figure 1.16**).[35]

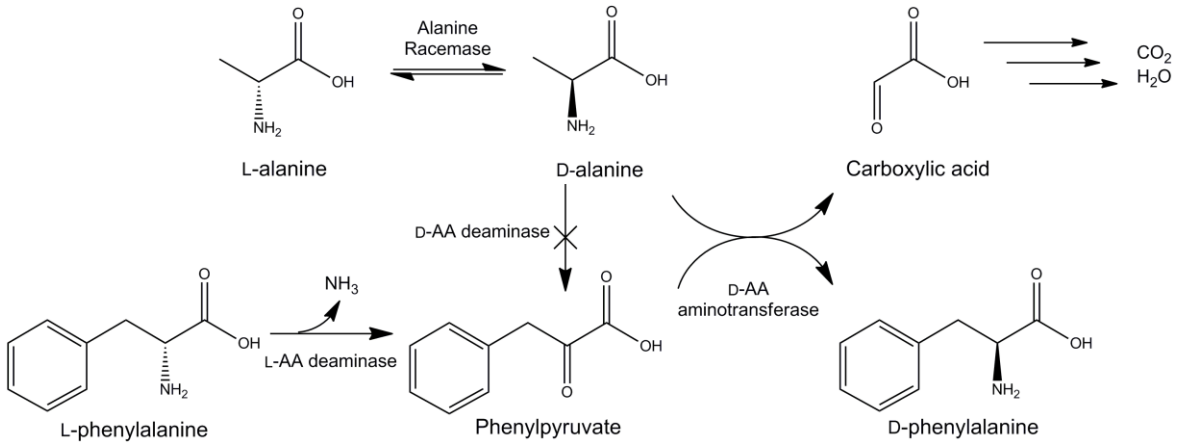

Figure 1.16 Production scheme of D-phenylalanine by fermentation in *E. coli*.[35]

D-amino acids can also be produced from racemate solutions by chemoenzymatic methods using an enantioselective L-amino acid oxidase and a chemical reductant. The enantioselective amino acid oxidase only oxidises the L-form of the amino acid, however the reductant will reduce the resulting imine into both L- and D-forms of the amino acid. The new L-amino acids are then oxidised again and so on until only the D-form remains.

Great Lakes Chemical Corp. developed this method using palladium on carbon (Pd-C) in ammonium formate buffer as the reduction agent (**Figure 1.17**) with yields of 90% with an enantiomeric purity of 99% *ee* being observed.[1] The same method can be used to produce L-amino acids from racemate solutions using an appropriate D-amino acid oxidase; however these tend to be less common in nature than L-amino acid oxidases, and this method is more commonly used to produce unnatural L-amino acids.

L-amino acid oxidases can also be used to resolve amino acids into a D-amino acid and the corresponding α-keto acid, which can then be separated using chromatography. Recently an L-amino acid oxidase from *Aspergillus fumigatus* has been shown to do this for alanine, phenylalanine and tyrosine.[36]

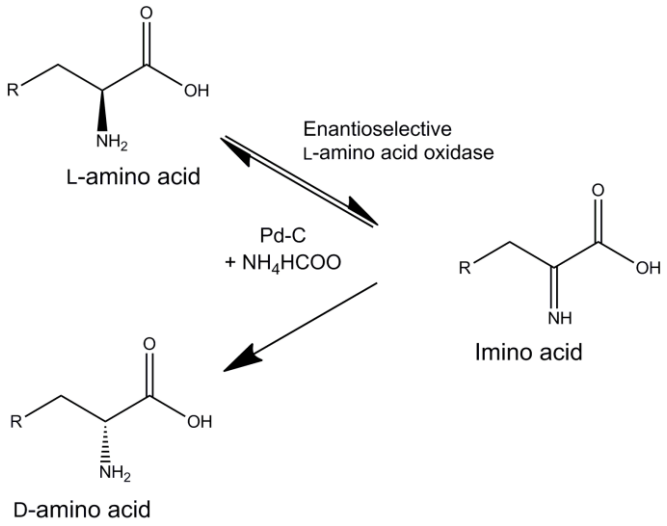

Figure 1.17 Racemisation of an amino acid to its D-form using an enantioselective L-amino acid oxidase and Pd-C in ammonia formate as a chemical reductant.

Lyases can also be used as biocatalysts in the synthesis of L-amino acids. Since 1958 L-aspartate has been made from fumarate using polyazetidine-immobilised *E. coli* cells containing L-aspartate ammonia lyase activity as a catalyst (**Figure 1.18**),[8] and this method could be used to produce *N*-substituted aspartic acids, as the aspartate ammonia lyase enzyme from *Bacillus* sp. YM55-1 has been shown to incorporate nucleophiles hydroxylamine and hydrazine into the fumarate substrate instead of ammonia.[37] Phenylalanine can also be made from *E*-cinnamic acid using the L-phenylalanine ammonia lyase from *Rhodotorula glutinis* as a catalyst (**Figure 1.19**),[38] however the fermentation method mentioned above is more economically viable.[1]

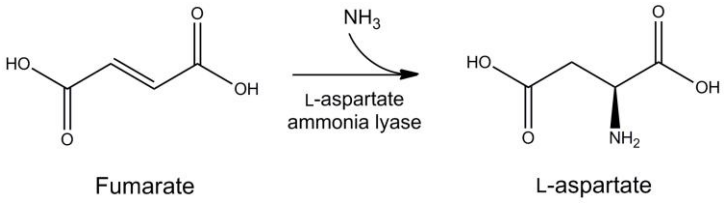

Figure 1.18 Synthesis of L-aspartate from fumarate using L-aspartate ammonia lyase.[37]

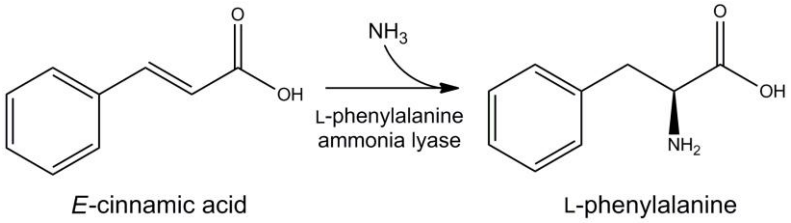

Figure 1.19 Synthesis of L-phenylalanine from *E*-cinnamic acid using L-phenylalanine ammonia lyase.[38]

Pseudomonas dacunhae cells immobilised with polyurethane and containing L-aspartate β-decarboxylase enzyme are also used to covert L-aspartate to L-alanine by removing the acid side chain (**Figure 1.20**),[39] although the release of carbon dioxide means that the reaction has to take

place in a pressure reactor in order to stop bubbles of carbon dioxide from disrupting the immobilised cell layers.[1] L-aspartate β-decarboxylase can also be used in a single reaction to convert fumarate into L-alanine and D-aspartate, which can be used to synthesise semisynthetic penicillin aspoxicillin. Fumarate is chemically synthesised into DL-aspartate, and the L-aspartate β-decarboxylase subsequently converts the L-aspartate into L-alanine, resulting in a mix of D-aspartate and L-alanine.[40]

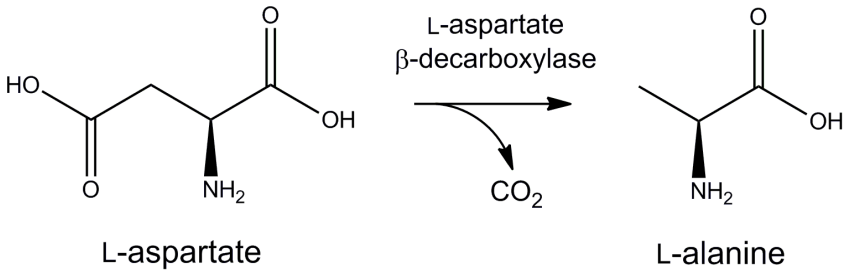

Figure 1.20 Synthesis of L-alanine from L-aspartate using L-aspartate β-decarboxylase.[39]

Amino acid dehydrogenases can be used to convert a 2-oxocarboxylic acid into a Schiff base, which is then reduced into an amino acid. This requires a co-substrate like NADH to provide the hydride ions, so the reaction has to be run alongside a co-substrate regeneration reaction, such as using the formate dehydrogenase from *Candia boidinii* to oxidise formate and reduce NAD^+, as formate is a cheap substrate (**Figure 1.21**).[41] The amino acid dehydrogenases do not have much substrate specificity, which means that non-proteinogenic amino acids can also be created. Degussa used a leucine dehydrogenase to synthesise L-*tert*-leucine, which is used as a building block for anti-cancer and anti-AIDS compounds, from trimethylpyruvic acid (**Figure 1.21**).[42]

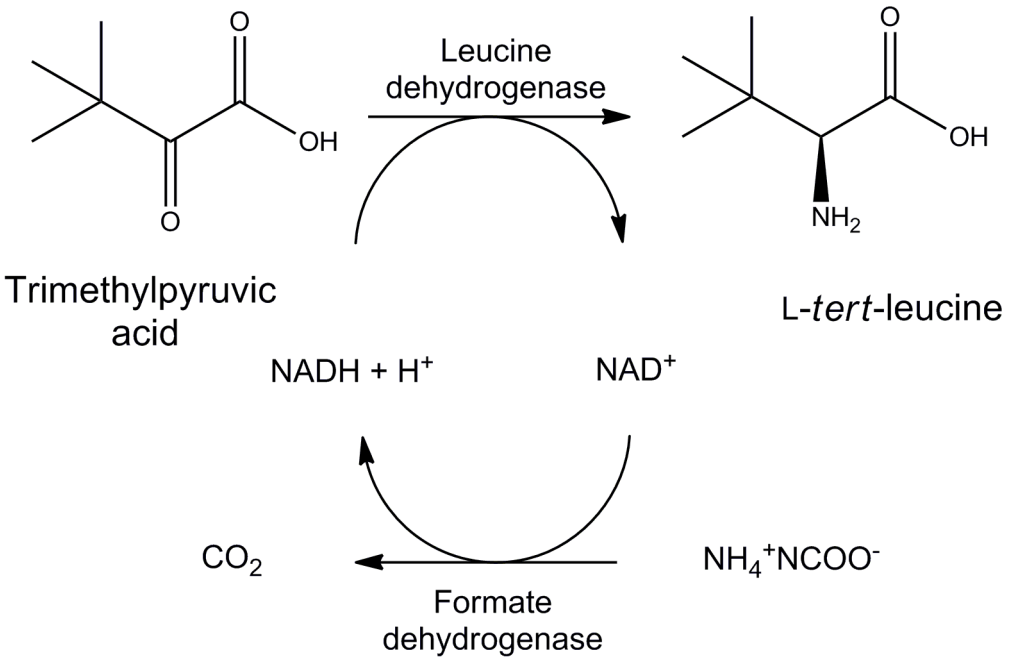

Figure 1.21 Degussa's method for production of L-*tert*-leucine using leucine dehydrogenase alongside NAD^+ regeneration reaction using formate dehydrogenase.[42]

Aminotransferases can also add an amine group to 2-oxocarboxylic acids, using other amino acids as an amine donor instead of needing a co-substrate. Like the dehydrogenases, these can be used to make non-proteinogenic amino acids.

One example of their use in industry is the production of L- or D-2-aminobutyric acid by Great Lakes Chemicals. Their method uses a genetically modified strain of *E. coli* as a catalyst in the production, which starts with the amine group from L-aspartate or D-aspartate (depending on which amino-acid aminotransferase enzyme is built into the strain) being transferred to 2-oxobutyric acid to form either L- or D-2-aminobutyric acid, as well as 2-oxalylacetic acid as a by-product. To avoid the *E. coli* cells generating L-alanine from the 2-oxalylacetic acid, the by-product is subsequently converted to acetoin, which is removed from the reaction by distillation. This distillation pushes the reaction equilibrium in favour of more 2-aminobutyric acid (**Figure 1.22**).[1]

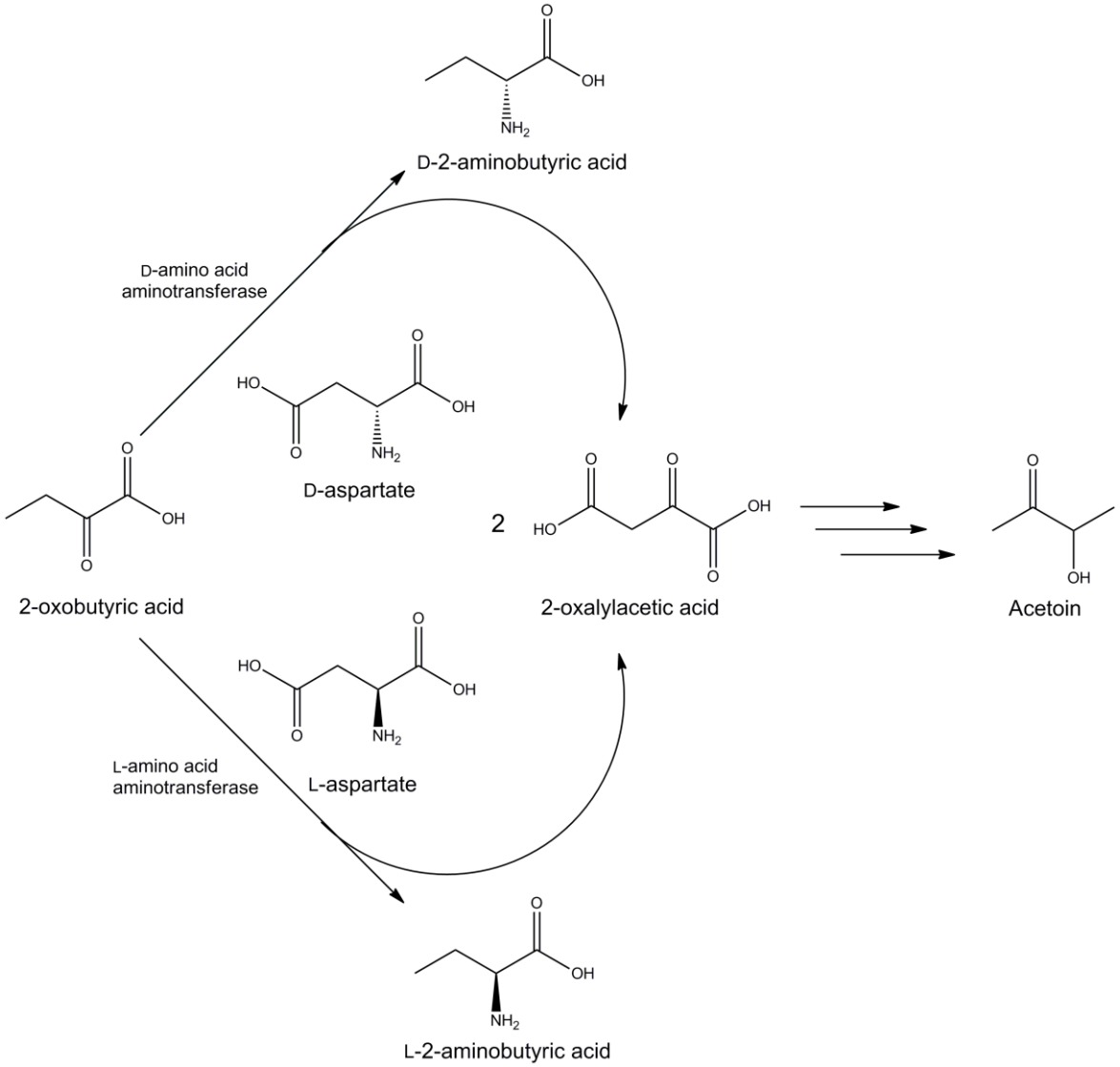

Figure 1.22 Great Lakes Chemicals' production method for L- and D-2-aminobutyric acid, using *E. coli* cells with amino acid aminotransferase activity as catalysts.[1]

Although L-serine can be extracted from keratin, an enzymatic method for its production has been developed by Genex Corporation. This method uses a two-step reaction catalysed by serine hydroxymethyltransferase (SHMT) enzyme from *E. coli*. The first step is a non-enzymatic reaction between formaldehyde and tetrafolate to form N^5,N^{10}-methylenetetrahydrofolate. SHMT then catalyses a reaction between N^5,N^{10}-methyenetetrahydrofolate and glycine that forms L-serine and tetrafolate, meaning only the formaldehyde and glycine have to be fed into the reaction.[8]

L-and D-amino acids can be produced by racemization of hydantoins (made by chemical synthesis), the racemic hydantoins spontaneously racemize at pH higher than 8, and can be treated with racemase to increase the rate. This means that the hydantoins can be treated with either a L- or D-enantiospecific hydantoinase to form a carbamoyl amino acid, which is subsequently treated with either L-or D-carbamoylase to form the respective amino acid with high enantiomeric purity (**Figure 1.23**).[1]

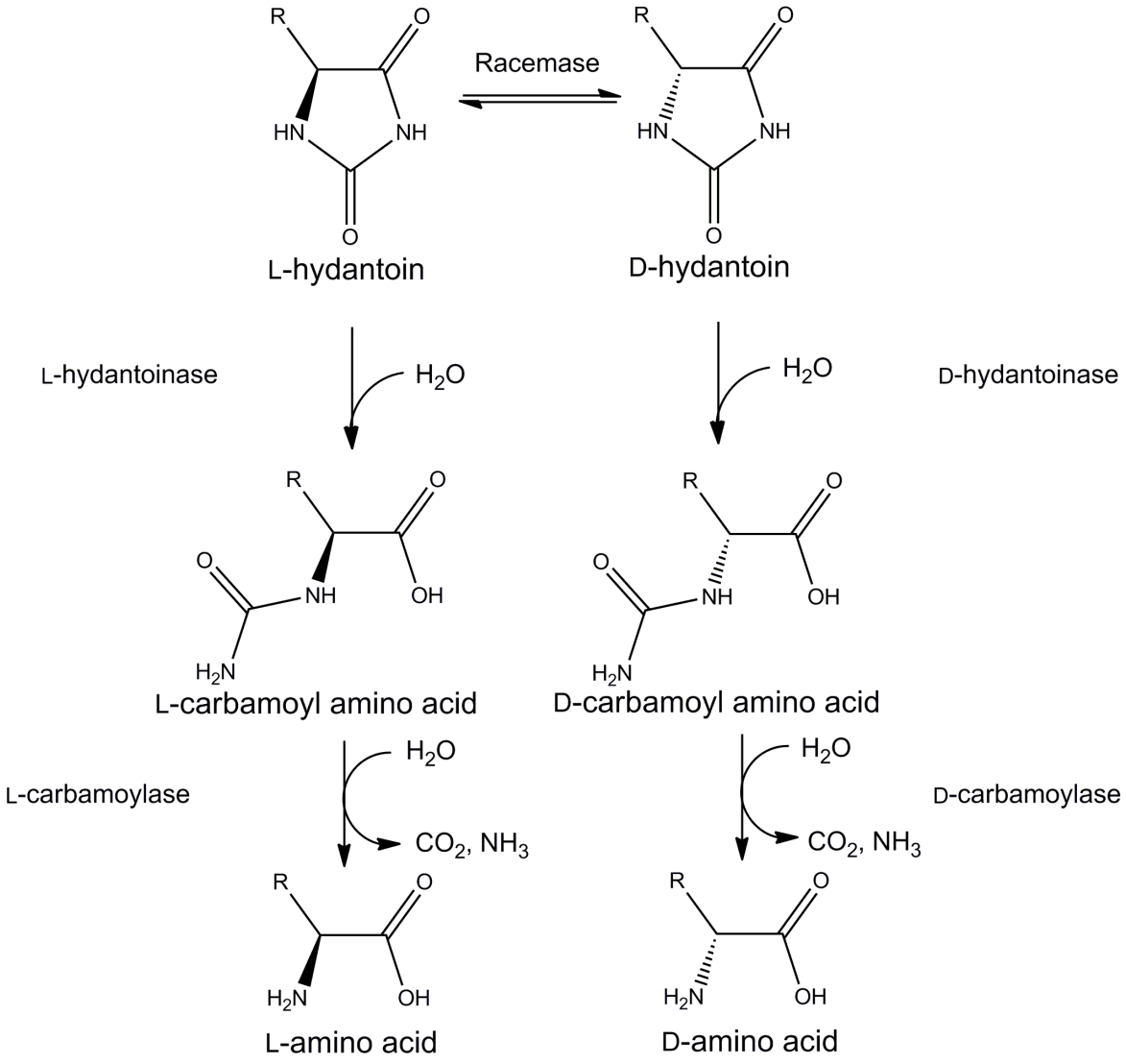

Figure 1.23 Method for production of amino acids by racemization of hydantoins.

The unnatural amino acids D-phenylglycine and D-hydroxyphenylglycine, used to produce β-lactam antibiotics, are usually produced using this method,[43] although a fermentation method for the production of D-phenylglycine has been developed by creating a strain of *E. coli* with the hydroxymandelate synthase enzyme from *Amycolatopsis orientalis*, the hydroxymandelate oxidase enzyme from *Streptomyces coelicolor*, and the D-(4-Hydroxy)phenylglycine aminotransferase enzyme from *Pseudomonas putida*. Phenylpyruvate produced by the cells is converted by the hydroxymandelate synthase into mandelate, which is subsequently converted to phenylglyoxylate by the hydroxymandelate oxidase. The D-(4-Hydroxy)phenylglycine aminotransferase then adds an amino group from L-glutamate to the phenylglyoxylate to make D-phenylglycine (**Figure 1.24**).[44]

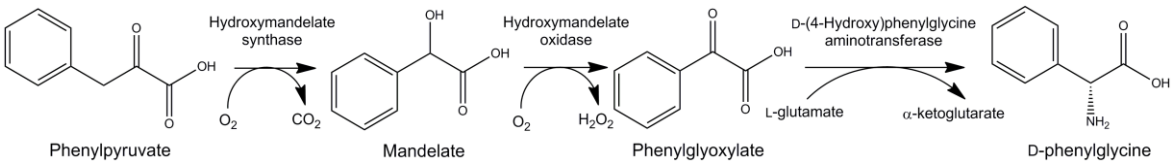

Figure 1.24 Fermentation route for the production of D-phenylglycine.[44]

As L-cysteine that has been extracted from human hair of animal products cannot be used for medical purposes, a method for the synthesis of L-cysteine has been developed that is based on the racemization of DL-2-amino-Δ^2-thiazoline-4-carboxylic acid (DL-ATC), which can be synthesized from α-chloroacrylic acid and thiourea. The DL-ATC is treated with a racemase and an enantiospecific L-ATC hydrolase, meaning all the substrate is converted to L-form and subsequently to (*S*)-carbamoyl-L-cysteine. The (*S*)-carbamoyl-L-cysteine is then hydrolysed to L-cysteine by a (*S*)-carbamoyl-L-cysteine hydrolase enzyme (**Figure 1.25**).

This reaction can be catalysed by cells from strains of *Pseudomonas* species containing all of these activities, as recent example of which is *Pseudomonas* sp. strain HUT-78 which contains a mutation deactivating the L-cysteine desulfhydrase enzyme, which usually decomposes the L-cysteine product.[45]

Enantiospecific L-acylases are also used to resolve D,L-amino acids produced by Strecker synthesis. The D,L-amino acids are acylated using the Schotten-Baumann reaction into D,L-*N*-acetyl-amino acids. The L-acylase then catalyses the reaction of L-*N*-acetyl-amino acids into L-amino acids, which are then removed by ion chromatography. The remaining D-*N*-acetyl-amino acids can then be racemized and reused (**Figure 1.26**). Degussa used this method to produce proteinogenic amino acids L-alanine, L-methionine, L-valine and L-tryptophan and some non-proteinogenic amino acids *O*-benzylserine, norleucine and norvaline.[46]

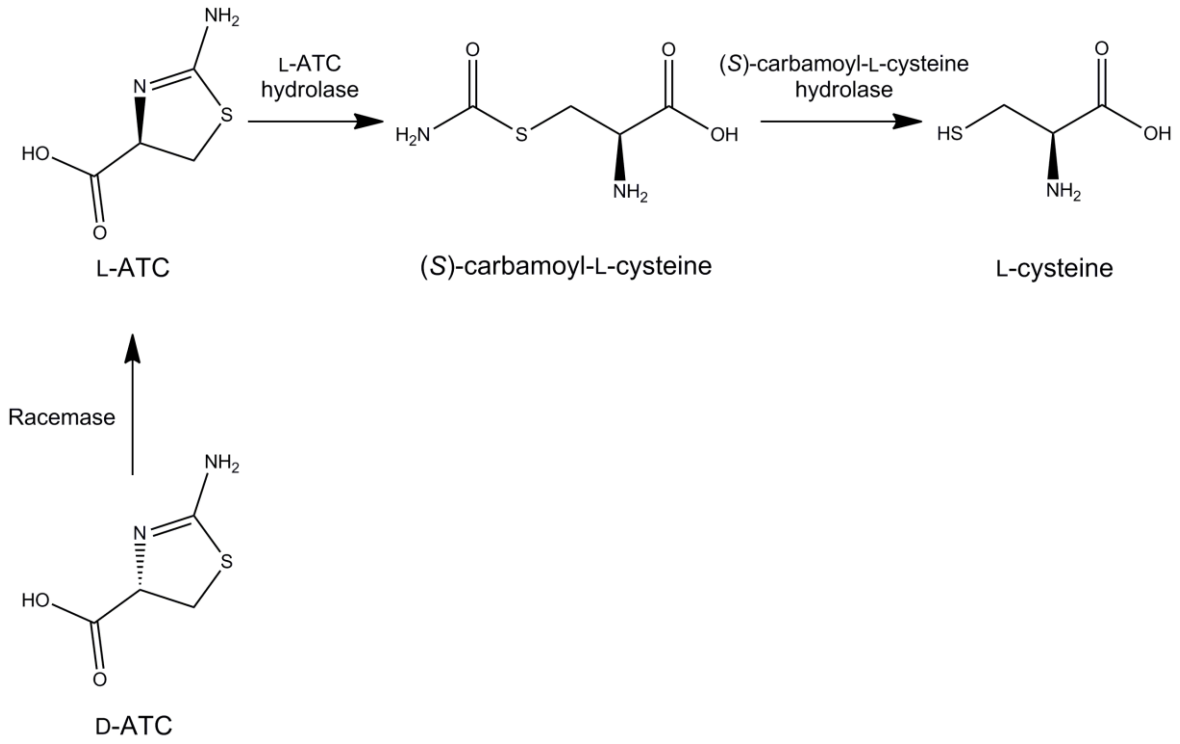

Figure 1.25 Production of L-cysteine from D,L-ATC.[45]

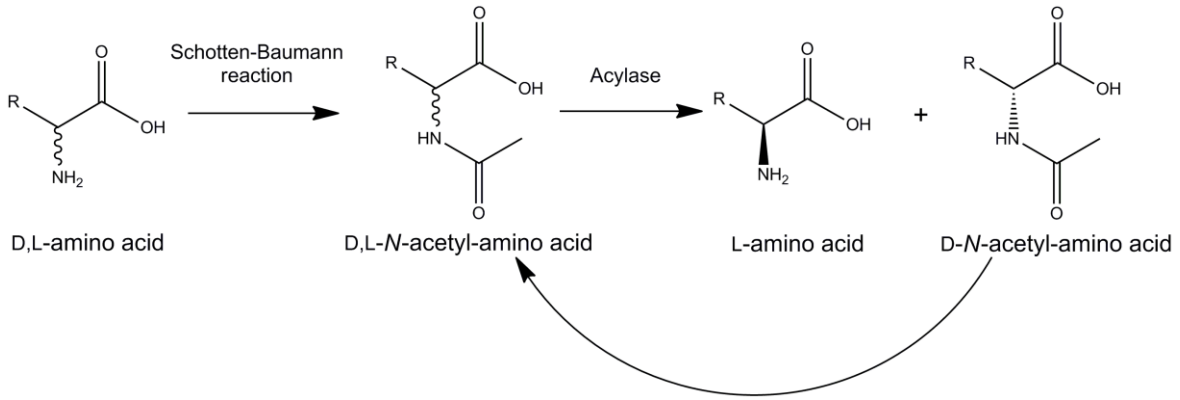

Figure 1.26 Resolution of D,L-amino acids using acylases.[46]

Enantiospecific amino acid amidases such as D-amino-peptidase from *Ochrobactrum anthropi* sp. SCRC Cl-38[47] or D-amino acid amide amidohydrolase from *Brevibacterium iodinum* TPU 5850[48] can also be used to racemize a variety of amino acid amines, which can be prepared by hydrolyzing amino nitriles (prepared using Strecker synthesis).[47] One disadvantage of this method is that the amino nitriles tend to be unstable substrates and will spontaneously revert back to cyanide, hydrogen and ammonia in alkaline solutions,[49] affecting yields unless mild reaction conditions are used.

1.3 Amino acid oxidases

Amino acid oxidases (AAOs) are enantioselective flavoenzymes that catalyse the oxidation of amino acids to imino acids, which in aqueous solutions will spontaneously hydrolyse into keto acids, producing hydrogen peroxide and ammonia as by-products (**Figure 1.27**).[50] They are related to amine oxidases (AOs), which are flavoenzymes that catalyse the oxidation of amines to imines, and subsequently ketones.[51] AAOs are found in species from bacteria to humans.[50]

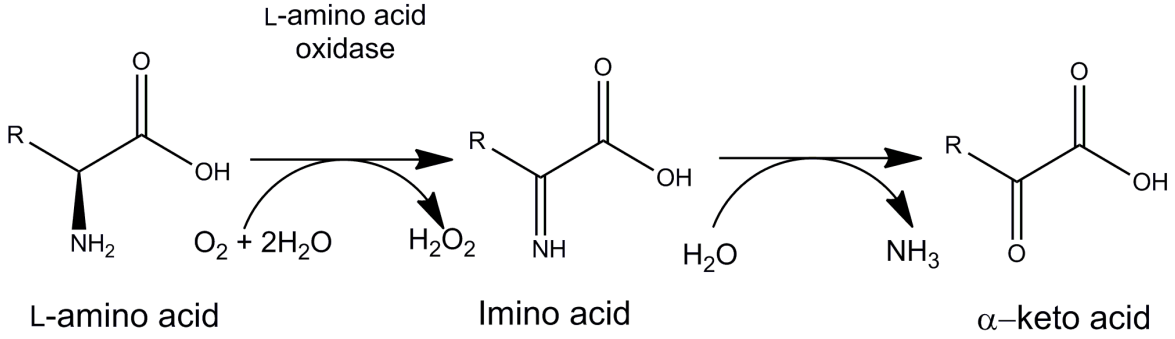

Figure 1.27 Reaction scheme for an L-amino acid oxidase.

1.3.1 Structure and Activity of AAOs

The monomeric forms of AAOs can range in size from around 39 kDa[52] to 85 kDa,[53] and usually contain one molecule of FAD cofactor per monomer. The monomers are usually described as having three domains; the FAD binding domain, substrate binding or capping domain and a helical domain thought to be involved in dimerisation of the protein.[54]

The active enzymes are usually homodimeric[54] although there are exceptions such as the homotetrameric aplysianin A enzyme from *Aplysia kurodai*, which oxidises basic L-amino acids arginine and lysine[53] and the tetrameric rat kidney L-AAO, which contains either one or half a monomer of flavin mononucleotide per subunit.[55] The effects of the quaternary structures of the oxidases on their activity have not been studied in depth, however the aplysianin A enzyme has higher binding affinity for its substrates than dimeric L-AAOs with activity against the same substrates (K_M of 3.34 μM against L-arginine and 2.38 μM against L-lysine,[53] compared with the L-AAO from *Rhodococcus opacus* (RoLAAO) which has K_M of 70 μM against L-arginine and 15 μM against L-lysine).[56]

The FAD binding domains of AAOs contain a common GR_2 motif for binding FAD. The secondary structure of the GR_2 motif contains the Rossmann fold, which consists of three β-strands and 2 α-helices in the pattern β1, α1, β2, α2 and β3 alternating on a parallel sheet. The overall motif structure has a parallel β-sheet containing β7, β8, β1, β2, and β3 strands, with the α1 and α2 helices

in the correct places to form the Rossmann fold, and an antiparallel other β-sheet containing the β4, β5 and β6 strands forming a crossover connection.[57]

There is some controversy as to how the amino acid oxidases catalyse the oxidation reaction. Two main mechanisms that have been suggested are a hydride transfer mechanism and the nucleophilic mechanism. The hydride transfer mechanism suggests that the role of the enzyme is to hold the substrate amino acid in the optimum position for the spontaneous transfer of the α-proton to the substrate to the N5 of the flavin (**Figure 1.28a**).[51]

The nucleophilic mechanism was first observed in amine oxidases but could be applicable to amino acid oxidases that contain a pair of aromatic residues, which sit at the base of the FAD molecule on the *re* side of the flavin ring, forming an "aromatic cage". The dipole moment of this aromatic cage increases the nucleophilicity of the substrate, allowing it to attack the C4a position of the flavin. This causes the N5 of the flavin ring to abstract the α-proton of the substrate, producing a benzylic carbanion intermediate that spontaneously rearranges to give the imine and reduced FAD (**Figure 1.28b**).[58]

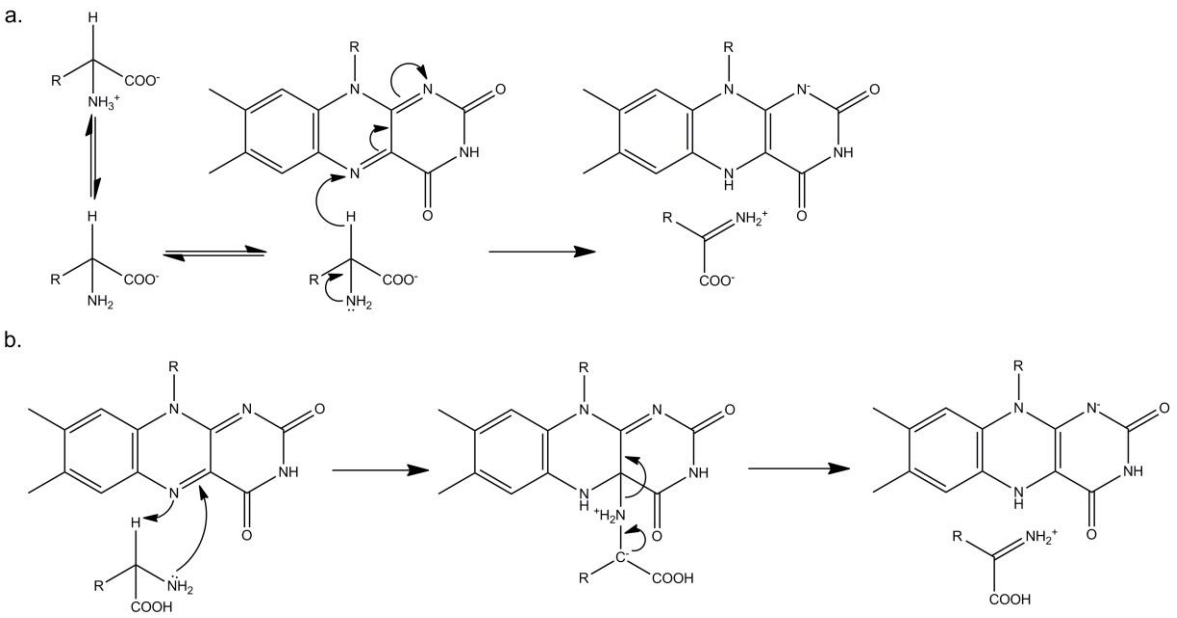

Figure 1.28 Possible reaction mechanisms for the oxidation of amino acids by amino acid oxidases. **a.** Hydride transfer mechanism. **b.** Nucleophilic mechanism.

Since the structure of pig kidney D-AAO was solved, the hydride transfer mechanism has been accepted as the mechanism for catalysis by D-AAOs, due to the lack of both an aromatic cage and any amino acid side chains that could act as a base for proton abstractions.[59] The structure of the D-AAO from *Rhodotorula gracilis* yeast also supported the hydride transfer mechanism, as the

substrates crystallised with the enzyme were held with the α-C-H bond pointing toward the N5 of flavin, and again no side chain capable of acting as a base were present in the active site.[60]

The mechanism of L-AAOs is more complex as L-AAOs have been considered to be in the structural group of monoamine oxidases (MAOs), as opposed to D-AAOs.[51] A mutational analysis of the human MAO-A and MAO-B enzymes was in support of the nucleophilic mechanism for MAOs. When one of the two residues comprising the aromatic cage (Y444 in MAO-A and Y435 in MAO-B) was mutated to aromatic residues with varying dipole moments the k_{cat}/k_M of the mutants were found to be proportional to the dipole moment of the aromatic cage residue. This suggested that the dipole moment of the aromatic cage residues is involved in the oxidation reaction, which supports the use of the nucleophilic mechanism for MAO proteins. It is also thought that the aromatic cage has a steric role in guiding the substrate towards the active site.[61]

The MAO-N protein from *Aspergillus niger* is also thought to use the nucleophilic mechanism, as it has two aromatic residues, Y430 and F466, in the same positions as the aromatic cage residues in MAO-A and MAO-B. The dipole effect is less pronounced in MAO-N as tryptophan has a dipole moment pointing away from the active site and phenylalanine does not have a permanent dipole moment. Interestingly, substrates with their own dipole effect, such as *para*-nitrobenzylamine, are poor substrates for MAO-B, as they cancel out the dipole effect of the aromatic cage. However, a N336S/M348K double mutant of MAO-N showed 30-fold higher activity against *para*-nitro-α-methylbenzylamine than the wild-type MAO-N, suggesting that a substrate with a dipole effect would be able to increase the activity of the MAO-N protein by compensating for the lack of a dipole moment in the aromatic cage, supporting the use of the nucleophilic mechanism.[62]

Although the possibilty of aromatic cages in L-AAOs has not been investigated, there are some structures of L-AAOs that have what appears to be an aromatic cage, and could possibly be using the nucleophilic mechanism. One example is the L-AAO from *Rhodococcus opacus*, which appears to have two tryptophan residues (W426 and W467) in the same place as the aromatic cage residues of MAO-N (**Figures 1.29, 1.30**)[54, 62] However there are also some doubts as to whether the MAO proteins use the nucleophilic mechanism, due to results of measurements of the oxidation of ^{15}N benzylamine by MAO-B, which appeared to be more consistent with a hydride transfer mechanism than the nucleophilic mechanism.[51]

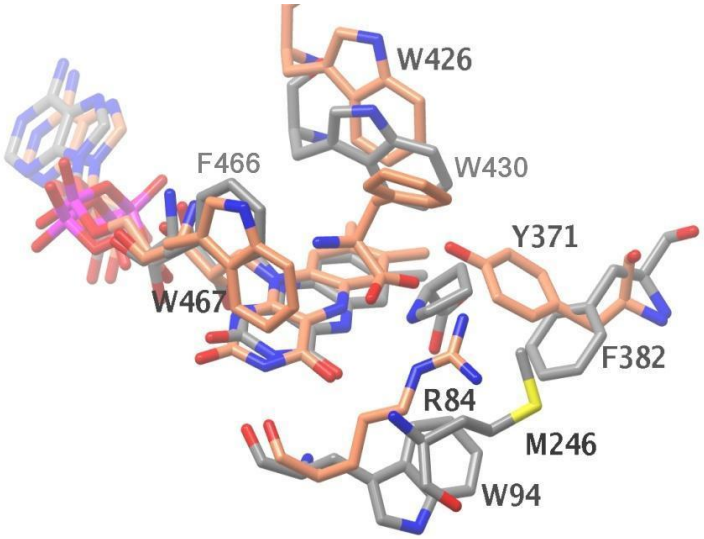

Figure 1.29 Superimposition of active site area of *Aspergillus niger* Mono Amine Oxidase (MAO-N)[62] (grey) and *Rhodococcus opacus* L-AAO (RoLAAO)[54] (coral)

However, there are L-AAOs that do not have aromatic cages and appear to abstract a proton from the amino acid substrate before reducing the substrate using the hydride transfer mechanism. One example of this is the L-AAO from *Calloselasma rhodostoma*, where the current understanding is that the H223 side chain deprotonates the substrate before it binds G464 at the active site, at which point the pair of electrons on the amino nitrogen atoms moves to the α-carbon of the substrate and the hydride of the α-carbon is transferred to the N5 of the flavin ring.[63]

The L-aspartate oxidase from *E. coli* uses a similar mechanism, however in this case the substrate, guided into the correct conformation by the E121 side chain,[64] has its a proton abstracted by the R290 residue after binding in the active site has occurred. The other proton is also transferred to the N5 of the flavin ring (**Figure 1.31**), although it is unknown if this happens at the same time as the proton abstraction or occurs afterwards. There is also some doubt as to which proton is abstracted by R290 and which is transferred to the flavin ring, however from the structure of the *E. coli* L-AspO solved by Bossi *et al.*[65] it appears most likely that the α-proton is abstracted by R290 and the β-proton is transferred to the flavin ring.[66]

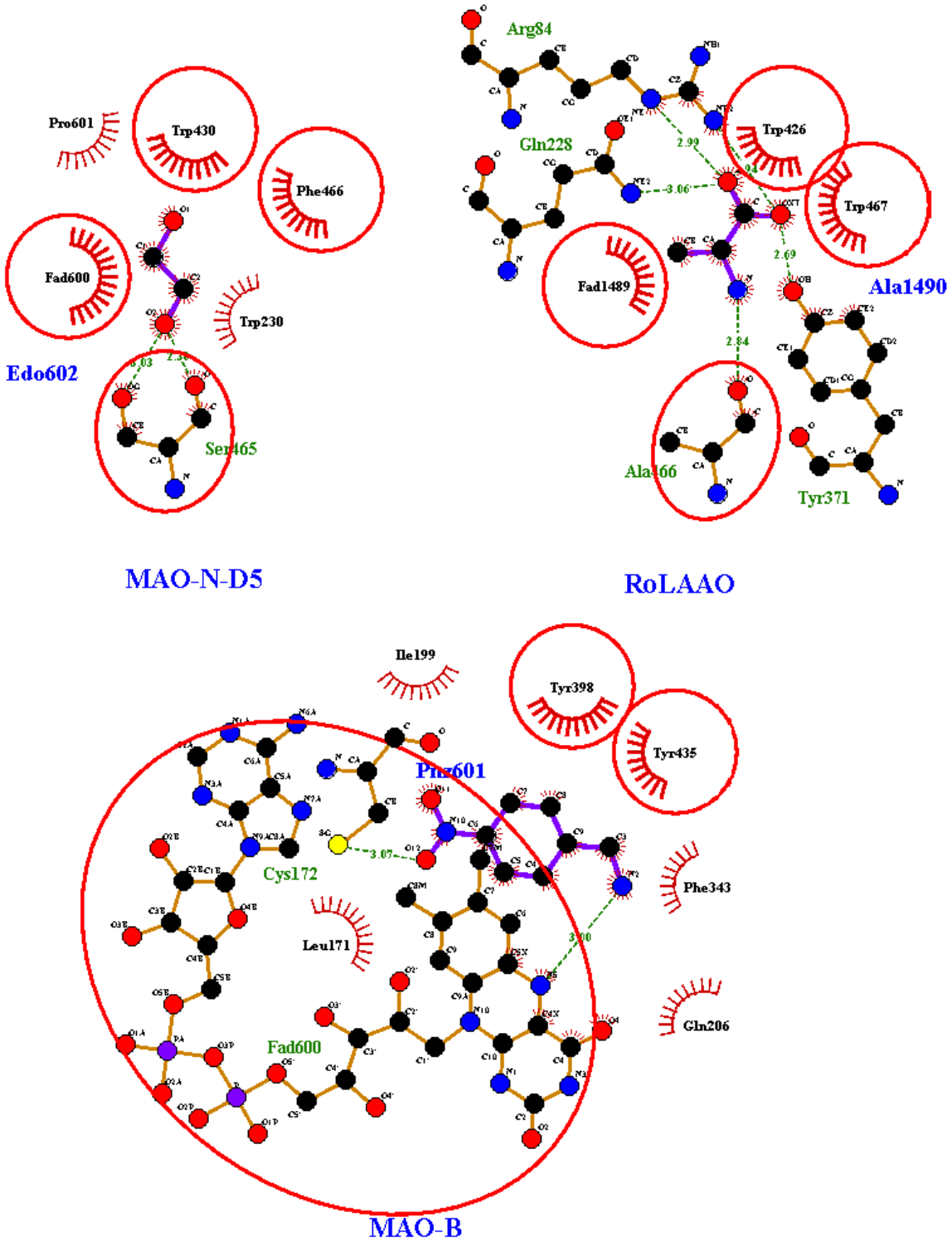

Figure 1.30 LigPlot+[67] comparison of the residues interacting with ligand in active site of a mutated form of the *Aspergillus niger* monoamine oxidase (MAO-N-D5)[62], the L-amino acid oxidase from *Rhodococcus opacus* (RoLAAO)[54] and the Human monoamine oxidase B (MAO-B)[61]. Hydrogen bonds are represented by dashed green lines, van der Waals contacts are represented by red combs and residues conserved between all three structures are circled in red.

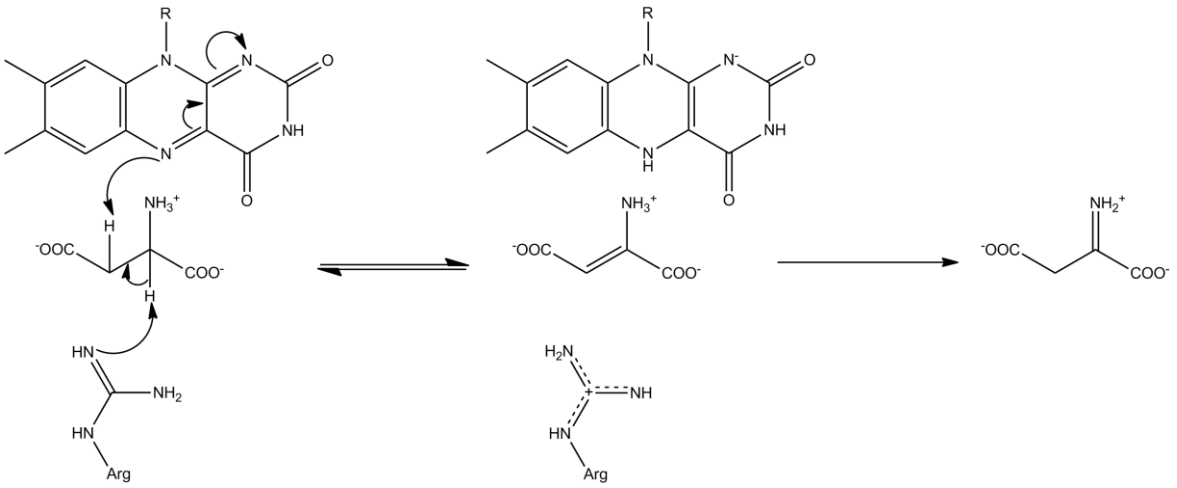

Figure 1.31 Mechanism of oxidation of L-aspartate by the *E. coli* L-AspO. The α-proton is abstracted by the R290 side chain, allowing the β-proton to transfer to the N5 of the flavin ring.[66]

1.3.2 Roles of AAOs in Nature

In microorganisms, D-AAOs metabolise D-amino acids in the environment to use as carbon and nitrogen sources.[50] In eukaryotic species they have a wider range of uses, however D-AAOs in some fish species are also involved in the metabolism of D-alanine, as the crustaceans and bivalve molluscs that they eat accumulate large concentrations of D-alanine, by racemizing L-alanine using an alanine racemize enzyme, to regulate osmotic pressure between cells.[68]

In humans D-AAO is involved in a range of neurobiological processes, most notably the regulation of D-serine levels. This is important as D-serine can act as an agonist of neuro-modulator *N*-methyl-D-aspartate-receptor (NMDA-receptor), and loss of NMDA-receptor activity is implied to be a cause of schizophrenia. In support of this, some studies have found that increased expression of D-AAO and its binding partner G72 can be a risk factor for developing schizophrenia.[69]

Brain tissue based D-AAOs are also involved in the regulation of D-alanine, which in the grey matter of Alzheimer's patients is found in 2.2-fold higher concentrations than in control groups and D-aspartate, which in the white matter of control groups is found in more than twice the concentration as in the white matter of Alzheimer's patients (although when these figures are expressed as a percentage of the total amount of DL-amino acid, the difference between Alzheimer's patients and the control groups are less noticeable).[70] D-alanine (along with D-serine) is also found in increased amounts in the ventricular cerebrospinal fluid (where amino acids from the brain are deposited) of Alzheimer's patients compared to control groups.[71]

In mammals, D-aspartate is found in the endocrine system as well as the central nervous system, and is involved in the regulation of several hormones. In the pineal gland D-aspartate produced by other tissues suppresses the secretion of melatonin from parenchyma cells.[72] D-aspartate and its derivative, *N*-methyl-D-aspartate, encourage the release of prolactin by acting on the pituitary and adenohypophysis glands respectively.[73] In rats, D-aspartate has been shown to induce testosterone synthesis in the testes[74] and the release of gonadotropin-releasing hormone (GnRH) from the hypothalamus, which allows D-Asp to induce secretion of luteinizing hormone (involved in triggering ovulation and inducing testosterone synthesis) from the pituitary gland.[75]

The L-arginine analogue N^G-nitro-L-arginine acts as a suppressor of nitric oxide synthase, which is involved in the regulation of basal blood pressure and peripheral vascular resistance. N^G-nitro-L-arginine is originally synthesized as the racemate form N^G-nitro-DL-arginine, however kidney based D-AAOs racemize the product by catalysing the oxidation of the N^G-nitro-D-arginine (which has no effect on nitric oxide synthase) to an α-keto acid, allowing it to be oxidised to the N^G-nitro-L-arginine.[76]

L-AAOs have a more diverse range of known roles in nature, as there are examples of L-AAOs that have narrow substrate specificity and are used for a more specific role. There are also many broad range L-AAOs, although the majority of these are found in snake venoms. The structure of a L-AAO from *Calloselasma rhodostoma* venom has a Y-shaped channel than allows oxygen to enter the active site and hydrogen peroxide to exit, however hydrogen peroxide is released near to a glycan moiety on the enzyme that allows it to bind to a host cell wall. This suggests that the role of these L-AAOs is to produce a large concentration of hydrogen peroxide at the host cell wall, causing the cell to initiate a stress response and undergo apoptosis.[63] Another toxic, broad range L-AAO has recently been characterized in the death cap *Amanita phalloides* mushroom.[77]

Other broad range L-AAOs can have antibiotic effects through the production of hydrogen peroxide. These can be produced by bacteria as a way of competing against other microbes. One example is the *Streptococcus oligofermentans* L-AAO, which is a factor in the inhibition of growth of *Streptococcus mutans* in the oral cavity, which is the primary cause of tooth decay.[78] *Pseudoalteromonas flavipulchra* strain C2, a marine bacteria found to associate with coral, can also use L-AAO derived H_2O_2 to disrupt the growth of other bacterial species and has shown anti-microbial activity against MRSA.[79]

A broad range L-AAO with anti-bacterial properties has also been found in mouse milk, again with the hydrogen peroxide providing the antimicrobial effect.[80] Broad range microbial L-AAOs can

also be used to metabolise L-amino acids in the environment, particularly in soils where they are an important source of nitrogen, as seen in the fungus *Hebeloma cylindrosporum*.[81]

The L-aspartate oxidase in eubacteria is known to catalyse the first step of the synthesis of quinolinic acid (the first substrate in the *de novo* synthesis of NAD) from L-aspartate and dihydroxyacetone phosphate (DHAP). The oxidase reduces L-aspartate to iminoaspartate, which is then condensed with DHAP by the quinolate synthase enzyme (**Figure 1.32**).[82]

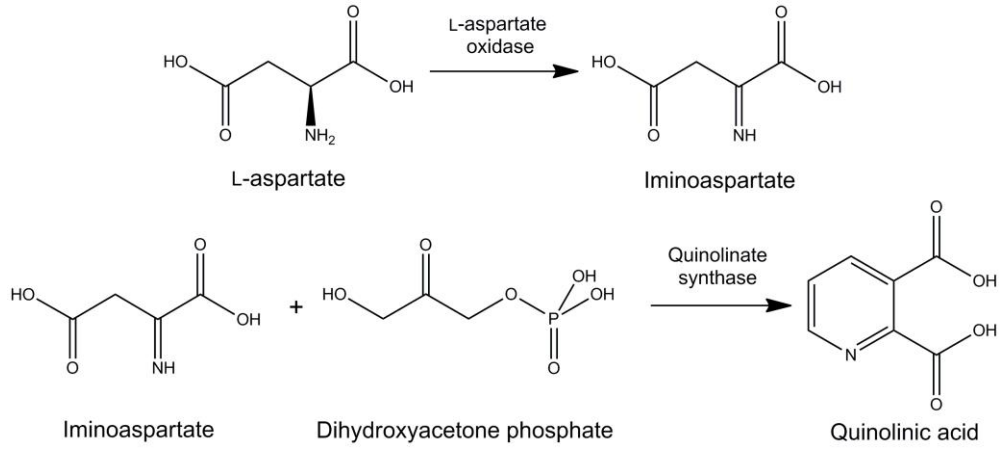

Figure 1.32 Synthesis of Quinolinic acid by L-aspartate oxidase and quinolinate synthase.[82]

Also, the human Interleukin-4–induced protein is a L-phenylalanine oxidase expressed and secreted by dendritic cells, which play a large role in the induction and regulation of the immune response. The protein has been shown to suppress the activity of T-lymphocyte cells, with memory T-cells being the most sensitive to suppression. The method of suppression appears to be that hydrogen peroxide produced by the enzyme down regulates the CD3 ξ-chain of the T-cell receptor at the protein level, with a preference for memory T-cells, resulting in reduced T-cell activity.[83]

1.3.3 Applications of AAOs

Several applications for D-AAOs are being developed. Enzymatic biosensors using D-AAOs have been developed for the measurement of D-AAs in food and beverages, which can be a sign of bacterial infection, and for the analysis of concentrations of D-serine in brain tissue *in vivo*. For food and beverages a graphite electrode with immobilised pig kidney D-AAO coupled with Prussian Blue, which acts as an electron mediator from hydrogen peroxide, has been shown to have a linear response to D-alanine concentrations between 5 μM and 200 μM.[84]

For *in vivo* detection of D-serine levels in brain tissue, a platinum microelectrode coated with a layer of the electron mediator poly-*m*-phenylenediamine and a layer of yeast *Rhodotorula gracilis*

D-AAO could detect concentrations of D-serine as low as 16 nM with a mean response time of two seconds. Unfortunately as the *Rhodotorula gracilis* D-AAO shows similar levels of activity towards D-alanine and D-serine, the microelectrode cannot be used to determine D-serine levels in other tissues due to the presence of D-alanine causing false positives.[85] For greater selectivity of these biosensors D-AAOs with single substrate specificities would need to be developed or found. In the case of the D-serine biosensor a mutant form of the *Trigonopsis variabilis* D-AAO that shows no activity against D-alanine, D-aspartate or D-proline has been created.[50]

D-AAO enzyme has also been suggested as a possible treatment for cancer, as cancer cells have low tolerance for oxidative stress. Polyethylene glycol (PEG) conjugated, recombinant pig kidney D-AAO was administered to tumour model mice using I.V. drip and was found to accumulate in greater concentrations in tumour cells compared with other organs. Two and four hours after PEG-D-AAO was administered, 0.5 mmol per mouse of D-proline was injected into the mice, and the subsequent hydrogen peroxide production was found to suppress tumour growth with no visible side effects.[86]

A couple of problems with D-AAO as a potential treated for cancer is the high K_M of the enzyme and the lack of oxygen in solid tumour cells. However Rosini *et al.* have optimised the D-AAO from *Rhodotorula gracilis* for activity at low oxygen levels, as well as increased activity at low levels of D-alanine, which could be used as a substitute for D-proline in this treatment method.[87]

D-AAOs can also be used to resolve racemic amino acids into the corresponding L-amino acids (using a chemical reductant as discussed in **Section 1.2.3**) or α-keto acid. One of the first examples of this was the use of pig kidney D-AAO to resolve racemic pipecolic acid into L-pipecolic acid, which is a component for the production of immunodepressants, and anticancer and neuroprotective drugs.[50]

The yeast *Trigonopsis variabilis* D-AAO has been used to produce the α-keto acid 4-methylthio-2-oxobutyric acid, which can induce apoptosis and is used as an anticancer drug, from racemic mixtures of methionine. The D-AAO was immobilised along with catalase enzyme in order to prevent the produced hydrogen peroxide from reacting with the 4-methylthio-2-oxobutyric acid, and the product was removed from the reaction solution using anion exchange chromatography.[88]

Also, D-AAO can be used alongside a glutaryl hydrolase to convert cephalosporin *C* into 7-aminocephalosporanic acid, which is used as a starting point for the synthesis of many cephalosporin based antibiotics. The D-AAO oxidises cephalosporin *C* into

ketoadipyl-7-aminocephalosporanic acid, which spontaneously decarboxylates into glutaryl-7-aminocephalosporanic acid. The glutaryl hydrolase then removes the glutaryl group to produce 7-aminocephalosporanic acid (**Figure 1.33**).[50]

Similarly to D-AAOs, L-AAOs can also be used as biosensors for their substrates, as evidenced by the development of L-glutamate biosensors using L-glutamate oxidase, which are useful as L-glutamate is the major excitatory neurotransmitter in the mammalian central nervous system. A recently developed biosensor consists of a platinum microelectrode covered with a permselective poly(phenylene diamine) membrane that prevents interference from oxidation of other compounds in biological samples such as urate or ascorbate. L-glutamate oxidase, from *Streptomyces* sp. X119-6, was then immobilised in a silica gel around the microelectrode. The resulting platinum electrode could then detect the generation of hydrogen peroxide by the L-glutamate oxidase specifically, with a linear dependence between 0.5 and 100 μmol of L-glutamate.[89]

L-glutamate oxidase has also been used alongside aspartate aminotransferase and a peroxidase from *Arthromyces ramosus* to form a biosensor for L-aspartate. L-aspartate is converted to L-glutamate by the aspartate aminotransferase, which is subsequently oxidised by L-glutamate oxidase to produce hydrogen peroxide. The hydrogen peroxide then reacts with the luminol, which produced luminescence that can be detected. Unfortunately this sensor requires the removal of any L-glutamate in the sample in order to determine L-aspartate levels.[90]

The L-lysine oxidase from *Trichoderma viride* has been used to develop biosensors to assay the content of essential amino acid L-lysine in nutrition dependant products, such as intravenous feeding solutions and cell and tissue culture mediums. A recent example uses L-lysine oxidase immobilised in monocrystalline natural diamond paste, which could measure L-lysine concentrations as low as 4 pmol L^{-1} and had linear dependence between 1 nmol L^{-1} and 100 nmol L^{-1}.[91]

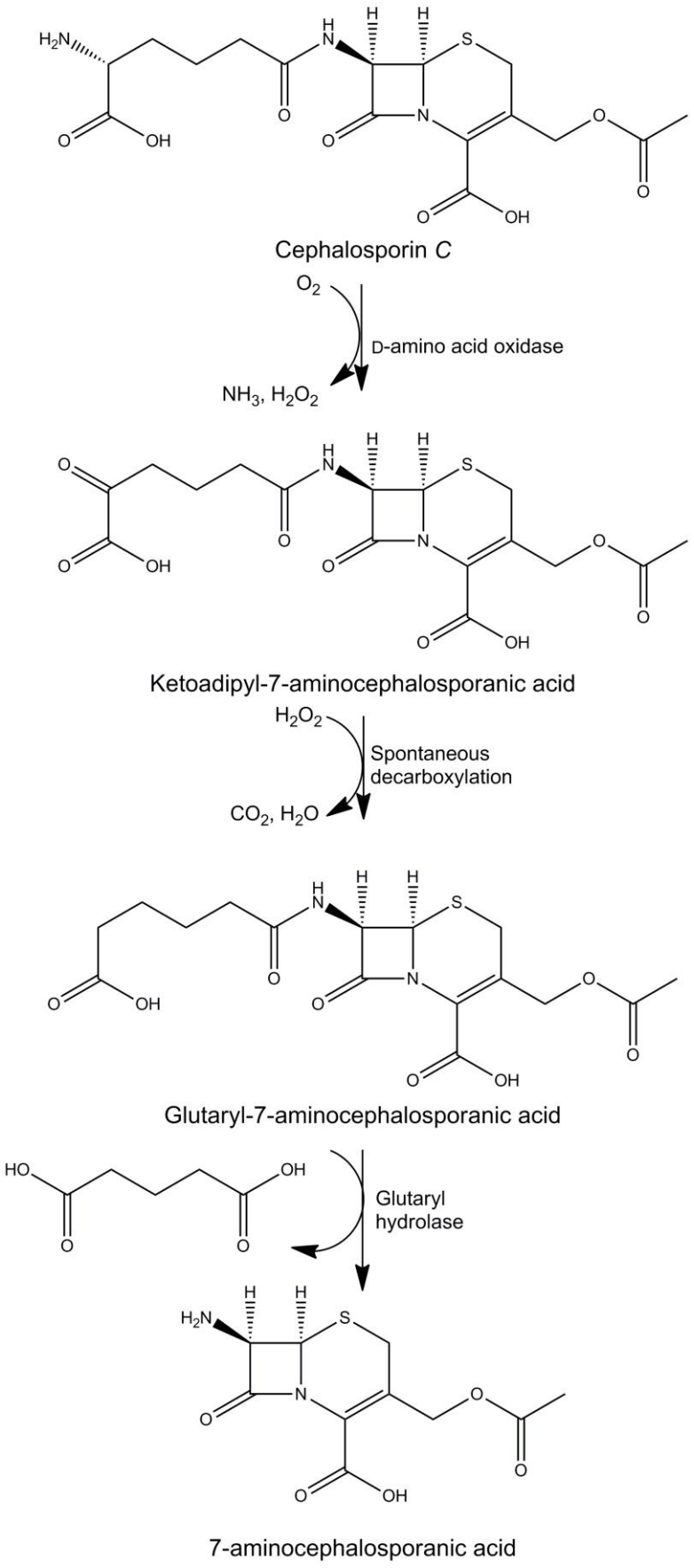

Figure 1.33 Method for the conversion of cephalosporin *C* into 7-aminocephaloporanic acid using D-AAO and a glutaryl hydrolase

L-lysine oxidase has also been shown to suppress DNA, RNA and protein synthesis in leukaemia L-5178Y, human ovary carcinoma, and Burkitt lymphoma tumour cells *in vitro*. This is thought to be due to its removal of L-lysine, which cannot be synthesised by mammals. Mice with grafted L1210 tumours survived 34-48% longer than a control group if they were injected with 70 U kg^{-1} of L-lysine oxidase, suggesting a possible use as an anti cancer agent.[92]

A broad range L-AAO from *Crotalus adamanteus* has been suggested for use as a pre-treatment to ready the body for treatment with melphalan, which is an anti-tumour agent designed to travel across the blood brain barrier. The disadvantage of melphalan is that it has to compete with large neutral L-amino acids like isoleucine, phenylalanine, valine *etc.* in order to cross the blood brain barrier. Moynihan *et al.* found that pre-treating mice models suffering from intracranial glioma with the L-AAO, and allowing time for it to deplete the levels of large neutral amino acids in the plasma, before treating the mice with anti-L-AAO serum and subsequently melphalan, increased the effectiveness of melphalan against the intracranial glioma.[93]

The *Crotalus adamanteus* L-AAO has also been used to assay the activity of peptide hydrolase from the intestinal mucosa. The assay is performed in two steps, the first involved allowing the peptide hydrolase to react with peptides, releasing single amino acids if the hydrolase is active. The second step involves addition of the L-AAO, horseradish peroxidase, *o*-dianisidine and sulphuric acid. If single peptides are present, the L-AAO releases hydrogen peroxide, causing the peroxidase to peroxidise the *o*-dianisidine into brown dianisidine quinonediimine, which has an absorbance around 450_{nm}.[94] The sulphuric acid then reacts with this to form a soluble pink product with absorbance around 530_{nm}.[95]

As mentioned in **Section 1.2.3** L-AAOs can also be used in biotransformations producing enantiomerically pure D-amino acids and α-keto acids from their L-amino acid substrates. They can also be used in other biotransformations, for example the L-amino acid oxidase from *Rhodococcus* sp. AIU Z-35-1 has been shown to convert N^{α}-benzyloxycarbonyl-L-lysine into the β-lactam antibiotic precursors N^{α}-benzyloxycarbonyl-L-aminoadipate-δ-semialdehyde and N^{α}-benzyloxycarbonyl-L-aminoadipic acid.[96]

Another potential therapeutic use for L-AAOs that has been suggested is that they could be used against bacterial infections, as the L-AAO from mouse milk has been found to prevent mastitis by killing bacteria[80] and could be used as an anti-bacterial agent outside of milk. It has also been suggested that L-AAOs could be added to cleaning products, such as detergent or toothpaste, along with a substrate in order to produce hydrogen peroxide as a bleaching agent, however these ideas have not been developed at this time.[55]

1.4 Objectives of Project

Amino acid oxidase enzymes could be used for the production of enantiomerically pure amino acids or as part of enzymatic biosensors for determining the concentrations of their substrates in food or biological samples (**Section 1.3.3**). This means that a range of amino acid oxidases, preferably with strong substrate specificity against various amino acid substrates, would be useful. In particular, Ingenza Ltd. has expressed an interest in L-tyrosine or L-alanine oxidases from a prokaryotic source, which would be more compatible with GMP guidelines than oxidases from other sources.

In the hope of finding an oxidase with natural activity against L-alanine or L-tyrosine, as well as increasing the repertoire of available oxidases, seven putative oxidases will be cloned and expressed in order to investigate their substrate specificities.

The Turner group has had some success in increasing the substrate range of MAO-N using directed evolution, starting with an increase in the enantiospecificity and range of substrates oxidised[97] and then creating versions that could oxidise secondary[98] and tertiary[99] amines. This suggests that it may be possible to introduce new substrate specificities into the related amino acid oxidases using directed evolution if they do not occur naturally.

Therefore, one target will be picked to undergo directed evolution attempts, either to introduce or improve activity against L-tyrosine or L-alanine. The choice of target will be based on the expression levels, solubility and substrate specificity of the enzyme, and whether the protein in question has been studied in depth by other groups.

1.4.1 Investigation of target oxidases

The L-AAO from *Synechococcus* sp. strain ATCC 27144, (also known as *Synechococcus elongatus* PCC 6301, UniProt code Z48565) (SLAAO) has previously been cloned and expressed in *E. coli* by Ingenza Ltd., who found that it was active against L-arginine and L-lysine, which is consistent with previously published data on the enzyme under the species name *S. elongates* PCC 6301, and a 100% identical L-AAO from the related *Synechococcus elongatus* PCC 7942 (UniProt code Q31PP3, now known as UDP-galactopyranose mutase), which were both found to be active specifically against basic amino acids, with L-arginine being the best substrate, followed by L-lysine and then L-histidine.[100] The SLAAO protein (UniProt code P72346) is estimated to be 54 kDa (estimation using ProtParam: http://web.expasy.org/protparam/ accessed 12/06/12).

To select other target proteins to be investigated, a BLAST search of the SLAAO was performed and six other putative oxidases were selected. Four of these were classed as putative L-AAOs, one as an amine oxidase and one as an oxidoreductase. The seven target proteins are summarized in **Table 1.1**

Table 1.1: Summary of seven target oxidases.

UniProt Code	Classification	Species	Known substrates	Abbreviation
P72346	L-amino acid oxidase	*Synechococcus* sp. strain ATCC 27144	L-arginine, L-lysine	SLAAO
Q8VPD4	L-amino acid oxidase	*Rhodococcus opacus*	L-alanine, L-histidine	RoLAAO
Q88MZ2	L-amino acid oxidase	*Pseudomonas putida*	L-aspartate	PpLAAO
O31616	L-amino acid oxidase	*Bacillus subtilis*	Glycine, sarcosine[101]	BsGO
Q8YKW9	L-amino acid oxidase	*Anabaena* sp. strain PCC 7120	-	AsAAO
Q5YV66	Oxidoreductase	*Nocardia farcinica*	-	NfOR
Q81RW3	Amine Oxidase	*Bacillus anthracis*	-	BaAO

The L-AAO from *Rhodococcus opacus* (RoLAAO) (UniProt code Q8VPD4) is a 53 kDa protein that has previously been purified and found to have a broad range of substrate activity, with L-alanine being the best substrate out of the proteinogenic amino acids.[56] The protein has also been crystallised previously and forms a homodimeric protein with three subunit domains, an FAD binding domain, a substrate binding domain and a helical dimerisation domain. Overall the structure is similar to that of many snake venom L-AAOs, and the RoLAAO protein is currently thought to use the hydride transfer mechanism to oxidise its substrates.[54]

The *nadB* gene from *Pseudomonas putida* encodes an L-AAO (PpLAAO) (UniProt code Q88MZ2), which is estimated to be around 59 kDa and has shown activity against L-aspartate when expressed in *E. coli* by Ingenza Ltd. Although no papers have been published about the *P. putida* protein, the homologous *E. coli* L-aspartate oxidase (L-AspO) shares 60% amino acid sequence identity and has been previously purified and has had its structure solved by crystallography.[65] The L-AspO protein is involved in the biosynthesis of NAD (**Figure 1.31**)[82] so it is possible that the PpLAAO protein is also involved in NAD biosynthesis. The L-AspO protein is currently thought to abstract a proton from its substrate before oxidising it using the hydride transfer mechanism.[67]

The glycine oxidase form *Bacillus subtilis* (BsGO) (UniProt code O31616) is a tetrameric protein made of 42 kDa monomers. Glycine oxidase can oxidise neutral D-amino acids such as D-alanine and D-proline, as well as glycine and sarcosine. The role of this protein in nature is not currently

understood.[102] The mechanism of activity for BsGO has also not been confirmed, although the hydride transfer mechanism appears to be the favoured mechanism.[103]

The *Anabaena* sp. strain PCC 7120 putative L-AAO (AsAAO) is a predicted enzyme found in the sequenced genome.[104] ProtParam (http://web.expasy.org/protparam/ accessed 12/06/12) estimates that the protein will be around 48 kDa in size. The *Nocardia farcinica* putative oxidoreductase (NfOR) (UniProt code Q5YV66) is also a predicted protein from the *N. farcinica* genome,[105] which is estimated to be around 49 kDa in size by ProtParam (http://web.expasy.org/protparam/ accessed 12/06/12). Finally the existence of the putative *Bacillus anthracis* amine oxidase (BaAO) (UniProt code Q81RW3) is predicted from the *B. anthracis* genome sequence.[106] It is estimated to be around 54 kDa (estimation using ProtParam: http://web.expasy.org/protparam/ accessed 12/06/12).

The amino acid sequence of these seven targets, along with known the known L-AAO from *C. rhodostoma* (CrLAAO) and the L-aspartate oxidase from *E. coli* are compared in **Figure B.1**.

The genes encoding these target proteins will be cloned and expressed in *E. coli* and the resulting cells and soluble protein fractions will be screened against potential amino acid and amine substrates in an attempt to determine substrate specificity of the enzymes. In order to investigate which residues of the proteins are involved in substrate activity and specificity, the target proteins will also be subjected to crystallisation screens for the X-ray determination of the protein structure, as well as possible mutational analysis of the active site residues.

1.4.2 Evolution of new substrate activity

Ingenza Ltd. has expressed an interest in L-tyrosine and L-alanine oxidases from a prokaryotic source, which could be created or developed from naturally occurring enzymes using directed evolution techniques.

The Turner group has had success creating variants of the MAO-N, capable of oxidising more substrates, using random mutagenesis and screening with a target substrate.[97, 98] However using random mutagenesis over the entire length of a gene sequence results in a large number of different combinations of mutations, and large numbers of transformants that need to be screened for activity. Directed evolution studies generally screen between 1,000-1,000,000 transformants, but some go as high as 1,000,000,000.[107] As this lab is not currently designed for high-throughput generation and screening of transformants, an approach that would potentially generate changes in substrate specificity with fewer transformants may be more efficient.

Reetz *et al.* suggest an iterative combinatorial active site saturation testing (CASTing) method where active site residues of the target protein are divided into groups, preferably ones that can be mutated using one primer set. The residues in each group are mutated together using site-directed saturation mutagenesis (SDSM) and the resulting transformants are screened for desired activity. Any transformants showing desired activity then undergo SDSM on the active site residues in one of the other groups. This can potentially continue until mutations in all of the groups have been covered.[108]

However, although active site residues do have a large effect on the activity and substrate specificity of enzymes, mutations in residues further away from the active site can also have a profound effect on the activity of the enzyme.[109] Because of this, a small scale random mutagenesis of the entire gene sequence of the target protein will be conducted alongside the CASTing procedure, with the intention of developing an amino acid oxidase with activity against L-alanine or L-tyrosine.

1.4.3 Summary

In summary, enantiomerically pure amino acids and amines have a variety of uses as substrates for the production of other enantiomerically pure chiral products or, in the case of L-amino acids, as additives for foodstuffs and nutritional products. Enantiomerically pure amino acids can be produced in a variety of ways, one of which uses enantioselective amino acid oxidases to resolve their respective substrate into the opposite enantiomer.

AAOs are a group of flavoenzymes, related to amine oxidases, which catalyse the enantiospecific oxidation of amino acids into imino acids and generate hydrogen peroxide and ammonia as by-products. Several possible uses have been suggested for them; however the most common uses are the aforementioned substrate deracemisation and their use in enzymatic amino acid biosensors.

Seven putative target oxidases (five L-AAOs, an oxidoreductase and an amine oxidase) were selected from a BLAST search of the SLAAO gene sequence to be investigated by cloning followed by protein expression and screening of the resulting samples for activity against amino acids and amines. Soluble proteins will also be purified and attempts to determine protein structure using X-ray crystallography will be initiated. Mutational analysis of the active site residues will also be performed, as part of the characterisation of the active site of the protein, if a structure can be determined. Directed evolution of one target with the intention of developing an oxidase with activity against L-alanine or L-tyrosine will also performed, using both a small scale random mutagenesis approach and the iterative CASTing approach.

Chapter 2 Materials and Methods

2.1 General Section

This general section describes common procedures such as agarose gel electrophoresis, SDS-PAGE, the transformation of chemically competent *E. coli* and Polymerase Chain Reaction (PCR)

2.1.1 Agarose gel electrophoresis

DNA was analysed with agarose gel electrophoresis. Agarose (electrophoresis grade) and SybrSafe DNA gel stain were purchased from Invitrogen. 1 kb DNA ladder was purchased from New England Biolabs.

A 1% (w/v) agarose gel contained 0.75 g agarose, 75 mL TAE buffer and 1 µL of 10000x SybrSafe DNA gel stain. Loading samples consisted of 75% (v/v) DNA solution and 25% (v/v) loading buffer. Electrophoreses with 1% agarose gels were conducted at 100 V for 1 h in TAE buffer. "1 kb DNA Ladder" was used as a standard to estimate the length of the DNA fragments, this marker contains single stranded DNA fragments 10 kb, 8 kb, 6 kb, 5 kb, 4 kb, 3 kb, 2 kb, 1.5 kb, 1 kb and 0.5 kb in length. The DNA was detected using a SYNGENE-UV-imager.

Loading buffer:	60 mM Tris/HCl, 2% (w/v) SDS, 0.2% (w/v) Bromophenol blue, 10% glycerol, 5% (v/v) β-mercaptoethanol, pH 6.8
TAE buffer:	40 mM Tris/acetate, 2 mM EDTA, pH 7.9

2.1.2 SDS-polyacrylamide gel electrophoresis (SDS-PAGE)

Protein samples were analysed with 12%-SDS-PAGE using Mighty Small gel electrophoresis equipment.[110] Acrylamide solution "30% ProtoGel" was purchased from National Diagnostics and "Low Molecular Weight Marker" was purchased from BioRad.

A 12%-resolving gel contained 1.6 mL H_2O, 1.25 mL buffer (1.5 M Tris/HCl, 0.4 % (w/v) SDS, pH 8.8), 2.1 mL acrylamide solution, 25 µL of 10% (w/v) APS and 4 µL of TEMED.
A stacking gel consisted of 1.6 mL H_2O, 0.65 mL buffer (0.5 M Tris/HCl, 0.4% (w/v) SDS, pH 6.8), 0.25 mL acrylamide solution, 16 µL of 10% APS, 4 µL of TEMED and 4 µL of 1% (w/v) Bromophenol Blue.

20 µL-loading samples contained 50% (v/v) protein solution and 50% (v/v) loading buffer. Loading samples were denatured at 95°C for 5 min. Electrophoreses were carried out at 200 V for 50 min in running buffer. "Low Molecular Weight Marker" was used as a standard to estimate the molecular weights of the proteins in the loading sample. This marker contains phosphorylase B (97.4 kDa), serum albumin (66.2 kDa), ovalbumin (45 kDa), carbonic anhydrase (31 kDa), trypsin inhibitor (21.5 kDa) and lysozyme (14.4 kDa).

After the electrophoresis, the SDS-gel was placed in staining solution and microwaved for 40 s. The SDS-gel was then washed with water and placed in destaining solution and microwaved for 40 s and then left to destain at room temperature. The destaining solution was exchanged several times in order to completely destain the SDS-gel. Pictures were taken using a Syngene Gene Genius Bioimaging System.

Loading buffer:	0.5 M Tris, 10% (w/v) glycerol, 2% (w/v) SDS, 0.005% Bromophenol Blue, 5% (v/v) β-mercaptoethanol, pH 6.8
Running Buffer:	25 mM Tris, 250 mM glycine, 0.1 % (w/v) SDS, pH 8.4
Staining Solution:	25% (v/v) propan-2-ol, 10% glacial acetic acid, 0.2% (w/v) Coomassie Brilliant BlueR
Destaining Solution:	5% (v/v) propan-2-ol and 7% (v/v) glacial acetic acid

2.1.3 Transformation of chemically competent *E. coli* with plasmid

Kanamycin sulphate was purchased from Invitrogen, chloramphenicol from Sigma-Aldrich, tetracycline from Merck/Calbiochem, the ingredients for LB-media from Fisher Scientific and agar was purchased from LAB M Ltd. Chemically competent *E. coli* Novablue singles, *E. coli* BL21-DE3, *E. coli* B834-DE3 and *E. coli* Rosetta2-DE3 were purchased from Merck/Novagen. Chemically competent *E. coli* XL10-Gold and *E. coli* BL21-Gold-DE3 were purchased from Agilent Technologies/Stratagene.

Cell genotypes are as follows:

Novablue singles: *endA1 hsdR17* (r_{K12}^{-} m_{K12}^{+}) *supE44 thi-1 recA1 gyrA96 relA1 lac* F′[*proA*$^{+}$*B*$^{+}$ *lacI*^{q}*ZΔM15*::Tn*10*] (Tet^{R})

BL21-DE3: F^{-} *ompT hsdS*$_B$ (r_B^{-} m_B^{-}) *gal dcm* (DE3)

B834-DE3: F^{-} *ompT hsdS*$_B$(r_B^{-} m_B^{-}) *gal dcm met* (DE3)

Rosetta2-DE3: F^{-} *ompT hsdS*$_B$(r_B^{-} m_B^{-}) *gal dcm* (DE3) pRARE*2* (Cam^{R})

XL10-Gold: Tet^R Δ(*mcrA*)*183* Δ(*mcrCB-hsdSMR-mrr*)*173 endA1 supE44 thi-1 recA1 gyrA96 relA1 lac* Hte [F´ *proAB lacI*q*Z*Δ*M15* Tn*10* (Tet^R) Amy Cam^R)
BL21-Gold-DE3: *E. coli* B F– *ompT hsdS*(rB– mB–) *dcm*+ Tet^R *gal* λ(DE3) *endA* Hte)

Chemically competent *E. coli* were thawed on ice and rapidly mixed with plasmid DNA under sterile conditions. The cells were incubated on ice for 30 min and then heat-shocked at 42°C. *E. coli* Novablue singles; *E. coli* BL21-DE3, *E. coli* B834-DE3 and *E. coli* Rosetta2-DE3 strains were heat-shocked for 45 s. *E. coli* XL10-Gold strains were heat-shocked for 30 s and *E. coli* BL21-Gold-DE3 strains were heat-shocked for 20 s. After that, the cells were incubated on ice for 5 min. 1 mL of sterile LB-media was added to *E. coli* BL21-DE3, *E. coli* B834-DE3 and *E. coli* Rosetta2-DE3 cells under sterile conditions and 1 mL of LB+ media was added to *E. coli* XL10-Gold cells. The cell suspension was then incubated at 37° for 60 min.

E. coli Novablue singles, *E. coli* BL21-DE3 and *E. coli* B834-DE3 strains were plated out onto LB-agar containing 30 μg/mL of kanamycin. *E. coli* Rosetta2-DE3 strains were plated out onto LB-agar containing 30 μg mL^{-1} of kanamycin and 34 μg mL^{-1} chloramphenicol. *E. coli* XL10-Gold strains were plated out onto LB-agar containing 30 μg mL^{-1} of kanamycin, 34 μg mL^{-1} chloramphenicol and 15 μg mL^{-1} tetracycline. *E. coli* BL21-Gold-DE3 strains were plated out onto LB-agar containing 30 μg mL^{-1} of kanamycin and 15 μg mL^{-1} tetracycline. Colonies were obtained after incubating the agar plates at 37°C overnight.

LB-media (V= 1 L): 10 g tryptone, 5 g yeast extract, 10 g NaCl, deionised H_2O
LB+ media (V= 1 L): 10 g tryptone, 5 g yeast extract, 10 g NaCl, 12.5 mL 1 M $MgCl_2$, 12.5 mL 1 M $MgSO_4$, 20 mL 20% (w/v) D-glucose, deionised H_2O
LB-agar (V= 1 L): 10 g tryptone, 5 g yeast extract, 10 g NaCl, 15 g agar, deionised H_2O

2.1.4 Transformation of electrocompetent *E. coli* with plasmid

Kanamycin sulphate, SOC media and electrocompetent *E. coli* Top10 (genotype F^- *mcr*A Δ(*mrr-hsd*RMS-*mcr*BC) φ80*lacZ*ΔM15 Δ*lac*X74 *rec*A1 *ara*D139 Δ(*ara-leu*) 7697 *gal*U *gal*K *rps*L (Str^R) *end*A1 *nup*G λ-) cells were purchased from Invitrogen. Electrocompetent *E. coli* BL21-DE3 cells were prepared as in **Section 2.1.5**. The ingredients for LB-media were purchased from Fisher Scientific and agar was purchased from LAB M Ltd. Electrocompetent *E. coli* BL21-DE3 cells were electroporated using a BioRad Gene Pulser electroporation system with pulse controller. Electrocompetent *E. coli* Top10 cells were electroporated using a BioRad *E. coli* Pulser.

Electrocompetent *E. coli* BL21-DE3 were thawed on ice and rapidly mixed with plasmid DNA under sterile conditions. Cells were incubated on ice for 1 min and then transferred to an ice-cold 0.1 cm electroporation cuvette. Electroporation cuvette was tapped firmly to ensure cells were at the bottom of the cuvette and that no bubbles were present. Cells were electroporated in the BioRad Gene Pulser at 2.5 kV with resistance set at 200 Ω and capacitance set to 25 μF. 950 μL of SOC media was then mixed with the cells and transferred to a fresh 15 mL tube under sterile conditions. Cells were incubated at 37°C with shaking at 180 r.p.m for 1 h. Cells were plated out on pre-warmed LB-agar containing 30 μg mL^{-1} of kanamycin. Colonies were obtained after incubating the agar plates at 37°C overnight.

Electrocompetent *E. coli* Top10 cells were thawed on ice and rapidly mixed with plasmid DNA. Cells were incubated on ice for 1 min and then transferred to an ice-cold 0.2 cm electroporation cuvette. Cells were electroporated at 2.5 kV in the *E. coli* Pulser. Cells were mixed with 950 μL SOC media and then transferred to a fresh 15 mL tube under sterile conditions. Cells were incubated at 37°C with shaking at 180 r.p.m for 90 min. Cells were plated out on pre-warmed LB-agar containing 30 μg mL^{-1} of kanamycin. Colonies were obtained after incubating the agar plates at 37°C overnight.

LB-media (V= 1 L): 10 g tryptone, 5 g yeast extract, 10 g NaCl, deionised H_2O
LB-agar (V= 1 L): 10 g tryptone, 5 g yeast extract, 10 g NaCl, 15 g agar, deionised H_2O

2.1.5 Production of electrocompetent *E. coli* cells

Chemically competent *E. coli* BL21-DE3 cells were purchased from Merck/Novagen. Ingredients for LB-media and glycerol were purchased from Fisher. Agar was purchased from LAB M Ltd. Falcon tubes were spun using a Harrier 18/80 centrifuge.

Chemically competent *E. coli* BL21-DE3 cells were spread over an LB-agar plate containing no antibiotics. The plate was incubated at 37°C overnight. One colony was used to inoculate each of two 5 mL starter cultures of LB-media, which were grown at 37°C with shaking at 180 r.p.m overnight. 8 mL of starter culture was then used to inoculate 800 mL of LB-media in a 2 L Erlenmeyer flask. Cells were grown at 37°C and 180 r.p.m until OD_{600} was between 0.7 and 0.9.

400 mL of the cells were transferred to eight chilled 50 mL Falcon tubes and kept on ice for 1 h, the remaining culture was kept in the flask and chilled on ice for 1 h. The cells in the eight Falcon tubes were then spun down by centrifugation at 3850 *g* and 4°C for 10 min. Supernatant was

discarded and the remaining culture was distributed equally between the eight 50 mL Falcon tubes. These were then spun down again at 3850 *g* and 4°C for 10 min.

The cell pellet in each Falcon tube was then resuspended in 5 mL of ice-cold 10% (v/v) glycerol, and the Falcon tubes were then filled to 50 mL with ice-cold 10% (v/v) glycerol. Cells were then spun down at 3850 *g* and 4°C for 10 min.

The cell pellet in each Falcon tube was then resuspended in 5 mL of ice-cold 10% glycerol and cells were then pooled equally between four of the Falcon tubes. These Falcon tubes were then filled up to 50 mL with ice-cold 10% (v/v) glycerol. Cells were then spun down at 3850 *g* and 4°C for 10 min and cell pellets were resuspended with 5 mL of ice-cold 10% (v/v) glycerol, then Falcon tubes were filled up to 50 mL with ice-cold 10% (v/v) glycerol.

Cells were then spun down at 3850 *g* and 4°C for 10 min and cell pellets were resuspended with 5 mL ice-cold 10% (v/v) glycerol and cells were pooled equally into two of the 50 mL Falcon tubes, which were then filled to 50 mL with ice-cold 10% (v/v) glycerol. Cells were then spun down at 3850 *g* and 4°C for 10 min.

Each of the two cell pellets was resuspended in 2.5 mL of ice-cold 10% (v/v) glycerol and dispensed in 100 µL aliquots into pre-chilled 1.5 mL Eppendorf tubes. These tubes were stored at -80°C.

LB-media (V= 1 L): 10 g tryptone, 5 g yeast extract, 10 g NaCl, deionised H_2O
LB-agar (V= 1 L): 10 g tryptone, 5 g yeast extract, 10 g NaCl, 15 g agar, deionised H_2O

2.1.6 Polymerase Chain Reaction (PCR)

KOD hot start DNA polymerase kit was purchased from Merck/Novagen, PfUTurbo hot start DNA polymerase kit was purchased from Agilent Technologies/Stratagene and Phusion hot start II High-fidelity DNA polymerase kit was purchased from New England Biolabs. dNTPs were purchased from Promega. High-purity salt-free primers were synthesized by Eurofins/MWG Biotech (Ebersberg, Germany). PCR cycling using 200 µL thin-walled PCR tubes was carried out with a Techne TC312 thermal cycler and PCR cycling using 500 µL thin-walled PCR tubes was carried out with a Techne TC312 thermal cycler. Gradient PCRs were carried out using an Eppendorf Mastercycler.

The conditions for PCR cycling are given in **Table 2.1**, the compositions of the PCR mixes are shown in **Table 2.2** and the primer sequences are listed in **Table 2.3**.

Table 2.1: Conditions for PCR cycling methods used for the amplification of DNA by PCR.

PCR Cycling	Initial denaturation	Denaturation	Annealing	Extension	Number of Cycles	Final extension
A	96°C, 5 min	96°C, 30 s	55°C, 30 s	72°C, 1 min	35	72°C, 5 min
B	96°C, 5 min	96°C, 30 s	55°C, 30 s	72°C, 90 s	35	72°C, 5 min
C	95°C, 2 min	95°C, 30 s	72°C, 30 s	72°C, 10 min	35	72°C, 15 min
D	95°C, 2 min	95°C, 30 s	52°C, 30 s	72°C, 10 min	25	72°C, 15 min
E	95°C, 2 min	95°C, 30 s	55°C, 30 s	72°C, 90 s	30	72°C, 5 min
F	95°C, 2 min	95°C, 30 s	64°C ± 6°C, 30 s	72°C, 10 min	25	72°C, 15 min
G	98°C, 2 min	98°C, 20 s	None	72°C, 6 min	35	72°C, 10 min
H	95°C, 2 min	95°C, 1 min	55 °C, 1 min	72°C 1.5 min	30	72°C, 10 min
I	95°C, 1 min	95°C, 50 s	60°C, 50 s	68°C 13min	25	N/A

Table 2.2: Composition of PCR mix used for the amplification of DNA by PCR.

PCR mix	V_{total} in µL	$V_{component}$	[Component] in PCR mix
A	50	33 µL H_2O (18.2 Ω· cm) 5 µL 5 x KOD buffer 3 µL 25 mM $MgSO_4$ 5 µL 2 mM (each) dNTPs 1 µL 20 µM forward primer 1 µL 20 µM reverse Primer 1 µL Template DNA 1 µL 1 U $µL^{-1}$ KOD Hot Start DNA polymerase	1 x KOD buffer 1.5 mM $MgSO_4$ 0.2 mM of each dNTP 0.4 µM forward primer 0.4 µM reverse primer 2% (v/v) template DNA 0.02 U $µL^{-1}$ KOD Hot Start DNA polymerase
B	50	28 µL H_2O (18.2 Ω· cm) 5 µL 10 x KOD buffer 3 µL 25 mM $MgSO_4$ 5 µL 2 mM (each) dNTPs 1 µL 20 µM forward primer 1 µL 20 µM reverse Primer 1 µL Template DNA 5 µL ≥99.5% DMSO 1 µL 1 U $µL^{-1}$ KOD Hot Start DNA polymerase	1 x KOD buffer 1.5 mM $MgSO_4$ 0.2 mM of each dNTP 0.4 µM forward primer 0.4 µM reverse primer 2% (v/v) template DNA 10% DMSO 0.02 U $µL^{-1}$ KOD Hot Start DNA polymerase
C	25	15.25 µL H_2O (18.2 Ω· cm) 2.5 µL 10 x PfU Turbo buffer 2.5 µL 2mM (each) dNTPs 0.5 µL 20 µM forward primer 0.5 µL 20 µM reverse primer 2 µL 10 ng $µL^{-1}$ YSBLIC3C-PpLAAO 1.25 µL ≥99.5% DMSO 0.5 µL 2.5 U $µL^{-1}$ PfUTurbo HotStart polymerase	1 x PfU Turbo buffer 0.2 mM of each dNTP 0.4 µM forward primer 0.4 µM reverse primer 0.8 ng $µL^{-1}$ YSBLIC3C-PpLAAO 5% DMSO 0.05 U $µL^{-1}$ PfUTurbo HotStart polymerase
D	25	14.25 µL H_2O (18.2 Ω· cm) 2.5 µL 5 x PfU Turbo buffer 2.5 µL 2mM (each) dNTPs 1 µL 10 µM forward primer 1 µL 10 µM reverse primer 2 µL 10 ng $µL^{-1}$ YSBLIC3C-PpLAAO 1.25 µL ≥99.5% DMSO 0.5 µL 2.5 U $µL^{-1}$ PfUTurbo HotStart polymerase	1 x PfU Turbo buffer 0.2 mM of each dNTP 0.4 µM forward primer 0.4 µM reverse primer 0.8 ng $µL^{-1}$ YSBLIC3C-PpLAAO 5% DMSO 0.05 U $µL^{-1}$ PfUTurbo HotStart polymerase

Table 2.2: Composition of PCR mix used for the amplification of DNA by PCR.

PCR mix	V_{total} in µL	$V_{component}$	[Component] in PCR mix
E	25	14 µL H_2O (18.2 Ω· cm) 2.5 µL 10 x KOD buffer 1.5 µL 25 mM $MgSO_4$ 2.5 µL 2 mM (each) dNTPs 0.5 µL 20 µM forward primer 0.5 µL 20 µM reverse Primer 0.5 µL Template DNA 2.5 µL ≥99.5% DMSO 0.5 µL 1 U μL^{-1} KOD Hot Start DNA polymerase	1 x KOD buffer 1.5 mM $MgSO_4$ 0.2 mM of each dNTP 0.4 µM forward primer 0.4 µM reverse primer 2% (v/v) template DNA 10% DMSO 0.02 U μL^{-1} KOD Hot Start DNA polymerase
F	25	14.25 µL H_2O (18.2 Ω· cm) 2.5 µL 10 x PfU Turbo buffer 2.5 µL 2mM (each) dNTPs 1 µL 10 µM forward primer 1 µL 10 µM reverse primer 2 µL 10 ng μL^{-1} YSBLIC3C-PpLAAO 1.25 µL ≥99.5% DMSO 0.5 µL 2.5 U μL^{-1} PfUTurbo HotStart polymerase	1 x PfU Turbo buffer 0.2 mM of each dNTP 0.4 µM forward primer 0.4 µM reverse primer 0.8 ng μL^{-1} YSBLIC3C-PpLAAO 5% DMSO 0.05 U μL^{-1} PfUTurbo HotStart polymerase
G	20	10.0 µL H_2O (18.2 Ω· cm) 4 µL 5 x Phusion HF buffer 2 µL 2 mM (each) dNTPs 0.5 µL 20 µM forward primer 0.5 µL 20 µM reverse primer 1 µL 10 ng μL^{-1} YSBLIC3C-PpLAAO 1 µL ≥99.5% DMSO 0.8 µL 5 mM $MgSO_4$ 0.2 µL 2 U μL^{-1} Phusion HotStart II polymerase	1 x Phusion HF buffer 0.2 mM (each) dNTPs 0.5 µM forward primer 0.5 µM forward primer 0.5 ng μL^{-1} YSBLIC3C-PpLAAO 5% DMSO 0.2 mM $MgSO_4$ 0.02 U μL^{-1} Phusion HotStart II polymerase
H	25	13.75 µL H_2O (18.2 Ω· cm) 2.5 µL 10 x KOD buffer 2.5 µL 2 mM (each) dNTPs 1.5 µL 25 mM $MgSO_4$ 1 µL 10 µM forward primer 1 µL 10 µM reverse primer 1 µL 10 ng μL^{-1} YSBLIC3C-PpLAAO 1.25 µL ≥99.5% DMSO 0.5 µL 1 U μL^{-1} KOD HotStart DNA polymerase	1 x KOD buffer 1.5 mM $MgSO_4$ 0.2 mM of each dNTP 0.4 µM forward primer 0.4 µM reverse primer 2% (v/v) template DNA 5% DMSO 0.02 U μL^{-1} KOD Hot Start DNA polymerase

Table 2.2: Composition of PCR mix used for the amplification of DNA by PCR.

PCR mix	V_{total} in µL	$V_{component}$	[Component] in PCR mix
I	50	28.5 µL H_2O (18.2 Ω· cm) 5 µL 5 x PfU Turbo buffer 5 µL 2mM (each) dNTPs 1 µL 10 µM forward primer 1 µL 10 µM reverse primer 6 µL 10 ng $µL^{-1}$ YSBLIC3C-PpLAAO 2.5 µL ≥99.5% DMSO 1 µL 2.5 U $µL^{-1}$ PfUTurbo HotStart polymerase	1 x PfU Turbo buffer 0.2 mM of each dNTP 0.2 µM forward primer 0.2 µM reverse primer 1.2 ng $µL^{-1}$ YSBLIC3C-PpLAAO 5% DMSO 0.05 U $µL^{-1}$ PfUTurbo HotStart polymerase
J	20	10.8 µL H_2O (18.2 Ω· cm) 4 µL 5 x Phusion HF buffer 2 µL 2 mM (each) dNTPs 0.5 µL 20 µM forward primer 0.5 µL 20 µM reverse primer 1 µL 10 ng $µL^{-1}$ YSBLIC3C-PpLAAO 1 µL ≥99.5% DMSO 0.2 µL 2 U $µL^{-1}$ Phusion HotStart II polymerase	1 x Phusion HF buffer 0.2 mM (each) dNTPs 0.5 µM forward primer 0.5 µM forward primer 0.5 ng $µL^{-1}$ YSBLIC3C-PpLAAO 5% DMSO 0.02 U $µL^{-1}$ Phusion HotStart II polymerase
K	20	8.8 µL H_2O (18.2 Ω· cm) 4 µL 5 x Phusion HF buffer 4 µL 2 mM (each) dNTPs 0.5 µL 20 µM forward primer 0.5 µL 20 µM reverse primer 1 µL 10 ng $µL^{-1}$ YSBLIC3C-PpLAAO 1 µL ≥99.5% DMSO 0.2 µL 2 U $µL^{-1}$ Phusion HotStart II polymerase	1 x Phusion HF buffer 0.4 mM (each) dNTPs 0.5 µM forward primer 0.5 µM forward primer 0.5 ng $µL^{-1}$ YSBLIC3C-PpLAAO 5% DMSO 0.02 U $µL^{-1}$ Phusion HotStart II polymerase
L	50	18 µL H_2O (18.2 Ω· cm) 5 µL 10 x Mutazyme® II Reaction Buffer 23 µL 95 ng $µL^{-1}$ pET-YSBLIC3C-PpLAAO 1 µL 10 mM (each) dNTP mix 1 µL 20 µM forward primer 1 µL 20 µM reverse primer 1 µL 2.5 U $µL^{-1}$ Mutazyme® II DNA polymerase	1 x Mutazyme® II Reaction Buffer 43.7 ng $µL^{-1}$ pET-YSBLIC3C-PpLAAO 0.2 mM of each dNTP 0.4 µM forward primer 0.4 µM reverse primer 0.05 U $µL^{-1}$ Mutazyme® II DNA polymerase
M	50	25 µL 2 x EZClone enzyme mix 0.5 µL 95 ng $µL^{-1}$ pET-YSBLIC3C-PpLAAO 500 ng megaprimer 3 µL EZclone solution H_2O (18.2 Ω· cm) to 50 µL	1 x EZClone enzyme mix 47.5 ng $µL^{-1}$ pET-YSBLIC3C-PpLAAO 10 ng $µL^{-1}$ megaprimer 6% (v/v) EZClone solution

Table 2.3: Sequences of primers used for the amplification of DNA by PCR.

Primer name/ Purification method	Primer sequence (5' to 3')
AsAAO-for/ HPSF	CCAGGGACCAGCAATGCAGCACAGGGAATTTACAGGCTGTATTCATAC
AsAAO-rev/ HPSF	GAGGAGAAGGCGCGTTATTATCGAGGAGCGGTAGAGCCAGCAAAGTG
BaAO-for/ HPSF	CCAGGGACCAGCAATGATGCAGCCATTAACGATGGAAAGAATGCTCC
BaAO-rev/ HPSF	GAGGAGAAGGCGCGTTATCACTTTTCGTTTACTTCATGAGCAACTCG
BsGO-for/ HPSF	CCAGGGACCAGCAATGAAAAGGCATTATGAAGCAGTGGTGATTGGAGG
BsGO-rev/ HPSF	GAGGAGAAGGCGCGTTATCATATCTGAACCGCCTCCTTGCGATCAATTC
NfOR-for/ HPSF	CCAGGGACCAGCAATGGTGGTGGACAGATCGGTGGATGTCGTC
NfOR-rev/ HPSF	GAGGAGAAGGCGCGTTATCACCGGAGGGCGGACGGGCTC
T7	TAATACGACTCACTATAGGG
T7-term	TATGCTAGTTATTGCTCAGCGGT
Q242A-for /HPLC	GGCGAACCTGGAATTCAACGCGTTCCACCCGACCT
Q242A-rev /HPLC	AGGTCGGGTGGAACGCGTTGAATTCCAGGTTCGCC
H244A-for /HPLC	TGGAATTCAACCAGTTCGCCCCGACCTGCCTGTATC
H244A-rev /HPLC	GATACAGGCAGGTCGGGGCGAACTGGTTGAATTCCA
P245A-for /HPLC	TTCAACCAGTTCCACGCGACCTGCCTGTATC
P245A-rev /HPLC	GATACAGGCAGGTCGCGTGGAACTGGTTGAA
L257A-for /HPLC	CAGGCCAAGAGCTTCGCGATCACCGAAGCCCT
L257A-rev /HPLC	AGGGCTTCGGTGATCGCGAAGCTCTTGGCCTG
T259A-for /HPLC	GAGCTTCCTGATCGCCGAAGCCCTGCG
T259A-rev /HPLC	CGCAGGGCTTCGGCGATCAGGAAGCTC
E260A-for /HPLC	TCCTGATCACCGCAGCCCTGCGCGG
E260A-rev /HPLC	CCGCGCAGGGCTGCGGTGATCAGGA
R290A-for /HPLC	AAGAGCTGGCCCCAGCGGACATCGTGGC
R290A-rev /HPLC	GCCACGATGTCCGCTGGGGCCAGCTCTT
V293A-for /HPLC	ACGGGACATCGCGGCCCGCGCCA
V293A-rev /HPLC	TGGCGCGGGCCGCGATGTCCCGT
H351A-for /HPLC	GGTGCCTGCGGCGGCTTACACCTGCGGC
H351A-rev /HPLC	GCCGCAGGTGTAAGCCGCCGCAGGCACC
Y352A-for /HPLC	TGCCTGCGGCGCATGCCACCTGCGGCGG
Y352A-rev /HPLC	CCGCCGCAGGTGGCATGCGCCGCAGGCA
R386A-for /HPLC	GCACGGCGCCAACGCCATGGCCAGCAAC
R386A-rev /HPLC	GTTGCTGGCCATGGCGTTGGCGCCGTGC
S389A-for /HPLC	CCAACCGCATGGCCGCCAACTCGCTGCTGG
S389A-rev /HPLC	CCAGCAGCGAGTTGGCGGCCATGCGGTTGG
S391A-for /HPLC	GCATGGCCAGCAACGCGCTGCTGGAATGT
S391A-rev /HPLC	ACATTCCAGCAGCGCGTTGCTGGCCATGC
PpLAAO-for/ HPSF	CCAGGGACCAGCAATGAGCCAACAATTCCAACATGATGTCCTGGTG
PpLAAO-rev/ HPSF	GAGGAGAAGGCGCGTTATCAGAGCGGGTTAAGGATGGTGTCCTTG
PNDTA-for/ HPLC	CGGTGGTGCCTGCGGCGNDTNDTACCTGCGGCGGGGTGAT
PNDTA-rev/ HPLC	ATCACCCCGCCGCAGGTAHNAHNCGCCGCAGGCACCACCG
PNDTB-for/ HPLC	ACCCACGCGAAGAGCTGGCCCCANDTGACATCNDTGCCCGCGCCATC
PNDTB-rev/ HPLC	GATGGCGCGGGCAHNGATGTCAHNTGGGGCCAGCTCTTCGCGTGGGT
PNDTC-for/ HPLC	CCTGCACGGCGCCAACNDTATGGCCNDTAACNDTCTGCTGGAATGTTTTG
PNDTC-rev/ HPLC	CAAAACATTCCAGCAGAHNGTTAHNGGCCATAHNGTTGGCGCCGTGCAGG

Table 2.3: Sequences of primers used for the amplification of DNA by PCR.

Primer name/ Purification method	Primer sequence (5' to 3')
PNDTD-for/ HPLC	GGCGAACCTGGAATTCAACNDTTTCNDTNDTACCTGCCTGTATCACCCAC
PNDTD-rev/ HPLC	GTGGGTGATACAGGCAGGTAHNAHNGAAAHNGTTGAATTCCAGGTTCGCC
PNDTE-for/ HPLC	CCCACAGGCCAAGAGCTTCNDTATCNDTNDTGCCCTGCGCGGCGAGGGCG
PekAsAAO-for/ HPSF	GCAAGTGTGGATCCAAAGGAGATATAGATATATACCATGGGCAGCAGC
PekAsAAO-rev/ HPSF	TGTGATAAGAATTCTTATTATCGAGGAGCGGTAGAGCCAGCAAAGTGAAT
PekBaAO-for/ HPSF	GCAAGTGTGGATCCAAAGGAGATATAGATATATACCATGGGCAGCAGC
PekBaAO-rev/ HPSF	TTATCAGAGGTACCTTATCACTTTTCGTTTACTTCATGAGCAACTCGAAT
PekNfOR-for/ HPSF	GCAAGTGTGGATCCAAAGGAGATATAGATATATACCATGGGCAGCAGC
PekNfOR-rev/ HPSF	TCTGATAAGAATTCTTATCACCGGAGGGCGGACGGGCTCGCGGCGTCG

2.2 Generation of target oxidases

As three of the seven prokaryotic oxidases (PpLAAO, RoLAAO and SLAAO) within the first fifteen BLAST results of an L-amino acid oxidase from *Synechococcus* sp. strain ATCC 27144 (**Table 3.1**) had been cloned previously by Gideon Grogan, The AsAAO, BaAO, BsGO and NfOR oxidases were generated by cloning the genes in the pET-YSBLIC-3C vector with ligation independent cloning. This section describes the amplification of four genes with polymerase chain reaction, cloning of the amplified genes, and analysis of the correct nucleotide sequence and overexpression of all seven target genes in *E. coli*.

2.2.1 PCR amplification of four target genes

The AsAAO, BaAO, BsGO and NfOR genes were amplified with PCR as in **Section 2.1**. The PCRs were separated with 1% agarose gel electrophoresis and purified using Sigma Aldrich's GenElute Gel Extraction kit. Each PCR product was eluted with 50 µL of H_2O (18.2 Ω· cm) and its concentration was determined using the dsDNA function of an Eppendorf Biophotometer, with an absorbance of 0.1 set equal to DNA concentration of 50 ng μL^{-1}. The PCR products were stored at -20°C.

The PCR methods and template DNA used are listed in **Table 2.4**, the conditions for the PCR cycling are given in **Table 2.1**, the composition of the PCR mix is shown in **Table 2.2** and the primer sequences are listed in **Table 2.3**.

Table 2.4: PCR methods, primers and template DNA used for the amplification of target genes (Please see **Table 2.1** for PCR cycling, **Table 2.2** for PCR mix and **Table 2.3** for primer sequences).

Gene name	PCR method	Primers	Template DNA
AsAAO	PCR mix A + PCR cycling A	AsAAO-for, AsAAO-rev	10 ng μL^{-1} *Anabaena* genomic DNA
BaAO	PCR mix A + PCR cycling A	BaAO-for, BaAO-rev	35 ng μL^{-1} Genomified *Bacillus anthracis* genomic DNA
BsGO	PCR mix B + PCR cycling B	BsGO-for, BsGO-rev	10 ng μL^{-1} *Bacillus subtilis* genomic DNA
NfOR	PCR mix B + PCR cycling B	NfOR-for, NfOR-rev	5 ng μL^{-1} *Nocardia farcinica* genomic DNA

2.2.2 Ligation Independent Cloning (LIC)

Ligation independent cloning was used to ligate the PCR products of target genes AsAAO, BaAO, BsGO and NfOR with a modified pET-28a vector, pET-YSBLIC-3C. LIC-qualified T4-DNA polymerase and buffer for the T4-DNA polymerase were purchased from Merck/Novagen. dATP and dTTP were purchased from Bioline. DTT was purchased from Melford and EDTA was purchased from Fisher Scientific. *BseRI* and NEBuffer 4 were purchased from New England Biolabs. The concentration of DNA was determined using an Eppendorf Biophotometer.

9 µg of circular pET-YSBLIC-3C was linearised using the Plasmid Linearisation mix, which was incubated at 37°C for 3 h. Linearised vector was separated using 1% agarose gel electrophoresis and purified using Sigma Aldrich's GenElute Gel Extraction kit. Vector was eluted using 50 µL of H_2O (18.2 Ω· cm), the concentration after extraction was 44 ng μL^{-1}.

In order to generate "sticky" single stranded overhangs, 2.2 µg of linear pET-YSBLIC-3C vector and 0.2 pmol of each PCR product were treated with T4-DNA polymerase using the Vector T4 polymerase mix and the Gene T4 polymerase mix, respectively. Vector and Gene T4 polymerase mixes were incubated at 22°C for 30 min, followed by incubation at 75°C for 20 min. The vector was cleaned up using Sigma Aldrich's GenElute PCR Clean-up kit, and eluted using 50 µL of H_2O (18.2 Ω· cm). The concentration after elution was 34 ng μL^{-1}.

2.5 µL of the gene PCR product and 1.5 µL of purified vector were mixed and incubated at room temperature for 20 min. 1.5 µL of 25 mM EDTA was added and the reaction was incubated at room temperature for another 15 min. 5.5 µL of the reaction was used to transform 25 µL of chemically competent *E. coli* Novablue Singles cells using heat shock.

Transformed colonies were used to inoculate 5 mL of LB-media containing 30 μg mL^{-1} kanamycin. These starter cultures were incubated at 37°C and shaking at 180 r.p.m overnight. The following day, the starter cultures were spun down at 16,000 *g* in an Eppendorf 5415 C centrifuge. Mutant plasmids were isolated using Sigma Aldrich's GenElute plasmid Miniprep kit, each plasmid was eluted using 100 μL of H_2O (18.2 Ω· cm) and stored at -20°C. Successful cloning of the genes into the pET-YSBLIC-3C vector was confirmed using restriction analysis and nucleotide sequencing.

Plasmid Linearisation mix:	1 x NEBuffer 4, 50 ng μL^{-1} pET-YSBLIC-3C, 0.2 U μL^{-1} *BseRI*
Vector T4 polymerase mix:	1 x T4 polymerase buffer, 22 ng μL^{-1} linear pET-YSBLIC-3C, 2.5 mM dTTP, 5 mM DTT, 0.05 U μL^{-1} T4-DNA polymerase
Gene T4 polymerase mix:	1 x T4 polymerase buffer, 0.01 pmol μL^{-1} gene PCR product, 2.5 mM dATP, 5 mM DTT, 0.05 U μL^{-1} T4-DNA polymerase
LB-media (V= 1 L):	10 g tryptone, 5 g yeast extract, 10 g NaCl, H_2O (18.2 Ω· cm)

2.2.3 Restriction analysis of the plasmids

To confirm the cloning of the genes in the pET-YSBLIC-3C vector, the plasmids encoding AsAAO, BaAO and NfOR were treated with the restriction endonucleases *NdeI* and *NcoI* and the plasmids encoding BsGO were treated with the restriction endonucleases *SacI* and *NcoI*. The restriction endonucleases and the NEBuffer 4 were purchased from New England Biolabs.

500 ng of each purified plasmid encoding AsAAO, BaAO or NfOR was treated using the *NdeI/NcoI* Restriction mix. 500 ng of each purified plasmid encoding BsGO was treated using the *SacI/NcoI* Restriction mix. Restriction mixes were mixed on ice, then incubated at 37°C for 3 h. Reactions were analysed using 1% agarose gel electrophoresis.

NdeI/NcoI Restriction mix (v= 10 μL):	1 x NEBuffer 4, 50 ng μL^{-1} plasmid DNA, 1 U μL^{-1} *NdeI*, 1 U μL^{-1} *NcoI*
SacI/NcoI Restriction mix (v= 10 μL):	1 x NEBuffer 4, 50 ng μL^{-1} plasmid DNA, 1 U μL^{-1} *SacI*, 1 U μL^{-1} *NcoI*

2.2.4 Analysis of recombinant genes by nucleotide sequencing

The correct nucleotide sequence of the plasmids encoding AsAAO, BaAO, BsGO, NfOR and PpLAAO was confirmed by nucleotide sequencing. The T7 and T7-term primers (**Table 2.3**) were used as sequencing primers. The sequencing reactions were carried out by the York University

Genomics group using an automated form of the Sanger sequencing method, where a PCR reaction is run in the presence of both dNTP and a smaller proportion of dideoxyNTPs (ddNTPs). The ddNTPs lack the 3' OH group necessary for the formation of phosphodiester bonds between nucleotides, causing the chains to terminate at any point if they incorporate a ddNTP. The different size chains are then separated by capillary tube electrophoresis, and as each type of ddNTP is labelled with a different fluorescent dye, the base of the ddNTP that caused the chain to terminated at each specific point in the sequence can be determined by recording the dye fluorescence of each DNA chain, which results in a chromatogram showing the peaks of each wavelength of fluorescence at specific points in the sequence (http://www.nature.com/scitable/topicpage/dna-sequencing-technologies-690).

The sequence chromatograms were analysed with the program Chromas lite, version 2.01 from Technelysium (free software). All five of the recombinant genes were found to be free of undesired mutations.

2.2.5 Overexpression analysis of target enzymes

The plasmids pET-YSBLIC-3C-AsAAO, pET-YSBLIC-3C-BaAO, pET-YSBLIC-3C-BsGO, pET-YSBLIC-3C-NfOR, pET-YSBLIC-3C-PpLAAO, pET-YSBLIC-3C-RoLAAO and pET-YSBLIC-3C-SLAAO, were used to overexpress the seven target genes in *E. coli* BL21-DE3, *E. coli* B834-DE3 and *E. coli* Rosetta 2-DE3 chemically competent cells. Negative controls using non recombinant pET-YSBLIC-3C plasmid were also carried out. AEBSF and IPTG were purchased from Melford. OD_{600} was measured using an Eppendorf Biophotometer.

Transformed *E. coli* BL21-DE3 and *E. coli* B834-DE3 cells were grown using 30 μg mL^{-1} kanamycin as the appropriate antibiotic. Transformed *E. coli* Rosetta 2-DE3 cells were grown using 30 μg mL^{-1} kanamycin and 34 μg mL^{-1} chloramphenicol as the appropriate antibiotics.

1 μL of recombinant plasmid was used to transform 25 μL of chemically competent cells using heat shock. Then 5 mL of sterile LB-media containing the appropriate antibiotics were inoculated with a single transformed colony. This starter culture was grown overnight at 37°C with shaking at 180 r.p.m. The next day three 5 mL aliquots of sterile LB-media containing the appropriate antibiotics were each inoculated with 100 μL of starter culture. The cells were incubated at 37°C with shaking at 180 r.p.m. Overexpression was induced with 1 mM IPTG when OD_{600} reach 0.5. One cell culture was incubated at 37°C for 3 h with shaking at 180 r.p.m, another cell cultures was incubated at 30°C for 5 h with shaking at 180 r.p.m and the final cell culture was incubated at 16°C overnight with shaking at 180 r.p.m.

The cells were harvested by centrifugation for 2 min at 16,000 *g* using an Eppendorf 5415 C centrifuge. The supernatant was discarded and the cell pellet was resuspended in 500 µL H_2O (18.2 Ω· cm). The cell suspension was sonicated on ice for 30 s at 15 microns. Cell debris was pulled down by spinning at 16,000 *g* for 2 min using an Eppendorf 5415 C centrifuge. The soluble supernatant was separated from the insoluble cell pellet. The cell pellet was then resuspended in 500 µL buffer 1. The soluble and insoluble fractions were analysed by SDS-PAGE.

LB-media (V= 1 L): 10 g tryptone, 5 g yeast extract, 10 g NaCl, H_2O (18.2 Ω· cm)
Buffer 1: 50 mM Tris/HCl, 300 mM NaCl, 20 µM AEBSF, pH 7.0

2.2.6 Overexpression of target enzymes for assay analysis

The plasmids pET-YSBLIC-3C-AsAAO, pET-YSBLIC-3C-BaAO, pET-YSBLIC-3C-BsGO and pET-YSBLIC-3C-PpLAAO were used to overexpress their respective target genes in *E. coli* BL21-DE3 chemically competent cells. The pET-YSBLIC-3C-NfOR plasmid was used to overexpress the NfOR protein in *E. coli* B834-DE3 chemically competent cells and the pET-YSBLIC-3C-SLAAO plasmid was used to overexpress the SLAAO protein in *E. coli* Rosetta 2-DE3 chemically competent cells. Non recombinant pET-YSBLIC-3C plasmid was also used to transform *E. coli* BL21-DE3 chemically competent cells, for use as negative controls. IPTG was purchased from Melford. OD_{600} and protein concentration were measured using an Eppendorf Biophotometer.

Transformed *E. coli* BL21-DE3 and *E. coli* B834-DE3 cells were grown using 30 µg mL^{-1} kanamycin as the appropriate antibiotic. Transformed *E. coli* Rosetta 2-DE3 cells were grown using 30 µg mL^{-1} kanamycin and 34 µg mL^{-1} chloramphenicol as the appropriate antibiotics.

1 µL of recombinant plasmid was used to transform 25 µL of chemically competent cells using heat shock. Then 5 mL of sterile LB-media containing the appropriate antibiotics was inoculated with a single transformed colony. This starter culture was grown overnight at 37°C with shaking at 180 r.p.m. For each starter culture a 10 mL aliquot of sterile LB-media containing the appropriate antibiotics was inoculated with 200 µL of starter culture. The cells were incubated at 37°C with shaking at 180 r.p.m. Overexpression was induced with 1 mM IPTG when OD_{600} reach 0.5. Cell cultures transformed with non recombinant pET-YSBLIC-3C, pET-YSBLIC-3C-BsGO, pET-YSBLIC-3C-NfOR and pET-YSBLIC-3C-SLAAO plasmids were left to grown at 37°C with shaking at 180 r.p.m for 3 h. Cell cultures transformed with pET-YSBLIC-3C-AsAAO, pET-YSBLIC-3C-BaAO and pET-YSBLIC-3C-PpLAAO plasmids were left to grown at 16°C with shaking at 180 r.p.m overnight.

The cells cultures were split into two 5 mL cultures and then harvested by centrifugation for 2 min at 16,000 *g* using an Eppendorf 5415 C centrifuge. The supernatant was discarded and the cell pellets were resuspended in 500 µL H_2O (18.2 Ω· cm). One cell suspension for each 10 mL culture was diluted to OD_{600} 1.5 with H_2O (18.2 Ω· cm) and stored at -20°C.

The remaining cell suspension was sonicated on ice for 30 s at 15 microns. Cell debris was pulled down by spinning at 16,000 *g* for 2 min using an Eppendorf 5415 C centrifuge. The soluble supernatant was separated from the insoluble cell pellet. The cell pellet was then resuspended in 500 µL H_2O (18.2 Ω· cm). Protein concentration was estimated using an Eppendorf Biophotometer and each soluble supernatant was diluted to a protein concentration of 2 mg mL^{-1} and stored at -20°C.

LB-media (V= 1 L): 10 g tryptone, 5 g yeast extract, 10 g NaCl, H_2O (18.2 Ω· cm)

2.2.7 Assay of target enzyme substrates

In order to determine the natural substrates of the seven target enzymes, a liquid phase horseradish peroxidase (HRP)-based assay was used to analyse the activity of the target enzymes against the twenty natural amino acids and the amines amylamine, phenylethylamine and AMBA.

TBHBA was purchased from Alfa Aesar. 4-AAP, HRP, L-alanine, L-arginine, L-asparagine, L-aspartate, L-glutamate, L-glutamine, glycine, L-Isoleucine, L-leucine, L-lysine, L-methionine, L-proline, L-serine, L-threonine, L-tryptophan, L-tyrosine, amylamine, phenylethylamine and AMBA were purchased from Sigma-Aldrich. L-cysteine, L-histidine, L-phenylalanine and L-valine were purchased from Sigma/Fluka. KH_2PO_4 and K_2HPO_4 were purchased from Fisher, 96-well flat bottomed plates were purchased from Corning Costar. A_{510} was measured on a BMG Labtech PolarStar Optima plate reader.

Reactions were repeated twice with each substrate, and two reactions using an assay solution with H_2O (18.2 Ω· cm) as substrate were used as control reactions. 10 µL of either 2 mg mL^{-1} soluble protein fraction or induced cells with OD_{600} of 1.5 were added to 190 µL of assay solution in an Eppendorf tube. Reactions were left to develop for 1 h before being spun down at 16,000 *g* for 1 min in an Eppendorf 5415 C centrifuge to remove any protein precipitant or cellular debris. The assay solution was then transferred to a 96 well flat-bottomed plate and A_{510} was measured. The mean absorbance of the control reactions was subtracted from all other absorbance readings before mean absorbance for each reaction was calculated. Assays were run with the substrate layout

shown in **Fig. 2.1**, positive control wells contained soluble protein fraction from cells transformed with pET-YSBLIC-3C-SLAAO plasmid and L-arginine as the substrate.

	1	2 3	4 5	6 7	8 9	10 11	12
A		-	-	-	-	-	
B		Glycine	L-threonine	L-methionine	L-tryptophan	Positive control	
C		L-asparagine	L-aspartate	L-serine	L-tyrosine	-	
D	-	L-histidine	L-valine	L-leucine	Amylamine	-	-
E		L-arginine	L-phenylalanine	L-glutamine	Phenylethylamine	-	
F		L-proline	L-isoleucine	L-cysteine	AMBA	-	
G		L-lysine	L-alanine	L-glutamate	H_2O (18.2 Ω· cm)	-	
H		-	-	-	-	-	

Fig. 2.1 Layout of substrates screened using the soluble HRP-based assay in a 96-well plate format. Wells marked with a dash were empty.

2 x Reaction Buffer (V= 50 mL): 100 mM KH_2PO_4/K_2HPO_4, 20 mg (TBHBA), 15 mg 4-AAP, pH 7.5

Assay solution: 1 x Reaction Buffer, 25 µg mL-1 HRP, 10 mM substrate

2.2.8 Effects of AIM and L-glutamate and L-arginine on solubility of AsAAO and BaAO

The ingredients for LB-media were purchased from Fisher Scientific, Kanamycin sulphate was purchased from Invitrogen, IPTG was purchased from Melford. Metal solution for Auto Induction Media[111] was prepared by previous YSBL staff.

2 µL of pET-YSBLIC-3C-AsAAO and pET-YSBLIC-3C-BaAO were each used to transform 50 µL of *E. coli* BL21-DE3 competent cells using heatshock. One colony of *E. coli* BL21-DE3-AsAAO and *E. coli* BL21-DE3-BaAO were each used to inoculate 5 mL of LB-media containing 30 µg ml^{-1} of kanamycin. These starter cultures were grown overnight at 37°C with shaking at 180 r.p.m. For each starter culture, two 10 mL cultures of LB-media containing 30 µg mL^{-1} kanamycin were each inoculated with 200 µL of starter culture. Cells were grown at 37°C with shaking at 180 r.p.m. Overexpression was induced with 1 mM IPTG when OD_{600} reached 0.5. Cells were left to express protein at 16°C with shaking at 180 r.p.m overnight.

For each starter culture, two 10 mL cultures of Auto Induction Media containing 30 µg mL^{-1} kanamycin were each inoculated with 200 µL of starter culture. These cultures were grown at 30°C with shaking at 180 r.p.m for 24 h.

Cells were harvested by centrifugation at 16,000 *g* for 1 min in an Eppendorf 5415 C centrifuge. One pellet from each media type was resuspended in 1 mL of buffer 1, and the other pellet was resuspended in 1 mL of buffer 2. Cells were lysed by sonication for 30 s and cell debris was spun down at 13,700 *g* for 5 min in an Eppendorf 5415 C centrifuge. Soluble protein supernatant was transferred to a fresh tube and insoluble cell pellets were resuspended in the same buffer as previously. Insoluble and soluble protein fractions were analysed by 12% SDS-PAGE.

LB-media (V= 1 L):	10 g tryptone, 5 g yeast extract, 10 g NaCl, H_2O (18.2 Ω· cm)
Auto induction media:	100 mM $MgSO_4$, 1 x metal mix, 1 x 5052 solution, 1 x NPS solution, 92.5 % (v/v) ZY media.
1000 x Metal mix:	50 mM $FeCl_3$-$6H_2O$ (prepared in 0.1 M HCl), 20 mM $CaCl_2$, 10 mM $MnCl_2$, 10 mM $ZnSO_4$-$7H_2O$, 2 mM $CoCl_2$-$6H_2O$, 4 mM $CuCl_2$-$2H_2O$, 2 mM $NiCl_2$-$6H_2O$, 2 mM Na_2MoO_4-$5H_2O$, 2 mM Na_2SeO_3-$5H_2O$, 2 mM H_3BO_3
50 x 5052 solution (V = 1 L):	250 g glycerol, 25 g glucose, 100 g a-lactose, H_2O (18.2 Ω· cm)
20 x NPS solution (V = 1 L):	6.6 g $(NH_4)_2SO_4$, 13.6 g KH_2PO_4, 142 g Na_2HPO_4, H_2O (18.2 Ω· cm), pH 6.75
ZY media (V = 1 L):	10 g tryptone, 5 g yeast extract, H_2O (18.2 Ω· cm)
Buffer 1:	50 mM Tris/HCl, 300 mM NaCl, 20 µM AEBSF, pH 7.0
Buffer 2:	50 mM Tris/HCl, 300 mM NaCl, 20 µM AEBSF, 50 mM L-glutamate, 50 mM L-arginine, pH 7.0

2.2.9 Effects of oxygen availability on solubility of AsAAO and BaAO

The ingredients for LB-media were purchased from Fisher Scientific, Kanamycin sulphate was purchased from Invitrogen, AEBSF and IPTG were purchased from Melford.

2 µL of pET-YSBLIC-3C-AsAAO and pET-YSBLIC-3C-BaAO were each used to transform 50 µL of *E. coli* BL21-DE3 competent cells using heatshock. Six colonies of *E. coli* BL21-DE3-AsAAO and *E. coli* BL21-DE3-BaAO were each used to inoculate 5 mL of LB-media containing 30 µg ml^{-1} of kanamycin. These starter cultures were grown overnight at 37°C with shaking at 180 r.p.m.

For each cell strain, three LB-media cultures of different volumes (0.5 L, 1.0 L, 1.5 L) containing 30 µg mL^{-1} kanamycin were prepared in 2 L Erlenmeyer flasks. These cultures were inoculated

with 1 starter culture per 0.5 L of culture and incubated at 37°C. Gene overexpression was induced using 1 mM IPTG once OD_{600} reached 0.5 and cells were left to grow at 16°C overnight.

10 mL of each culture's cells was harvested by centrifugation for 1 min at 16,000 *g* in an Eppendorf 5415 C centrifuge. Cell pellets were resuspended in 1 mL of buffer 1 and sonicated for 30 s at 15 microns. Insoluble material was separated by centrifugation for 5 min at 13,700 *g* in an Eppendorf 5415 C centrifuge. Soluble supernatant was transferred to a fresh tube and the insoluble pellet was resuspended in 1 mL buffer 1. Insoluble and soluble protein fractions were analysed by 12% SDS-PAGE.

LB-media (V= 1 L):	10 g tryptone, 5 g yeast extract, 10 g NaCl, H_2O (18.2 Ω· cm)
Buffer 1:	50 mM Tris/HCl, 300 mM NaCl, 20 µM AEBSF, pH 7.0

2.2.10 Solubility screen of BaAO

The ingredients for LB-media were purchased from Fisher Scientific, Kanamycin sulphate was purchased from Invitrogen, AEBSF and IPTG were purchased from Melford. Lindwall solubility screen conditions[112] were prepared by previous YSBL staff.

2 µL of pET-YSBLIC-3C-BaAO was used to transform 50 µL of *E. coli* BL21-DE3 competent cells using heat-shock. One colony of *E. coli* BL21-DE3-BaAO was used to inoculate 5 mL of LB-media containing 30 µg ml^{-1} of kanamycin. This starter culture was grown overnight at 37°C with shaking at 180 r.p.m. 1.2 mL of starter culture was used to inoculate 62 mL of LB-media containing 30 µg mL^{-1} kanamycin. Cells were grown at 37°C with shaking at 180 r.p.m. Overexpression was induced with 1 mM IPTG when OD_{600} reached 0.5. Cells were left to express protein at 16°C with shaking at 180 r.p.m overnight.

The culture was split into thirty two 2 mL aliquots, which were harvested by centrifugation at 16,000 *g* for 1 min in an Eppendorf 5415 C centrifuge. 200 µL of each of the thirty solubilisation screen conditions suggested by Lindwall *et al.*[112] was used to resuspend a single cell pellet, and 200 µL of H_2O (18.2 Ω· cm) was used to resuspend the final cell pellet as a control. Cells were sonicated for 20 s at 15 microns and then spun down at 13,700 *g* for 5 min in an Eppendorf 5415 C centrifuge to remove cell debris. Soluble supernatant was transferred to a fresh tube and the insoluble cell pellet from the pellet resuspended in H_2O was resuspended in 200 µL H_2O (18.2 Ω· cm). This insoluble and the soluble samples were analysed by 12% SDS-PAGE.

To determine the effectiveness of the solubilisation screen conditions 4 and 15 at higher volumes of culture, 4 colonies of *E. coli* BL21-DE3-BaAO were each used to inoculate 5 mL of LB-media containing 30 μg ml^{-1} of kanamycin. These starter cultures were grown overnight at 37°C with shaking at 180 r.p.m. Each 5 mL starter culture was used to inoculate 500 mL of LB-media containing 30 μg mL^{-1} kanamycin. Cells were grown at 37°C with shaking at 180 r.p.m. Overexpression was induced with 1 mM IPTG when OD_{600} reached 0.5. Cells were left to express protein at 16°C with shaking at 180 r.p.m overnight.

Cells were spun down for 15 min at 5,100 *g* using the GS3 rotor of a RC-5B Sorvall Centrifuge. 50 mL of solubilisation screen condition 4, 50 mL of solubilisation screen condition 15, 50 mL of buffer 1 and 50 mL of H_2O (18.2 Ω· cm) were each used to resuspend one cell pellet. Cells were lysed by sonication and cell debris was spun down at 26,900 *g* for 15 min in the SS34 rotor of a RC-5B Sorvall Centrifuge. Soluble supernatant was transferred to a fresh tube and insoluble cell pellet was resuspended in the same buffer as previously. Insoluble and soluble samples were analysed by 12% SDS-PAGE.

LB-media (V= 1 L): 10 g tryptone, 5 g yeast extract, 10 g NaCl, H_2O (18.2 Ω· cm)

Buffer 1: 50 mM Tris/HCl, 300 mM NaCl, 20 μM AEBSF, pH 7.0

Solubility Screen conditions:[112]

1: 100 mM Tris, 10 % glycerol, pH 7.6

2: 100 mM Tris, 50 mM LiCl, pH 7.6

3: 100 mM HEPES, 50 mM $(NH_4)_2SO_4$, 10% glycerol, pH 7.0

4: 100 mM HEPES, 100 mM KCl, pH 7.0

5: 100 mM Tris, 50 mM NaCl, 10% isopropanol, pH 8.2

6: 100 mM K_2HPO_4/KH_2PO_4, 50 mM $(NH_4)_2SO_4$, 1% Triton X-100, pH 6.0

7: 100 mM triethanolamine, 100 mM KCl, 10 mM DTT, pH 8.5

8: 100 mM Tris, 100 mM sodium glutamate, 10 mM DTT, pH 8.2

9: 250 mM K_2HPO_4/KH_2PO_4, 0.1% CHAPS, pH 6.0

10: 100 mM triethanolamine, 50 mM LiCl, 5 mM EDTA, pH 8.5

11: 100 mM sodium acetate, 100 mM glutamine, 10 mM DTT, pH 5.5

12: 100 mM sodium acetate, 100 mM KCl, 0.1% *n*-octyl-β-D-glucoside, pH 5.5

13: 100 mM HEPES, 1 M $MgSO_4$, pH 7.0

14: 100 mM HEPES, 50 mM LiCl, 0.1% CHAPS, pH 7.0

15: 100 mM K_2HPO_4/KH_2PO_4, 2.5 mM ZnCl, pH 4.3

16: 100 mM Tris, 50 mM NaCl, 5 mM calcium acetate, pH 7.6

17: 100 mM triethanolamine, 50 mM $(NH_4)_2SO_4$, 10 mM $MgSO_4$, pH 8.5

18: 100 mM Tris, 100 mM KCl, 2 mM EDTA, 1% Triton X-100, pH 8.2

19: 100 mM sodium acetate, 1 M $MgSO_4$, pH 5.5

20: 100 mM Tris, 2 M NaCl, 0.1% *n*-octyl-β-D-glucoside, pH 7.6

21: 100 mM Tris, 1 M $(NH_4)_2SO_4$, 10 mM DTT, pH 8.2

22: 100 mM sodium acetate, 50 mM LiCl, 5 mM calcium acetate, pH 5.5

23: 100 mM HEPES, 100 mM sodium glutamate, 5 mM DTT, pH 7.0

24: 100 mM triethanolamine, 100 mM sodium glutamate, 0.02% *n*-octyl-β-D-glucoside, 10% glycerol, pH 8.5

25: 100 mM Tris, 50 mM NaCl, 100 mM urea, pH 8.2

26: 100 mM triethanolamine, 100 mM KCl, 0.05% dextran sulfate, pH 6.0

27: 100 mM K_2HPO_4/KH_2PO_4, 50 mM $(NH_4)_2SO_4$, 0.05% dextran sulfate, pH 6.0

28: 100 mM HEPES, 50 mM LiCl, 0.1% deoxycholate, pH 7.0

29: 100 mM Tris, 100 mM KCl, 0.1% deoxycholate, 25% glycerol, pH 7.6

30: 100 mM potassium acetate, 50 mM NaCl, 0.05% dextran sulfate, 0.1% CHAPS, pH 5.5

2.3 Protein Purification and Characterisation

2.3.1 Overexpression of PpLAAO for protein purification

The ingredients for LB-media were purchased from Fisher Scientific, Kanamycin sulphate was purchased from Invitrogen, IPTG was purchased from Melford. Transformed cell cultures were grown in media containing 30 μg mL^{-1} kanamycin as the appropriate antibiotic.

1 μL of wild type pET-YSBLIC-3C-PpLAAO plasmid was used to transform 25 μL of *E. coli* BL21-DE3 chemically competent cells using heatshock. Four colonies of *E. coli* BL21-DE3-PpLAAO were each used to inoculate a 10 mL LB-media starter culture containing appropriate antibiotic under sterile conditions. These starter cultures were incubated overnight at 37°C with shaking at 180 r.p.m. Two 2 L Erlenmeyer flasks containing 1 L of LB media and appropriate antibiotic were each inoculated with 20 mL of starter culture under sterile conditions. The cell cultures were incubated at 37°C and shaking at 180 r.p.m until OD_{600} reached 0.5. Overexpression was induced by adding 1 mL of 1 M IPTG to each flask to give a final concentration of 1 mM IPTG. The cell culture was incubated at 37°C for 3 h with shaking at 180 r.p.m. The cells were

harvested by centrifugation for 15 min at 5,100 *g* using the GS3 rotor of a RC-5B Sorvall Centrifuge. The supernatant was discarded and the cell pellet was stored at -20°C.

LB-media (V= 1 L): 10 g tryptone, 5 g yeast extract, 10 g NaCl, H_2O (18.2 Ω· cm)

2.3.2 Purification of PpLAAO protein

PpLAAO was purified by metal affinity chromatography, followed by gel filtration chromatography. Prepacked HiTrap Chelating HP column was purchased from GE Healthcare. 120 mL HiLoad 16/60 Superdex 75 column was purchased from Pharmacia Biotech. Buffers 1-3, H_2O (18.2 Ω· cm) and 20% (v/v) ethanol were filtered through a 0.22 µM Whatman filter before use. The Prepacked HiTrap Chelating HP Column was loaded using peristaltic pump and gradient was run using AKTA Purifier P-900. The 120 mL HiLoad 16/60 Superdex 75 column was operated using an AKTA Purifier P-900. 1.6 mL semi-micro cuvettes were purchased from Sarstedt. AEBSF was purchased from Melford.

The cell pellets from 2 L of *E. coli* BL21-DE3-PpLAAO culture were thawed at room temperature and resuspended in 100 mL of buffer 1. The cell suspension was cooled on ice for 20 min. The cells were then sonicated on ice for 5 x 30 sec at 15 microns. Cell debris was spun down for 15 min at 26,900 *g* at 4°C using a Sorvall RC5B centrifuge and SS34 rotor. The supernatant was decanted and filtered through a 0.45 µm ACRODISC filter, followed by 0.2 µm ACRODISC filter. Filtered supernatant was then loaded onto a 5 mL HiTrap Chelating HP Column pre-charged with 0.1 M $NiSO_4$ using a peristaltic pump, the flow rate was 1 mL min^{-1}. After loading, resin was washed with 25 mL of buffer 1 at 1 mL min^{-1}. The column was then transferred to an AKTA Explorer and a gradient from buffer 2 to buffer 3 was run starting at 100% buffer 2 to 100% buffer 3 over 100 mL, with a flow rate of 1 mL min^{-1}. 4 mL fractions were collected. SDS-PAGE showed which sample fractions contained the desired protein by approximate monomer molecular weight (~60 kDa).

Sample fractions containing desired protein were combined and protein concentration was determined using Coomassie (Bradford) assay. BSA standards were prepared by dissolving BSA powder in buffer 1. BSA solutions were used at 0 µg mL^{-1}, 25 µg mL^{-1}, 125 µg mL^{-1}, 250 µg mL^{-1}, 500 µg mL^{-1}, 750 µg mL^{-1}, 1000 µg mL^{-1}, 1500 µg mL^{-1} and 2000 µg mL^{-1} BSA. A protein solution dilution was prepared by adding 10 µL of protein solution to 90 µL of buffer 1. Protein solutions were used at full concentration and at a 1 in 10 dilution.

10 µL of each BSA solution and 10 µL of each protein solution were added to 500 µL of Coomassie (Bradford) assay reagent in a 1.6 mL semi-micro cuvette and incubated for 10 min at room temperature. The A_{595} was measured using the Bradford setting of an Eppendorf Biophotometer. The absorbance of BSA was plotted against [BSA] as shown in **Fig. 2.2**, and the line of regression was used to determine the concentration of PpLAAO.

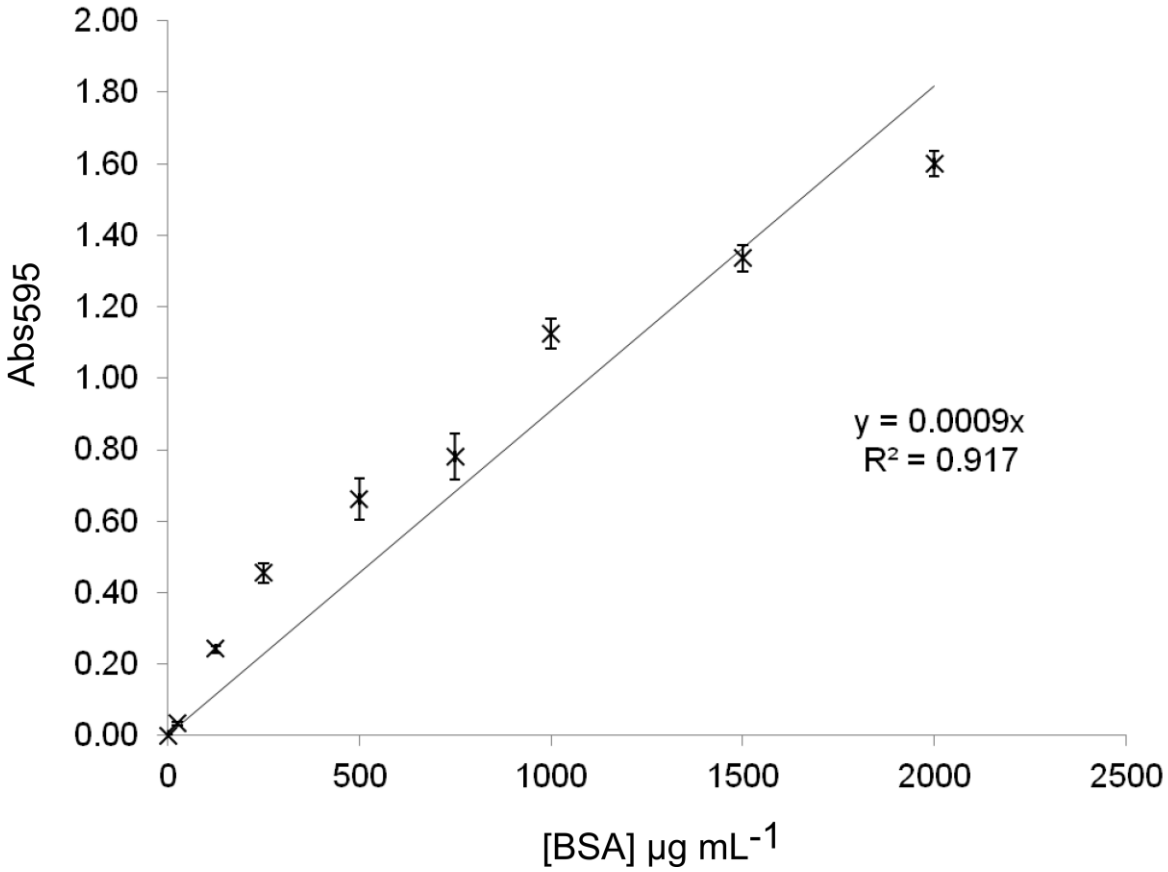

Fig. 2.2 Example of a Bradford calibration used to determine the concentration of PpLAAO protein.

The combined protein sample was diluted to a final concentration of 1 mg mL^{-1} using buffer 1. C3 His tag protease was added to a ratio of 1:100 mg protein. Protein was incubated at 4°C overnight and digestion was checked by SDS-PAGE. The digested protein was then loaded onto a 5 mL HiTrap Chelating HP column per-charged with 0.1 M $NiSO_4$ using peristaltic pump, flow rate was 1 ml min^{-1} and flow-through was collected. Resin was washed with 30 mL buffer 1, followed by 30 mL buffer 2 and then 30 mL buffer 4, flow rate was 1 mL min^{-1} and flow-through was collected. Resin was then washed with 30 mL buffer 3, flow rate was 1 mL min^{-1} and flow-through was collected. The collected flow-through was analysed on SDS-PAGE to determine protein content. Samples containing cleaved protein were then concentrated down to a volume of 4 mL using MWCO 30000 Vivaspin 20 tubes, spinning at 4066 g using the GSA rotor .

Gel filtration chromatography was then used to purify the protein further: A 2 mL aliquot was loaded onto a prepacked and pre-equilibrated 120 mL HiLoad 16/60 Superdex 75 column using a 2 mL loop on an AKTA Explorer. Resin was washed with 120 mL of buffer 1, flow rate was 1 mL min^{-1}, and 4 mL fractions were collected. SDS-PAGE showed which sample fractions contained the desired protein by approximate monomer molecular weight (~60 kDa). These fractions were then pooled and concentrated to 2 mg mL^{-1} using MWCO 30000 Vivaspin 20 tubes. Concentrated protein was snap frozen in liquid nitrogen and stored at -80°C.

The approximate purified protein molecular weight was determined using a calibration of the 120 mL HiLoad 16/60 Superdex 75 column performed by the EMBL (http://www.embl.de/pepcore/pepcore_services/protein_purification/chromatography/hiload16-60_superdex75/ Accessed 17/01/2012), which determined the equation of the calibration curve to be:

$$V_{elution} = 252.6 - 39.6 \times \log(M_r)$$

Meaning that molecular weight could be determined using the equation:

$$M_r = \text{antilog}\left(\frac{252.6 - V_{elution}}{39.6}\right)$$

As the elution volume of the purified protein was 52 mL, this makes the molecular weight 116320, or 116.32 kDa, which is roughly twice the size of the protein, suggesting that the purified protein is in a dimeric form.

Buffer 1: 50 mM Tris/HCl, 300 mM NaCl, 20 µM AEBSF, pH 7.0
Buffer 2: 50 mM Tris/HCl, 300 mM NaCl, 20 µM AEBSF, 30 mM Imidazole pH 7.0
Buffer 3: 50 mM Tris/HCl, 300 mM NaCl, 20 µM AEBSF, 500 mM Imidazole pH 7.0
Buffer 4: 50 mM Tris/HCl, 300 mM NaCl, 20 µM AEBSF, 70 mM Imidazole pH 7.0

2.3.3 Liquid phase assay of activity of wild type PpLAAO against wild type and target substrates

TBHBA was purchased from Alfa Aesar, 4-AAP, HRP, L-aspartate, L-asparagine, L-tyrosine, L-alanine and L-homoserine were purchased from Sigma-Aldrich, KH_2PO_4 and K_2HPO_4 were purchased from Fisher, 1 mL cuvettes purchased from Sarstedt. A_{510} was measured on a GBC Cintra 10 spectrophotometer.

The Cintra 10 spectrophotometer was programmed to measure A_{510} every 1 s for 6 min. 950 µL of assay solution was pipetted into a 1 mL cuvette. 50 µL of H_2O (18.2 Ω· cm) was added and cuvette was placed in the background solution position of the Cintra 10. 950 µL of assay solution was pipetted into a second 1 mL cuvette. The cuvette was placed in the front position of the Cintra 10. The Cintra 10 was set running for 10 s to ensure that the solution absorbance was stable. The front cuvette was removed from the Cintra 10 and 50 µL of 2 mg mL^{-1} PpLAAO protein was quickly added to the assay solution. The cuvette was mixed by inverting three times before being placed back into the Cintra 10. A_{510} continued to be measured for the remainder of the program.

After the program had finished, the absorbance values at 174 and 226 s were recorded for reactions containing L-aspartate. For reactions containing L-asparagine absorbance values at 250 and 300 s were recorded. The absorbance values at 275 s and 325 s were recorded for reactions containing L-alanine, L-homoserine and L-tyrosine.

Activity was measured in this way with 0.22 mM, 0.43 mM, 0.87 mM, 1.74 mM, 3.48 mM, 6.99 mM and 13.92 mM L-aspartate; 3.00 mM, 6.00 mM, 12.00 mM, 24.01 mM, 48.02 mM and 96.04 mM L-asparagine; 50 mM, 100 mM, 150 mM, 200 mM, 250 mM, 300 mM 350 mM, 400 mM, 500 mM L-glutamate; 1.42 mM, 2.84 mM, 5.68 mM, 11.3 mM, 22.7 mM, 45.5 mM and 91 mM L-alanine; 0.77 mM, 1.42 mM, 2.84 mM, 5.68 mM, 11.3 mM, 22.7 mM, 45.5 mM and 91 mM L-homoserine; 1.42 mM, 2.84 mM, 5.68 mM, 11.3 mM and 22.7 mM L-tyrosine in the assay solution. Activity was measured three times for each concentration of each substrate.

The rate of change in absorbance, in absorbance unit min^{-1}, for each concentration of each substrate was determined using the equation:

$$\frac{60}{50} \text{ x } \textit{Later time point - Earlier time point}$$

As the red quinonimine complex product of the HRP reaction has an extinction coefficient of 29,400 M^{-1} cm^{-1}, and the 1 mL cuvettes used have a path length of 1 cm, the Beer Lambert law was used to determine the change in concentration of the quinonimine complex, which should be equal to the change in concentration of the substrate, using the following calculation:

$$V_0(\text{Concentration change rate } (M\,min^{-1})) = \frac{V_0\,(AbsUnits\,min^{-1})}{29400\ M^{-1}\,cm^{-1} \text{ x } 1\ cm}$$

The SigmaPlot version 12 software with Enzyme Kinetics Module was used to plot Michaelis-Menten graphs and determine V_{max} and K_M against L-aspartate and L-asparagine. As the size of the PpLAAO protein is 59215 Da, the concentration of protein in mM per mg of protein could be determined:

$$[PpLAAO]\ (\text{mM}) = \frac{1}{59215\ Da} = 1.689 \text{ x } 10^{-5}\ mM\ mg^{-1}\ (of\ protein)$$

Therefore, k_{cat} could be determined as follows:

$$k_{cat} = \frac{V_{max}(nM\ min^{-1}\ mg^{-1}\ (\text{of protein})}{1.689 \text{ x } 10^{-5}\ mM\ mg^{-1}\ (\text{of protein})}$$

2 x Reaction Buffer (V= 50 mL):	100 mM KH_2PO_4/K_2HPO_4, 20 mg (TBHBA), 15 mg 4-AAP, pH 7.5
Assay solution:	1 x Reaction Buffer, 25 µg mL^{-1} HRP, and varied concentration of substrate

2.3.4 Liquid phase stability assay of wild type PpLAAO against L-aspartate over pH

TBHBA was purchased from Alfa Aesar, 4-AAP, HRP and L-aspartate were purchased from Sigma-Aldrich, KH_2PO_4 and K_2HPO_4 were purchased from Fisher, 96-well flat bottomed plates were purchased from Corning Costar. A_{510} was measured on a BMG Labtech PolarStar Optima plate reader.

Reactions were repeated four times at each pH, and four reactions using an assay solution with pH 7.4 and H_2O (18.2 Ω· cm) as substrate were used as control reactions. 10 µL of 1 mg mL^{-1} PpLAAO protein was added to 190 µL of assay solution in an Eppendorf tube. Reactions were left to develop for 1 h before being spun down at 16,000 *g* for 1 min in an Eppendorf 5415 C centrifuge to remove any protein precipitant. The assay solution was then transferred to a 96 well flat-bottomed plate and A_{510} was measured. The mean absorbance of the control reactions was subtracted from all other absorbance readings before mean absorbance for each reaction was calculated. Assays were run at pH 4.7, 5.8, 6.2, 6.6, 7.0, 7.4, 7.8 and 8.2.

2 x Reaction Buffer (V= 50 mL):	100 mM KH_2PO_4/K_2HPO_4, 20 mg (TBHBA), 15 mg 4-AAP, varying pH
Assay solution:	1 x Reaction Buffer, 25 µg mL^{-1} HRP, 10 mM L-aspartate

2.3.5 Liquid phase stability assay of wild type PpLAAO against L-aspartate over temperature

TBHBA was purchased from Alfa Aesar, 4-AAP, HRP and L-aspartate were purchased from Sigma-Aldrich, KH_2PO_4 and K_2HPO_4 were purchased from Fisher, 96-well flat bottomed plates were purchased from Corning costar. Proteins were incubated at various temperatures in 200 µL thin walled PCR tubes purchased from Axygen, using a Techne TC-312 Thermocycler and an

Eppendorf Mastercycler gradient PCR machine. A_{510} was measured on a BMG Labtech PolarStar Optima plate reader.

40 µL of protein was kept at 4°C, 10°C, 20°C, 30°C, 40°C, 50°C or 60°C for 5 min, 10 min, 20 min, 30 min, 45 min or 60 min. Protein was then cooled on ice or 3 h. Three reactions for each temperature and time combinations were setup. Three assays using protein kept at 4°C and deionised H_2O (18.2 Ω· cm) as substrate were setup was control reactions.

10 µL of 1 mg mL^{-1} PpLAAO protein was added to 190 µL of assay solution in an Eppendorf tube. Reactions were left to develop for 1 h before being spun down at 16,000 *g* for 1 min in an Eppendorf 5415 C centrifuge to remove any protein precipitant. The assay solution was then transferred to a 96 well flat-bottomed plate and A_{510} was measured. The mean absorbance of the control reactions was subtracted from all other absorbance readings before mean absorbance for each reaction was calculated.

2 x Reaction Buffer (V= 50 mL):	100 mM KH_2PO_4/K_2HPO_4, 20 mg (TBHBA), 15 mg 4-AAP, pH 7.4
Assay solution:	1 x Reaction Buffer, 25 µg mL^{-1} HRP, 10 mM L-aspartate

2.3.6 Overexpression and purification of PpLAAO for crystallisation

PpLAAO protein was overexpressed and purified as in **Sections 2.3.1** and **2.3.2**. However, after the protein was run through the 120 mL HiLoad 16/60 Superdex 75 column, fractions containing the protein were pooled together and concentrated to 100 mg mL^{-1} using MWCO 30000 Vivaspin 20 tubes. Concentrated protein was stored at 4°C.

2.3.7 Crystallisation screening of PpLAAO

Purified and His-tag cleaved PpLAAO protein was subjected to several 96-well crystallisation screens, using the sitting drop diffusion method. Screens were transferred from 96-deep-well block format to 96-well MRC plates using a Robbins Scientific Hydra™ 96. Protein drops were set up using a TTP Labtech Mosquito®. Index crystallisation screen was purchased from Hampton. PACT crystallisations screen was purchased from Qiagen. AEBSF was purchased from Melford.

For CSS 1+ 2 screens 6 µL of 1 M MES pH 5.6 was added to all wells in columns 1-6 of the MRC plate, and 6 µL of Tris pH 8.0 was added to all wells in columns 7-12. For all screens 54 µL of

crystallisations screen was transferred from the deep-well blocks to the MRC plate using the Hydra^{TM} 96. The Mosquito® was then used to create crystallisation drops containing 150 µL of well solution and 150 µL of protein solution.
The combinations of crystal screen and protein solution tried are listed in **Table 2.5**.

Table 2.5: Combinations of crystallization screens and protein solutions trialled during attempts to create crystals of PpLAAO protein.

Crystallisation Screen	Protein Solution
Index	10 mg mL^{-1} PpLAAO in buffer 1
Index	30 mg mL^{-1} PpLAAO in buffer 1
Index	30 mg mL^{-1} PpLAAO in buffer 2
Index	45 mg mL^{-1} PpLAAO in buffer 1
Index	60 mg mL^{-1} PpLAAO in buffer 1
Index	100 mg mL^{-1} PpLAAO in buffer 1
PACT	30 mg mL^{-1} PpLAAO in buffer 1
PACT	45 mg mL^{-1} PpLAAO in buffer 1
PACT	60 mg mL^{-1} PpLAAO in buffer 1
PACT	100 mg mL^{-1} PpLAAO in buffer 1
CSS 1 + 2	60 mg mL^{-1} PpLAAO in buffer 1

Buffer 1: 50 mM Tris/HCl, 300 mM NaCl, 20 µM AEBSF, pH 7.0
Buffer 2: 50 mM Tris/HCl, 300 mM NaCl, 20 µM AEBSF, 1 mM FAD, pH 7.0

2.3.8 Native gel and Dynamic Light Scattering analysis of wild type PpLAAO

Tris and AEBSF were purchased from Melford. HCl, NaCl, Imidazole, glycerol, propanol and glacial acetic acid were purchased from Fisher. Acrylamide solution "30% ProtoGel" was purchased from National Diagnostics. APS and TEMED were purchased from Sigma-Aldrich. MicroPasteur pipettes were purchased from Alpha laboratories.

Purified wild type PpLAAO was analysed on a 7.5% native-PAGE gel using Mighty Small gel electrophoresis equipment.[110]

A 7.5%-resolving gel contained 2.45 mL H_2O (18.2 Ω· cm), 1.25 mL buffer (1.5 M Tris/HCl, pH 8.8), 1.25 mL acrylamide solution, 25 µL of 10% (w/v) APS and 4 µL of TEMED.
A stacking gel consisted of 1.6 mL H_2O (18.2 Ω· cm), 0.65 mL buffer (0.5 M Tris/HCl, pH 6.8), 0.25 mL acrylamide solution, 16 µL of 10% APS, 4 µL of TEMED and 4 µL of 1% (w/v) Bromophenol Blue. 20 µL-loading samples contained 50% (v/v) protein solution and 50% (v/v) loading buffer. Electrophoreses were carried out at 100 V for 120 min in running buffer, with water running through the gel apparatus to ensure that the equipment did not overheat.

After the electrophoresis, the native-gel was placed in staining solution and microwaved for 40 s. The SDS-gel was then washed with water and placed in destaining solution and microwaved for 40 s and then left to destain at room temperature. The destaining solution was exchanged several times in order to completely destain the native-gel. Pictures of the gel were taken using a Syngene Gene Genius Bioimaging System.

Wild type PpLAAO protein was analysed by Dynamic Light Scattering (DLS) using a Protein Solutions DynaPro DLS machine with Temperature controlled Microsampler manipulated used the Dynamic 5-26 programme. 500 µL of 1 mg ml^{-1} wild type PpLAAO protein and 500 µL of filtered buffer 1 were spun down at 16,000 *g* for 10 min in an Eppendorf 5415 C centrifuge. The DLS cuvette was rinsed with H_2O (18.2 Ω· cm) for 2 min and left in a beaker of fresh H_2O (18.2 Ω· cm) for a further 2 min. DLS cuvette was dried with compressed air and cleaned wiped with an optical-grade cloth.

500 µL of H_2O (18.2 Ω· cm) was placed in the DLS cuvette using a micropasteur pipette and the cuvette was placed in the DLS machine at 20°C. Counts were measured to ensure that they were less than 12,000. H_2O was removed from the cuvette and replaced with 500 µL of buffer 1. Counts were measured to ensure that they were still below the 12,000 threshold level. Buffer 1 was replaced with 500 µL of 1 mg mL^{-1} PpLAAO protein. Counts were measured for 30 s to ensure that the levels were stable before data collection was started. Data collection was left to run until at least 15 statistically accurate blue bars of data had accumulated.

Buffer 1:	50 mM Tris/HCl, 300 mM NaCl, 20 µM AEBSF, pH 7.0
Loading buffer:	0.5 M Tris, 10% (w/v) glycerol, 0.2% (w/v) Bromophenol Blue, pH 6.8
Running Buffer:	25 mM Tris, 250 mM glycine, pH 8.4
Staining Solution:	25% (v/v) propan-2-ol, 10% glacial acetic acid, 0.2% (w/v) Coomassie Brilliant BlueR
Destaining Solution:	5% (v/v) propan-2-ol and 7% (v/v) glacial acetic acid

2.3.9 Analysis of effects of different buffers on wild type PpLAAO

Guanidine HCl (G. HCl), Tris and AEBSF were purchased from Melford. Urea, HCl, NaCl, Imidazole, glycerol, propanol and glacial acetic acid were purchased from Fisher. Acrylamide solution "30% ProtoGel" was purchased from National Diagnostics. SB12, LDAO, TMAO, β-OG, APS and TEMED were purchased from Sigma-Aldrich. NSDB-201 was purchased from

Calbiochem. Vivaspin 20s with 30,000 MWCO were purchased from Sartorius stedim. MicroPasteur pipettes were purchased from Alpha laboratories.

PpLAAO protein purified as in **Section 2.3.6** was concentrated to 20 mg mL^{-1} in a Vivaspin 20 spun at 3,400 *g* in a Harrier 18/80 centrifuge. 50 µL of protein was mixed with 450 µL of each of the following protein buffers: 10 mM LDAO, 10 mM SB12, 0.5% β-OG, 500 mM TMAO, 250 mM NDSB-201, 50 mM Urea, 100 mM Urea, 200 mM Urea, 50 mM G. HCl, 100 mM G. HCL and 200 mM G. HCl.

The protein solutions remixed with 500 mM TMAO, 250 mM NDSB-201, 50 mM Urea, 100 mM Urea, 200 mM Urea, 50 mM G. HCl, 100 mM G. HCl and 200 mM G. HCl were analysed by Dynamic Light Scattering (DLS) using a Protein Solutions DynaPro DLS machine with Temperature controlled Microsampler manipulated used the Dynamic 5-26 programme. 500 µL of 2 mg mL^{-1} PpLAAO protein and 500 µL of filtered protein buffer were spun down at 16,000 *g* for 10 min in an Eppendorf 5415 C centrifuge. The DLS cuvette was rinsed with H_2O (18.2 Ω· cm) for 2 min and left in a beaker of fresh H_2O (18.2 Ω· cm) for a further 2 min. DLS cuvette was dried with compressed air and cleaned wiped with an optical-grade cloth.

500 µL of H_2O (18.2 Ω· cm) were placed in the DLS cuvette using a micropasteur pipette and the cuvette was placed in the DLS machine at 20°C. Counts were measured to ensure that they were less than 12,000. H_2O was removed from the cuvette and replaced with 500 µL of protein buffer. Counts were measured to ensure that they were still below the 12 k threshold level. Protein buffer was replaced with 500 µL of 2 mg mL^{-1} PpLAAO protein. Counts were measured for 30 s to ensure that the levels were stable before data collection was started. Data collection was left to run until at least 15 statistically accurate blue bars of data had accumulated. The 100 mM and 200 mM G. HCl solutions were aborted as protein precipitation was too great for accurate readings to be collected.

PpLAAO protein in buffer 1 was also analysed using DLS as above, but with the temperature at 4°C, 12°C and 20°C. An analysis at 37°C was attempted but the protein precipitated.

All the remixed protein solutions other than the 100 mM and 200 mM G. HCl solutions were analysed on a 7.5% native-PAGE gel using Mighty Small gel electrophoresis equipment.[110]

A 7.5%-resolving gel contained 2.45 mL H_2O (18.2 Ω· cm), 1.25 mL buffer (1.5 M Tris/HCl, pH 8.8), 1.25 mL acrylamide solution, 25 µL of 10% (w/v) APS and 4 µL of TEMED.

A stacking gel consisted of 1.6 mL H_2O (18.2 Ω· cm), 0.65 mL buffer (0.5 M Tris/HCl, pH 6.8), 0.25 mL acrylamide solution, 16 µL of 10% APS, 4 µL of TEMED and 4 µL of 1% (w/v) Bromophenol Blue.
20 µL-loading samples contained 50% (v/v) protein solution and 50% (v/v) loading buffer. Electrophoresis was carried out at 100 V for 120 min in running buffer, with water running through the gel apparatus to ensure that the equipment did not overheat.

After the electrophoresis, the native-gel was placed in staining solution and microwaved for 40 s. The SDS-gel was then washed with water and placed in destaining solution and microwaved for 40 s and then left to destain at room temperature. The destaining solution was exchanged several times in order to completely destain the native-gel. Pictures of the gel were taken using a Syngene Gene Genius Bioimaging System.

Buffer 1:	50 mM Tris/HCl, 300 mM NaCl, 20 µM AEBSF, pH 7.0
Loading buffer:	0.5 M Tris, 10% (w/v) glycerol, 0.2% (w/v) Bromophenol Blue, pH 6.8
Running Buffer:	25 mM Tris, 250 mM glycine, pH 8.4
Staining Solution:	25% (v/v) propan-2-ol, 10% glacial acetic acid, 0.2% (w/v) Coomassie Brilliant BlueR
Destaining Solution:	5% (v/v) propan-2-ol and 7% (v/v) glacial acetic acid

2.3.10 Effects of cold purification and G. HCl concentration on PpLAAO quaternary form

G. HCl, Tris and AEBSF were purchased from Melford. NaCl, Imidazole, glycerol, propanol and glacial acetic acid were purchased from Fisher. Acrylamide solution "30% ProtoGel" was purchased from National Diagnostics. APS and TEMED were purchased from Sigma-Aldrich. Vivaspin 20s with 30,000 MWCO were purchased from Sartorius. MicroPasteur pipettes were purchased from Alpha Laboratories.

PpLAAO protein was overexpressed and purified as in **Sections 2.3.1-2.3.2**, however the AKTA used was kept in a refrigerator set at 4°C, and extra care was made to ensure that protein was kept at ice temperature at all times during purification. Protein was diluted to 1 mg mL^{-1} and 10 µL of the purified protein was analysed on a 7.5% native-PAGE gel using Mighty Small gel electrophoresis equipment.[110]

After purification, the protein was concentrated to 20 mg mL^{-1} in a Vivaspin 20 spun at 3,400 *g* in a Harrier 18/80 centrifuge. 50 µL of protein was mixed with 450 µL of ice-cold, pH 7.0 G. HCl at

the following concentrations; 5 mM, 10 mM, 15 mM, 20 mM, 25 mM, 30 mM, 35 mM, 40 mM, 45 mM. Remixed protein samples were kept at 4°C overnight and amount of precipitation was observed visually. Precipitated protein was spun down at 16,000 *g* for 10 min in an Eppendorf 5415 C centrifuge and each sample was analysed on a 7.5% native-PAGE gel using Mighty Small gel electrophoresis equipment.[110]

A 7.5%-resolving gel contained 2.45 mL H_2O (18.2 Ω· cm), 1.25 mL buffer (1.5 M Tris/HCl, pH 8.8), 1.25 mL acrylamide solution, 25 µL of 10% (w/v) APS and 4 µL of TEMED.
A stacking gel consisted of 1.6 mL H_2O (18.2 Ω· cm), 0.65 mL buffer (0.5 M Tris/HCl, pH 6.8), 0.25 mL acrylamide solution, 16 µL of 10% APS, 4 µL of TEMED and 4 µL of 1% (w/v) Bromophenol Blue.
20 µL-loading samples contained 50% (v/v) protein solution and 50% (v/v) loading buffer. Electrophoresis was carried out at 100 V for 120 min in running buffer, with water running through the gel apparatus to ensure that the equipment did not overheat.

After the electrophoresis, the native gel was placed in staining solution and microwaved for 40 s. The SDS-gel was then washed with water and placed in destaining solution and microwaved for 40 s and then left to destain at room temperature. The destaining solution was exchanged several times in order to completely destain the native gel. Pictures of the gel were taken using a Syngene Gene Genius Bioimaging System.

Buffer 1:	50 mM Tris/HCl, 300 mM NaCl, 20 µM AEBSF, pH 7.0
Loading buffer:	0.5 M Tris, 10% (w/v) glycerol, 0.2% (w/v) Bromophenol Blue, pH 6.8
Running Buffer:	25 mM Tris, 250 mM glycine, pH 8.4
Staining Solution:	25% (v/v) propan-2-ol, 10% glacial acetic acid, 0.2% (w/v) Coomassie Brilliant BlueR
Destaining Solution:	5% (v/v) propan-2-ol and 7% (v/v) glacial acetic acid

A 24-well crystallisation plate was set up at 4°C using the hanging drop vapour diffusion method, with the wells containing the solutions shown in **Fig 2.2**. The tray was kept at 4°C and checked in the microscope periodically to see if crystals had developed.

1.0 M AS	1.5 M AS	2.0 M AS	2.5 M AS	3.0 M AS	3.5 M AS
10% PEG 4K	15% PEG 4K	20% PEG 4K	25% PEG 4K	30% PEG 4K	35% PEG 4K
15% PEG 3350 0.2 M AS	20% PEG 3350 0.2 M AS	25% PEG 3350 0.2 M AS	30% PEG 3350 0.2 M AS	35% PEG 3350 0.2 M AS	

Fig 2.3 Layout of well solutions in 24-well crystallisation screen of PpLAAO protein**.** AS = Ammonium sulfate.

2.4 Generation of active site residue mutants of PpLAAO

PfUTurbo HotStart DNA polymerase kit was purchased from Agilent Technologies/Stratagene. dNTPs were purchased from Promega. High-purity salt free primers were purchased from MWG/Eurofins. PCRs were carried out in either 200 µL or 500 µL thin-walled PCR tubes using a Techne TC-312 thermal cycler. *DpnI* Restriction enzyme was purchased from New England Biolabs. Chemically competent *E. coli* BL21-Gold-DE3 were purchased from Agilent Technologies/Stratagene. Electrochemically competent *E. coli* BL21-DE3 were prepared as in **Section 2.1.5**. Transformed *E. coli* BL21-DE3 cells were grown using 30 µg mL^{-1} kanamycin as the appropriate antibiotic. Transformed *E. coli* BL21-Gold-DE3 cells were grown using 30 µg mL^{-1} kanamycin and 15 µg mL^{-1} tetracyclin as the appropriate antibiotic.

Stratagene's QuikChange method of Site Directed Mutagenesis was used to introduce mutations into the YSBLIC3C-PpLAAO plasmid, using PCR cycle C (**Table 2.1**), PCR mix C (**Table 2.2**) and the primer pairs (**Table 2.3**) listed in **Table 2.6**. Each reaction was treated with 1 µL of *DpnI* restriction enzyme and incubated at 37°C for 3 h. 2 µL of the restricted reaction product was used to transform 50 µL of the cell strain listed in **Table 2.6**.

The number of colonies listed in **Table 2.6** were each used to inoculate a 5 mL starter culture containing appropriate antibiotics. These cultures were grown at 37°C with shaking at 180 r.p.m overnight. The next morning 100 µL of starter culture was used to inoculate a fresh 5 mL culture of LB-media containing appropriate antibiotics, and the remaining started culture pulled down by spinning at 16,000 *g* for 1 min using an Eppendorf 5415 C centrifuge, the supernatant was discarded and cell pellets were stored at -20°C**.**

Table 2.6: Primers and PCR tubes used to generate Alanine substituted mutants of the PpLAAO active site residues using the Stratagene QuikChange method and cell strains transformed with resulting plasmid (Please see **Table 2.3** for primer sequences).

Mutation	Primers	PCR tube size	Cell Strain	Number of colonies grown
Q242A	Q242A-for, Q242A-rev	200 µL	Electrocompetent *E. coli* BL21-DE3	10
H244A	H244A-for, H244A-rev	200 µL	Chemically competent *E. coli* BL21-Gold-DE3	1
P245A	P245A-for, P2425-rev	200 µL	Chemically competent *E. coli* BL21-Gold-DE3	3
L257A	L257A-for, L257A-rev	200 µL	Chemically competent *E. coli* BL21-Gold-DE3	3
T259A	T259A-for, T259A-rev	200 µL	Chemically competent *E. coli* BL21-Gold-DE3	12
E260A	E260A-for, E260A-rev	200 µL	Chemically competent *E. coli* BL21-Gold-DE3	2
R290A	R290A-for, R290A-rev	500 µL	Chemically competent *E. coli* BL21-Gold-DE3	3
V293A	V293A-for, V293A-rev	500 µL	Chemically competent *E. coli* BL21-Gold-DE3	10
H351A	H351A-for, H351A-rev	500 µL	Electrocompetent *E. coli* BL21-DE3	2
Y352A	Y352A-for, Y352A-rev	500 µL	Chemically competent *E. coli* BL21-Gold-DE3	2
R386A	R386A-for, R386A-rev	500 µL	Electrocompetent *E. coli* BL21-DE3	2
S389A	S389A-for, S389A-rev	500 µL	Chemically competent *E. coli* BL21-Gold-DE3	10
S391A	S391A-for, S391A-rev	500 µL	Chemically competent *E. coli* BL21-Gold-DE3	2

The fresh cell cultures were incubated at 37°C with shaking at 180 r.p.m until OD_{600} was at 0.5. Overexpression was induced by adding 5 µL of 1 M IPTG to give a final concentration of 1 mM IPTG. The cell culture was incubated at 37°C for 3 h with shaking at 180 r.p.m. The cells were harvested by centrifugation for 1 min at 16,000 *g* using an Eppendorf 5415 C centrifuge. The supernatant was discarded and the cell pellet was resuspended in 500 µL buffer 1. The cell suspension was sonicated on ice for 30 s at 15 microns. Cell debris was pulled down by spinning at 16,000 *g* for 1 min using an Eppendorf 5415 C centrifuge. The soluble supernatant was separated from the insoluble cell pellet. The cell pellet was then resuspended in 500 µL buffer 1. The soluble and insoluble fractions were analysed by 12.5% SDS-PAGE.

Plasmid DNA from cell strains that appeared to produce correctly sized protein (~60 kDa) was purified from the cell pellets stored at -20°C using Sigma-Aldrich's GenElute DNA Miniprep Kit, plasmids were then sent for sequencing by the York University Genomics group (**Section 2.2.4**) using the T7 and T7-term primers (**Table 2.3**).

LB media (V= 1 L): 10 g tryptone, 5 g yeast extract, 10 g NaCl, H_2O (18.2 Ω· cm)

LB-agar (V= 1 L): 10 g tryptone, 5 g yeast extract, 10 g NaCl, 15 g agar, H_2O (18.2 Ω· cm)

Buffer 1: 50 mM Tris/HCl, 300 mM NaCl, 20 µM AEBSF, pH 7.0

2.5 Purification and characterisation of active site PpLAAO mutants

2.5.1 Overexpression of active site PpLAAO mutant proteins for purification

Chemically competent *E. coli* BL21-DE3 cells were purchased from Merck/Novagen. Ingredients for LB-media were purchased from Fisher. Agar was purchased from Lab M Ltd. Kanamycin sulfate was purchased from Invitrogen. IPTG was purchased from Melford. OD_{600} was measured using an Eppendorf Biophotometer. Transformed cell cultures were grown in media containing 30 µg mL^{-1} kanamycin as the appropriate antibiotic.

1 µL of each mutated form of the pET-YSBLIC-3C-PpLAAO plasmid made as in **Section 2.4** was used to transform 25 µL of *E. coli* BL21-DE3 chemically competent cells using heatshock. For each mutation, two of the resulting colonies were each used to inoculate a 10 mL LB-media starter cultures containing appropriate antibiotic under sterile conditions. These starter cultures were incubated overnight at 37°C with shaking at 180 r.p.m. A 2 L Erlenmeyer flask containing 1 L of LB media and appropriate antibiotic was inoculated with 20 mL of starter culture under sterile conditions. The cell cultures were incubated at 37°C and shaking at 180 r.p.m until OD_{600} reached 0.5. Overexpression was induced by adding 1 mL of 1 M IPTG to give a final concentration of 1 mM IPTG. The cell culture was incubated at 37°C for 3 h with shaking at 180 r.p.m. The cells were harvested by centrifugation for 15 min at 5,100 *g* using the GS3 rotor of a RC-5B Sorvall Centrifuge. The supernatant was discarded and the cell pellet was stored at -20°C.

LB media (V= 1 L): 10 g tryptone, 5 g yeast extract, 10 g NaCl, H_2O (18.2 Ω· cm)

2.5.2 Purification of active site PpLAAO mutant protein

Active site mutants of PpLAAO were purified by anion exchange chromatography, followed by gel filtration chromatography. Prepacked HiTrap Chelating HP column was purchased from GE Healthcare. 120 mL HiLoad 16/60 Superdex 75 column was purchased from Pharmacia Biotech. Buffers 1-3, H_2O (18.2 Ω· cm) and 20% (v/v) ethanol were filtered through a 0.22 µM Whatman filter before use. The Prepacked HiTrap Chelating HP Column was loaded using peristaltic pump and gradient was run using AKTA Purifier P-900. The 120 mL HiLoad 16/60 Superdex 75 column was operated using an AKTA Purifier P-900. AEBSF was purchased from Melford.

The cell pellets from the 1 L cultures of *E. coli* BL21-DE3-Active site PpLAAO mutant were thawed at room temperature and resuspended in 50 mL of buffer 1. The cell suspension was cooled on ice for 20 min. The cells were then sonicated on ice for 5 x 30 sec at 15 microns. Cell debris was spun down for 15 min at 26,900 *g* at 4°C using a Sorvall RC5B centrifuge and SS34 rotor. The supernatant was decanted and filtered through a 0.45 µm ACRODISC filter, followed by 0.2 µm ACRODISC filter. Filtered supernatant was then loaded onto a 5 mL HiTrap Chelating HP Column pre-charged with 0.1 M $NiSO_4$ using a peristaltic pump, the flow rate was 1 mL min^{-1}. After loading, resin was washed with 25 mL of buffer 1 at 1 mL min^{-1}. The column was then transferred to an AKTA Explorer and a gradient from buffer 2 to buffer 3 was run starting at 100% buffer 2 to 100% buffer 3 over 100 mL, with a flow rate of 1 mL min^{-1}. 4 mL fractions were collected. SDS-PAGE showed which sample fractions contained the desired protein by approximate monomer molecular weight (~60 kDa). Samples with pure protein were combined and concentrated to 2 mL aliquots using a MWCO 30000 Vivaspin 20 tube.

Gel filtration chromatography was then used to purify the protein further: A 2 mL aliquot was loaded onto a prepacked and pre-equilibrated 120 mL HiLoad 16/60 Superdex 75 column using a 2 mL loop on an AKTA Explorer. Resin was washed with 120 mL of buffer 1, flow rate was 1 mL min^{-1}, and 4 mL fractions were collected. SDS-PAGE showed which sample fractions contained the desired protein by approximate monomer molecular weight (~60 kDa). These fractions were then pooled and concentrated to 2 mg mL^{-1} using MWCO 30000 Vivaspin 20 tubes. Concentrated protein was snap frozen in liquid nitrogen and stored at -80°C.

Buffer 1: 50 mM Tris/HCl, 300 mM NaCl, 20 µM AEBSF, pH 7.0
Buffer 2: 50 mM Tris/HCl, 300 mM NaCl, 20 µM AEBSF, 30 mM Imidazole pH 7.0
Buffer 3: 50 mM Tris/HCl, 300 mM NaCl, 20 µM AEBSF, 500 mM Imidazole pH 7.0

2.5.3 Activity assay of active site PpLAAO mutant proteins against target substrates

TBHBA was purchased from Alfa Aesar, 4-AAP, HRP, L-aspartate, L-asparagine, L-tyrosine, L-alanine and L-homoserine were purchased from Sigma-Aldrich, KH_2PO_4 and K_2HPO_4 were purchased from Fisher, 1 mL cuvettes purchased from Sarstedt. A_{510} was measured on a GBC Cintra 10 spectrophotometer.

The initial rate activity of the purified wild type PpLAAO protein and the purified protein from PpLAAO mutants Q242A, H244A, P245A, L257A, T259A, R290A, H351A, Y352A, R386A, S389A and S391A were all measured against L-aspartate, L-asparagine, L-homoserine and L-glutamate as follows:

The Cintra 10 spectrophotometer was programmed to measure A_{510} every 0.1 s for 5 min. 950 µL of assay solution was pipetted into a 1 mL cuvette. 50 µL of H_2O (18.2 Ω· cm) was added and cuvette was placed in the background solution position of the Cintra 10. 950 µL of assay solution was pipetted into a second 1 mL cuvette. The cuvette was placed in the front position of the Cintra 10. The Cintra 10 was set running for 10 s to ensure that the solution absorbance was stable. The front cuvette was removed from the Cintra 10 and 50 µL of 2 mg mL^{-1} protein was quickly added to the assay solution. The cuvette was mixed by inverting three times before being placed back into the Cintra 10. A_{510} continued to be measured for the remainder of the program.

After the program had finished the absorbance values at 239.9 and 299.9 s were recorded.

Activity was measured in this way with 1.563 mM, 3.125 mM, 6.25 mM, 12.5 mM, 25 mM, 37.5 mM 50 mM, of each of L-aspartate, L-asparagine, L-homoserine and L-glutamate. Activity was measured three times for each concentration of each substrate.

The rate of change in absorbance, in absorbance unit min^{-1}, for each concentration of each substrate was determined using the equation:

$$\frac{60}{50} \text{ x } \textit{Later time point - Earlier time point}$$

As the red quinonimine complex product of the HRP reaction has an extinction coefficient of 29,400 M^{-1} cm^{-1}, and the 1 mL cuvettes used have a path length of 1 cm, the Beer Lambert law was used to determine the change in concentration of the quinonimine complex, which should be equal to the change in concentration of the substrate, using the following calculation:

$$V_0(\text{Concentration change rate } (M\,min^{-1})) = \frac{V_0\,(AbsUnits\,min^{-1})}{29400\ M^{-1}\,cm^{-1} \text{ x } 1\ cm}$$

Grafit version 7.0 and GraphPad Prism 5 software were used to plot Michaelis-Menten graphs and determine V_{max} and K_M against L-aspartate and L-asparagine. As the size of the PpLAAO protein is 59215 Da, the concentration of protein in mM per mg of protein could be determined:

$$[PpLAAO]\ (\text{mM}) = \frac{1}{59215\ Da} = 1.689 \text{ x } 10^{-5}\ mM\,mg^{-1}\ (of\,protein)$$

Therefore, k_{cat} could be determined as follows:

$$k_{cat} = \frac{V_{max}(nM\,min^{-1}\ mg^{-1}\ (\text{of protein})}{1.689 \text{ x } 10^{-5}\ mM\,mg^{-1}\ (\text{of protein})}$$

2 x Reaction Buffer (V= 50 mL): 100 mM KH_2PO_4/K_2HPO_4, 20 mg (TBHBA) in 1 mL DMSO, 15 mg 4-AAP, pH 7.5

Assay solution: 1 x Reaction Buffer, 25 µg mL^{-1} HRP, and varied concentration of substrate

2.6 Generation of SDSM CASTing libraries

2.6.1 Building of SDSM CASTing library A

The annealing temperature of the Stratagene QuikChange reaction was optimized in 200 µL thin-walled PCR tubes using an Eppendorf Mastercycler gradient PCR machine. *DpnI* restriction enzyme was purchased from New England Biolabs. The ingredients for LB-media were purchased from Fisher, kanamycin sulphate was purchased from Invitrogen, tetracycline was purchased from Merck/Calbiochem. AEBSF and IPTG were purchased from Melford. OD_{600} was measured using an Eppendorf Biophotometer. Other PCRs were carried out in 200 µL thin-walled PCR tubes in a Techne TC-312 PCR machine.

The PCR mix was pipetted in 200 µL thin-walled PCR tubes. Stratagene's QuikChange method of SDSM mutagenesis was used to introduce mutations into the YSBLIC3C-PpLAAO plasmid using PCR cycle D (**Table 2.1**) and PCR mix D (**Table 2.2**) and the PNDTA-for and PNDTA-rev primers (**Table 2.3**). Reactions were performed in duplicate, then mixed together to produce a total reaction volume of 50 µL. 25 µL of reaction product was analysed with 1 % agarose gel electrophoresis (**Section 3.1.1**). The remaining 25 µL of the PCR mix was mixed with 1 µL of *DpnI*. The reaction was incubated at 37°C for 3 h. 2 µL of this reaction was cooled down on ice and used to transform 25 µL of *E. coli* XL10-Gold cells using heat shock (**Section 2.1.3**). 6 single colonies were each used to inoculate 5 mL of LB-media containing 30 µg mL^{-1} kanamycin, 34 µg mL^{-1} chloramphenicol and 15 µg mL^{-1} tetracycline. These started cultures were incubated at 37°C and shaking at 180 r.p.m overnight.

The following day, the starter cultures were spun down at 16,000 *g* in an Eppendorf 5415 C centrifuge. Mutant plasmids were isolated using Sigma Aldrich's GenElute plasmid Miniprep kit. To check size of the gene insert, the inserts of each plasmid was amplified by PCR (**Section 3.1.5**) using PCR cycle E (**Table 2.1**), PCR mix E (**Table 2.2**) and the PpLAAO-for and PpLAAO-rev primers (b). The reactions were analysed with 1% agarose gel electrophoresis.

The concentration of DNA in the purified plasmids was determined by measuring the absorption at 280 nm using the dsDNA function on the Eppendorf Biophotometer, with an absorbance of 0.1 equal to DNA concentration of 50 ng μL^{-1}. The plasmids were then concentrated to between 100 and 150 ng μL^{-1} using a GeneVac miVac DNA concentrator. Each plasmid was then sequenced by the York University Genomics group using the T7 and T7-term primers (**Table 2.3**). Multiple sequence alignments were performed using the CLUSTALW2 program version 2.0.12 hosted by

the European Bioinformatics Institute (http://www.ebi.ac.uk/Tools/msa/clustalw2/ Accessed 10/02/2010).

1 µL of each of 4 of the purified mutant plasmids was used to transform *E. coli* Rosetta2-DE3 competent cells using heat shock. One colony from each plate was used to inoculate 5 mL of LB-media containing 30 µg mL^{-1} kanamycin and 34 µg mL^{-1} chloramphenicol. These starter cultures were incubated at 37°C and shaking at 180 r.p.m overnight. The following day 100 µL of started culture was used to inoculate a fresh 5 mL culture of LB-media containing 30 µg mL^{-1} kanamycin and 34 µg mL^{-1} chloramphenicol. These cultures were incubated at 37°C and shaking at 180 r.p.m until OD_{600} was at 0.5. Overexpression was induced by adding 5 µL of 1 M IPTG to give a final concentration of 1 mM IPTG. The cell culture was incubated at 37°C for 3 h with shaking at 180 r.p.m. The cells were harvested by centrifugation for 2 min at 16,000 *g* using an Eppendorf 5415 C centrifuge. The supernatant was discarded and the cell pellet was resuspended in 500 µL buffer 1. The cell suspension was sonicated on ice for 30 s at 15 microns. Cell debris was pulled down by spinning at 16,000 *g* for 2 min using the Eppendorf 5415 C centrifuge. The soluble supernatant was separated from the insoluble cell pellet. The cell pellet was then resuspended in 500 µL buffer 1. The soluble and insoluble fractions were analysed by SDS-PAGE.

PCR mixes were pipetted into 6 200 µL thin-walled PCR tubes. Stratagene's QuikChange method of SDSM mutagenesis was used to introduce mutations into the YSBLIC3C-PpLAAO plasmid using PCR cycle F (**Table 2.1**) and PCR mix F (**Table 2.2**) with the PNDTA-for and PNDTA-rev primers (**Table 2.3**), with the tubes placed in positions 2, 4, 6, 8, 10 and 12 of the Mastercycler gradient PCR machine. PCR products were analysed with 1 % agarose gel electrophoresis.

Based on these results, the Stratagene QuikChange reaction was repeated. PCR mixes were pipetted into two 200 µL thin-walled PCR tubes. The pET-YSBLIC3C-PpLAAO plasmid was used as a template for the PCR. The PCR was carried out as in section 3.1.5, using PCR cycling C (**Table 2.1**) and PCR mix F (**Table 2.2**) and the PNDTA-for and PNDTA-rev primers (**Table 2.3**). The two products were mixed together to make a total reaction volume of 50 µL. 25 µL of the PCR mix was analysed with 1% agarose gel electrophoresis. The remaining 25 µL of PCR mix was mixed with 1 µL of *DpnI* restriction enzyme. The mixture was incubated at 37°C for 3 h. 2 µL of reaction product was cooled and used to transform 25 µL of *E. coli* BL21-Gold-DE3 competent cell using heat shock.

Nine colonies were each used to inoculate 5 mL of LB-media containing 30 µg mL^{-1} kanamycin and 15 µg mL^{-1} tetracycline. These starter cultures were incubated at 37°C and shaking at 180 r.p.m overnight. The following day 100 µL of started culture was used to inoculate a fresh 5 mL culture

of LB-media containing 30 μg mL^{-1} kanamycin and 15 μg mL^{-1} tetracycline. These cultures were incubated at 37°C and shaking at 180 r.p.m until OD_{600} was at 0.5. Overexpression was induced by adding 5 μL of 1 M IPTG to give a final concentration of 1 mM IPTG. The cell culture was incubated at 37°C for 3 h with shaking at 180 r.p.m. The cells were harvested by centrifugation for 2 min at 16,000 *g* using an Eppendorf 5415 C centrifuge. The supernatant was discarded and the cell pellet was resuspended in 500 μL buffer 1. The cell suspension was sonicated on ice for 30 s at 15 microns. Cell debris was pulled down by spinning at 16,000 *g* for 2 min using an Eppendorf 5415 C centrifuge. The soluble supernatant was separated from the insoluble cell pellet. The cell pellet was then resuspended in 500 μL buffer 1. The soluble and insoluble fractions were analysed by 12.5% SDS-PAGE.

Mutant PNDTA plasmids were purified from the remaining 4.9 mL of starter culture using Sigma-Aldrich's GenElute Plasmid Miniprep kit. The concentration of DNA in the purified plasmids was determined by measuring the absorption at 280 nm using the dsDNA function on the Eppendorf BioPhotometer, with an A_{280} of 1 equal to a DNA concentration of 50 μg mL^{-1}. The plasmids were then concentrated to between 100 and 150 ng μL^{-1} using a GeneVac miVac DNA concentrator. Each plasmid was then sequenced by the University of York Genomics department using the T7 and T7-term primers (**Table 2.3**). Sequencing data output was analysed using the Chromas Lite programme developed by Technelysium Pty Ltd. Sequence alignments with the wild type-PpLAAO DNA sequence were performed using the Align program (needle method) hosted by the European Bioinformatics Institute (http://www.ebi.ac.uk/Tools/emboss/align/ Accessed 04/07/2010).

Ten more transformations of *E. coli* BL21-Gold-DE3 were performed using the PCR product mixed with *DpnI*, resulting in over 430 colonies. Colonies were scrubbed off the plates under sterile conditions by pipetting 2 mL of LB-media over each plate and resuspending the colonies by wiping the plate with glass spreader. The resuspended cells were the collected with a pipette and pooled together. Cells were spun down at 16,000 *g* for 2 min using the Eppendorf 5415 C centrifuge. The mutant plasmid library was then purified using Sigma Aldrich's GenElute Midiprep kit and stored at -20°C until needed.

LB-media (V= 1 L): 10 g tryptone, 5 g yeast extract, 10 g NaCl, H_2O (18.2 Ω· cm)

Buffer 1: 50 mM Tris/HCl, 300 mM NaCl, 20 μM AEBSF, pH 7.0

2.6.2 Building of SDSM CASTing library D

DpnI restriction enzyme was purchased from New England Biolabs. The ingredients for LB-media were purchased from Fisher, kanamycin sulphate was purchased from Invitrogen, tetracycline was purchased from Merck/Calbiochem. AEBSF and IPTG were purchased from Melford. OD_{600} was measured using an Eppendorf Biophotometer. PCRs were carried out in 200 µL thin-walled PCR tubes in a Techne TC-312 PCR machine.

Stratagene's QuikChange method of SDSM mutagenesis was used to introduce mutations into the YSBLIC3C-PpLAAO plasmid twice using PCR cycle G (**Table 2.1**) and PCR mix G (**Table 2.2**) along with and the PNDTD-for and PNDTD-rev primers (**Table 2.3**). PCR product was mixed with 1 µL of *DpnI* restriction enzyme and incubated at 37°C for 3 h. Duplicate PCRs were mixed to make a total reaction volume of 40 µL. 20 µL of product was analysed with 1% agarose gel electrophoresis, the remainder was stored at -20°C.

2 µL of *DpnI* treated PNDTD PCR product was used to transform 75 µL of E. coli Top10 electrocompetent cells using electroporation. This produced around 400 colonies. Five colonies from the transformation were each used to inoculate 5 mL of LB media containing 30 µg mL^{-1} of kanamycin. These starter cultures were incubated at 37°C with shaking at 180 r.p.m overnight. Plasmid DNA was purified using Sigma-Aldrich's GenElute Miniprep kit. To determine gene insert size, the plasmid DNA was amplified by PCR using PCR cycle condition A (**Table 2.1**), PCR mix H (**Table 2.2**) and the PpLAAO-for and PpLAAO-rev primers (**Table 2.3**). Product was analysed using 1% agarose gel electrophoresis.

Purified plasmids were sent for nucleotide sequencing (**Section 2.2.4**). The T7 and T7-term primers (**Table 2.3**) were used as sequencing primers. The sequencing reactions were carried out by the York University Genomics group. The sequence chromatograms were analysed with the program Chromas lite, version 2.01 from Technelysium (free software).

Transformations of the *E. coli* Top10 Electrocompetent cells using 2µL of *DpnI* treated PNDTD PCR product were repeated until around 3000 colonies had been produced. Colonies were scrubbed off the plates under sterile conditions by pipetting 2 mL of LB-media over each plate and resuspending the colonies by wiping the plate with glass spreader. The resuspended cells were the collected with a pipette and pooled together. Cells were spun down at 16,000 *g* for 2 min using the Eppendorf 5415 C centrifuge. The mutant plasmid library was then purified using Sigma Aldrich's GenElute Midiprep kit. The concentration of DNA in the purified library was determined to be 87

ng μL^{-1} using the dsDNA function of an Eppendorf Biophotometer. The purified PNDTD plasmid library was stored at -20°C until needed.

LB-media (V= 1 L): 10 g tryptone, 5 g yeast extract, 10 g NaCl, H_2O (18.2 Ω· cm)

Buffer 1: 50 mM Tris/HCl, 300 mM NaCl, 20 µM AEBSF, pH 7.0

2.6.3 Attempts to build SDSM libraries B, C and E using PfUTurbo HotStart Polymerase

PfUTurbo HotStart DNA polymerase kit was purchased from Agilent Technologies/Stratagene. dNTPs were purchased from Promega. High-purity salt free primers were purchased from MWG/Eurofins. PCRs were carried out in 200 µL thin-walled PCR tubes in a Techne TC-312 PCR machine.

Stratagene's QuikChange method of SDSM mutagenesis was used to introduce mutations into the YSBLIC3C-PpLAAO plasmid. The PCR mixes listed in **Table 2.7** were used along with PCR cycle C (**Table 2.1**) to amplify the YSBLIC3C-PpLAAO plasmid. This was done using the PNDTB-for/PNDTB-rev and the PNDTC-for/PNDTC-rev primer pairs (**Table 2.3**). The PCR mixes listed in **Table 2.8** were used along with PCR cycle C (**Table 2.1**) to amplify the YSBLIC3C-PpLAAO plasmid. This was done using the PNDTE-for/PNDTE-rev primer pairs (**Table 2.3**). PCR products were analysed with 1% agarose gel electrophoresis.

Table 2.7: Composition of PCR mix used for the amplification of DNA by PCR using PfU Turbo HotStart polymerase with PNDTB-for/PNDTB-rev and PNDTC-for/PNDTC-rev primer pairs.

	H_2O (18.2 Ω· cm)/ µL	10 * PfU Buffer/ µL	2 mM (each) dNTPs/ µL	10 µM F Primer/ µL	10 µM R Primer/ µL	10 ng μL^{-1} PpLAAO Plasmid/ µL	≥99.5% DMSO/ µL	PfUTurbo HotStart Polymerase/ µL
Optimisation condition 1	13.75	2.5	2.5	1.0	1.0	2.0	1.25	0.5
Optimisation condition 2	10.0	2.5	5.0	1.0	1.0	2.0	1.25	0.5
Optimisation condition 3	14.25	2.5	2.5	2.0	2.0	2.0	1.25	0.5
Optimisation condition 4	13.0	2.5	2.5	1.0	1.0	3.0	1.25	0.5
Optimisation condition 5	12.25	2.5	2.5	1.0	1.0	4.0	1.25	0.5
Optimisation condition 6	13.25	2.5	2.5	1.0	1.0	2.0	2.5	0.5

Table 2.8: Composition of PCR mix used for the amplification of DNA by PCR using PfU Turbo HotStart polymerase with PNDTE-for and PNDTE-rev primers.

	H_2O (18.2 Ω· cm)/ µL	10 * PfU Buffer/ µL	2 mM (each) dNTPs/ µL	10 µM F Primer/ µL	10 µM R Primer/ µL	10 ng $µL^{-1}$ PpLAAO Plasmid/ µL	≥99.5% DMSO/ µL	PfUTurbo HotStart Polymerase/ µL
Optimisation condition 1	16.25	2.5	2.5	0.5	0.5	1.0	1.25	0.5
Optimisation condition 2	13.75	2.5	5.0	0.5	0.5	1.0	1.25	0.5
Optimisation condition 3	15.25	2.5	2.5	1.0	1.0	1.0	1.25	0.5
Optimisation condition 4	15.25	2.5	2.5	0.5	0.5	2.0	1.25	0.5
Optimisation condition 5	14.25	2.5	2.5	0.5	0.5	3.0	1.25	0.5
Optimisation condition 6	15.00	2.5	2.5	0.5	0.5	1.0	2.5	0.5

2.6.4 PNDTE library SDSM reaction and transformation

PfUTurbo hot start DNA polymerase kit was purchased from Agilent Technologies/Stratagene. dNTPs were purchased from Promega. High-purity salt free primers were purchased from MWG/Eurofins. *DpnI* restriction enzyme was purchased from New England Biolabs. PCRs were carried out in 200 µL thin-walled PCR tubes in a Techne TC-312 PCR machine.

Stratagene's QuikChange method of SDSM mutagenesis was used to introduce mutations into the YSBLIC3C-PpLAAO plasmid using PCR cycle C (**Table 2.1**) and PCR mix I (**Table 2.2**) along with the PNDTE-for and PNDTE-rev primers (**Table 2.3**). PCR product was mixed with 1 µL of *DpnI* restriction enzyme and incubated at 37°C for 3 h. 20 µL of product was analysed with 1% agarose gel electrophoresis.

2 µL of the *DpnI* digested product were used to transform 75 µL of *E .coli* Top10 electrocompetent cells.

2.6.5 Attempts to build SDSM libraries B, C and E using Phusion Polymerase

Phusion hot start II High-fidelity DNA polymerase kit was purchased from New England Biolabs. dNTPs were purchased from Promega. High-purity salt free primers were purchased from MWG/Eurofins. PCRs were carried out in 200 µL thin-walled PCR tubes in a Techne TC-312 PCR machine.

Stratagene's QuikChange method of SDSM mutagenesis was used to introduce mutations into the YSBLIC3C-PpLAAO plasmid. The PCR mixes listed in **Table 2.9** were used along with PCR cycle G (**Table 2.1**) to amplify the YSBLIC3C-PpLAAO plasmid. This was done using the PNDTB-for/PNDTB-rev and the PNDTE-for/PNDTE-rev primer pairs (**Table 2.3**). The PCR mixes listed in **Table 2.10** were used along with PCR cycle G (**Table 2.1**) to amplify the YSBLIC3C-PpLAAO plasmid. This was done using the PNDTC-for/PNDTC-rev primer pairs (**Table 2.3**). PCR products were analysed with 1% agarose gel electrophoresis.

Table 2.9: Composition of PCR mix used for the amplification of DNA by PCR using Phusion HotStart II polymerase with PNDTB-for/PNDTB-rev and PNDTE-for/PNDTE-rev primer pairs.

	H_2O (18.2 Ω· cm)/ µL	5 * Phusion Buffer/ µL	2 mM (each) dNTPs/ µL	20 µM F Primer / µL	20 µM R Primer/ µL	10 ng $µL^{-1}$ PpLAAO Plasmid/ µL	≥99.5% DMSO/ µL	5 mM $MgSO_4$/ µL	Phusion HotStart II Polymerase / µL
Optimisation condition 1	11.2	4.0	2.0	0.5	0.5	1.0	0.6	0	0.2
Optimisation condition 2	9.2	4.0	4.0	0.5	0.5	1.0	0.6	0	0.2
Optimisation condition 3	11.7	4.0	2.0	0.25	0.25	1.0	0.6	0	0.2
Optimisation condition 4	11.7	4.0	2.0	0.5	0.5	0.5	0.6	0	0.2
Optimisation condition 5	10.8	4.0	2.0	0.5	0.5	1.0	1.0	0	0.2
Optimisation condition 6	10.4	4.0	2.0	0.5	0.5	1.0	0.6	0.8	0.2

Table 2.10: Composition of PCR mix used for the amplification of DNA by PCR using Phusion HotStart II polymerase with the PNDTC-for/PNDTC-rev primer pair.

	H_2O (18.2 Ω· cm)/ µL	5 * Phusion Buffer/ µL	2 mM (each) dNTPs/ µL	20 µM F Primer / µL	20 µM R Primer/ µL	10 ng $µL^{-1}$ PpLAAO Plasmid/ µL	≥99.5 % DMSO/ µL	5 mM $MgSO_4$/ µL	Phusion HotStart II Polymerase/ µL
Optimisation condition 1	9.2	4.0	4.0	0.5	0.5	1.0	0.6	0	0.2
Optimisation condition 2	7.2	4.0	6.0	0.5	0.5	1.0	0.6	0	0.2
Optimisation condition 3	9.7	4.0	4.0	0.25	0.25	1.0	0.6	0	0.2
Optimisation condition 4	9.7	4.0	4.0	0.5	0.5	0.5	0.6	0	0.2
Optimisation condition 5	8.8	4.0	4.0	0.5	0.5	1.0	1.0	0	0.2
Optimisation condition 6	8.4	4.0	4.0	0.5	0.5	1.0	0.6	0.8	0.2

Stratagene's QuikChange method of SDSM mutagenesis was used to introduce mutations into the YSBLIC3C-PpLAAO plasmid using PCR cycle G (**Table 2.1**) and PCR mix J (**Table 2.2**) along

with the PNDTB-for and PNDTB-rev and the PNDTE-for and PNDTE-rev primers (**Table 2.3**). Stratagene's QuikChange method of SDSM mutagenesis was used to introduce mutations into the YSBLIC3C-PpLAAO plasmid using PCR cycle G (**Table 2.1**) and PCR mix K (**Table 2.2**) along with the PNDTC-for and PNDTC-rev primers (**Table 2.3**). PCR product was mixed with 1 µL of *DpnI* restriction enzyme and incubated at 37°C for 3 h. 20 µL of product was analysed with 1% agarose gel electrophoresis. 2 µL of each of the *DpnI* digested products from the PNDTB and PNDTC reactions was used to transform 75 µL of *E. coli* Top10 electrocompetent cells.

Four colonies from the PNDTB reactions were each used to inoculate 5 mL of LB media containing 30 µg mL^{-1} of kanamycin. These starter cultures were incubated at 37°C with shaking at 180 r.p.m overnight. Plasmid DNA was purified using Sigma-Aldrich's GenElute Miniprep kit. To determine gene insert size, the plasmid DNA, along with the wild-type YSBLIC-3C-PpLAAO plasmid, was amplified by PCR using PCR cycle condition A (**Table 2.1**), PCR mix H (**Table 2.2**) and the PpLAAO-for and PpLAAO-rev primers (**Table 2.3**). Product was analysed using 1% agarose gel electrophoresis.

LB-media (V=1 L): 10 g tryptone, 5 g yeast extract, 10 g NaCl, H_2O (18.2 Ω·cm)

2.6.6 Attempts to build SDSM libraries B and C using KOD HotStart Polymerase

KOD HotStart DNA polymerase kit was purchased from Novagen. dNTPs were purchased from Promega. High-purity salt free primers were purchased from MWG/Eurofins. PCRs were carried out in 200 µL thin-walled PCR tubes in a Techne TC-312 PCR machine.

Stratagene's QuikChange method of SDSM mutagenesis was used to introduce mutations into the YSBLIC3C-PpLAAO plasmid. The PCR mixes listed in **Table 2.11** were used along with PCR cycle C (**Table 2.1**) to amplify the YSBLIC3C-PpLAAO plasmid. This was done using the PNDTB-for/PNDTB-rev and the PNDTC-for/PNDTC-rev primer pairs (**Table 2.3**). PCR products were analysed with 1% agarose gel electrophoresis.

Table 2.11 Composition of PCR mix used for the amplification of DNA by PCR using KOD HotStart polymerase with the PNDTB-for/PNDTB-rev and PNDTC-for/PNDTC-rev primer pairs.

	H2O (18.2 Ω·cm) / µL	10 * KOD Buffer/ µL	25 mM $MgSO_4$/ µL	2 mM (each) dNTPs/ µL	10 µM F Primer/ µL	10 µM R Primer/ µL	10 ng μL^{-1} PpLAAO Plasmid/ µL	≥99.5% DMSO/ µL	K.O.D HotStart Polymerase/ µL
Optimisation condition 1	13.75	2.5	1.5	2.5	1.0	1.0	1.0	1.25	0.5
Optimisation condition 2	10.0	2.5	1.0	2.5	2.0	2.0	2.0	2.5	0.5
Optimisation condition 3	14.25	2.5	1.0	2.5	1.0	1.0	1.0	1.25	0.5
Optimisation condition 4	13.0	2.5	1.0	2.5	1.0	1.0	1.0	2.5	0.5
Optimisation condition 5	12.25	2.5	1.0	2.5	2.0	2.0	1.0	1.25	0.5
Optimisation condition 6	13.25	2.5	1.0	2.5	1.0	1.0	2.0	1.25	0.5
Optimisation condition 7	12.5	2.5	1.5	2.5	1.0	1.0	1.0	2.5	0.5
Optimisation condition 8	10.5	2.5	1.5	2.5	2.0	2.0	1.0	2.5	0.5
Optimisation condition 9	11.5	2.5	1.5	2.5	1.0	1.0	2.0	2.5	0.5

Stratagene's QuikChange method of SDSM mutagenesis was used to introduce mutations into the YSBLIC3C-PpLAAO plasmid in 2x 25 µL reactions using PCR cycle C (**Table 2.1**) and PCR mix H (**Table 2.2**) with either the PNDTB-for and PNDTB-rev primers (**Table 2.3**) or the PNDTC-for and PNDTC-rev primers (**Table 2.3**). The 2 products were mixed together to make a total reaction volume of 50 µL. 25 µL of the PCR mix were analysed with 1% agarose gel electrophoresis (**Section 3.1.1**). The remaining 25 µL of PCR mix were mixed with 1 µL of *DpnI* restriction enzyme. The mixture was incubated at 37°C for 3 h. 2 µL of reaction product were cooled and used to transform 75 µL of *E. coli* Top10 Electrocompetent cells using electroporation.

Six colonies from the PNDTB reactions were each used to inoculate 5 mL of LB media containing 30 µg mL^{-1} of kanamycin. These starter cultures were incubated at 37°C with shaking at 180 r.p.m overnight. Plasmid DNA was purified using Sigma-Aldrich's GenElute Miniprep kit. To determine gene insert size, the plasmid DNA was amplified by PCR using PCR cycle condition A (**Table 2.1**), PCR mix H (**Table 2.2**) and the PpLAAO-for and PpLAAO-rev primers (**Table 2.3**). Product was analysed using 1% agarose gel electrophoresis.

LB-media (V=1 L): 10 g tryptone, 5 g yeast extract, 10 g NaCl, H_2O (18.2 Ω·cm)

2.7 Random mutagenesis of wild type PpLAAO gene sequence

PpLAAO gene sequence was mutagenized at a low range frequency using the Genemorph® II EZClone Domain Mutagenesis Kit, purchased from Stratagene. High-purity salt-free primers were synthesized by Eurofins/MWG Biotech (Ebersberg, Germany). Sigma-Aldrich GenElute Gel Purification Kit was purchased from Sigma-Aldrich. Materials for LB media were purchased from Fisher. PCR cycling was carried out using 500 µL thin-walled PCR tubes and a Techne TC312 thermal cycler. A control reaction was carried out as according to the Genemorph® II EZClone Domain Mutagenesis Kit instructions.

In order to create a target amount of 2-7 mutations in the gene sequence per transformant (1.25- 4.4 mutation kb^{-1}) the Genemorph® II EZClone Domain Mutagenesis Kit instructions recommend using an initial target quantity of 500-1000 ng of wild type gene DNA, which equates to 2.2-4.4 µg of wild-type pET-YSBLIC3C-PpLAAO plasmid using the following equation:

$$\frac{Target\ quantity\ (ng)}{Gene\ sequence\ size\ (kb)}\ \text{x}\ Total\ plasmid\ size\ (kb) = Amount\ of\ template\ needed\ (ng)$$

$$\frac{500\ ng}{1605\ kb}\ \text{x}\ 6963\ kb = 2169\ ng = 2.1\ \mu g$$

2.2 µg of wild-type pET-YSBLIC3C-PpLAAO was mutagenized using PCR cycle H (**Table 2.1**), PCR mix L (**Table 2.2**) and the PpLAAO-for and PpLAAO-rev primers (**Table 2.3**). 2.5 µL of the PCR megaprimer product and 2.5 µL (50 ng) of a 1.1 kb gel standard included in the Genemorph® II EZClone Domain Mutagenesis Kit were analysed by 1% agarose gel electrophoresis. The remaining product was then run on a 1% agarose gel and purified using the Sigma Aldrich GenElute Gel purification kit.

The megaprimer product was inserted into the pET-YSBLIC3C plasmid with Stratagene's EZClone reaction, using PCR cycle I (**Table 2.1**), PCR mix M (**Table 2.2**) and the megaprimer product. Reactions were cooled on ice to below 37°C. 1 µL of *DpnI* restriction enzyme (included in the kit) was added to the reaction product and mixed gently before incubation at 37°C for 2 h.

45 µL of *E. coli* XL10-Gold supercompetent cells were transformed with 1.5 µL of the *DpnI* treated reaction product as in **Section 2.1**. Ten 50 µL aliquots of the outgrowth solution were each plated onto one LB-agar plates containing 30 µg mL^{-1} of kanamycin, 34 µg mL^{-1} chloramphenicol and 15 µg mL^{-1} tetracycline. This resulted in over 4000 colonies. 10 colonies were each used to inoculate 5 mL of LB-media containing 30 µg mL^{-1} of kanamycin, 34 µg mL^{-1} chloramphenicol and

15 μg mL^{-1} tetracycline and were grown overnight at 37°C with shaking at 180 r.p.m. Cells were then spun down at 16,000 *g* using an Eppendorf 5415 C centrifuge and pellets were stored at -20°C until needed.

Colonies were scrubbed off the plates by pipetting 2 mL of LB+ media to each plate and resuspending the colonies into the media using a glass spreader under sterile conditions. Resuspended colonies were collected using a pipette and spun down at 16,000 *g* using an Eppendorf 5415 C centrifuge. Mutated plasmids were purified using Sigma-Aldrich's GenElute Plasmid Miniprep Kit and stored at -20°C until needed.

LB+ media (V= 1 L): 10 g tryptone, 5 g yeast extract, 10 g NaCl, 12.5 mL 1 M $MgCl_2$, 12.5 mL 1 M $MgSO_4$, 20 mL 20% (w/v) D-glucose, H_2O (18.2 Ω·cm)

LB-agar (V= 1 L): 10 g tryptone, 5 g yeast extract, 10 g NaCl, 15 g agar, H_2O (18.2 Ω·cm)

LB media (V= 1 L): 10 g tryptone, 5 g yeast extract, 10 g NaCl, H_2O (18.2 Ω·cm)

2.8 Screening of Random Mutagenesis and SDSM CASTing libraries

2.8.1 Solid Phase HRP assay of Random Mutagenesis and SDSM CASTing libraries A and D

Colonies lifted using Whatman filter paper. DAB tablets and HRP were purchased from Sigma-Aldrich, KH_2PO_4/K_2HPO_4 buffer solution was provided by Ingenza Ltd.

1 μL of purified PNDTA plasmid library (prepared as in **Section 2.6**) was used to transform *E. coli* BL21-DE3 Electrocompetent cells using electrophoresis. Cells were diluted by 6 times in LB-media and 120 μL aliquots of diluted cells were each spread over one LB-agar plate containing 30 μg mL kanamycin and 100 μM IPTG.

2 μL of purified PNDTD plasmid library (prepared as in **Section 2.6**) was used to transform 50 μL of *E. coli* Rosetta-2-DE3 competent cells using heat shock. 100 μL aliquots were each spread over one LB-agar plate containing 30 μg mL^{-1} kanamycin, 34 μg mL^{-1} chloramphenicol and 100 μM IPTG.

2 μL of purified random mutagenesis plasmid library (prepared as in **Section 2.7**) was used to transform 50 μL of *E. coli* Rosetta-2-DE3 competent cells using heat shock. 100 μL aliquots were each spread over one LB-agar plate containing 30 μg mL^{-1} kanamycin, 34 μg mL^{-1} chloramphenicol and 100 μM IPTG.

Resulting colonies were lifted off of the plates onto filter paper under sterile conditions by placing an 8 cm disk of filter paper directly onto the LB-agar and rubbing with a glass spreader until wet through. Filter paper was lifted off of plate and placed colony side up into a sealable box containing damp tissue paper. Boxes were sealed and frozen overnight at -80°C.

The next morning the filter papers containing colonies were thawed at room temperature for one h. Fresh 8 cm filter paper disks were placed into 8 cm round petri dishes containing 2 mL of assay solution and allowed to soak up assay solution. One thawed filter paper was placed colony side up into each petri dish. Petri dishes were then placed with lids on into a sealed box containing damp tissue paper. The sealed box was left in the dark to allow assays to develop. Colonies showing oxidase activity turned brown compared to colonies containing no active oxidase (**Figure 2.4**).

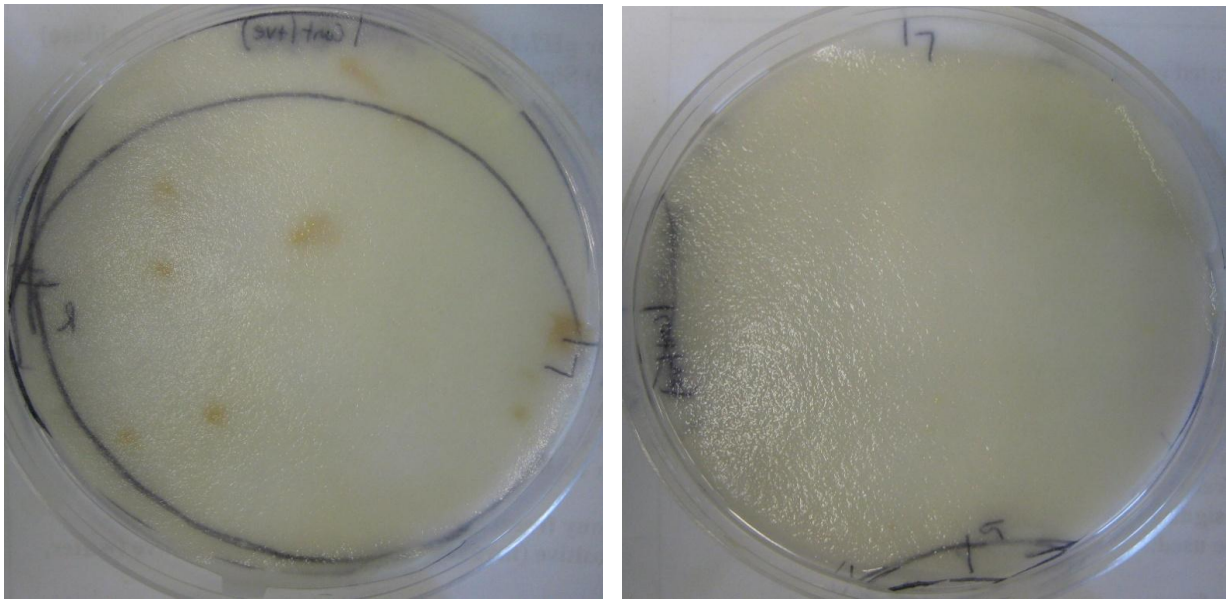

Figure 2.4 Example of solid phase HRP-based oxidase assay. **a.** Wild-type PpLAAO colonies screened with 20 mM L-aspartate as substrate, brown colour shows presence of H_2O_2 produced by active oxidase. b Wild-type PpLAAO colonies screened with H_2O (18.2 Ω·cm) as substrate, no brown colour development seen.

The PNDTA library was screened with 20 mM L-aspartate, 1 mM, 2 mM, 4 mM, 10 mM and 20 mM LD-asparagine and 40 mM, 60 mM, 80 mM and 100 mM L-homoserine as substrate. Screens were left to develop for 4 d.

The PNDTD library was screened with 40 mM LD-aspartate (1 plate), 100 mM L-homoserine (8 plates), 100 mM L-alanine (10 plates) and 25 mM L-tyrosine (10 plates) as substrate. The screens against L-aspartate and L-homoserine were left to develop for 4 d, the screen against L-alanine was left to develop for 1 d and the screen against L-tyrosine was left to develop for 2 d. The wild-type

control was screened with 40 mM LD-aspartate and H_2O (18.2 Ω·cm) as substrate. Photos of the plate assays were then taken using an Apple iPod Touch Generation 4.

The random mutagenesis library was screened against 20 mM L-aspartate, 20 mM L-tyrosine, 20 mM L-arginine, 20 mM L-glutamate and 20 mM L-glutamine. Screens were left to develop for 1 d.

Assay solution: 1 DAB tablet per 20 mL, 100 mM KH_2PO_4/K_2HPO_4, 25 μg mL^{-1} HRP, varied concentration of substrate, pH 7.5

2.8.2 Analysis of potential hits from CASTing library A

BugBuster was purchased from Novagen. Benzonase, TBHBA, Lysozyme and 96-well flat-bottomed plates were provided by Ingenza Ltd. Bradford reagent was purchased from BioRad. HRP and 4-AAP were purchased from Sigma-Aldrich. Protein concentration was determined using the Bradford assay setting of an Eppendorf BioPhotometer.

Two colonies from the PNDTA screen against 2 mM LD-asparagine (Referred to as LD-Asn-O1 and 2) and one colony from the PNDTA screen against 40 mM L-homoserine (Referred to as L-Hse-O) deemed to have potential oxidase activity were picked from the filter paper and used to inoculate 5 mL LB-media contained 30 μg mL^{-1} kanamycin. These starter cultures were incubated at 37°C with shaking at 180 r.p.m overnight. 100 μL of starter culture was used to inoculate a fresh 5 mL culture of LB-media containing 30 μg mL^{-1} kanamycin. Culture was incubated at 32°C with shaking at 180 r.p.m until OD_{600} reached 0.5. Overexpression was induced by adding 5 μL of 1 M IPTG, to give a final concentration of 1 mM IPTG. Cells were incubated at 32°C with shaking at 180 r.p.m for 5 h. OD_{600} was measured and a volume of cells equivalent to 1 mL of a culture with OD_{600} at 5.0 was spun down at 16,000 *g* using a benchtop centrifuge. Cell pellets were stored at -20°C.

Cell pellets were resuspended in 161 μL of resuspension solution. Resuspended cells were incubated at 30°C with shaking at 200 r.p.m for 30 min to lyse. Cell debris was spun down at 16,000 *g* for 1 min using a benchtop centrifuge. Soluble supernatant was transferred to a fresh Eppendorf tube. 20 μL of lysate was diluted with 180 μL of H_2O (18.2 Ω·cm) three times. 50 μL of diluted lysate was mixed with 1450 μL of Bradford reagent. A reagent/lysate mixture was left for 15 min at room temperature to develop. A_{595} was measured using the Bradford setting on an Eppendorf Biophotometer three times for each dilution. Protein concentration was determined using a standard curve for protein concentration that had been set previously. The mean of the three readings was calculated and used to determine the mean concentration of protein in each cell lysate.

10 µL of lysate was pipetted into a single well of a 96-well plate three times for each substrate tested. 190 µL of assay solution was added to each well. Each lysate was tested against 100 mM L-homoserine, 20 mM LD-asparagine, 20 mM L-aspartate and H_2O (18.2 Ω·cm).

$Abs_{510\ nm}$ over 5 min was measured using Ingenza's 96-well plate reader. The plate was then left at room temperature to develop for 1 h, and A_{510} was measured using the 96-well plate reader. Rate of reaction was determined by subtracting the absorbance at 0 min from the absorption after 5 min. The mean rate of reaction of the control reactions using H_2O (18.2 Ω·cm) as a substrate was subtracted from the rates of the other reactions to remove any background absorbance. The mean absorption measurement of the control reactions after 1 h was also subtracted from the absorption of the other reactions after 1 h.

LB-media (V=1 L):	10 g tryptone, 5 g yeast extract, 10 g NaCl, H_2O (18.2 Ω·cm)
Resuspension solution (V= 161 µL):	150 µL BugBuster, 25 U Benzonase, 0.15 µg Lysozyme
2 x Reaction Buffer (V= 50 mL):	100 mM KH_2PO_4/K_2HPO_4, 20 mg (TBHBA), 15 mg 4-AAP, pH 7.5
Assay solution:	1 x Reaction Buffer, 25 µg mL^{-1} HRP, and varied concentration of substrate

2.8.3 Analysis of potential Screening Hits from CASTing library D

TBHBA was purchased from Alfa Aesar. 4-AAP, HRP, L-alanine, L-asparagine, L-aspartate and L-tyrosine were purchased from Sigma-Aldrich. KH_2PO_4 and K_2HPO_4 were purchased from Fisher, AEBSF was purchased from Melford and 96-well flat bottomed plates were purchased from Corning Costar. A_{510} was measured on a BMG Labtech PolarStar Optima plate reader.

Three colonies from the PNDTD screen against L-aspartate (labelled Asp1-3) seven colonies from the PNDTD screen against L-homoserine (labelled H1-7), ten colonies from the PNDTD screen against L-alanine (labelled Ala1-10) and five colonies from the screen against L-tyrosine (labelled Tyr1-5) that had developed a brown colour (**Figures 6.16-6.19**) were picked from the filter paper and used to inoculate 5 mL of LB-media containing 30 µg mL^{-1} kanamycin and 34 µg mL^{-1} chloramphenicol. These starter cultures were grown overnight at 37°C with shaking at 180 r.p.m. (Cultures Asp3, H1, H7 and Tyr4 failed to grow).

The next morning 100 µL of starter culture was used to inoculate 5 mL of fresh LB-media containing 30 µg mL^{-1} kanamycin and 34 µg mL^{-1} chloramphenicol. The remaining starter culture

was spun down at 16,000 *g* in an Eppendorf 5415 C centrifuge and stored at -20°C. The fresh cultures were grown at 37°C with shaking at 180 r.p.m until OD_{600} reached 0.5. Gene overexpression was induced with 1 mM of IPTG and cells were left to grow at 16°C overnight. Cells were spun down at 16,000 *g* for 1 min using an Eppendorf 5415 C centrifuge. Cell pellets were resuspended in 500 µL of buffer 1 and sonicated for 20 s at 15 microns. Cell debris was then spun down for 5 min at 13,700 *g* in the Eppendorf 5415 C centrifuge. Soluble supernatant was transferred into a fresh eppendorf tube and the insoluble pellet was resuspended in 500 µL of buffer 1. Insoluble protein samples were analysed on 12% SDS-PAGE.

Based on those results (**Figure 6.20**) the Ala3, Ala5 and Ala6 pellets stored earlier were mini-prepped using the Sigma-Aldrich Gen Elute Plasmid Miniprep kit to purify the plasmids. Plasmids were concentrated to between 100-150 ng μL^{-1} and then sent for sequencing (**Section 2.2.4**) using the T7 and T7-term primers (**Table 2.3**) by the York University Genomics group. The sequence chromatograms were analysed with the program Chromas lite, version 2.01 from Technelysium (free software).

Buffer 1:	50 mM Tris/HCl, 300 mM NaCl, 20 µM AEBSF, pH 7.0
2 x Reaction Buffer (V= 50 mL):	100 mM KH_2PO_4/K_2HPO_4, 20 mg (TBHBA), 15 mg 4-AAP, pH 7.5
Assay solution:	1 x Reaction Buffer, 25 µg mL^{-1} HRP, and varied concentration of substrate

2.8.4 Analysis of three error-prone PCR mutants

TBHBA was purchased from Alfa Aesar. 4-AAP, HRP, L-alanine, L-asparagine, L-aspartate, L-glutamate, L-glutamine and L-tyrosine were purchased from Sigma-Aldrich. KH_2PO_4 and K_2HPO_4 were purchased from Fisher, AEBSF was purchased from Melford and 96-well flat bottomed plates were purchased from Corning Costar. A_{510} was measured on a BMG Labtech PolarStar Optima plate reader.

Five colonies from the epPCR screen against L-aspartate (labelled PPM 1-5) were picked from the filter paper and used to inoculate 5 mL of LB-media containing 30 µg mL^{-1} kanamycin and 34 µg mL^{-1} chloramphenicol. These starter cultures were grown overnight at 37°C with shaking at 180 r.p.m. The next morning 100 µL of starter culture was used to inoculate 5 mL of fresh LB-media containing 30 µg mL^{-1} kanamycin and 34 µg mL^{-1} chloramphenicol. The remaining starter culture was spun down at 16,000 *g* in an Eppendorf 5415 C centrifuge and stored at -20°C.

The fresh cultures were grown at 37°C with shaking at 180 r.p.m until OD_{600} reached 0.5. Gene overexpression was induced with 1 mM of IPTG and cells were left to grow at 16°C overnight. Cells were spun down at 16,000 *g* for 1 min using an Eppendorf 5415 C centrifuge. Cell pellets were resuspended in 500 µL of buffer 1 and sonicated for 20 s at 15 microns. Cell debris was then spun down for 5 min at 13,700 *g* in the Eppendorf 5415 C centrifuge. Soluble supernatant was transferred into a fresh eppendorf tube and the insoluble pellet was resuspended in 500 µL of buffer 1. Insoluble and soluble protein samples were analysed on 12% SDS-PAGE.

Soluble protein fractions were tested for activity against 20 mM L-aspartate using the assay solution. Assays were prepared in a 1.5 mL Eppendorf tube and left to develop for 1 h. Colour development was determined by visual inspection.

The cells pellets stored earlier were mini-prepped using the Sigma-Aldrich Gen Elute Plasmid Miniprep kit to purify the plasmids. Plasmids were concentrated to between 100-150 ng μL^{-1} and then sent for sequencing (**Section 2.2.4**) using the T7 and T7-term primers by the York University Genomics group. The sequence chromatograms were analysed with the program Chromas lite, version 2.01 from Technelysium (free software). Distance of mutated residues from active site of the *E. coli* L-aspartate oxidase structure created by Bossi *et al.*[65] was calculated using Coot.[113]

Buffer 1:	50 mM Tris/HCl, 300 mM NaCl, 20 µM AEBSF, pH 7.0
2 x Reaction Buffer (V= 50 mL):	100 mM KH_2PO_4/K_2HPO_4, 20 mg (TBHBA), 15 mg 4-AAP, pH 7.5
Assay solution:	1 x Reaction Buffer, 25 µg mL^{-1} HRP, 20 mM L-aspartate

Chapter 3 Cloning, Expression and Assay of Targets

In order to increase the available repertoire of oxidases, particularly ones with activity against L-alanine and L-tyrosine, and to determine which oxidase would be worth focusing on, seven target oxidases; all within the first fifteen BLAST homology results of the L-amino acid oxidase (L-AAO) from *Synechococcus* ATCC 27144, in organisms for which we had access to genomic DNA and described as putative L-AAOs, Oxidoreductases (ORs) or Amine Oxidases (AOs) (**Table 3.1**) (**Figure 3.1**), were selected to be cloned using Ligation Independent Cloning (LIC) into the modified pET28a plasmid, pET-YSBLIC3C.

Table 3.1: Summary of seven target oxidases to be cloned into pET-YSBLIC3C.

UniProt Code	Classification	Species	Known substrates	Abbreviation
P72346	L-amino acid oxidase	*Synechococcus* sp. strain ATCC 27144	L-arginine, L-lysine	SLAAO
Q8VPD4	L-amino acid oxidase	*Rhodococcus opacus*	L-alanine, L-histidine	RoLAAO
Q88MZ2	L-amino acid oxidase	*Pseudomonas putida*	L-aspartate	PpLAAO
O31616	L-amino acid oxidase	*Bacillus subtilis*	Glycine, sarcosine[101]	BsGO
Q8YKW9	L-amino acid oxidase	*Anabaena* sp. strain PCC 7120	-	AsAAO
Q5YV66	Oxidoreductase	*Nocardia farcinica*	-	NfOR
Q81RW3	Amine Oxidase	*Bacillus anthracis*	-	BaAO

The pET-YSBLIC3C vector was made from Novagen's pET28a3C plasmid, which contains a 3C protease recognition site and hexa-histidine (His_6) purification tag (**Figure 3.2a**), however recognition sites *AscI* and *BseRI* have been added, and thymine bases in the His_6 tag have been replaced with cytosines (**Figure 3.2b**). When the *BseRI* restriction site is cleaved it causes staggered cleavage 8 bp to 10 bp upstream of the site on both strands, which results in the linearised plasmid having 2 bp long 3' overhangs. These overhangs on the plasmids are treated with bacteriophage T4 DNA polymerase in the presence of dTTP, which results in the excision of the 3' overhangs up to the first thymine on the 3' side, leaving a 14-15 bp 5' overhang on each side.[114]

The desired gene insert for the pET-YSBLIC3C plasmid can then be amplified using primers with LIC-specific additions, which when treated with T4 DNA polymerase in the presence of dATP result in 5' overhangs complementary to those on the pET-YSBLIC3C plasmid, allowing for a ligation reaction that is independent of a ligase enzyme to be performed.[114]


Q8VPD4_RoLAAO
Q5YV66_NfOR
P72346_SLAAO
Q81RW3_BaAO
Q8YKW9_AsAAO
O31616_BsGO
Q88MZ2_PpLAAO

```
Q8VPD4_RoLAAO      FP-YdhynsdrgvVvayYssGKrqEAfeslthrqRlAkaIaEgseihGek-YTrdisssf
Q5YV66_NfOR        Fd--ntppagspGVLvgFleGRhaDAcsrmdhptRrAqvIdDlagyfGprarTpidyiEk
P72346_SLAAO       id-itgnegggyGntffYlnGRnkDAmlarPkseRaqaiVdqfrsdlpdl-Fdevvtlad
Q81RW3_BaAO        YPsYgihtpgaatVLasYtwadealtwdslPdreRiryaLkNlaeiyGeivYSefvtgts
Q8YKW9_AsAAO       w-----drpektGILhaYlkGekgleidgfegktQqqklLqhwekilpgv--Snysvrsy
O31616_BsGO        YhdHcyivprksGrLvvgatmKpgD-wsetPdlgglesvMkkaktmlpai---qnmkvDr
Q88MZ2_PpLAAO      iPvvpaahytcgGVMv--------DdcghtdvpglyaigetsftglhGanrmAsnsllEc

Q8VPD4_RoLAAO      sgSWrRt--------------kYSesAWanwagsGgshggaatpeYek-llEPvdkIy-F
Q5YV66_NfOR        --dWade--------------eYSrGcy------GaftapgtltrfghalrpfiGplH-w
P72346_SLAAO       F-AWgeq--------------pwirGSf------Ggpplgga--wmirewttPeGlIH-F
Q81RW3_BaAO        F-SWsKn--------------pYScGAf------tafepgqElelFpy-itsPsGkVH-F
Q8YKW9_AsAAO       FhSWtKd--------------iwSkGgW------ayptdeqEkklFpe-lgKseGkIy-F
O31616_BsGO        F--Wa----------------------------Glrpgtk DgkpYigrhpEdsrilf-a
Q88MZ2_PpLAAO      F-vygRaaaadiqahleqvampkalpgWda----sqvtdsdEdviiahnwdElrrfmwdY

Q8VPD4_RoLAAO      AGdHlsna-iaWqhGALt----------SardVvthI----------------------
Q5YV66_NfOR        AGteTatrwaGYidGAaE----------SGhRtAREI----------------------
P72346_SLAAO       AGdfTTmk-sGWvEGAIE----------SGlRaARqI----------------------
Q81RW3_BaAO        AGeHTTlt-hGWmQGAIE----------SGiRVAhEV----------------------
Q8YKW9_AsAAO       AGeHTskt-rGWlQGALE----------SGlKaAQEI----------------------
O31616_BsGO        AGhfrngillapatGALi----------SdliMnKEV----------------------
Q88MZ2_PpLAAO      vGivrTskrlqraQhrIrllldeidefySnyKVSRdlielrnlaqvaelmilsamqrkes

Q8VPD4_RoLAAO      --------hervaqEa-----------
Q5YV66_NfOR        --------aaaldprhDaaspsalR--
P72346_SLAAO       --------dpgaqpEaDtflrQeqRcn
Q81RW3_BaAO        --------nek----------------
Q8YKW9_AsAAO       --------hfagstapr----------
O31616_BsGO        --------nqdwlhafridrkEavqi-
Q88MZ2_PpLAAO      rglhytldypgmldEakdtilnpl---
```

Figure 3.1 MUSCLE sequence alignment of the seven targets selected to be cloned into pET-YSBLIC3C. Identical residue highlighted in blue, similar residues highlighted in grey.

a.

3C Protease

5′-TATA**CCATGG**GCAGCAGCCATCATCATCATCATCACAGCAGCGGCCTGGAAGTTCTGTTCCAGGGGCCC**CATATG**GCTAGCATGACTGGT-3′

3′-ATAT**GGTACC**CGTCGTCGGTAGTAGTAGTAGTAGTGTCGTCGCCGGACCTTCAAGACAAGGTCCCCGGG**GTATAC**CGATCGTACTGACCA-5′

MetGlySerSerHisHisHisHisHisHisSerSerGlyLeuGluValLeuPheGlnGlyProHisMetAlaSerMetThrGly

b.

LIC

AscI

5′-TATA**CCATGG**GCAGCAGCCATCATCACCACCACCACAGGCGCGCCTTCTCCTCACTGTTCCAGGGGCCC**CATATG**GCTAGCATGACTGG-3′

3′-TATA**GGTACC**CGTCGTCGGTAGTAGTGGTGGTGGTGTCCGCGCGGAAGAGGAGTGACAAGGTCCCCGGG**GTATAC**CGATCGTACTGACC-5′

MetGlySerSerHisHisHisHisHisHis *BseRI*

Figure 3.2 a. Cloning region of Novagen pET28a derivative pET28a3C, sequences coding for His_6 protein purification tag and the 3C protease recognition site are underlined. Recognition sequences for *NcoI* (CCATGG) and *NdeI* (CATATG) are highlighted in bold. **b.** LIC region of pET-YSBLIC3C. Recognition sequences for *AscI* (GGCGCGCC) and *BseRI* (GAGGAG) are underlined and labelled. Recognition sequences for *NcoI* (CCATGG) and *NdeI* (CATATG) are highlighted in bold.

Cloned targets were then used to transform *E. coli* BL21-DE3, B834-DE3 and Rosetta-2-DE3 competent protein expression strains to assess expression levels and solubility of each target.

Whole cells and soluble protein fractions of each target protein were then screened for activity against all 20 natural amino acids and three amines, amylamine, phenylethylamine and AMBA.

3.1 Cloning of targets into pET-YSBLIC3C plasmid

The L-AAOs from *Synechococcus* sp. strain ATCC 27144, *Rhodococcus opacus* and *Pseudomonas putida* (SLAAO, RoLAAO and PpLAAO, respectively) had already been cloned into the pET-YSBLIC3C vector by the Technology Facility of the University of York. The L-AAOs from *Bacillus subtilis* and *Anabaena* sp. strain PCC 7120 (BsGO and AsAAO respectively), the oxidoreductase from *Nocardia farcinica* (NfOR) and the amine oxidase from *Bacillus anthracis* (BaAO) were amplified from genomic DNA via PCR as in **Section 2.2.1** (**Figure 3.3**).

The non recombinant pET-YSBLIC3C vector was cut with restriction endonuclease *BseRI*, a LIC-qualified T4 DNA polymerase was used to excise the 3' strand of the amplified gene insert and the restricted pET-YSBLIC3C plasmid up to the first adenine and thymine nucleotide, respectively, leaving 5' overhangs with complementary sequences between the amplified gene insert and the restricted pET-YSBLIC3C plasmid.

The gene insert was then annealed to the pET-YSBLIC3C plasmid and transformed into *E. coli* Novablue competent cells as in **Section 2.2.2**. Several colonies from each target transformation were picked for plasmid purification. The size of the insert was checked by restriction analysis (**Section 2.2.3, Figure 3.4)** and plasmids with the correctly sized insert (AsAAO 4, BaAO 4, BsGO 1 and NfOR 2) were sent for sequencing (**Section 2.2.4**). All sequences were as expected with no undesired mutations.

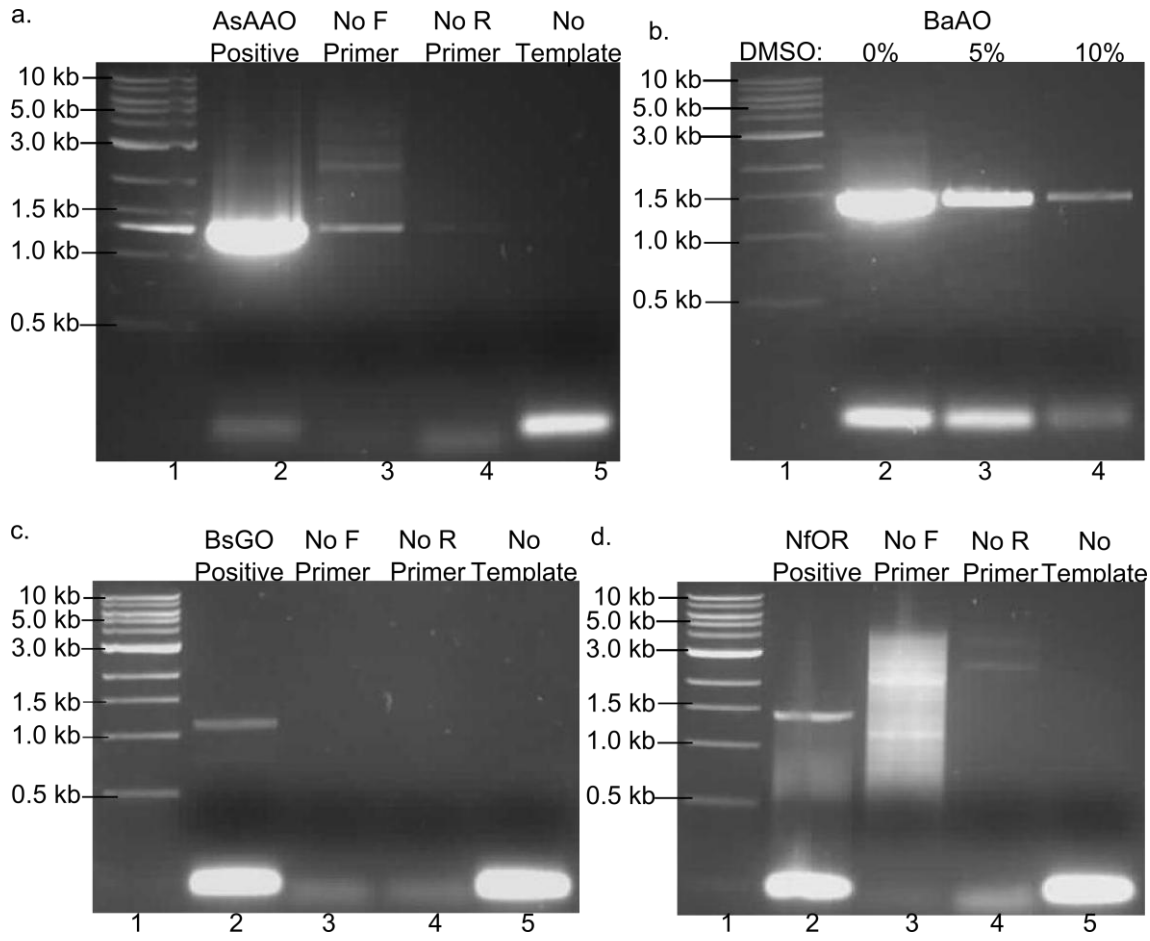

Figure 3.3: 1% agarose gel separations of DNA from PCR amplification of cloning targets. **a.** Amplification of AsAAO from *Anabaena* genomic DNA: Lane 1, 1 kb DNA Ladder (0.5 kb, 1 kb, 1.5 kb, 2 kb, 3 kb, 4 kb, 5 kb, 6 kb, 8 kb, 10 kb); Lane 2, Positive reaction (1281 bp); Lane 3, forward primer negative control; Lane 4, reverse primer negative control; Lane 5, template negative control. **b.** Amplification of BaAO from *Bacillus anthracis* genomified DNA: Lane 1, 1 kb DNA Ladder (0.5 kb, 1 kb, 1.5 kb, 2 kb, 3 kb, 4 kb, 5 kb, 6 kb, 8 kb, 10 kb); Lane 2, positive reaction in 0% DMSO (1437 bp); Lane 3, positive reaction in 5% DMSO; Lane 4, positive reaction in 10% DMSO. **c.** Amplification of BsGO from *Bacillus subtilis* genomic DNA: Lane 1, 1 kb DNA Ladder (0.5 kb, 1 kb, 1.5 kb, 2 kb, 3 kb, 4 kb, 5 kb, 6 kb, 8 kb, 10 kb); Lane 2, Positive reaction (1110 bp); Lane 3, forward primer negative control; Lane 4, reverse primer negative control; Lane 5, template negative control. **d.** Amplification of NfOR from *Nocardia* genomic DNA: Lane 1, 1 kb DNA Ladder (0.5 kb, 1 kb, 1.5 kb, 2 kb, 3 kb, 4 kb, 5 kb, 6 kb, 8 kb, 10 kb); Lane 2, Positive reaction (1392 bp); Lane 3, forward primer negative control; Lane 4, reverse primer negative control; Lane 5, template negative control.

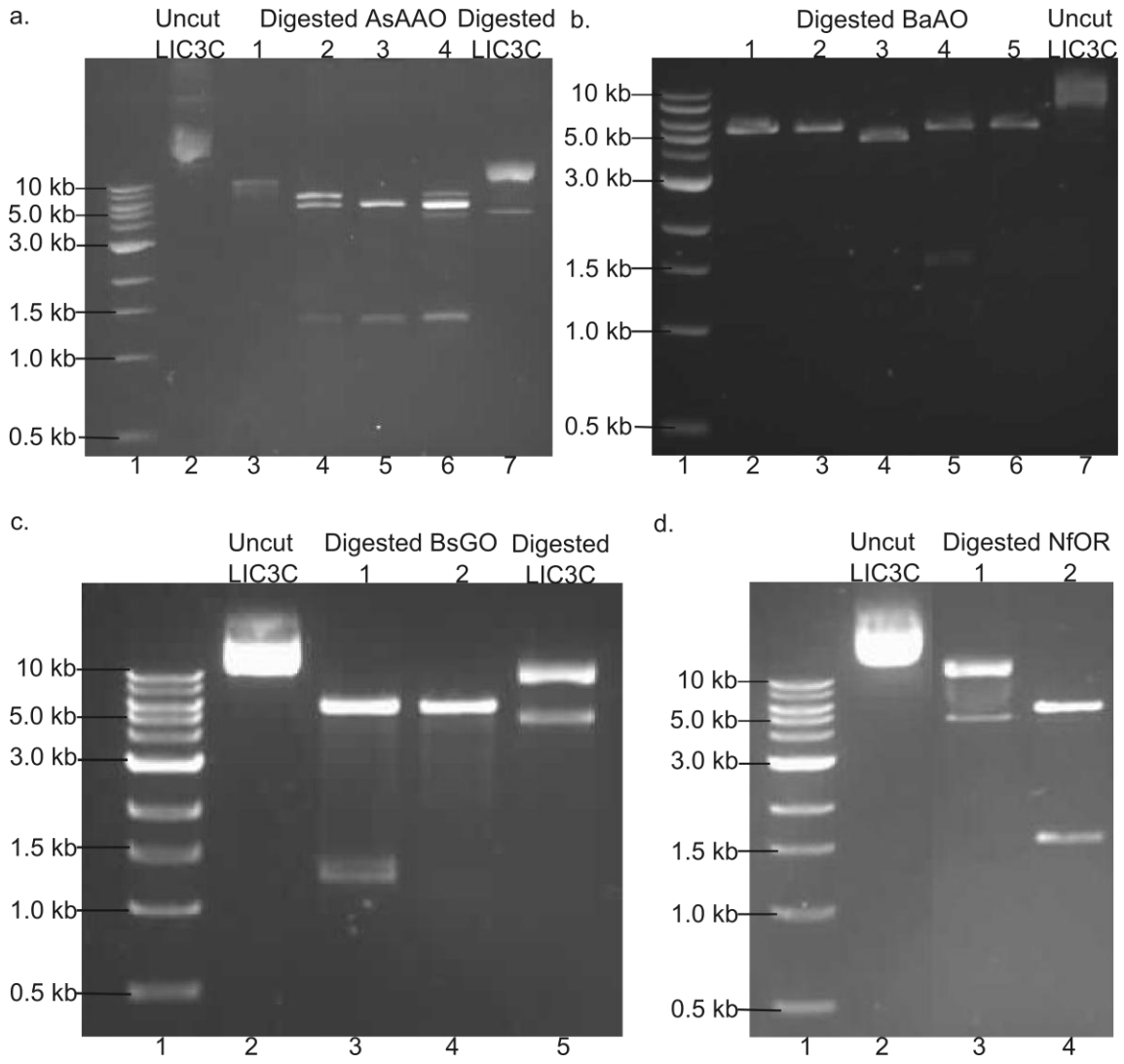

Figure 3.4: 1% agarose gel separation of restriction digest of potential AsAAO plasmids: Lane 1, 1kb DNA Ladder (0.5 kb, 1 kb, 1.5 kb, 2 kb, 3 kb, 4 kb, 5 kb, 6 kb, 8 kb, 10 kb); Lane 2, Uncut LIC3C vector; Lane 3-6, digested AsAAO colonies 1-4; Lane 7, Control colony. **b.** 1% PAGE gel separation of restriction digest of potential BaAO plasmids: Lane 1, 1kb DNA Ladder (0.5 kb, 1 kb, 1.5 kb, 2 kb, 3 kb, 4 kb, 5 kb, 6 kb, 8 kb, 10 kb); Lane 2-6, digested BaAO colonies 1-5; Lane 7, Uncut LIC3C vector. **c.** 1% PAGE gel separation of restriction digest of potential BsGO plasmids: Lane 1, 1kb DNA Ladder (0.5 kb, 1 kb, 1.5 kb, 2 kb, 3 kb, 4 kb, 5 kb, 6 kb, 8 kb, 10 kb); Lane 2, Uncut LIC3C vector; Lane 3-4, digested BsGO colonies 1-2; Lane 5, Control colony. **d.** 1% PAGE gel separation of restriction digest of potential NfOR plasmids: Lane 1, 1kb DNA Ladder (0.5 kb, 1 kb, 1.5 kb, 2 kb, 3 kb, 4 kb, 5 kb, 6 kb, 8 kb, 10 kb); Lane 2, Uncut LIC3C vector; Lane 3-4 digested NfOR colonies 1-2.

3.2 Expression and solubility of targets

The seven cloned targets and the non recombinant pET-YSBLIC3C vector were each used to transform *E. coli* BL21-DE3, B834-DE3 and Rosetta-2-DE3 competent protein productions strains. For each target and strain, gene overexpression was induced at 16°C overnight, 30°C for 5 hours and 37°C for 3 hours. Cells were then sonicated and separated into insoluble and soluble protein fractions as in **Section 2.2.5**. Protein fractions were the analysed using 12% SDS-PAGE (**Figures 3.5 - 3.12**).

The pET-YSBLIC3C vector was used as a negative control (**Figure 3.5)**.

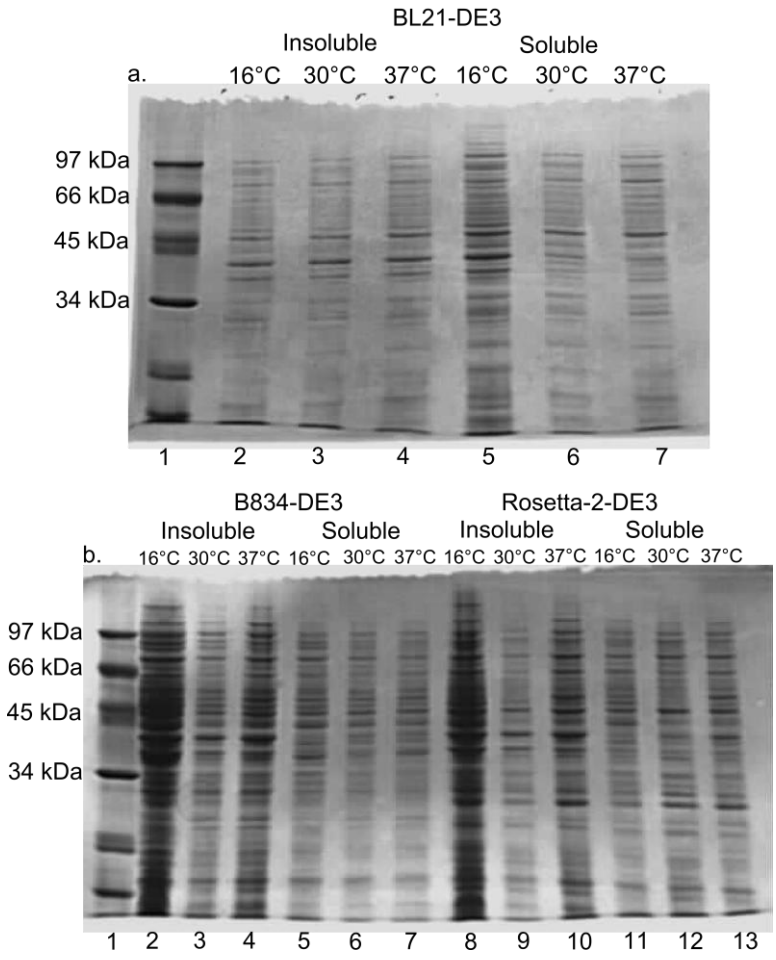

Figure 3.5: **a.** SDS-PAGE separation of protein from *E. coli* BL21-DE3 transformed with non recombinant pET-YSBLIC3C plasmid: Lane 1, low range molecular weight marker; Lane 2-4, BL21-pET-YSBLIC3C insoluble fraction 16/30/37°C induction; Lane 5-7, BL21- pET-YSBLIC3C soluble fraction 16/30/37°C induction. **b**. SDS-PAGE separation of protein from *E. coli* B834-DE3 and Rosetta-2-DE3 transformed with non recombinant pET-YSBLIC3C plasmid. Lane 1, low range molecular weight marker; Lane 2-4, B834-pET-YSBLIC3C insoluble fraction 16/30/37°C induction; Lane 5-7, B834-pET-YSBLIC3C soluble fraction 16/30/37°C induction; Lane 8-10, Rosetta-2-pET-YSBLIC3C insoluble fraction 16/30/37°C; Lane 11-13 Rosetta-2-pET-YSBLIC3C soluble fraction 16/30/37°C induction.

The pET-YSBLIC3C-AsAAO strains all expressed genes encoding proteins close to the correct size (48 kDa), however protein solubility was poor even at lower induction temperatures (**Figure 3.6**).

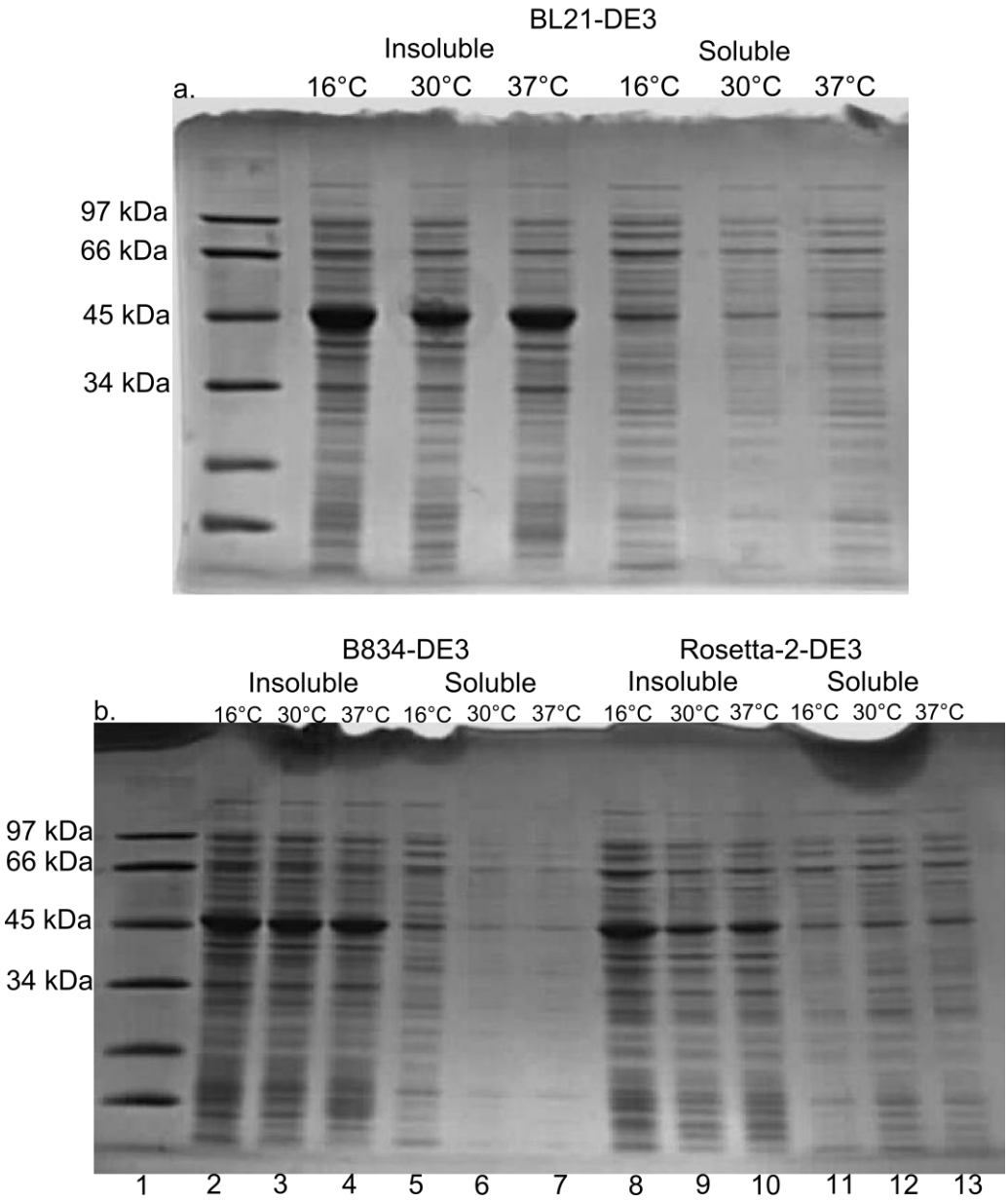

Figure 3.6: **a.** SDS-PAGE separation of protein from *E. coli* BL21-DE3 transformed with pET-YSBLIC3C-AsAAO: Lane 1, low range molecular weight marker; Lane 2-4, BL21- pET-YSBLIC3C-AsAAO insoluble fraction 16/30/37°C induction (48 kDa); Lane 5-7, BL21- pET-YSBLIC3C-AsAAO soluble fraction 16/30/37°C induction (48 kDa). **b**. SDS-PAGE separation of protein from *E. coli* B834-DE3 and Rosetta-2-DE3 transformed with pET-YSBLIC3C-AsAAO. Lane 1, low range molecular weight marker; Lane 2-4, B834- pET-YSBLIC3C-AsAAO insoluble fraction 16/30/37°C induction (48 kDa); Lane 5-7, B834 pET-YSBLIC3C--AsAAO soluble fraction 16/30/37°C induction (48 kDa); Lane 8-10, Rosetta-2- pET-YSBLIC3C-AsAAO insoluble fraction 16/30/37°C (48 kDa); Lane 11-13 Rosetta-2- pET-YSBLIC3C-AsAAO soluble fraction 16/30/37°C induction (48 kDa).

The pET-YSBLIC3C-BaAO strains again showed good expression of a protein around the correct size (54 kDa) but poor solubility, although solubility showed a slight increase at lower induction temperatures (**Figure 3.7**).

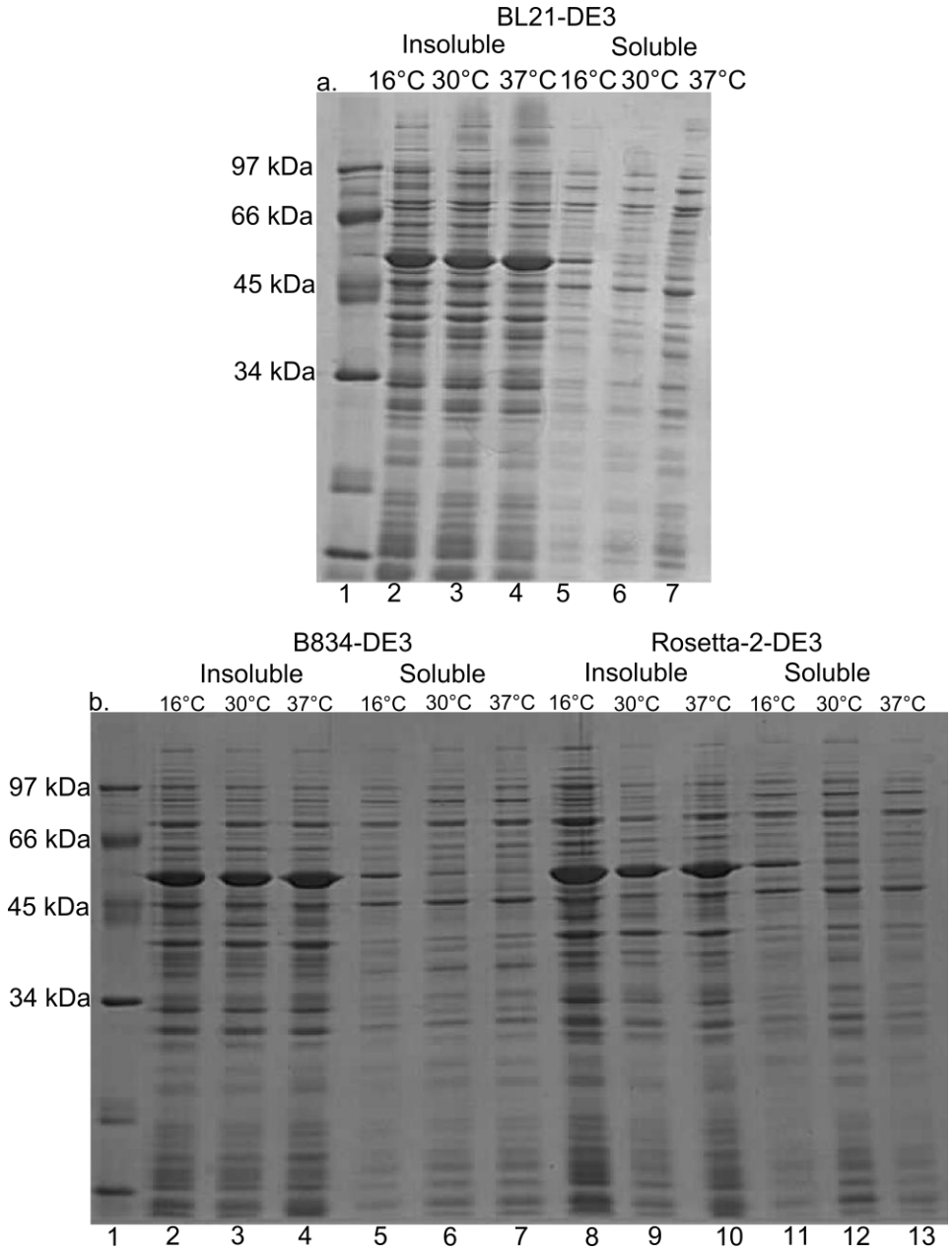

Figure 3.7: **a.** SDS-PAGE separation of protein from *E. coli* BL21-DE3 transformed with pET-YSBLIC3C-BaAO: Lane 1, low range molecular weight marker; Lane 2-4, BL21-pET-YSBLIC3C-BaAO insoluble fraction 16/30/37°C induction (54 kDa); Lane 5-7, BL21-pET-YSBLIC3C-BaAO soluble fraction 16/30/37°C induction (54 kDa). **b**. SDS-PAGE separation of protein from *E. coli* B834-DE3 and Rosetta-2-DE3 transformed with pET-YSBLIC3C-BaAO. Lane 1, low range molecular weight marker; Lane 2-4, B834-pET-YSBLIC3C-BaAO insoluble fraction 16/30/37°C induction (54 kDa); Lane 5-7, B834-pET-YSBLIC3C-BaAO soluble fraction 16/30/37°C induction (54 kDa); Lane 8-10, Rosetta-2-pET-YSBLIC3C-BaAO insoluble fraction 16/30/37°C (54 kDa); Lane 11-13 Rosetta-2-pET-YSBLIC3C-BaAO soluble fraction 16/30/37°C induction (54 kDa).

The protein encoded by the pET-YSBLIC3C-BsGO strains appeared to be slightly larger on the SDS-PAGE than the expected 42 kDa. All strains showed good expression and reasonable solubility at all induction temperatures, although solubility appeared to be highest in the BL21-pET-YSBLIC3C-BsGO strain (**Figure 3.8**).

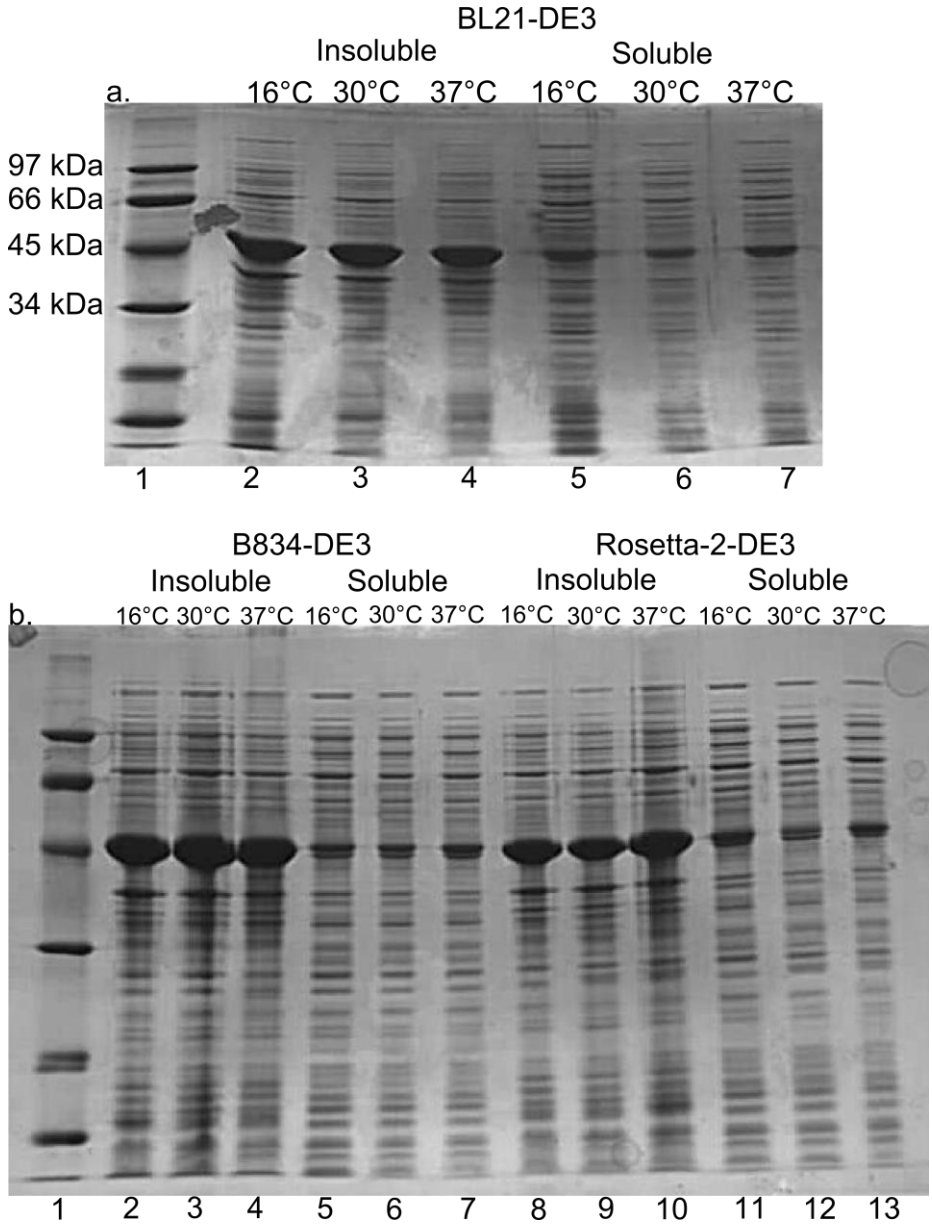

Figure 3.8: **a.** SDS-PAGE separation of protein from *E. coli* BL21-DE3 transformed with pET-YSBLIC3C-BsGO: Lane 1, low range molecular weight marker; Lane 2-4, BL21-pET-YSBLIC3C-BsGO insoluble fraction 16/30/37°C induction (42 kDa); Lane 5-7, BL21-pET-YSBLIC3C-BsGO soluble fraction 16/30/37°C induction (42 kDa). **b**. SDS-PAGE separation of protein from *E. coli* B834-DE3 and Rosetta-2-DE3 transformed with pET-YSBLIC3C-BsGO: Lane 1, low range molecular weight marker; Lane 2-4, B834-pET-YSBLIC3C-BsGO insoluble fraction 16/30/37°C induction (42 kDa); Lane 5-7, B834-pET-YSBLIC3C-BsGO soluble fraction 16/30/37°C induction (42 kDa); Lane 8-10, Rosetta-2-pET-YSBLIC3C-BsGO insoluble fraction 16/30/37°C induction (42 kDa); Lane 11-13 Rosetta-2-pET-YSBLIC3C-BsGO soluble fraction 16/30/37°C induction (42 kDa).

The pET-YSBLIC3C-NfOR protein was not expressed at the correct size (49 kDa) unless induced at high temperatures, at lower temperatures a smaller protein around 40 kDa appears to be produced instead. The best expression appears to be in Rosetta-2-pET-YSBLIC3C-NfOR strains induced at 37°C; however solubility was still poor in all strains (**Figure 3.9**).

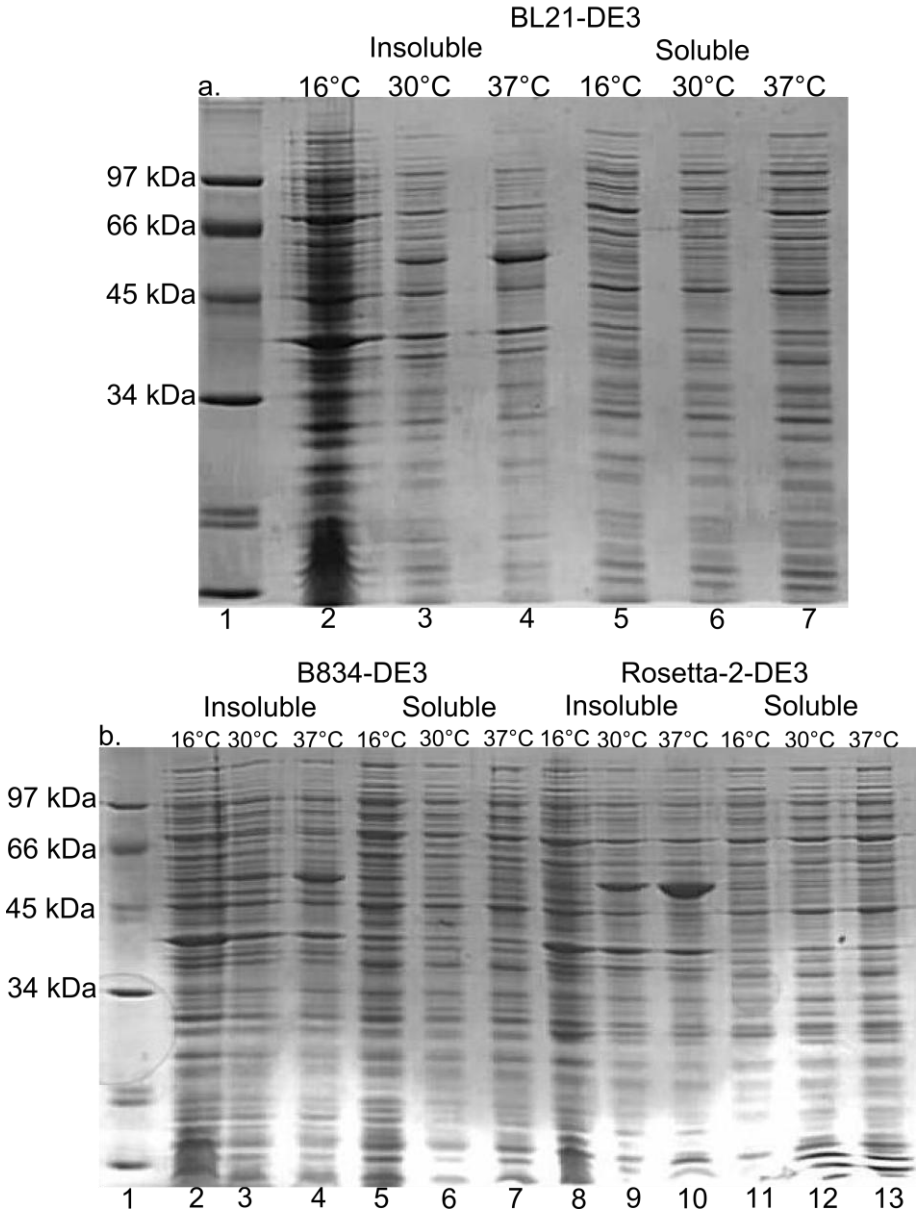

Figure 3.9: **a.** SDS-PAGE separation of protein from *E. coli* BL21-DE3 transformed with pET-YSBLIC3C-NfOR. Lane 1, low range molecular weight marker; Lane 2-4, BL21-pET-YSBLIC3C-NfOR insoluble fraction 16/30/37°C induction (49 kDa); Lane 5-7, BL21-pET-YSBLIC3C-NfOR soluble fraction 16/30/37°C induction (49 kDa). **b.** SDS-PAGE separation of protein from *E. coli* B834-DE3 and Rosetta-2-DE3 transformed with pET-YSBLIC3C-NfOR. Lane 1, low range molecular weight marker; Lane 2-4, B834-pET-YSBLIC3C-NfOR insoluble fraction 16/30/37°C induction (49 kDa); Lane 5-7, B834-pET-YSBLIC3C-NfOR soluble fraction 16/30/37°C induction (49 kDa); Lane 8-10, Rosetta-2-pET-YSBLIC3C-NfOR insoluble fraction 16/30/37°C induction (49 kDa); Lane 11-13 Rosetta-2-pET-YSBLIC3C-NfOR soluble fraction 16/30/37°C induction (49 kDa).

The BL21-pET-YSBLIC3C-PpLAAO strain showed good expression and high solubility of a protein around the expected size (59 kDa), particularly when gene overexpression was induced at low temperatures. The other pET-YSBLIC3C-PpLAAO strains appeared to produce less protein, although soluble protein is still present from the Rosetta-2-pET-YSBLIC3C-PpLAAO strain (**Figure 3.10**).

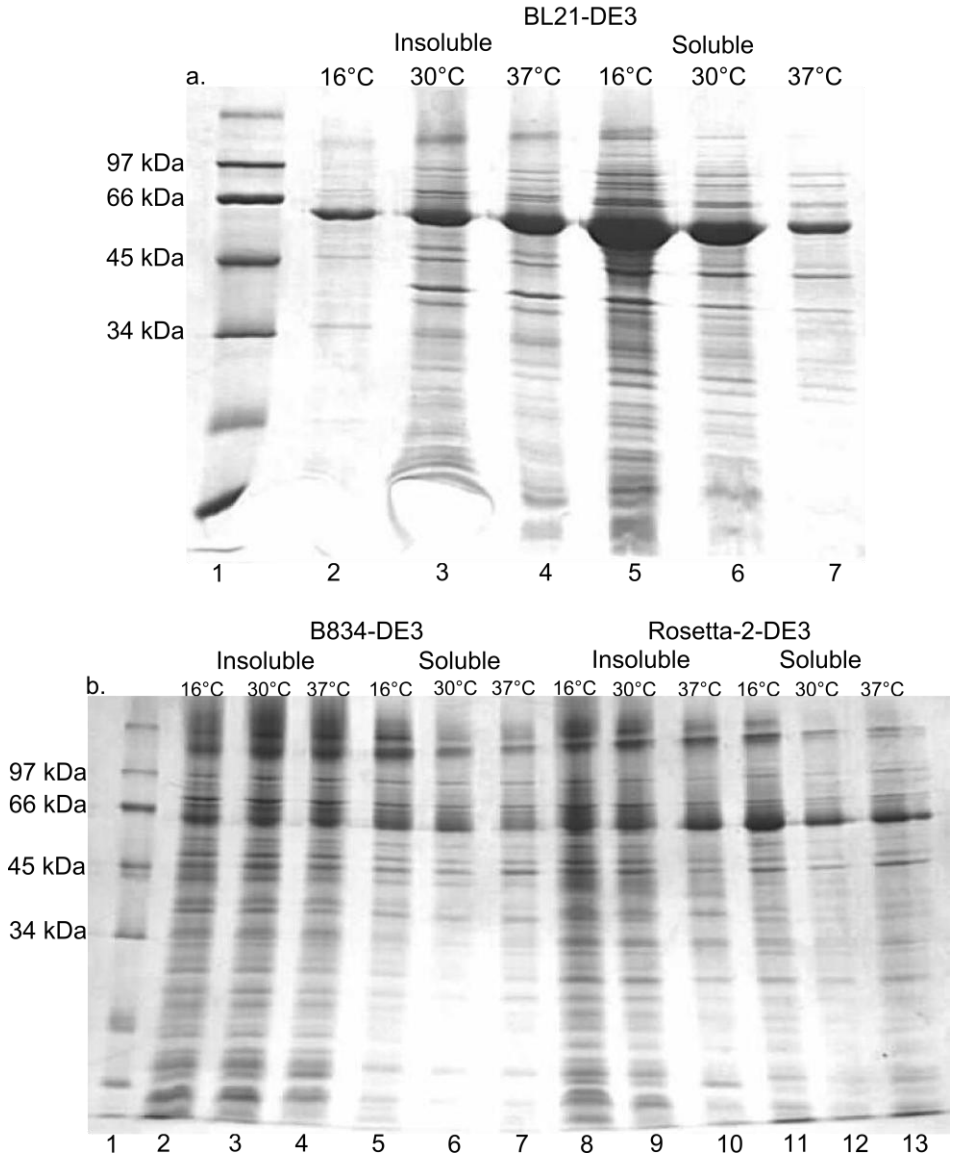

Figure 3.10: **a.** SDS-PAGE separation of protein from *E. coli* BL21-DE3 transformed with pET-YSBLIC3C-PpLAAO. Lane 1, low range molecular weight marker; Lane 2-4, BL21-pET-YSBLIC3C-PpLAAO insoluble fraction 16/30/37°C induction (59 kDa); Lane 5-7, BL21-pET-YSBLIC3C-PpLAAO soluble fraction 16/30/37°C induction (59 kDa). **b.** SDS-PAGE separation of protein from *E. coli* B834-DE3 and Rosetta-2-DE3 transformed with pET-YSBLIC3C-PpLAAO. Lane 1, low range molecular weight marker; Lane 2-4, B834-pET-YSBLIC3C-PpLAAO insoluble fraction 16/30/37°C induction (59 kDa); Lane 5-7, B834-pET-YSBLIC3C-PpLAAO soluble fraction 16/30/37°C induction (59 kDa); Lane 8-10, Rosetta-2-pET-YSBLIC3C-PpLAAO insoluble fraction 16/30/37°C induction (59 kDa); Lane 11-13 Rosetta-2-pET-YSBLIC3C-PpLAAO soluble fraction 16/30/37°C induction (59 kDa).

The pET-YSBLIC3C-RoLAAO strains all produced protein at the correct size (53 kDa), although the BL21-pET-YSBLIC3C-RoLAAO strain expressed a small (14 kDa) protein when induced at 16°C and 30°C and the Rosetta-2-YSBLIC3C-RoLAAO strain expressed the small 14 kDa protein when induced at 37°C. Despite the apparently high expression none of the strains appeared to contain soluble protein (**Figure 3.11**). Because of this and a preliminary test of the expressed proteins activity against its known substrates L-alanine and L-histidine (**Table 3.1**) that showed no activity from the samples, no further work was done using the RoLAAO target.

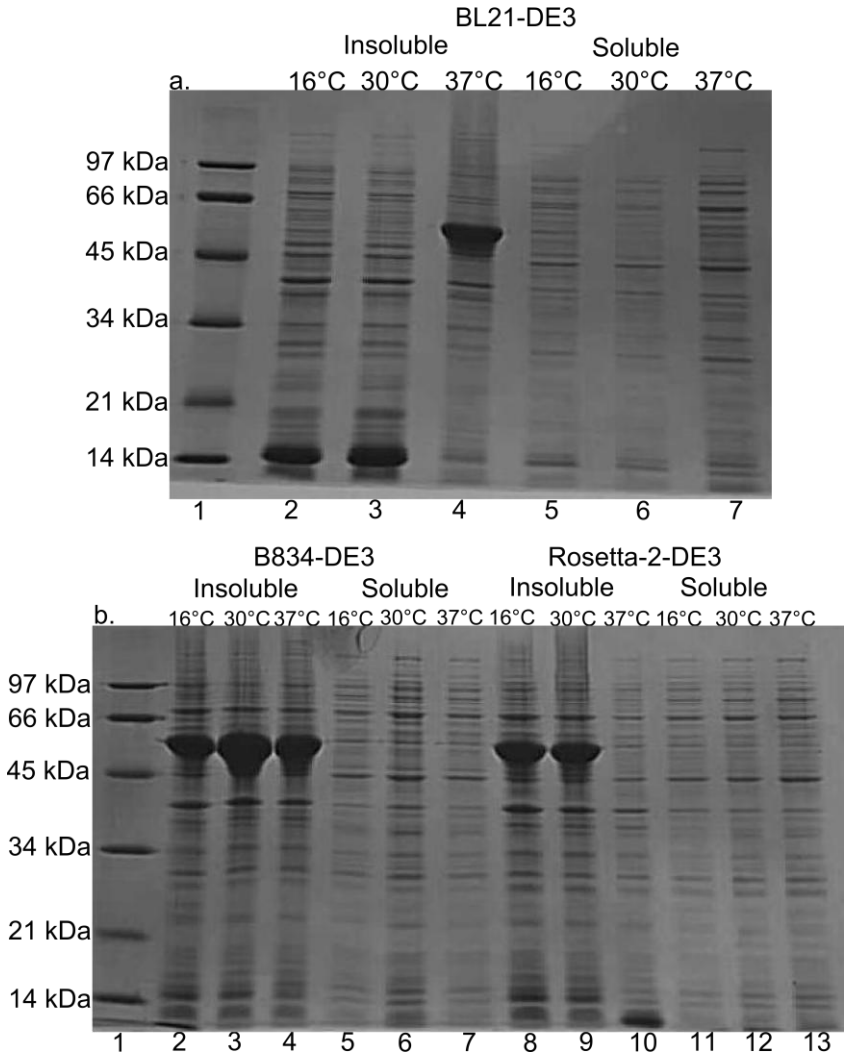

Figure 3.11: **a.** SDS-PAGE separation of protein from *E. coli* BL21-DE3 transformed with pET-YSBLIC3C-RoLAAO. Lane 1, low range molecular weight marker; Lane 2-4, BL21-pET-YSBLIC3C-RoLAAO insoluble fraction 16/30/37°C induction (53 kDa); Lane 5-7, BL21-pET-YSBLIC3C-RoLAAO soluble fraction 16/30/37°C induction (53 kDa). **b.** SDS-PAGE separation of protein from *E. coli* B834-DE3 and Rosetta-2-DE3 transformed with pET-YSBLIC3C-RoLAAO. Lane 1, low range molecular weight marker; Lane 2-4, B834-pET-YSBLIC3C-RoLAAO insoluble fraction 16/30/37°C induction (53 kDa); Lane 5-7, B834-pET-YSBLIC3C-RoLAAO soluble fraction 16/30/37°C induction (53 kDa); Lane 8-10, Rosetta-2-pET-YSBLIC3C-RoLAAO insoluble fraction 16/30/37°C induction (53 kDa); Lane 11-13 Rosetta-2-pET-YSBLIC3C-RoLAAO soluble fraction 16/30/37°C induction (53 kDa).

The pET-YSBLIC3C-SLAAO strains all showed high expression but poor solubility of a protein around the expected size of 54 kDa, at all induction temperatures (**Figure 3.12**).

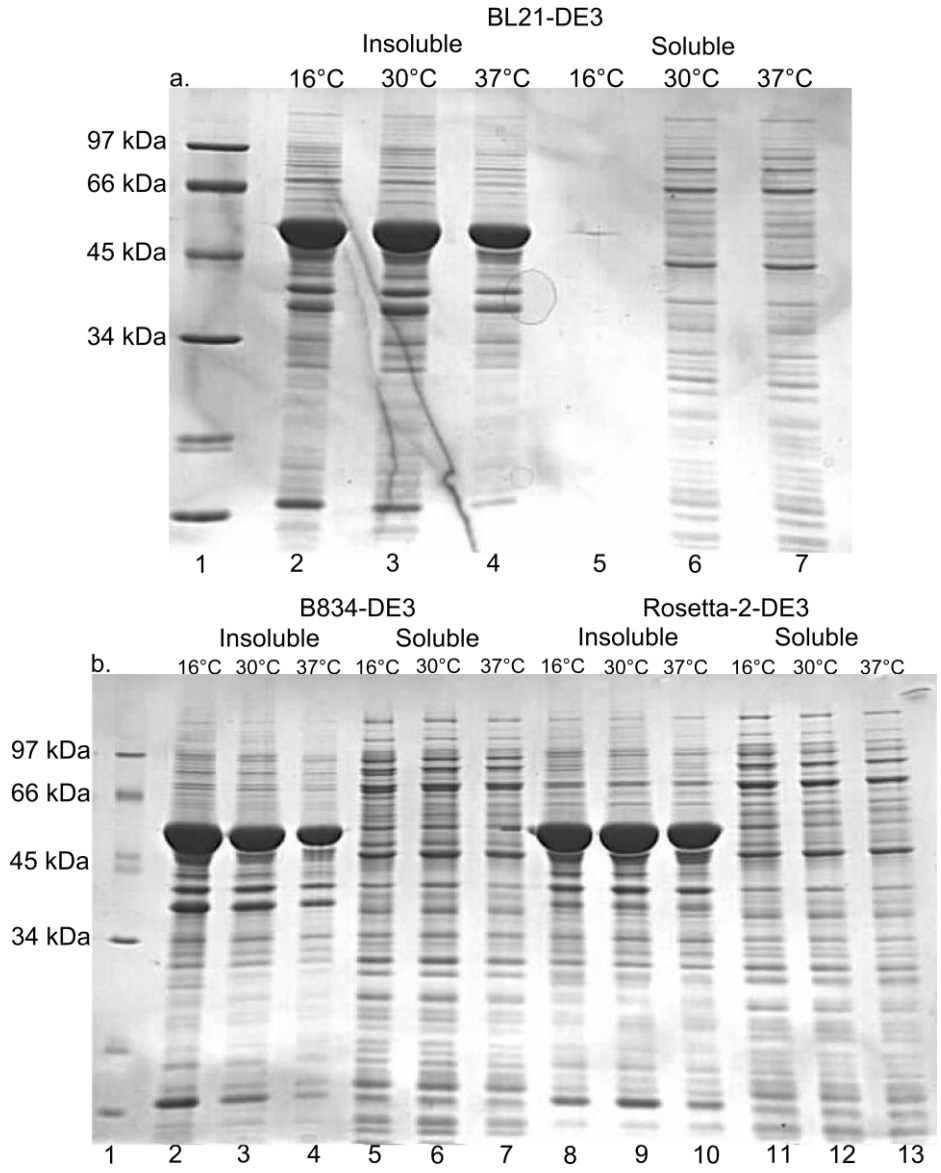

Figure 3.12: **a.** SDS-PAGE separation of protein from *E. coli* BL21-DE3 transformed with pET-YSBLIC3C-SLAAO. Lane 1, low range molecular weight marker; Lane 2-4, BL21-pET-YSBLIC3C-SLAAO insoluble fraction 16/30/37°C induction (54 kDa); Lane 5-7, BL21-pET-YSBLIC3C-SLAAO soluble fraction 16/30/37°C induction (54 kDa). **b.** SDS-PAGE separation of protein from *E. coli* B834-DE3 and Rosetta-2-DE3 transformed with pET-YSBLIC3C-SLAAO. Lane 1, low range molecular weight marker; Lane 2-4, B834-pET-YSBLIC3C-SLAAO insoluble fraction 16/30/37°C induction (54 kDa); Lane 5-7, B834-pET-YSBLIC3C-SLAAO soluble fraction 16/30/37°C induction (54 kDa); Lane 8-10, Rosetta-2-pET-YSBLIC3C-SLAAO insoluble fraction 16/30/37°C induction (54 kDa); Lane 11-13 Rosetta-2-pET-YSBLIC3C-SLAAO soluble fraction 16/30/37°C induction (54 kDa).

Based on these results, the optimal expression conditions for each target were chosen (**Table 3.2**), these were used to express protein as in **Section 2.2.6**.

Table 3.2: Summary of expression conditions for six target proteins to be assayed.

Plasmid	*E. coli* Cell Strain	Overexpression Temperature	Overexpression Time
Non recombinant pET-YSBLIC-3C	BL21-DE3	37°C	3 h
pET-YSBLIC-3C-AsAAO	BL21-DE3	16°C	Overnight
pET-YSBLIC-3C-BaAO	BL21-DE3	16°C	Overnight
pET-YSBLIC-3C-BsGO	BL21-DE3	37°C	3 h
pET-YSBLIC-3C-NfOR	B834-DE3	37°C	3 h
pET-YSBLIC-3C-PpLAAO	BL21-DE3	16°C	Overnight
pET-YSBLIC-3C-SLAAO	Rosetta-2-DE3	37°C	3 h

3.3 Activity assay of target oxidases

The remaining six target enzymes were assayed for activity using a horseradish peroxidase (HRP) based assay developed by Ingenza Ltd. to determine the levels of H_2O_2 being produced as a by-product of the oxidase activity, as described in **Section 2.2.7**. The assay contains 4-aminoantipyrine (4-AAP) and 2,4,6,tribromo-3-hydroxybenzoic acid (TBHBA), which in the presence of HRP combine with the H_2O_2 to form a soluble red quinoneimine complex. This can be seen visibly and qualitative measurement can be performed by reading the absorbance of light at 510 nm. This assay was used in a plate format (**Figure 3.13**) to screen induced whole cells and the induced soluble protein fraction of each of the remaining target enzymes against all 20 natural amino acids, amylamine, phenylethylamine and AMBA as in **Section 2.2.7**.

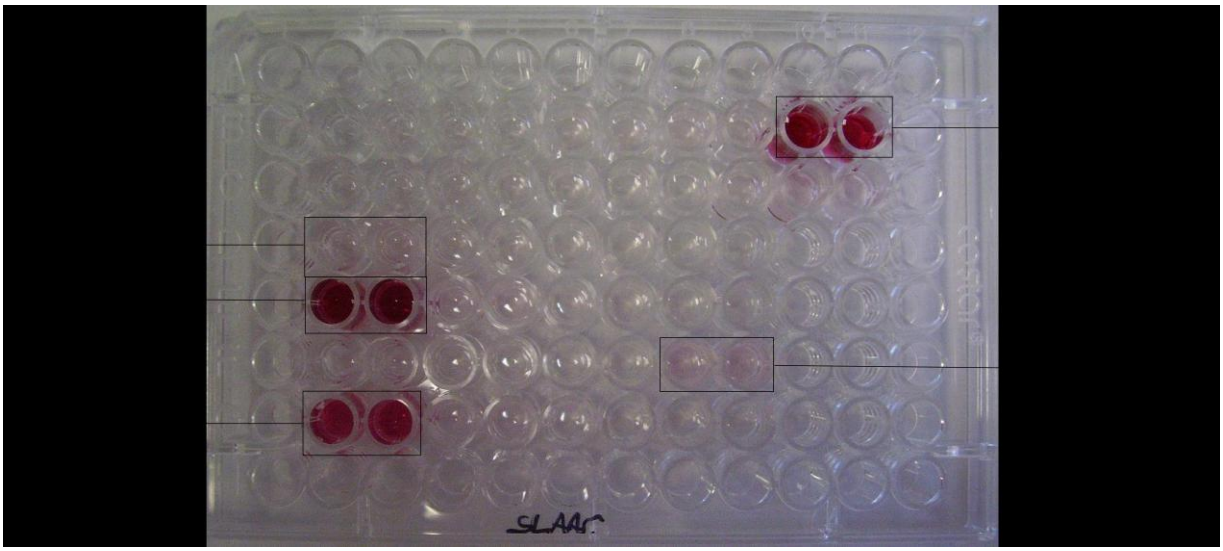

Figure 3.13 Example of horseradish peroxidase assay (active oxidase activity produces pink colour). Photograph of soluble SLAAO assay plate, annotation shows the substrate and [average absorbance-control absorbance] of a few substrates as an example.

The non recombinant pET-YSBLIC-3C was used as a negative control. No significant activity was seen against any of the substrates (**Figure 3.14**), although a very low level of activity was seen in all assays against AMBA, regardless of the protein sample used (**Figure 3.14-3.20**).

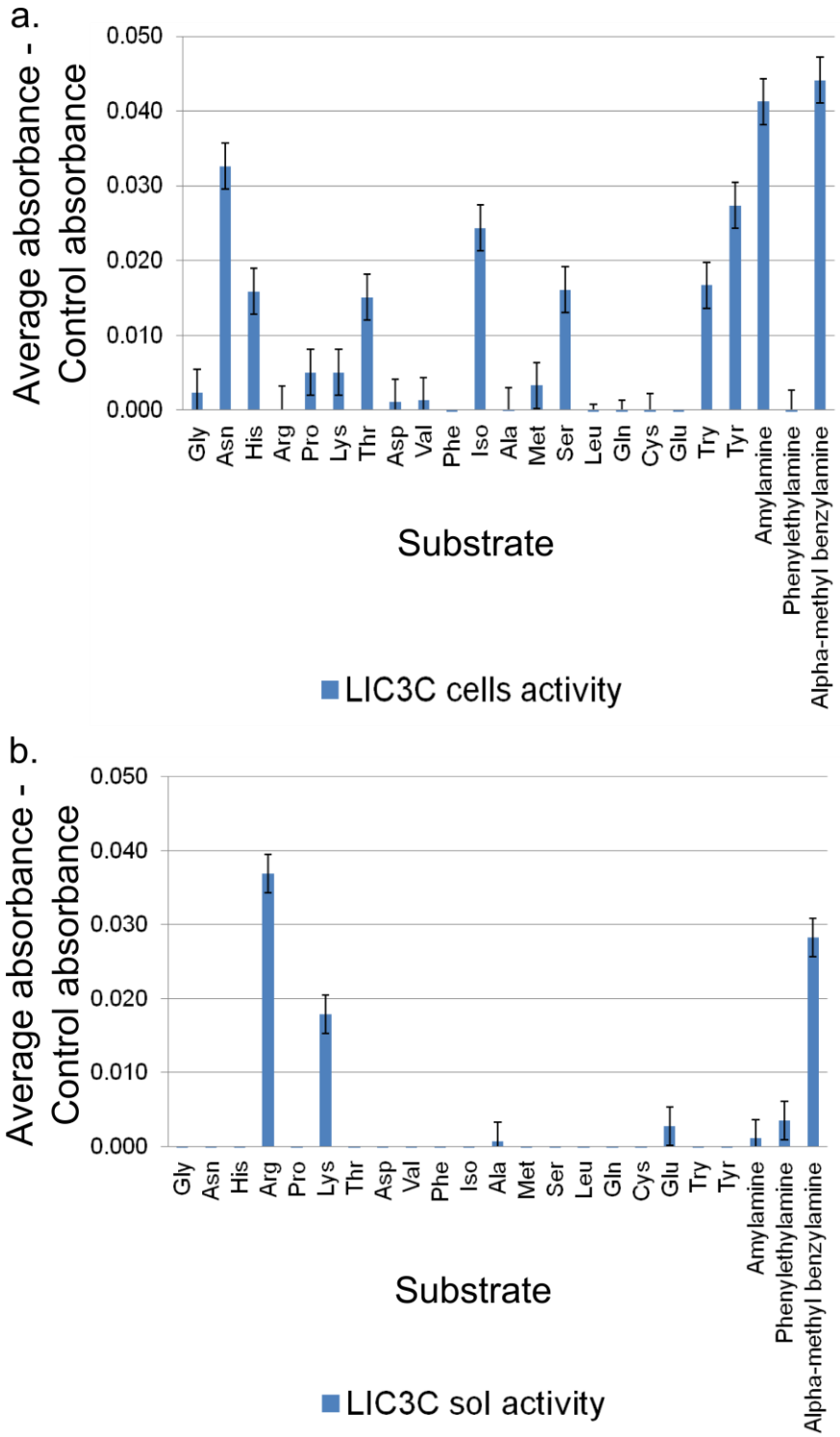

Figure 3.14 a. 1 h end point of the activity of induced BL21-pET-YSBLIC3C cells against the natural amino acids, amylamine, phenylethylamine and α-methylbenzylamine **b.** 1 h end point activity of induced BL21-pET-YSBLIC3C soluble cell fraction against the natural amino acids, amylamine, phenylethylamine and α-methylbenzylamine.

The AsAAO cells appeared to show a small level of activity against L-tyrosine, with an A_{510} reading of 0.080 (**Figure 3.15**), however later tests did not show this activity (data not shown). The soluble protein fraction did not show any significant activity against any of the substrates (**Figure 3.15**); however this may be because there was very little soluble protein produced (**Figure 3.6**).

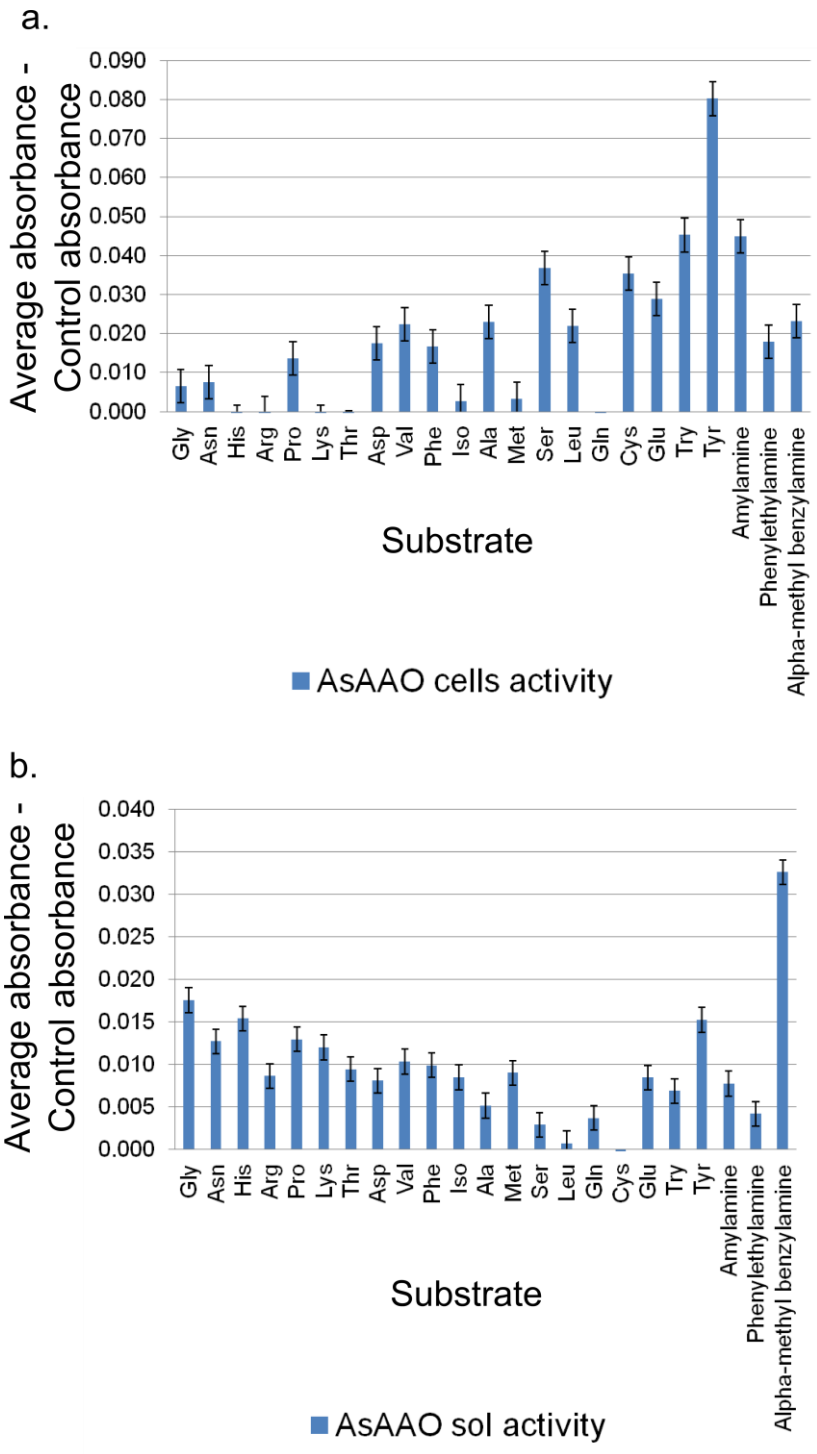

Figure 3.15 a. 1 h end point of the activity of induced BL21-pET-YSBLIC3C-AsAAO cells against the natural amino acids, amylamine, phenylethylamine and α-methylbenzylamine **b.** 1 h end point activity of induced BL21-pET-YSBLIC3C-AsAAO soluble cell fraction against the natural amino acids, amylamine, phenylethylamine and α-methylbenzylamine.

Neither the BaAO whole cells or soluble fraction showed any significant activity against any of the substrates tested (**Figure 3.16**), although there was a very small amount of absorbance against the three amines in the soluble protein assays (A_{510} of 0.014, 0.014 and 0.013 for amylamine, phenylethylamine and AMBA respectively) (**Figure 3.16**), this is unlikely to be significant compared to more active protein. The low activity may be due to the lack of soluble protein produced (**figure 3.7**).

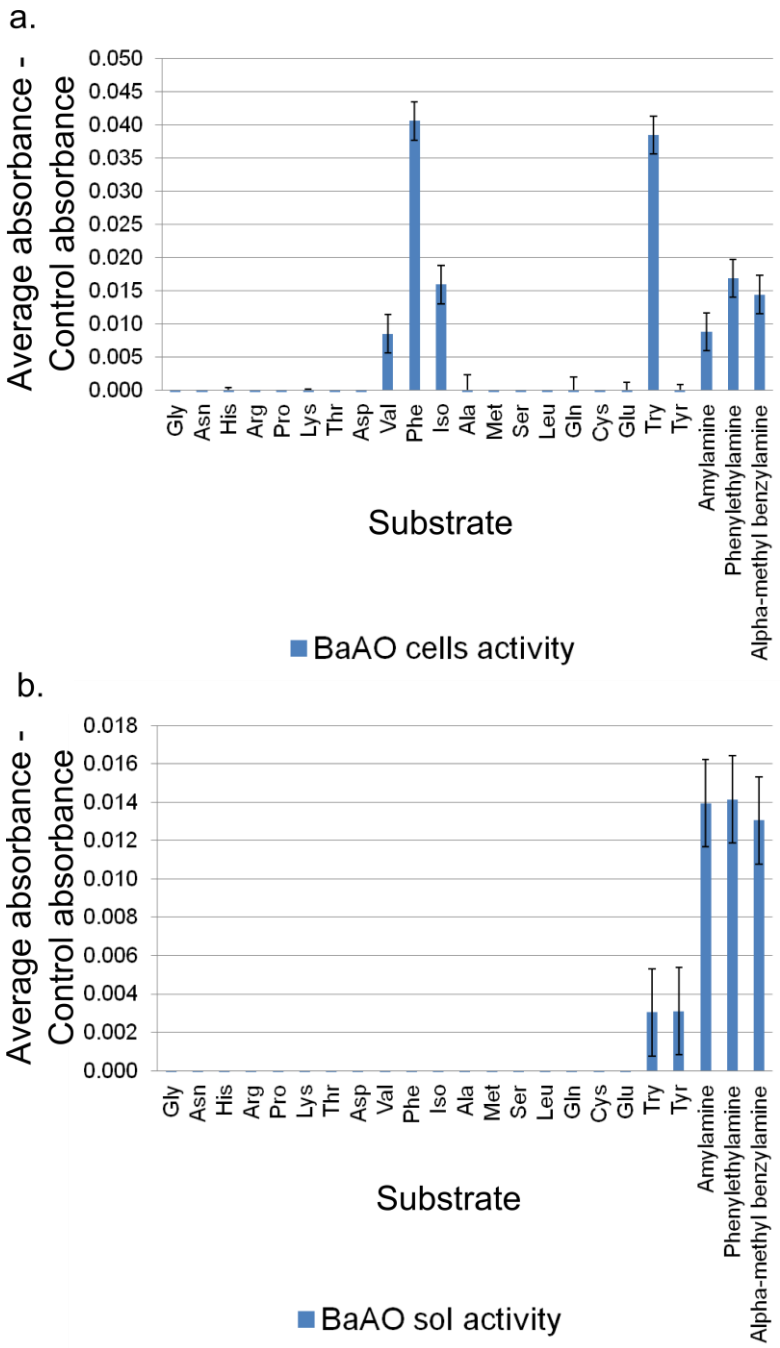

Figure 3.16 a. 1 h end point of the activity of induced BL21-pET-YSBLIC3C-BaAO cells against the natural amino acids, amylamine, phenylethylamine and α-methylbenzylamine **b.** 1 h end point activity of induced BL21-pET-YSBLIC3C-BaAO soluble cell fraction against the natural amino acids, amylamine, phenylethylamine and α-methylbenzylamine.

The BsGO whole cells showed activity against its known substrate, glycine (**Table 3.1**) with A_{510} at 0.372, as well as lower activity against L-asparagine (A_{510} was 0.162); however the soluble protein fraction did not show any significant activity against any of the substrates (**Figure 3.17**). The activity against L-asparagine is surprising given that BsGO is known to be active against neutral D-amino acids, rather than L-amino acids.[102]

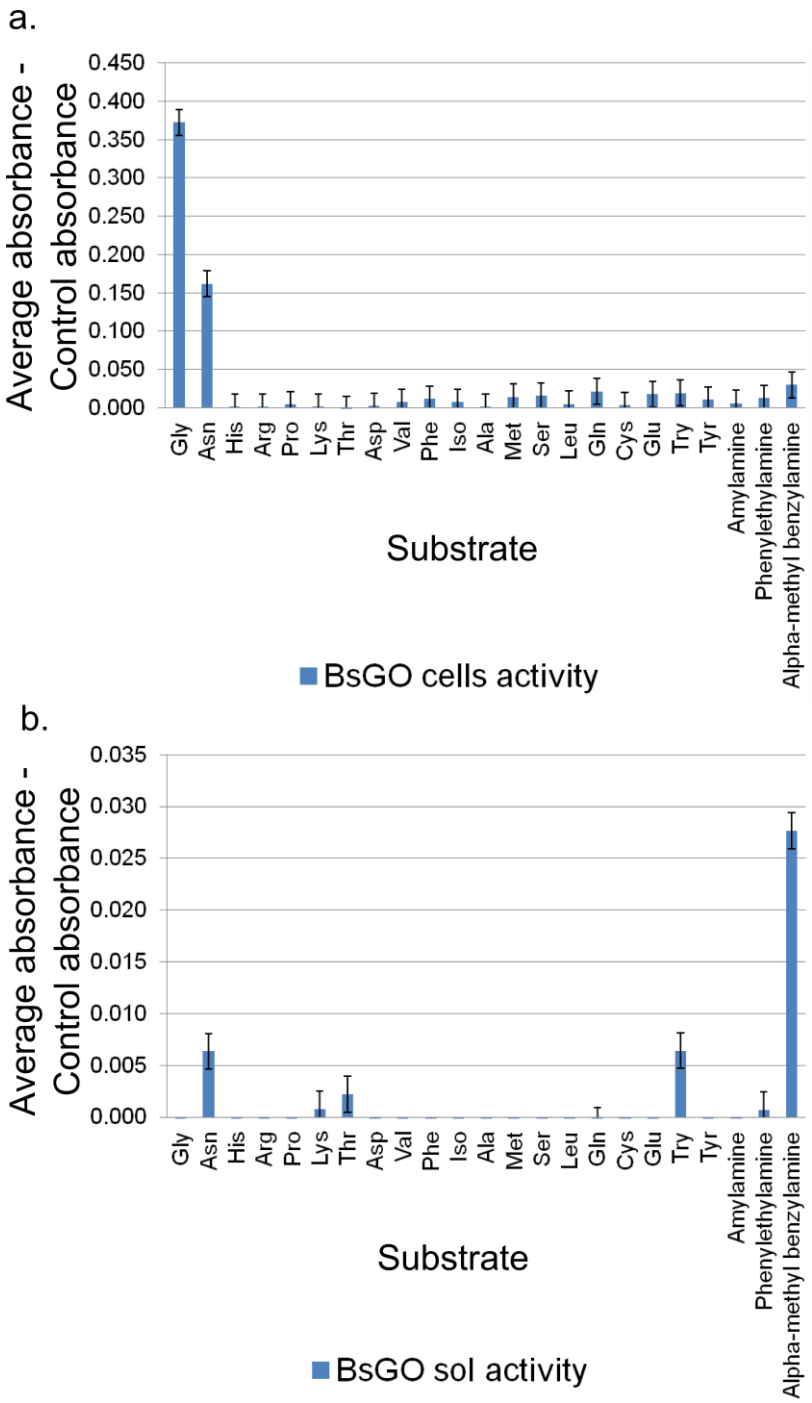

Figure 3.17 a. 1 h end point of the activity of induced BL21-pET-YSBLIC3C-BsGO cells against the natural amino acids, amylamine, phenylethylamine and α-methylbenzylamine **b.** 1 h end point activity of induced BL21-pET-YSBLIC3C-BsGO soluble cell fraction against the natural amino acids, amylamine, phenylethylamine and α-methylbenzylamine.

Neither of the NfOR whole cells or soluble protein fractions showed any significant activity against the substrates tested (**Figure 3.18**). Again this may be due to the lack of soluble protein (**Figure 3.9**)

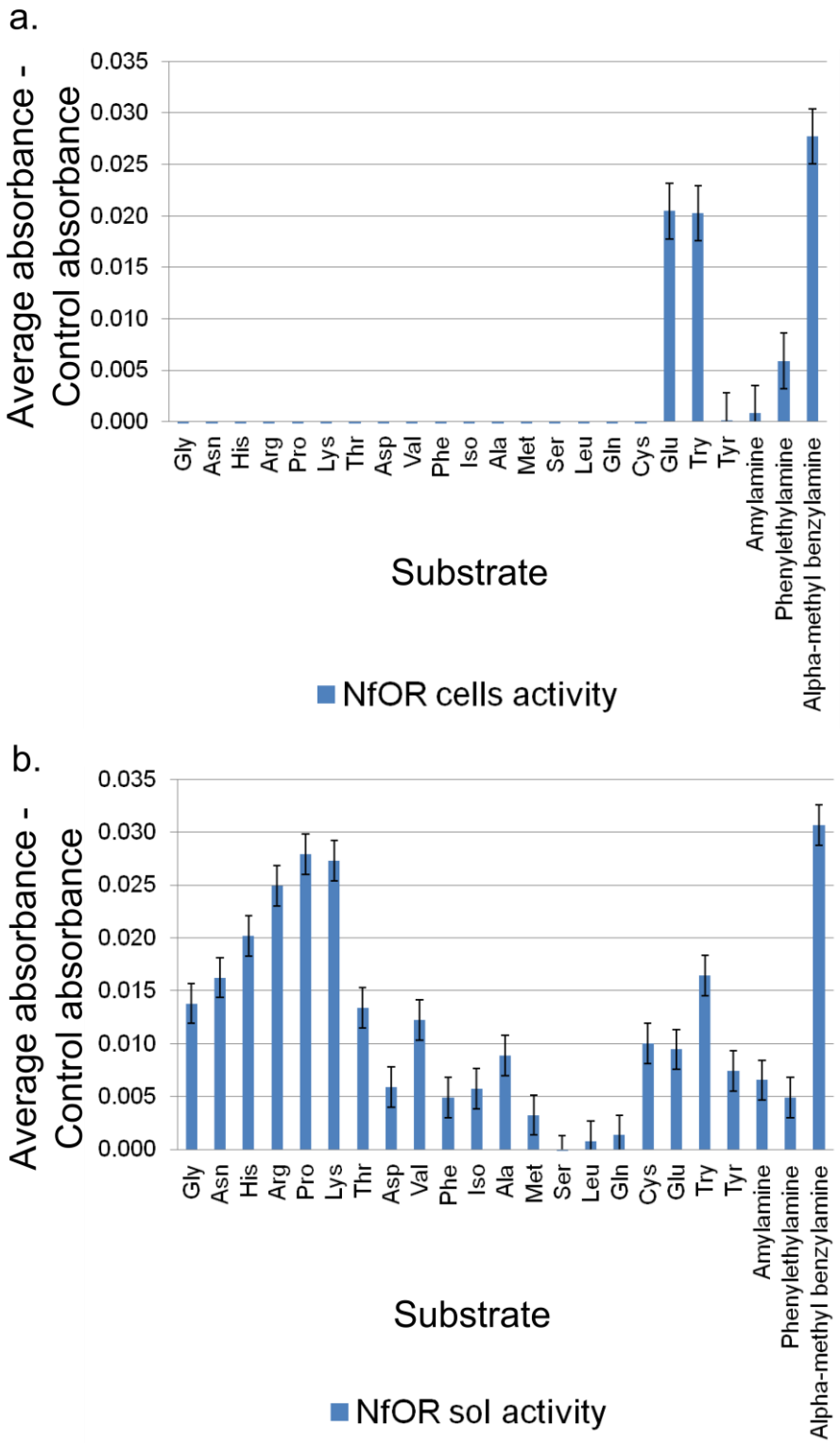

Figure 3.18 a. 1 h end point of the activity of induced B834-pET-YSBLIC3C-NfOR cells against the natural amino acids, amylamine, phenylethylamine and α-methylbenzylamine **b.** 1 h end point activity of induced B834-pET-YSBLIC3C-NfOR soluble cell fraction against the natural amino acids, amylamine, phenylethylamine and α-methylbenzylamine.

The PpLAAO cells showed activity against glycine (A_{510} was 0.578), and a lower amount of activity against L-asparagine (A_{510} was 0.220). The soluble protein fraction showed similar activity against glycine and L-asparagine (A_{510} of 0.478 and 0.098 respectively) and also showed activity against L-aspartate with A_{510} at 0.166 (**Figure 3.19**).

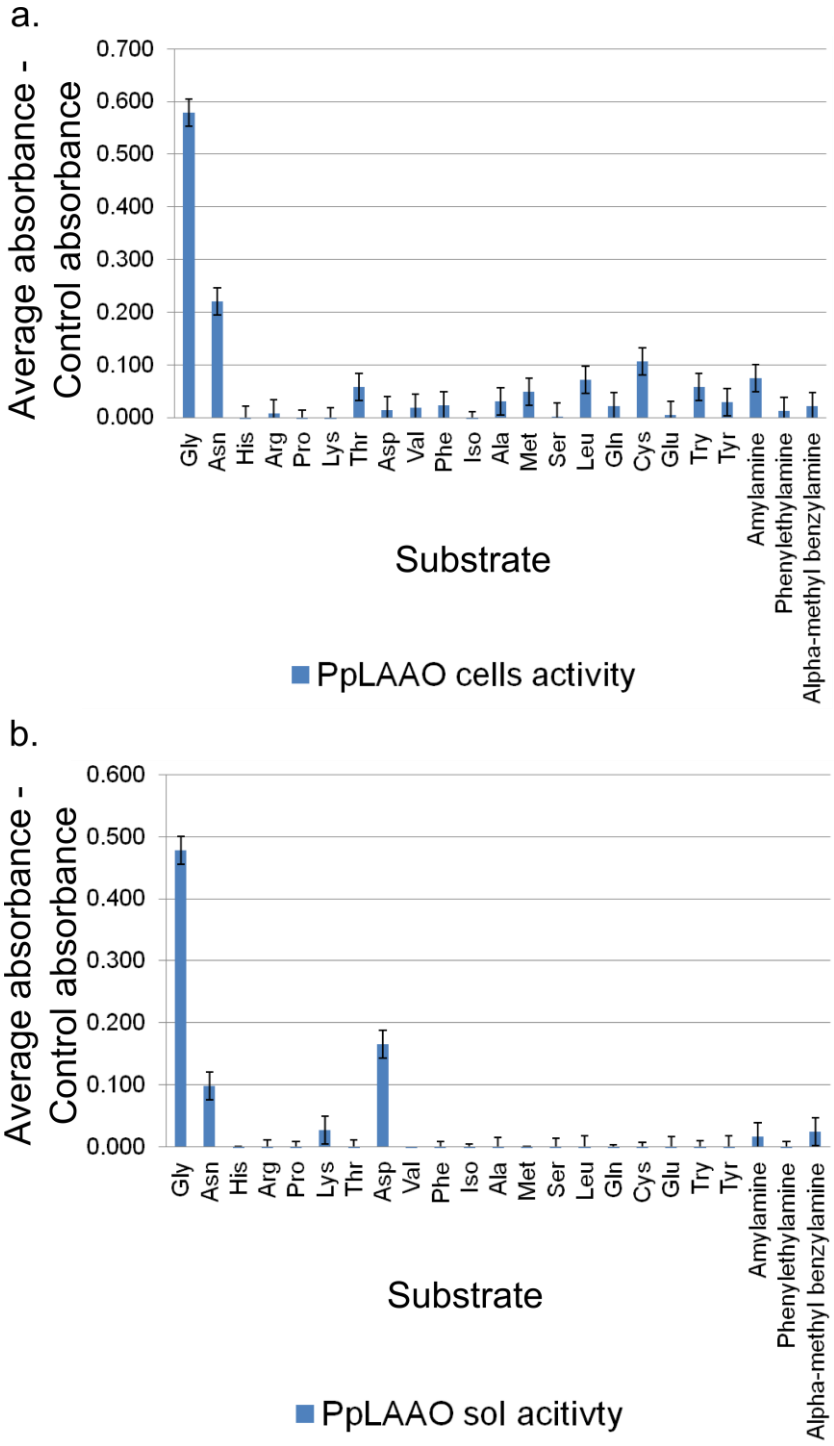

Figure 3.19 a. 1 h end point of the activity of induced BL21-pET-YSBLIC3C-PpLAAO cells against the natural amino acids, amylamine, phenylethylamine and α-methylbenzylamine **b.** 1 h end point activity of induced BL21-pET-YSBLIC3C-PpLAAO soluble cell fraction against the natural amino acids, amylamine, phenylethylamine and α-methylbenzylamine.

The SLAAO whole cells and soluble protein both showed very high activity against known substrate L-arginine (3.712 and 3.643 respectively) and showed high activity against known substrate L-lysine (A_{510} was 2.619 with whole cells and 1.831 with the soluble protein fraction). Both whole cells and soluble protein also showed a lower amount of activity against L-histidine (A_{510} of 0.164 and 0.135 respectively) (**Figure 3.20**), which is consistent with other *Synechococcus* L-AAOs.[100]

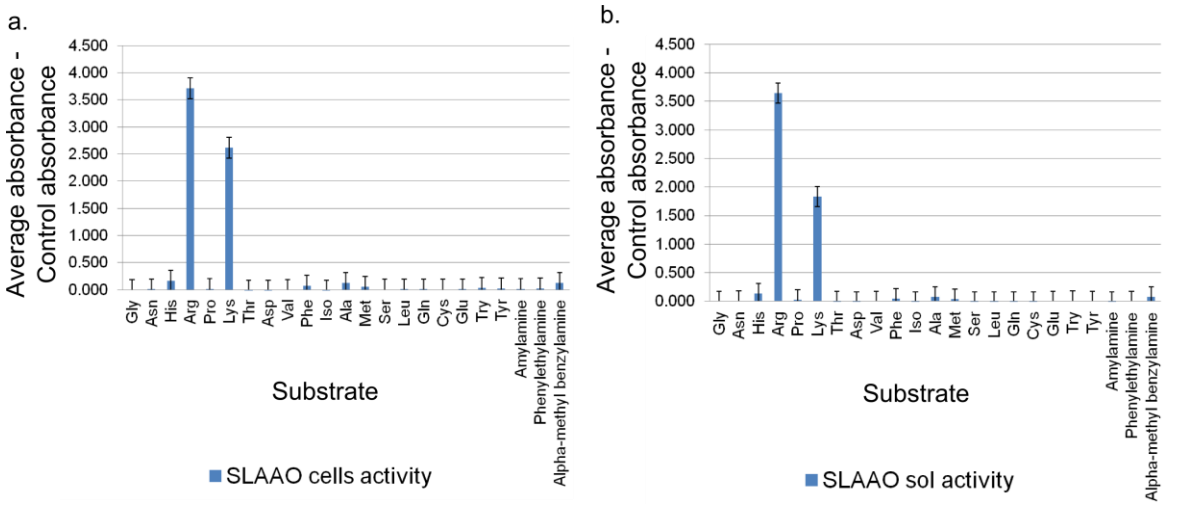

Figure 3.20 a. 1 h end point of the activity of induced Rosetta-2-pET-YSBLIC3C-SLAAO cells against the natural amino acids, amylamine, phenylethylamine and α-methylbenzylamine **b.** 1 h end point activity of induced Rosetta-2-pET-YSBLIC3C-SLAAO soluble cell fraction against the natural amino acids, amylamine, phenylethylamine and α-methylbenzylamine.

Based on these results it was decided that PpLAAO would be used as a target for further studies, due to its high solubility, activity against L-aspartate and L-asparagine and the fact that the *P. putida* version of the L-aspartate oxidase protein has not previously been purified or characterised in depth, although the 60% identical *E. coli* homologue has a structure solved using crystallisation[65] and the effects of some active site residues have been determined through mutagenesis studies.[64, 118]

As both the AsAAO and BaAO targets appeared to potentially show activity against some interesting substrates (L-tyrosine for AsAAO and the amines for BaAO) attempts were made to increase the solubility of these enzymes so they could be studied further.

3.4 Attempts to increase solubility of AsAAO and BaAO

Both the AsAAO and BaAO targets appear to produce protein, however in both cases the protein is insoluble (**Figures 3.15 and 3.16**). Because of this attempts were made to increase the solubility of these two proteins. Auto induction media (AIM)[111] is routinely used to increase the solubility of

proteins that are weakly soluble when expressed in colonies grown in LB-media. Golovanov *et al.*[115] also found that adding 50 mM of L-glutamate and 50 mM of L-arginine increased the maximum solubility and stability of several proteins, so the effects of these methods were tested on each protein as in **Section 2.2.8**. However no change in solubility was in when using the AIM, the 50 mM L-glutamate and 50 mM L-arginine, or both in conjunction (**Figures 3.21-3.22**).

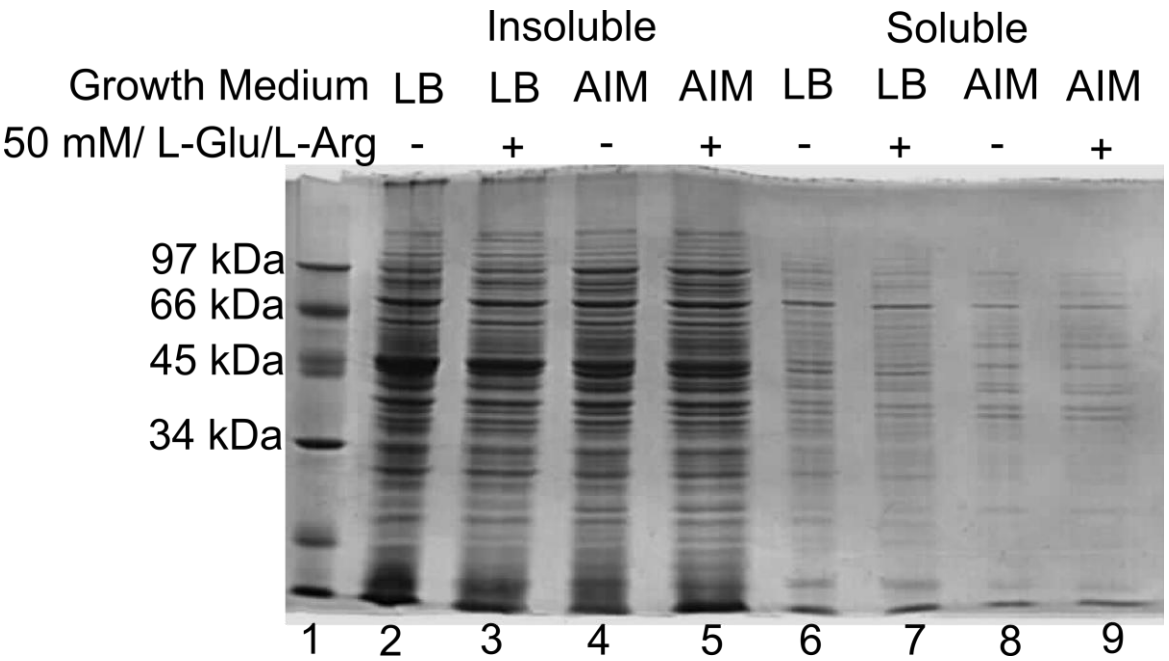

Figure 3.21 SDS-PAGE separation of protein from *E. coli* BL21-DE3 transformed with pET-YSBLIC3C-AsAAO, showing effects of auto-induction media (AIM) and adding 50 mM L-glutamate and 50 mM L-arginine on soluble expression: Lane 1, low range molecular weight marker; Lane 2-3, BL21- pET-YSBLIC3C-AsAAO insoluble fraction grown in LB without/with 50 mM L-Glu and 50 mM L-Arg (48 kDa); Lane 4-5, BL21- pET-YSBLIC3C-AsAAO insoluble fraction grown in AIM without/with 50 mM L-Glu and 50 mM L-Arg (48 kDa); Lane 6-7, BL21- pET-YSBLIC3C-AsAAO soluble fraction grown in LB without/with 50 mM L-Glu and 50 mM L-Arg (48 kDa); Lane 8-9, BL21- pET-YSBLIC3C-AsAAO soluble fraction grown in AIM without/with 50 mM L-Glu and 50 mM L-Arg (48 kDa).

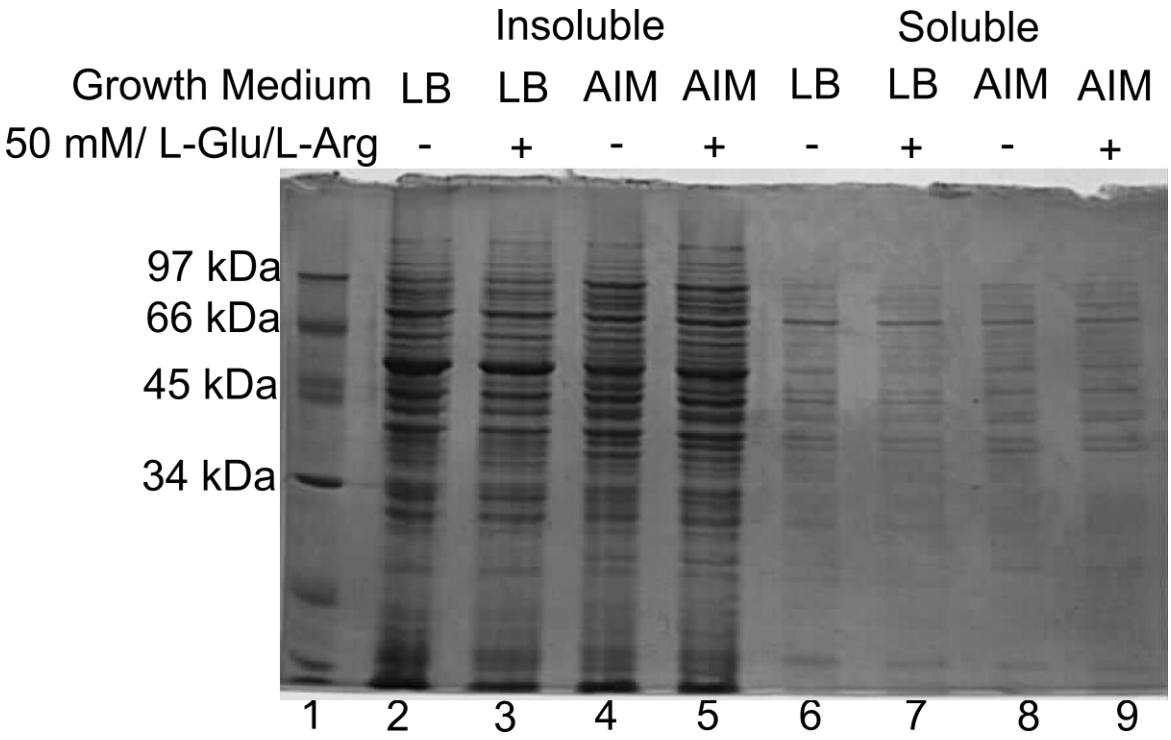

Figure 3.22 SDS-PAGE separation of protein from *E. coli* BL21-DE3 transformed with pET-YSBLIC3C-BaAO, showing effects of auto-induction media (AIM) and adding 50 mM L-glutamate and 50 mM L-arginine on soluble expression: Lane 1, low range molecular weight marker; Lane 2-3, BL21- pET-YSBLIC3C-BaAO insoluble fraction grown in LB without/with 50 mM L-Glu and 50 mM L-Arg (55 kDa); Lane 4-5, BL21- pET-YSBLIC3C-BaAO insoluble fraction grown in AIM without/with 50 mM L-Glu and 50 mM L-Arg (55 kDa); Lane 6-7, BL21- pET-YSBLIC3C-BaAO soluble fraction grown in LB without/with 50 mM L-Glu and 50 mM L-Arg (55 kDa); Lane 8-9, BL21- pET-YSBLIC3C-BaAO soluble fraction grown in AIM without/with 50 mM L-Glu and 50 mM L-Arg (55 kDa).

The level of oxygen available to the culture often has an effect on the solubility of produced proteins.[116] To see if this would have any effect on the AsAAO or BaAO targets three different volumes of culture (0.5 L, 1.0 L and 1.5 L) were each grown in a 2 L Erlenmeyer flask and protein overexpression was induced as normal (**Section 2.2.9**). To see if this had any effect on solubility 500 mL of each culture was spun down and analysed using SDS-PAGE, however no improvements in solubility were seen in either target. (**Figure 3.23**).

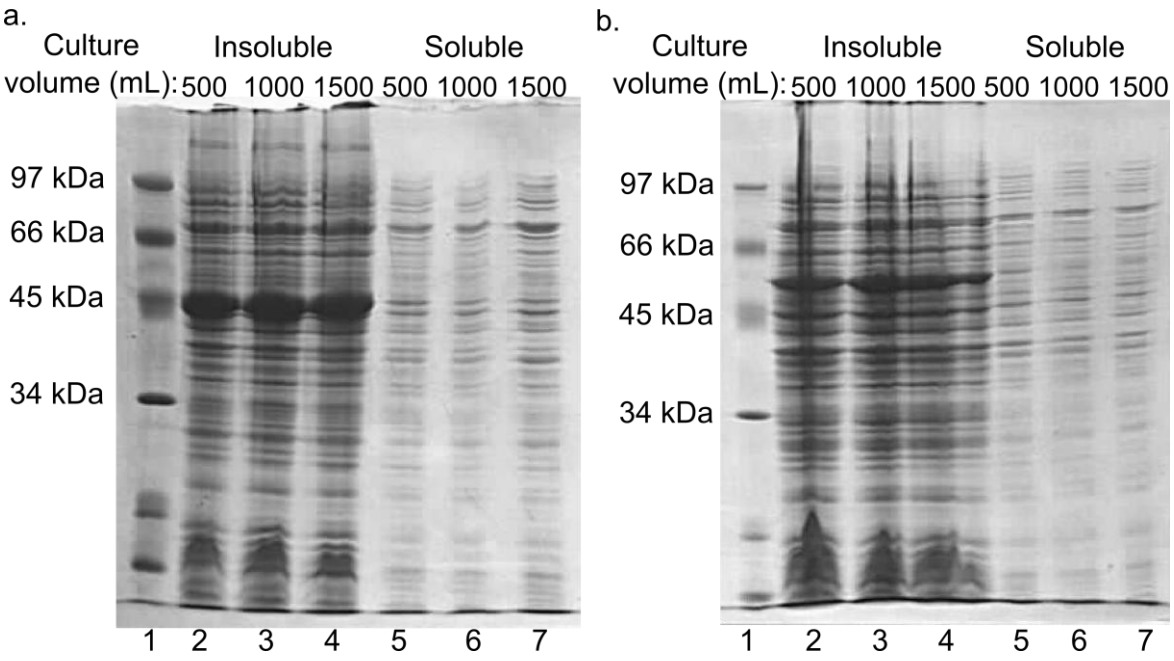

Figure 3.23 a. SDS-PAGE separation of protein from *E. coli* BL21-DE3 transformed with pET-YSBLIC3C-AsAAO, showing effects of changing culture volume in 2L Erlenmeyer flask: Lane 1, BioRad low weight molecular marker; Lane 2-4, Lane 2-3, BL21- pET-YSBLIC3C-AsAAO insoluble fractions from 500/1000/1500 mL culture; Lane 5-7, BL21- pET-YSBLIC3C-AsAAO soluble fractions from 500/1000/1500 mL culture. **b.** SDS-PAGE separation of protein from *E. coli* BL21-DE3 transformed with pET-YSBLIC3C-BaAO, showing effects of changing culture volume in 2L Erlenmeyer flask: Lane 1, BioRad low weight molecular marker; Lane 2-4, BL21- pET-YSBLIC3C-BaAO insoluble fractions from 500/1000/1500 mL culture; Lane 5-7, BL21- pET-YSBLIC3C-BaAO soluble fractions from 500/1000/1500 mL culture.

A solubility screen developed by Lindwall *et al.*[112] to screen various resuspension conditions was used on the BaAO target protein to determine if the solubility could be increased as in **Section 2.2.10**. Conditions 4 (100 mM HEPES, 100 mM KCl, pH 7.0) and 15 (100 mM KH_2PO_4/K_2HPO_4, 2.5 mM $ZnCl_2$, pH 4.3) appeared to increase the solubility of the protein (**Figure 3.24**).

The production of the BaAO protein was scaled up to two 1 L cultures, which were split into four 500 mL cultures. Each of these cultures was spun down and resuspended in a different buffer condition; H_2O, Solubility screen condition 4, Solubility screen condition 15 and a Tris resuspension buffer (50 mM Tris/HCl, 300 mM NaCl, 20 µM AEBSF, pH 7.0). The solubility of the protein in each condition was analysed using SDS-PAGE. From these results it appeared that the Tris based buffer resulted in the most solubility (**Figure 3.25**). However attempts to purify the BaAO protein using NiNTA column failed as no protein bound to the nickel column (data not shown).

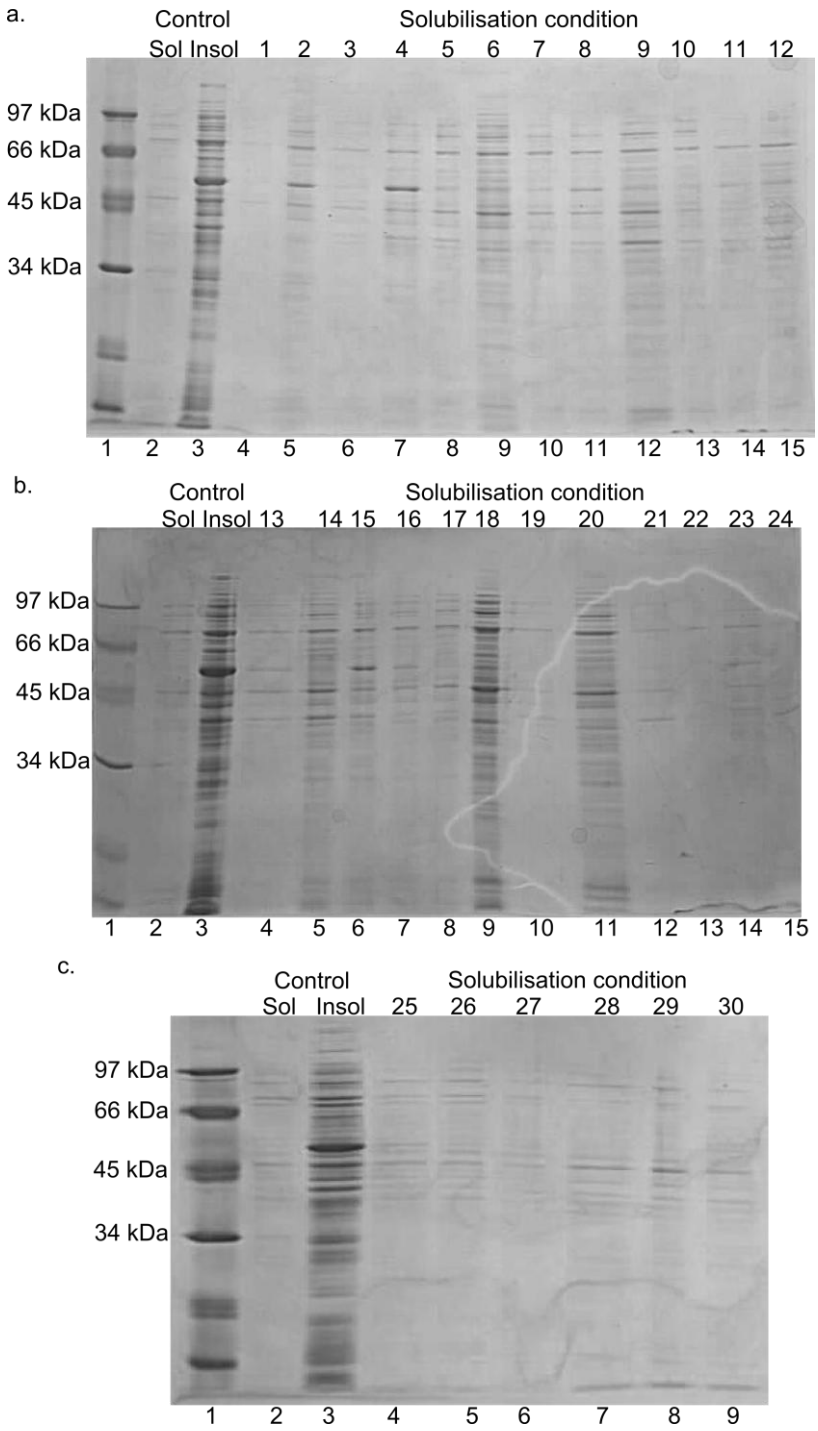

Figure 3.24 SDS-PAGE separation of protein from *E. coli* BL21-DE3 transformed with pET-YSBLIC3C-BaAO, treated with solubilisation screen conditions**: a.** Lane 1, BioRad low range molecular weight marker; Lane 2-3, BL21- pET-YSBLIC3C-BaAO soluble/insoluble fraction, resuspended in H_2O (55 kDa); Lane 4-15, BL21- pET-YSBLIC3C-BaAO soluble fractions resuspended in solubilisation conditions 1-12 c. **b.** Lane 1, BioRad low range molecular weight marker; Lane 2-3, BL21-pET-YSBLIC3C-BaAO soluble/insoluble fraction, resuspended in H_2O (55 kDa); Lane 4-15, BL21-pET-YSBLIC3C-BaAO soluble fractions resuspended in solubilisation conditions 16-24 c. **c.** Lane 1, BioRad low range molecular weight marker; Lane 2-3, BL21- pET-YSBLIC3C-BaAO soluble/insoluble fraction, resuspended in H_2O (55 kDa); Lane 4-9, BL21-pET-YSBLIC3C-BaAO soluble fractions resuspended in solubilisation conditions 25-30 (55 kDa).

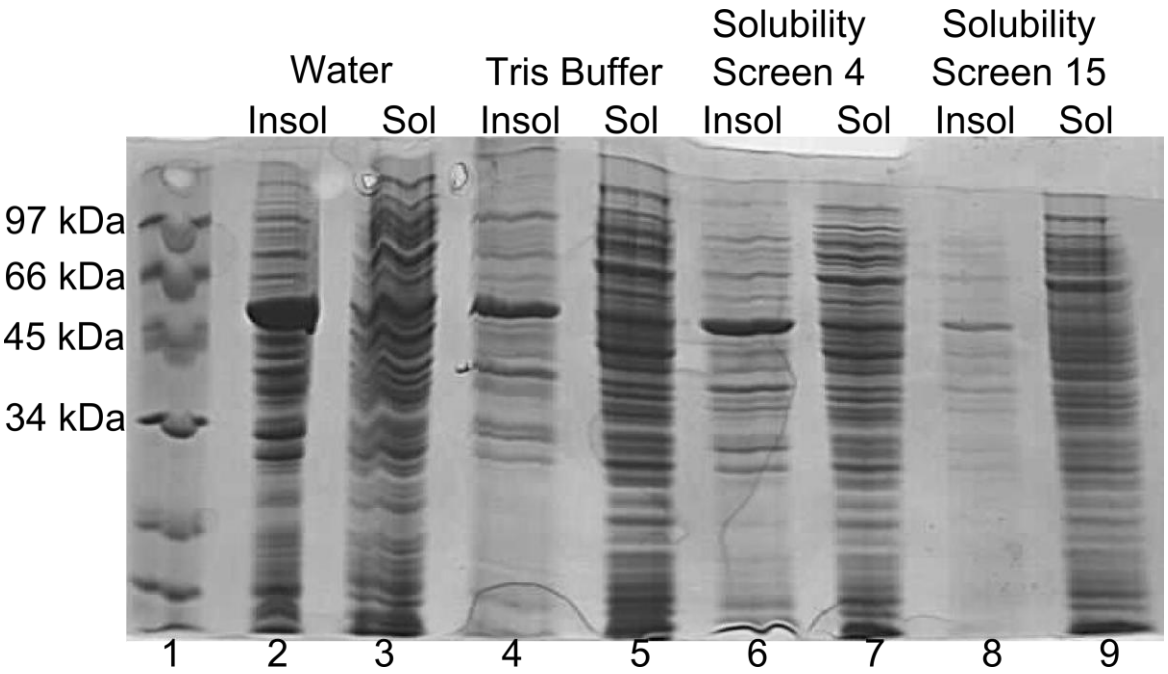

Figure 3.25 SDS-PAGE separation of protein from 1 L cultures of *E. coli* BL21-DE3 transformed with pET-YSBLIC3C-BaAO, sonicated in different resuspension buffers**:** Lane 1, BioRad low range molecular weight marker; Lane 2-3, BL21- pET-YSBLIC3C-BaAO Insoluble/Soluble fraction, resuspended in H_2O (55 kDa); Lane 2-3, BL21- pET-YSBLIC3C-BaAO Insoluble/Soluble fraction, resuspended in Tris buffer (55 kDa); Lane 2-3, BL21- pET-YSBLIC3C-BaAO Insoluble/Soluble fraction, resuspended in the Solubility Screen condition 4 (55 kDa); Lane 2-3, BL21- pET-YSBLIC3C-BaAO Insoluble/Soluble fraction, resuspended in the Solubility Screen condition 15 (55 kDa).

3.5 Conclusions

Seven target oxidases were successfully cloned into the pET-YSBLIC-3C expression vector. These cloned targets were used to transform the *E. coli* protein production strains Bl21-DE3, B834-DE3 and Rosetta-2-DE3 and the genes were overexpressed with different induction temperatures and times to determine which combination of strain and induction temperature would result in the highest level of soluble protein production for each cloned target. These optimum conditions were then used to produce whole cells and soluble protein fractions for each cloned target, which were then screened for activity against the twenty proteinogenic amino acids and three amines.

From work done by Ingenza Ltd. and Geueke & Hummel[56] the *Rhodococcus opacus* L-AAO (RoLAAO) is active against a range of proteinogenic substrates, notably L-alanine and L-histidine. However, when the gene was overexpressed in the *E. coli* expression strains no soluble protein was produced under any condition (**Figure 3.11**) and a preliminary test of the induced whole cells and soluble fractions against L-alanine and L-histidine did not detect any activity (data not shown), suggesting that the protein was not being expressed in an active form in any of the *E.coli* strains

used. In some of the conditions used the *E. coli* cells appear to be over expressing a protein around 14 kDa in size, as opposed to the expected 53 kDa RoLAAO protein (**Figure 3.11**), which might suggest that the produced protein is being subjected to protein cleavage by the *E. coli* expression strains used. However it is also possible that the 14 kDa protein is due to overexpression of a non-specific, native *E.coli* protein and either DNA fingerprinting or a His-tag based immunoblot of the gel would have to be used to determine if this was the case.

Another reason for the insolubility of the protein maybe that it need other factors to help it fold that are not present in the *E. coli* expression strains used, such as chaperone proteins. There is also the possibility is that any hydrogen peroxide produced by the RoLAAO protein reacting with L-alanine or L-histidine in the cell cytoplasm may be producing reactive oxygen species that would damage the DNA and protein inside the cells, resulting in cell death and poor protein expression. As looking into these issues would have taken time, and because the RoLAAO protein is already more understood than some of the other target proteins, it was decided that this was not a suitable target for further work.

The *Synechococcus* sp. strain ATCC 27144 (*aka Synechococcus elongates* PCC 6301) L-AAO (SLAAO) was known to be active against L-arginine and L-lysine. When expressed in *E. coli* the gene did not appear to produce any soluble protein (**Figure 3.13**) however when tested for activity both the whole cells and soluble protein fractions with the overexpressed gene showed high activity against L-arginine and L-lysine, as well as low activity against L-histidine (**Figure 3.20**). As the protein has previously been found to mainly precipitate in cell membrane fractions[100] it may be that the protein is folding in an active state in the membrane, although the portion of the protein located in the soluble fraction is also highly active. However as the protein has already been partially characterised by others[100] and the low solubility would suggest that it may be difficult to purify in high quantities, it was decided that it would be worth investigating a less well understood or easier to purify target, and no further work was done on this target.

The *Bacillus subtilis* L-AAO (BsGO) was a known glycine oxidase and has been shown to oxidise sarcosine[101] and neutral D-amino acids.[103] When cloned and overexpressed in *E. coli* BL21-DE3 cells at 37°C for 3 h gene produced a reasonable amount of soluble protein (**Figure 3.8**), and induced whole cells showed activity against glycine as well as some lower activity against L-asparagine, although this activity was lost in the soluble protein fraction (**Figure 3.17**). This might suggest that the BsGO protein requires a factor that is present in the *E. coli* expression strains to oxidise its substrates. This would make working with the pure form of the protein difficult, and as other groups have already worked on this protein[101, 102] it was disregarded as a target.

The putative *Nocardia farcinica* oxidoreductase (NfOR) did not have any known substrates. Unfortunately, when the gene was overexpressed at lower temperatures the produced protein appeared to be smaller than expected, at around 40 kDa instead of 49 kDa and although protein produced at higher induction temperatures were of the correct size (**Figure 3.9**) there was no soluble protein produced, and neither the induced whole cells or soluble fraction showed any activity against the screened substrates (**Figure 3.18**).

As with the RoLAAO protein, this could be due to proteolysis by the *E. coli* expression strain, a lack of chaperone proteins or damage to the expressing cells by hydrogen peroxide produced by the active protein. The NfOR gene sequence is also quite GC rich (74% GC content), which may cause poor gene expression in the *E. coli*, which has a lower overall GC content of 50%.[117] In an attempt to counteract this effect, the NfOR gene sequence was cloned into a *Corynebacterium glutamicum* pEKEx2 shuttle expression vector to see if expressing the gene in an organism that had genes with a higher GC content than *E. coli* would help produce more soluble protein. Unfortunately no produced protein could be seen from *C. glutamicum* (**Appendix**).

The putative L-AAO from *Anabaena* sp. strain PCC 7120 (AsAAO) also had no known substrates. The protein produced in *E. coli* was of the correct size, however no soluble protein was produced (**Figure 3.6**) and no activity was seen against any of the substrates screened (**Figure 3.15**). Attempts were made to increase the solubility of the produced protein using Auto Induction Media (AIM),[111] by adding 50 mM L-glutamate and 50 mM L-arginine[115] to the protein resuspension buffer and by adjusting the amount of soluble oxygen available to the bacterial culture,[116] unfortunately none of these methods resulted in a noticeable increase in the solubility of the produced protein (**Figures 3.21, 3.23a**).

As with the RoLAAO and NfOR genes, the lack of soluble protein could be the lack of chaperone proteins available in the expressions trains used or damage to the expressing cells by hydrogen peroxide produced by active AsAAO protein. Although the AsAAO gene sequence has a low GC content (42%), attempts were made to clone it into the pEKEx2 shuttle vector for expression in *C. glutamicum*, however the cloning was not successful (**Appendix**) and work on the AsAAO target was stopped.

The putative *Bacillus anthracis* AO (BaAO) has no known substrates. When the gene was cloned and expressed in *E. coli* very little soluble protein was produced, although the protein that was produced was all of the expected size (**Figure 3.7**). Unfortunately no activity was seen from either the whole cells or soluble fraction of the induced *E. coli* cells. As with AsAAO attempts were made to solubilise the protein using AIM,[111] by adding 50 mM L-glutamate and 50 mM L-arginine[115] to

the protein resuspension buffer and by adjusting the amount of soluble oxygen available to the bacterial culture[116] but none of these methods had any noticeable effect on protein solubility (**Figure 3.22, 3.23b**).

A solubilisation screen develop by the Lindwall group[112] was also tested against the BaAO produced protein and two of the conditions appeared to increase the solubility of the protein (**Figure 3.24**) however when these were compared with the Tris based buffer in a larger scale production the two conditions from the Lindwall screen appeared to have no noticeable effect on protein solubility (**Figure 3.25**). As there appeared to be some soluble protein, an attempt was made to purify the protein using a NiNTA column, however no protein bound to the column (data not shown) suggesting that the protein that appeared to be the soluble BaAO protein may just have been a normal protein produced by the *E. coli* expression strain. Like the other insoluble proteins, the lack of soluble protein could have been caused by a lack of chaperone protein or damage by hydrogen peroxide produced by the active protein.

Although the BaAO protein only has a GC content of 35%, attempts were made to clone the gene into the pEKEx2 shuttle vector for expression in *C. glutamicum*, to see if a different expression host would help increase solubility of the protein. Unfortunately, cloning was unsuccessful (**Appendix**) the BaAO target was disregarded as a target.

From work done by Ingenza Ltd. the *Pseudomonas putida* L-AAO (PpLAAO) protein was known to have activity against L-aspartate. The gene produced a highly soluble protein when overexpressed in *E. coli* BL21-DE3 cells with an induction temperature of 16°C (**Figure 3.10**). When screened for activity the whole cells and soluble protein fraction of the induced strain both showed high activity against glycine and low activity against L-asparagine. The soluble protein fraction also showed activity against L-aspartate that was slightly higher than that against L-asparagine. The loss of activity against L-aspartate in the whole cells is likely to have been due to problems transporting the L-aspartate across the bacterial cell membrane. As the PpLAAO protein was highly soluble, showed varying activity against three substrates and had not been studied in depth previously, it was decided that it was the best target to characterise by purification, crystallisation and mutational analysis. These reasons also make it the most optimal target to use as a model for directed evolution of an L-alanine or L-tyrosine oxidase, as none of the targets showed natural activity against these substrates.

Chapter 4 Characterisation of PpLAAO protein

The BL21-DE3-YSBLIC-3C-PpLAAO soluble protein extracts appeared to show activity against glycine, L-aspartate and L-asparagine (**Figure 3.18**). It was also very soluble (**Figure 3.9**), suggesting that it would be easy to purify in large quantities. It has also not been studied in depth, so it is not well understood. For these reasons the PpLAAO protein was selected to be purified and characterised using the soluble phase HRP-based assay used in **Section 3.3** to determine kinetic constants for its activity against glycine, L-aspartate, L-asparagine and target substrates L-glutamate L-tyrosine, L-alanine and L-homoserine as well as the pH preference and temperature stability of the purified PpLAAO protein. Attempts to crystallise the protein in order to determine the structure of the protein by X-ray diffraction were also started.

4.1 Purification of PpLAAO protein

Chemically competent *E. coli* BL21-DE3 cells were transformed with the YSBLIC-3C-PpLAAO plasmid, then grown in a 2 L culture and used to overexpress the gene encoding the PpLAAO protein as in **Section 2.3.1**. This culture was harvested and sonicated, and the PpLAAO protein was purified by metal affinity chromatography using a prepacked HiTrap Chelating HP column. The His-tag was then cleaved from the protein using C3-protease and cleaved His-tags were removed from the protein solution using metal affinity chromatography using the prepacked HiTrap Chelating HP column. The pure protein was then purified further by gel filtration chromatography using a 120 mL HiLoad 16/60 Superdex 75 column as in **Section 2.3.2**, protein from all steps were analysed using SDS-PAGE to ensure protein was purified (**Figure 4.1**).

The protein eluted from the 120 mL HiLoad 16/60 Superdex 75 column after 52 mL (**Figure 4.2**), allowing protein size to be calculated at roughly 116 kDa (**Section 2.3**), as wild type PpLAAO protein is 59 kDa, this suggests that the protein is in a dimeric form. Protein concentration was determined by measuring the absorption of the protein solution at 280nm and determining protein concentration using the theoretical extinction coefficient as detailed in **section 2.3.2**. Protein yield from 2 L of culture was 20 mg.

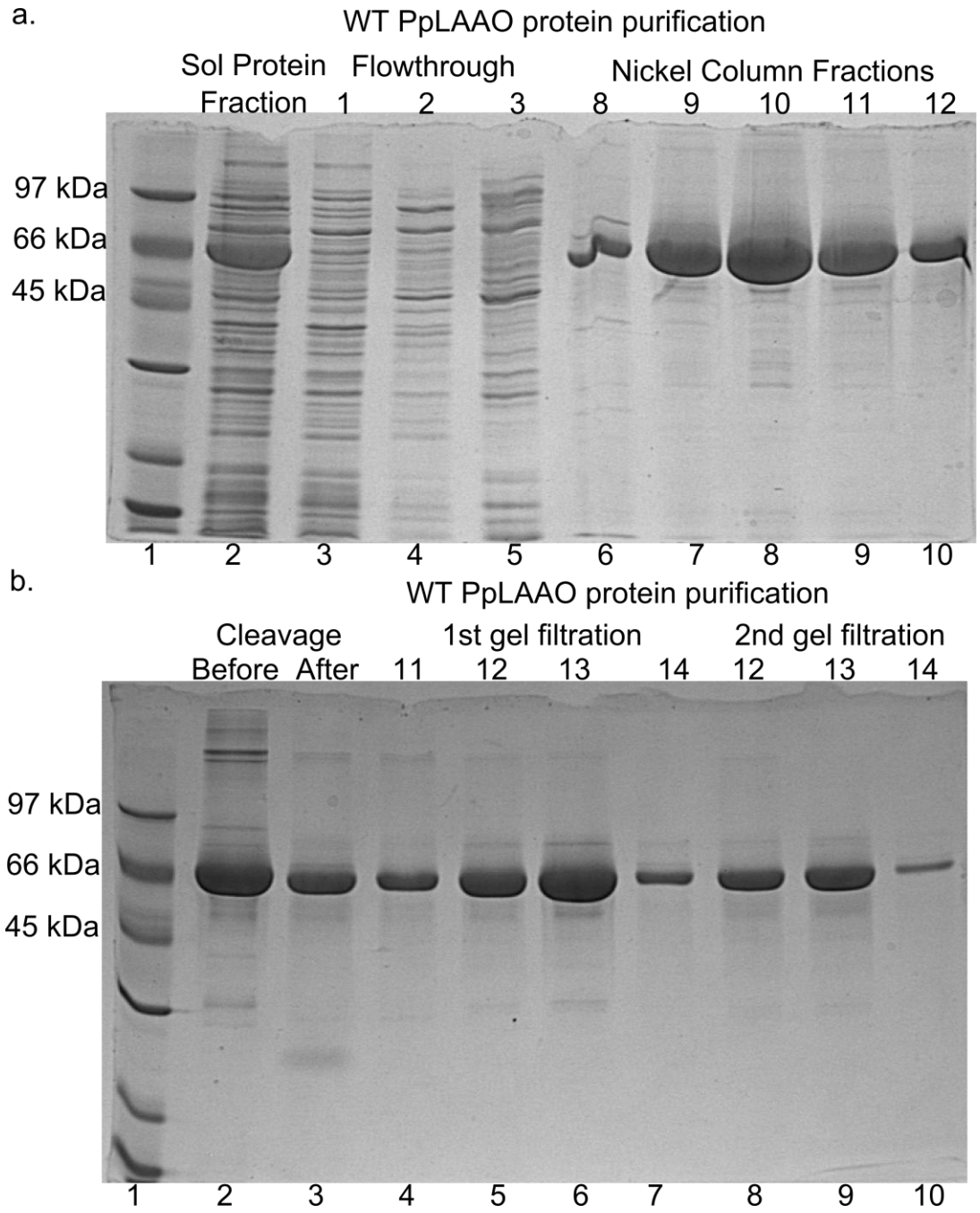

Figure 4.1: **a.** SDS-PAGE separation of protein purified from *E. coli* BL21-DE3 transformed with pET-YSBLIC3C-PpLAAO using metal affinity based chromatography. Lane 1, low range molecular weight marker; Lane 2, Soluble fraction of sonicated BL21-pET-YSBLIC3C-PpLAAO induced culture (60 kDa); Lane 3-5, Protein flow-through from column loading of soluble fraction of sonicated BL21-pET-YSBLIC3C-PpLAAO induced culture; Lane 6-10, protein fractions 8-12 from FPLC imidazole gradient of loaded BL21-pET-YSBLIC3C-PpLAAO protein (60 kDa). **b.** SDS-PAGE separation of protein from *E. coli* BL21-DE3 transformed with pET-YSBLIC3C-PpLAAO, cleaved and purified via gel filtration chromatography. Lane 1, low range molecular weight marker; Lane 2-3, BL21-pET-YSBLIC3C-PpLAAO FPLC fractions before/after C3-protease cleavage (60 kDa); Lane 4-7, BL21-pET-YSBLIC3C-PpLAAO fractions 11-14 from 1st gel filtration chromatography run (60 kDa); Lane 8-10, BL21-pET-YSBLIC3C-PpLAAO fractions 12-14 from 2nd gel filtration chromatography run (60 kDa).

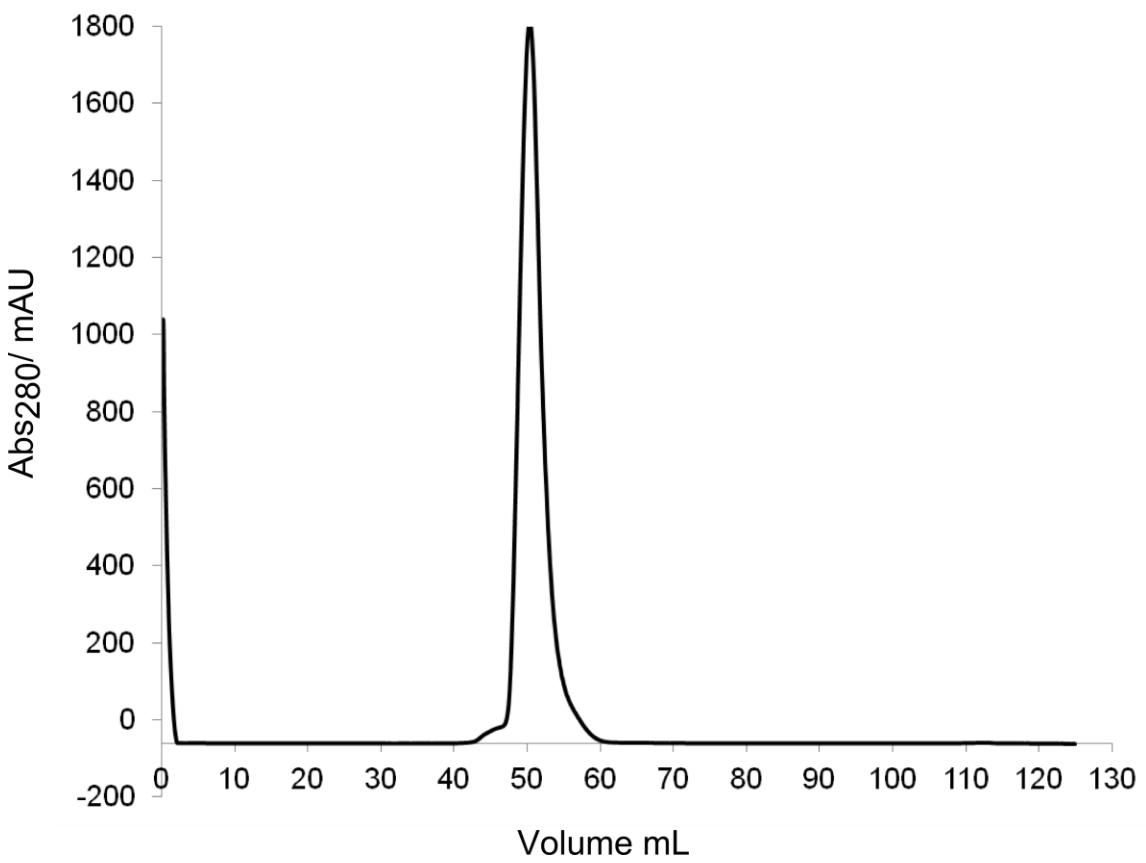

Figure 4.2 Abs280 trace of solution from gel filtration chromatography of purified PpLAAO using 120 mL HiLoad 16/60 Superdex 75 column.

4.2 Characterisation of PpLAAO protein

In order to determine the effects that any mutagenesis would have on the activity of the protein, the kinetic constants of the purified wild-type PpLAAO protein were tested against glycine, L-aspartate, L-asparagine and target substrates L-glutamate, L-homoserine, L-alanine and L-tyrosine using the HRP-based assay in 1 mL cuvettes in order to record the change in Abs_{510} over time (**Section 2.3.3**).

The activity against glycine seen previously had been lost in the purified protein, and no significant activity was seen against the target substrates L-homoserine, L-alanine and L-tyrosine (data not shown); however activity against L-aspartate and L-asparagine was still present and low levels of activity were also seen against L-glutamate. (**Figures 4.3-5, Table 4.1**). Activity against L-aspartate was quite high, with a k_{cat} of 10.6 s^{-1} and a k_{cat}/K_M of 4684 M^{-1} s^{-1} (**Figure 4.3, Table 4.1**).

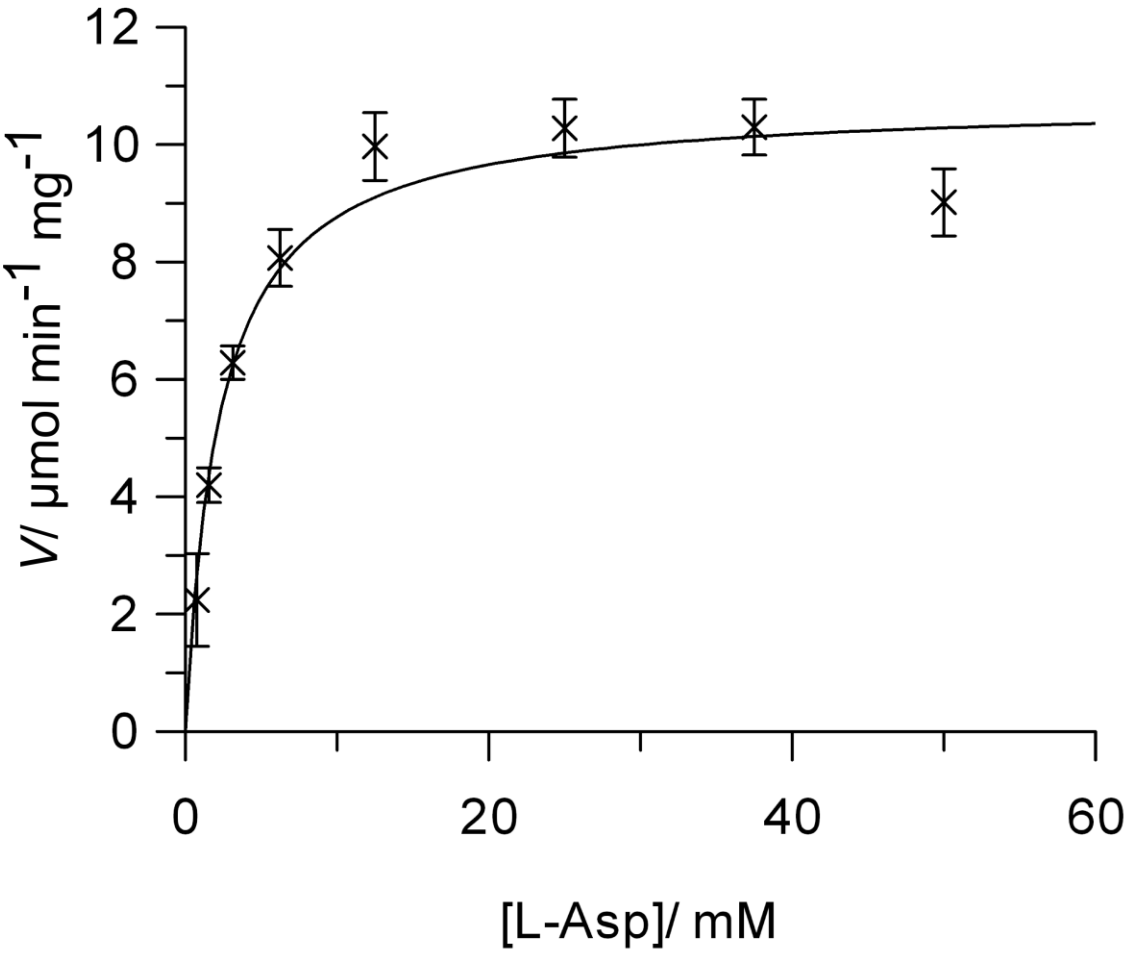

Figure 4.3 Rate of H_2O_2 production of PpLAAO against L-aspartate substrate concentration.

The determination of kinetic constants for the activity against L-asparagine was more difficult, as the rates of activity increased steadily over concentration up to 12.5 mM, but then decreased over higher concentrations of L-asparagine (**Figure 4.4**). This meant that the Michaelis Menten equations did not really fit the data, causing the calculated K_M to be unrealistically low, with an apparent k_{cat} of 4.5 s^{-1} and an apparent k_{cat}/K_M of 7298 M^{-1} s^{-1} (**Table 4.1**). Unfortunately there was not enough data to model the reaction using a substrate inhibition equation accurately, and an attempt to do so resulted in calculated V_{max} of 10244 nM min^{-1} mg $enzyme^{-1}$, K_M of 6264 mM and K_i of 0.01241 mM, which is also unrealistic.

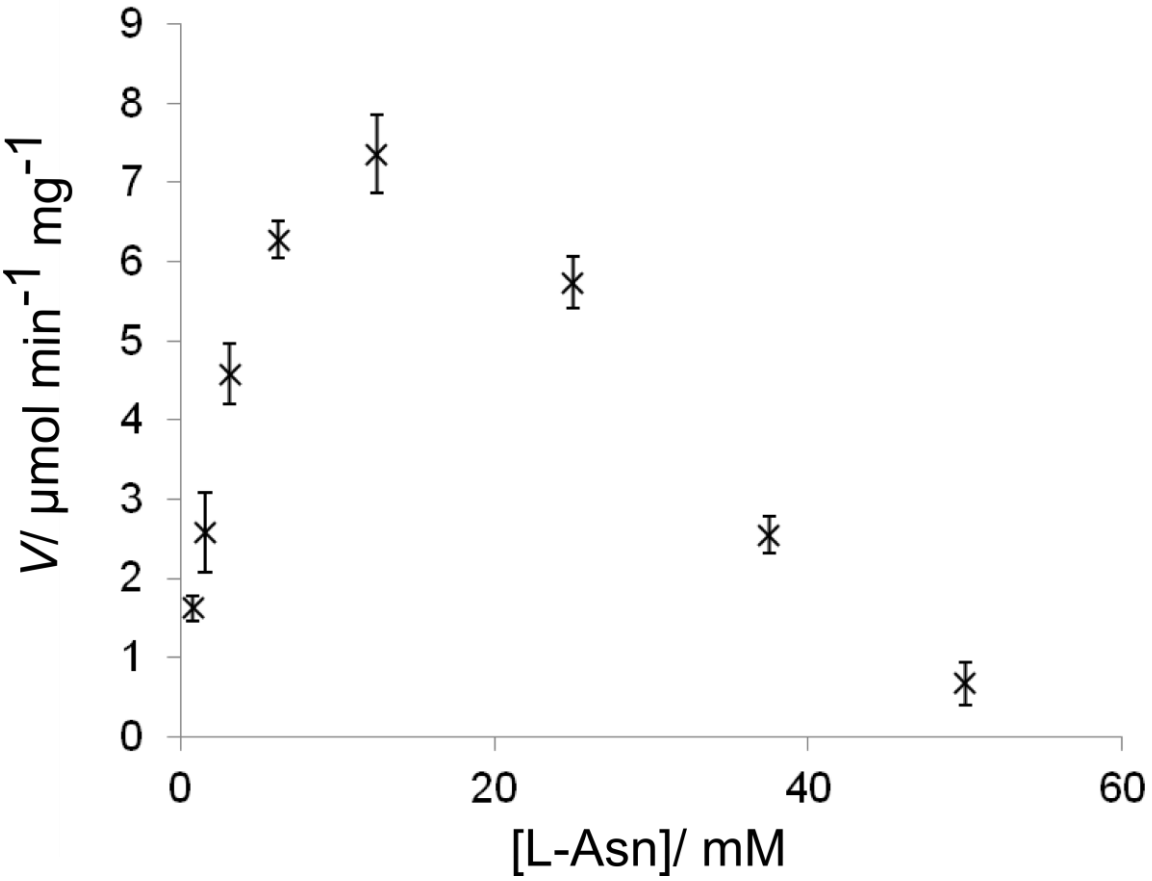

Figure 4.4 Rate of H_2O_2 production of PpLAAO against L-asparagine substrate concentration.

Despite the similarity between the L-aspartate and L-glutamate side chains, the activity against L-glutamate was very low (**Figure 4.5**), which is likely the reason the activity was not detected in the 96-well plate assay screen (**Figure 3.19**). The K_M against L-glutamate of 345 mM was 150-fold higher than that of L-aspartate and the k_{cat} against L-glutamate was 10-fold lower than the k_{cat} against L-aspartate (**Table 4.1**).

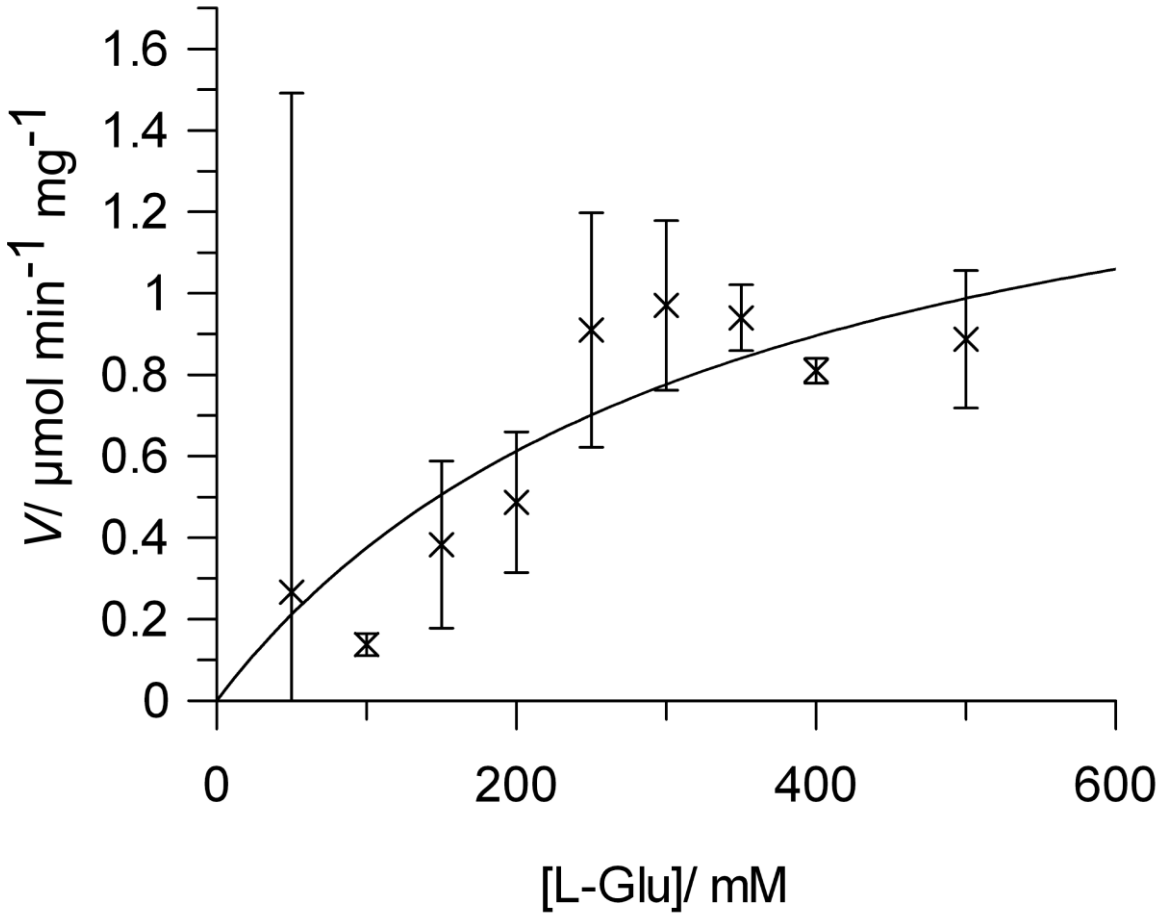

Figure 4.5 Rate of H_2O_2 production of PpLAAO against L-glutamate substrate concentration.

Table 4.1 Kinetic parameters of PpLAAO enzyme against L-aspartate and L-glutamate and unreliable calculated kinetic parameters against L-asparagine.

Substrate	V_{max} (nM min^{-1} mg $enzyme^{-1}$)	K_M (mM)	k_{cat} (s^{-1})	k_{cat}/K_M (M^{-1} s^{-1})
L-aspartate	10.75	2.263	10.60	4684
L-asparagine	(4.564)	(0.6166)	(4.50)	(7305)
L-glutamate	1.67	345	1.65	4.77

The pH optimum of the protein was determined using the liquid phase HRP based assay in a 96-well plate as in **Section 2.3.4**, with the 60 min end-point of reactions against L-aspartate at pH 4.7, 5.8, 6.2, 6.6, 7.0, 7.4, 7.8 and 8.2 being measured at A_{510}. From these reactions the optimum pH for the wild-type oxidation reaction of PpLAAO appears to be around 7.5 (**Figure 4.6**), although this may be affected by the pH optimum of the HRP enzyme on which the assay is reliant.

The effects of temperature on the protein was measured by incubating the purified protein at temperatures of 4°C, 10°C, 20°C, 30°C, 40°C, 50°C and 60°C for 5 min, 10 min, 20 min, 30 min, 45 min or 60 min. These incubated protein samples were then left on ice for 3 hours and then tested for activity against L-aspartate using the liquid phase HRP-based assay as in **Section 2.3.5**. The 60

min end point of these reactions was measured at A_{510}. Visually, the purified protein did not precipitate at temperatures of 30°C or lower, but began precipitating after 5 min at temperatures of 40°C and higher. Despite the protein having precipitated at 40°C, the activity of the protein samples treated at 40°C was still at the same levels as protein incubated at lower temperatures (**Figure 4.6**), suggesting any denaturation at 40°C is reversible. Protein activity dropped rapidly when incubated at 50°C (**Figure 4.6**).

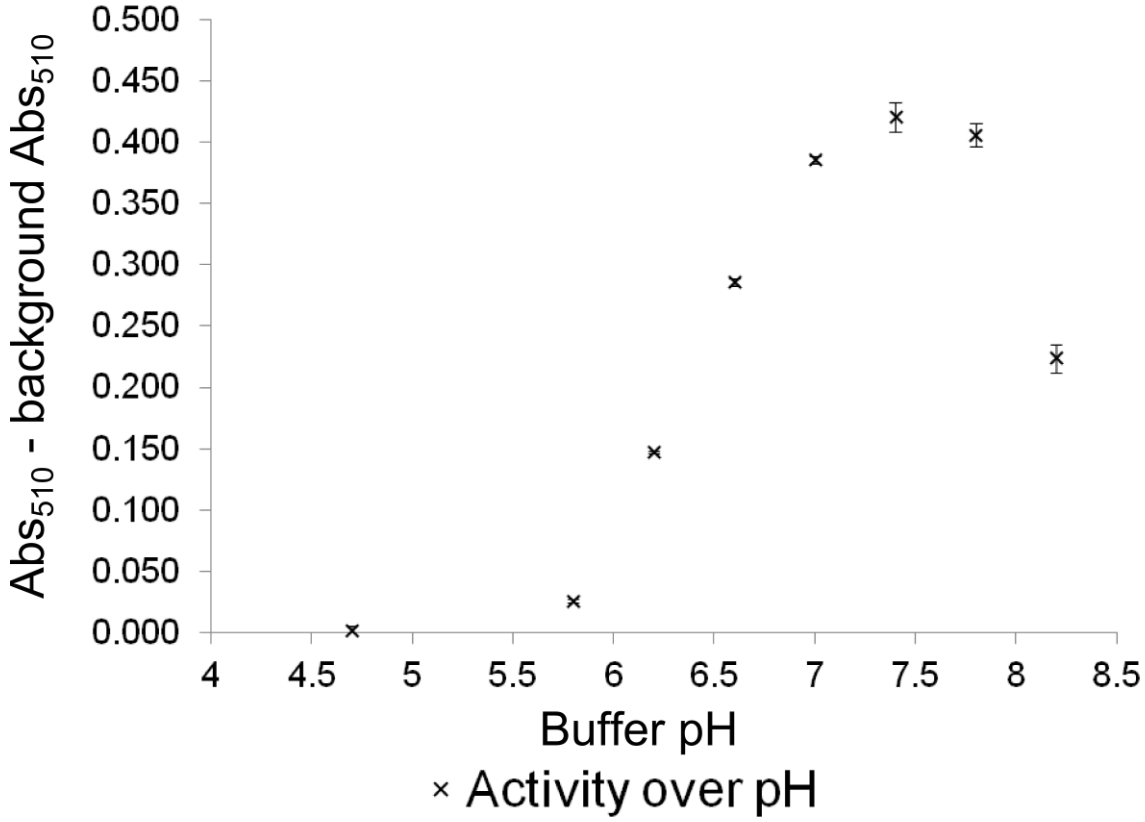

Figure 4.6 1 h end point of the activity assay of purified wild-type PpLAAO protein against L-aspartate over the pH of the reaction buffer.

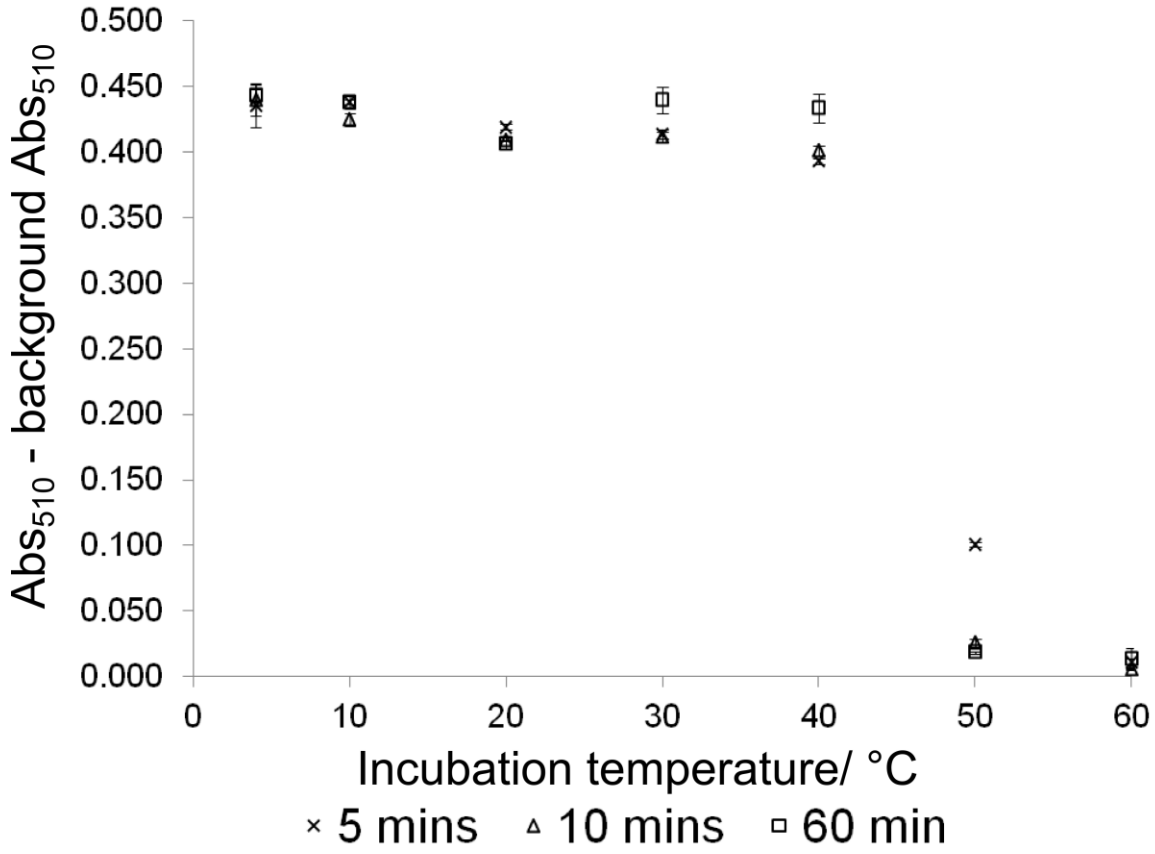

Figure 4.7 1 h end point of the activity assay of temperature-treated purified wild-type PpLAAO protein against L-aspartate over the incubation temperature of the protein, for incubation times of 5 min, 10 min and 60 min.

4.3 Attempts to crystallise PpLAAO protein

In an attempt to create protein crystals suitable for use in X-ray structure determination, the purified PpLAAO protein was concentrated to 10 mg mL^{-1}, 30 mg mL^{-1}, 45 mg mL^{-1}, 60 mg mL^{-1}, and 100 mg mL^{-1} as in **Section 2.3.6**. These proteins preparations were added to wells containing the 96-well Index crystallisation screen as in **Section 3.2.7**, along with a sample of the 30 mg ml^{-1} protein which had 1 mM of FAD added to the protein. However none of these screens produced protein crystals. 96 well crystallisation screens were also set up with 30 mg mL^{-1}, 45 mg mL^{-1}, 60 mg mL^{-1}, and 100 mg mL^{-1} of protein against the PACT crystallisation screen, and 60 mf mL^{-1} against the CSS 1+2 crystallisation screen, however no protein crystals were produced.

As crystallisation trials were showing large amounts of precipitation but no crystal formation, the purified wild type PpLAAO protein was run down a 7.5% native gel and subjected to Dynamic Light Scattering (DLS) as in **Section 2.3.8** in order to determine if the protein was in a homologous form while in solution.

Despite the protein eluting from the gel filtration column in a single peak (**Figure 4.2**) the native gel showed the protein separating into at least 5 separate bands (**Figure 4.8**). This is unlikely to be caused by protein aggregation as the protein formed separate bands rather than smearing. It could have been caused by different post-translational modifications to the protein changing the electronegativity of the protein by different amounts, or the protein could form different quaternary structures while in solution. Data from the DLS suggests that the protein is forming different sized quaternary structures, as it showed mass readings that are equivalent to both monomer and dimer forms of PpLAAO present in the solution, as well as several larger aggregated forms of the protein (**Table 4.2**).

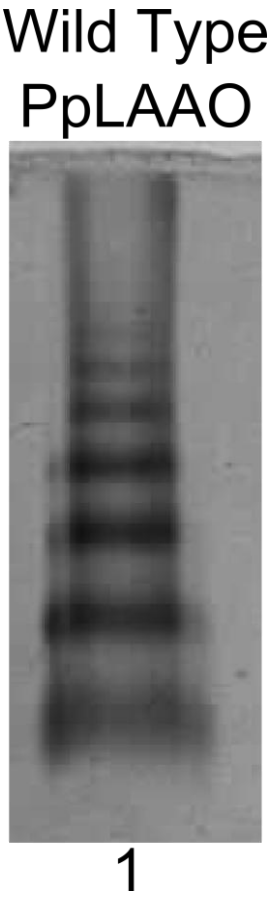

Figure 4.8 7.5% Native gel separation of wild type PpLAAO protein. Lane 1, 20 µL 1 mg mL^{-1} wild type PpLAAO protein.

Table 4.2 Table showing regularization data from the DLS analysis of wild type PpLAAO at 20°C. Possible quaternary structure determined by comparing the Radius to the Rh readings from the Results Summary of the DLS analysis (data not shown).

Radius (nm)	Possible Quaternary Structure	% Intensity	% Mass
2.899		1.61	4.95
3.841	Monomer	56.8	75.0
5.090	Dimer	35.3	20.0
6.744		0.000	0.000
36.50		3.25	0.00501
48.36		0.000	0.000
3295		3.10	2.72 E^{-6}

The formation of various different quaternary structures could be due to the protein forming disulphide cross-links between cysteine residues after purification. Because of this the purified protein was concentrated down and then diluted into several detergents (10 mM LDAO, 10 mM SB12, 0.5% β-OG, 500 mM TMAO, 250 mM NDSB-201) and varying concentration of precipitates (50 mM Urea, 100 mM Urea, 200 mM Urea, 50 mM G. HCl, 100 mM G. HCL and 200 mM G. HCl) (**Section 2.3.9**) in order to see if they could force the protein into a monomeric state that would be suitable for crystallisation.

The protein solutions remixed with 500 mM TMAO, 250 mM NDSB-201, 50 mM Urea, 100 mM Urea, 200 mM Urea, 50 mM G. HCl, 100 mM G. HCl and 200 mM G. HCl were analysed by DLS (**Section 2.3.9**), although the protein solutions remixed with 100 mM G. HCl and 200 mM G. HCl were too precipitated to get a reliable data set.

The solutions remixed with 500 mM TMAO, 250 mM NDSB-201, 50 mM Urea, 100 mM Urea and 200 mM Urea all still showed various quaternary states, similar to the protein in the original Tris/NaCl/AEBSF resuspension buffer (data not shown). However the protein remixed with 50 mM G. HCl had precipitated. However after the precipitation had been spun down by centrifugation, the remaining protein appeared to be in a mostly monomeric form (**Table 4.3**), which suggests that using a gradient of low concentration of G. HCl may allow the protein to be kept in a monomeric state.

Table 4.3 Comparison of the % Intensity and % Mass of the Monomeric and Dimeric forms of the protein (determined by comparing Radius in Regularization Data to Rh and MW in Results Summary of DLS analysis) in 50 mM Tris, 300 mM NaCl, 20 μM AEBSF and 50 mM G. HCl.

	Tris/NaCl/AEBSF		50 mM G. HCl	
Quaternary Structure	% Intensity	% Mass	Quaternary Structure	% Intensity
Monomer	56.8	75.0	2.92	95.0
Dimer	35.3	20.0	0.00	0.00

All of the remixed protein solutions, except for the 100 mM and 200 mM G. HCl, were analysed by 7.5% native gel as in S**ection 2.3.9**. The 10 mM LDAO, 10 mM SB12, 0.5% β-octylglucopyranoside and 200 mM Urea all caused a reduction in the larger forms of the protein compared to the Tris/NaCl/AEBSF buffer, but there were still at least three different forms of the protein in these solutions (**Figure 4.9**). The 250 mM NDSB-201 appears to have caused an increase in the number of forms of the PpLAAO protein compared to the Tris/NaCl/AEBSF buffer and the protein remixed in the 500 mM TMAO and the 50 mM and 100 mM Urea appears to have aggregated as the protein is smeared in the gel, especially in the 500 mM TMAO solution.

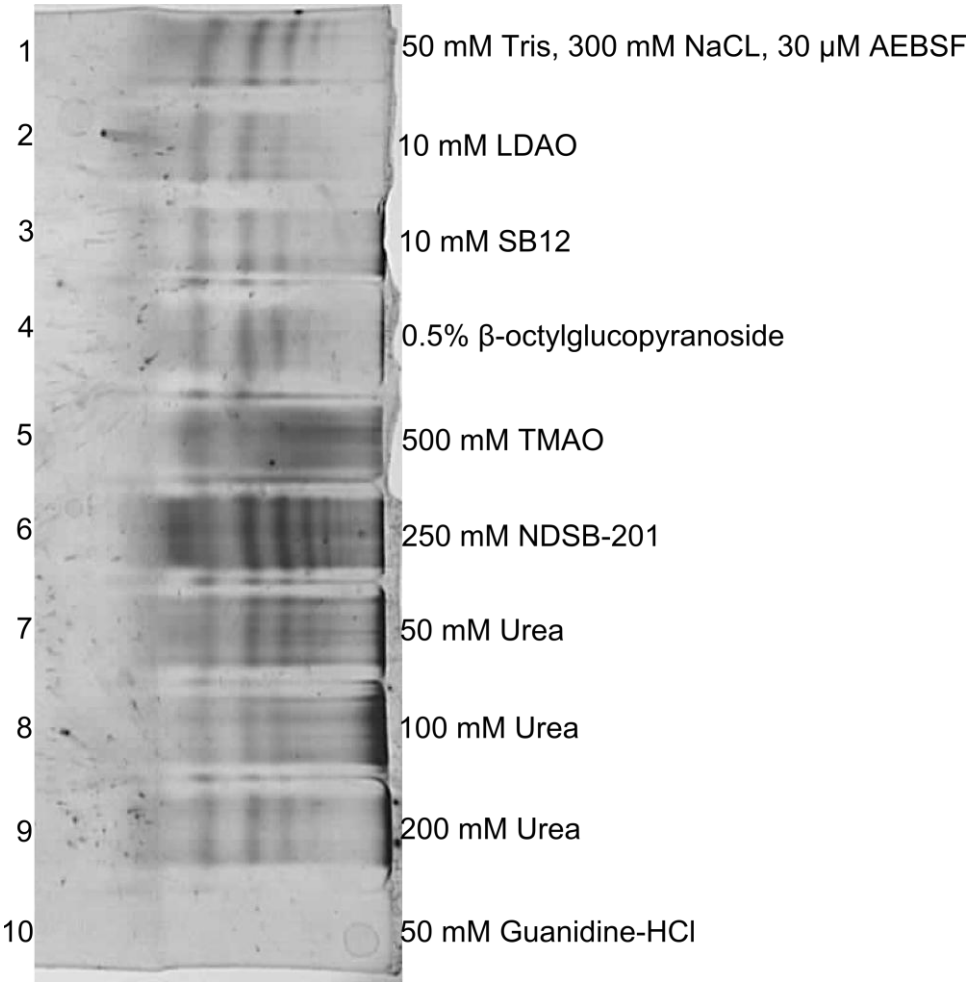

Figure 4.9 7.5% Native-gel analysis of wild-type PpLAAO protein in various buffers. Lane 1, Original 50 mM Tris, 300 mM NaCl and 20 µM AEBSF buffer; Lane 2, 10 mM LDAO, Lane 3, 10 mM SB12; Lane 4, 0.5% β-OG; Lane 5, 500 mM TMAO; Lane 6, 250 mM NDSB-201; Lane 7-9, 50 mM, 100 mM and 200 mM Urea; Lane 10, 50 mM G. HCl.

The wild type protein in the original Tris/NaCl/AEBSF buffer was also analysed at temperatures of 4°C, 12°C and 20°C to determine if the temperature of the protein had any effect on the protein form in solution (**Section 2.3.9**). The results suggested that while at cooler temperatures the protein was more likely to be in monomeric form (**Table 4.4**). It's possible that the preparation and

purification steps done at 20°C may have caused the protein to form larger complexes, meaning that preparing, purifying and crystallising the protein in a cold room may help the protein stay in monomeric form and be more likely to crystallise.

Table 4.4 Comparison of the % Intensity and % Mass of the Monomeric and Dimeric forms of the protein (determined by comparing Radius in Regularization Data to Rh and MW in Results Summary of DLS analysis) at 20°C, 12°C and 4°C.

	20°C		12°C		4°C	
Quaternary Structure	% Intensity	% Mass	% Intensity	% Mass	% Intensity	% Mass
Monomer	56.8	75.0	72.9	90.0	50.3	83.4
Dimer	35.3	20.0	18.7	9.94	27.8	13.1

Due to these observations, protein was re-purified taking extra care to ensure all steps were done at cold temperatures as in **Section 2.3.10**. This protein prep was analysed on a 7.5% native gel as in **Section 2.3.10** however the protein still separated into several distinct bands similar to those seen in **Figure 4.7** (data not shown).

The remaining protein was concentrated down and diluted with ice-cold 5 mM, 10 mM, 15 mM, 20 mM, 25 mM, 30 mM, 35 mM, 40 mM and 45 mM G. HCl at pH 7.0 as in **Section 2.3.10,** as the protein did not precipitate immediately, the solutions were stored at 4°C overnight. The next morning all solutions of protein had precipitated equally. Protein was spun down to remove precipitation and samples were analysed using 7.5% native-PAGE gel, however none of the samples contained enough free protein to be visible on the gel (data not shown).

A 24-well crystallisation tray was set up at 4°C as in **Section 2.3.10**, to see if the precipitants ammonium sulphate, PEG 4k or PEG 3.5k at a cold temperature could result in production of crystals, however no crystals developed from the tray.

4.4 Conclusions

The PpLAAO protein was purified from *E. coli* BL21-DE3 cells using metal affinity chromatography and the attached C terminal His-tag was removed using C3-protease. The cleaved protein was then purified further using gel filtration chromatography. The position of the gel filtration elution peak (**Figure 4.2**) suggested that the protein is around 116 kDa in solution, roughly corresponding to a dimeric form of the 59 kDa PpLAAO protein. The soluble HRP based assay solution used to screen the target oxidases for activity in **Section 3.3** was then used to determine the rate of activity over substrate concentration of the purified PpLAAO protein against glycine, L-aspartate and L-asparagine.

The activity seen previously against glycine (**Figure 3.19**) had been lost in the purified PpLAAO protein, with no detectable activity been seen (data not shown). This may be due to another soluble protein produced by *E. coli* that was converting the glycine in the reaction solution into a different substrate that could be oxidised by the PpLAAO protein during the previous assays, or possibly the PpLAAO protein needs a different cofactor to oxidise glycine that is lost during the protein purification.

The protein showed high activity against L-aspartate with a k_{cat} of 10.6 s^{-1} and a k_{cat}/K_M of 4684 M^{-1} s^{-1} (**Figure 4.3**, **Table 4.1**), which is roughly ten-fold higher than the k_{cat}/K_M of the *E. coli* L-AspO, which is 306 M^{-1} s^{-1}.[118] It also showed lower activity against L-asparagine, although a loss of activity at the higher concentrations of L-asparagine made it difficult to accurately fit the data to either a Michaelis Menten or a substrate inhibition based equation. This meant that the apparent K_M and V_{max} of L-asparagine were calculated to be lower than expected from looking at the data points, resulting in an apparent k_{cat} of 4.5 s^{-1} and k_{cat}/K_M of 7298 M^{-1} s^{-1}. There was also some very low activity against L-glutamate, with a k_{cat} of 1.65 s^{-1} and a k_{cat}/K_M of 4.77 M^{-1} s^{-1}, which had been too low to be detected in the screens performed previously (**Scetion 3.3**).

The effect of pH on the PpLAAO protein was determined by measuring the 1 h end point of reactions against L-aspartate at different pH of reaction buffers. PpLAAO was most active around pH 7.5 (**Figure 4.5**), however this may be affected by the pH optimum of the HRP enzyme, which is required for the assay. The effects of temperature on the purified protein were determined by incubating samples of the purified protein at varying temperatures and varying times, then measuring the activity of the protein samples against L-aspartate once the protein had cooled back down. The protein activity was unaffected when the sample was incubated between 4°C and 30°C. Although protein precipitation could be seen after 5 min at 40°C, the activity of the protein incubated at 40°C from 5 min to 1 h was still at the same levels as protein kept at lower temperatures, suggesting that the protein is reversibly denatured at 40°C.

Incubation at 50°C caused the protein to lose most of its activity after just 5 min, and protein incubation at 60°C for 5 min caused it to lose all activity against L-aspartate, suggesting that the protein is irreversibly denatured at temperatures above 50°C (**Figure 4.6**).

Attempts were then made to crystallise the purified protein for use in X-ray structure determination using 96-well crystallisations screens. However the protein showed a large amount of precipitation, but no crystals were formed. Because of this the native gel and DLS analysis were used to determine if the protein was in a homogenous form in solution, as heterogeneous forms of proteins often fail to crystallise.

Despite the protein eluting from the gel filtration column in one peak (**Figure 4.2**), the native gel showed the protein forming at least five distinct bands (**Figure 4.7**). One potential reason for the separate bands could either be due to a difference in the protein charge possibly caused by post-translational modification of the protein. The separate bands could also the protein grouping into several different quaternary forms of the protein in solution, which would have to have happened after purification by gel filtration.

The DLS analysis suggested that the protein was forming different sized quaternary structures in solution. There were several different protein mass sizes, some of which were equivalent to monomeric and dimeric forms of PpLAAO and several larger aggregated forms of the protein. Despite the protein apparently purifying as a dimer, the majority of the protein mass in the DLS was formed by the monomeric form of the protein (**Table 4.2**), suggesting the proteins quaternary structure partially broke down after the gel filtration.

It is possible that the different quaternary forms of the protein could be caused by cross-links formed after the purification. The purified protein was resuspended into several detergents to see if these would have any effect on any cross-linking that was occurring. The protein was also resuspended into low concentrations of precipitates urea and guanidine hydrochloride (G. HCl) as they could have forced the protein into a monomeric form suitable for crystallisation.

Although some detergents and 200 mM Urea reduced the number of bands the protein split into when run on a native gel (**Figure 4.8**) none caused the protein to remain in a single form. A low concentration of 50 mM G. HCl caused the majority of the protein to precipitate, however the protein that remained in solution was entirely monomeric (**Table 4.3**). The protein was resuspended in lower concentration of G. HCl in an attempt to force the protein into a monomeric form without causing larger amounts of it to precipitate, but large amounts of the protein precipitated when as little as 5 mM of G. HCl was added.

DLS analysis of the purified PpLAAO protein repeated at 4°C, 12°C and 20°C suggested that the protein was more likely to be in a monomeric form at lower temperatures (**Table 4.4**). Because of this the protein purification was repeated, except that the metal affinity chromatography and the gel filtration chromatography were both performed at a temperature of 4°C, and extra care was taken to ensure the protein was kept ice-cold at all times. However this protein sample still separated into several bands when analysed on native gel, indicating that the protein temperature is not the only cause of the heterogeneous form of the protein in solution.

Chapter 5 Site Directed Mutagenesis of PpLAAO protein

As the activity of the wild-type PpLAAO protein has been characterised, one step towards identifying what factors determine the activity and substrate specificity of the PpLAAO enzyme and how active it is as a catalyst would be to attempt to rationally mutate the protein based on the structure of its active site. As the structure of PpLAAO is still unsolved (**Section 4.3**) the structure of a homologous L-aspartate oxidase (L-AspO) from *E. coli*[119, 65] was used as a starting point for this mutagenesis.

The thirteen active site residues were individually mutated to alanine residues in order to determine the effects of each active site residue on the overall efficiency and substrate specificity of the PpLAAO protein.

5.1 Comparison of PpLAAO and *E. coli* L-AspO

As attempts to crystallise the PpLAAO protein for use in structure determination were unsuccessful (**Section 4.3**), a homologous structure of the protein would be useful for use as a starting point when deciding what changes to make as part of a rational design approach towards identifying what factors determine substrate specificity of the PpLAAO enzyme.

L-AspO is a 60 kDa monomeric flavoprotein that catalyses the first step of the *de novo* production of NAD.[119] The structure for the R386L mutant of L-AspO in complex with succinate has been solved by Bossi *et al.*[65] and it has 63% sequence homology with the PpLAAO protein (**Figure 5.1**). The active site of the *E. coli* enzyme is divided into a flavin binding domain, comprised of residues Q50, G51, G52, E121 (122 in the *P. putida* enzyme), H351, R386L, S389, S391 and L392 and a capping domain, including residues H244, L257, L258, T259, E260, S261 and R290.

Further work by Tedeschi *et al.*[118] on the role of the active site residues shows that the T259 and H244 from the capping domain bind the C1 carboxylate of the succinate ligand and the backbone N-H of S389 and H351 are bound to the C2 succinate carboxylate. The E121 (122 in the *P. putida* enzyme) residue is conserved in L-aspartate oxidases and is thought to be essential for binding the amino group of the L-aspartate substrate.[65] The R290 residue from the capping domain is also thought to be important in interactions with the amino acid substrate.

In order to determine if the active site structure of the L-AspO protein is similar enough to that of PpLAAO for it to be used as the basis of a site directed mutagenesis strategy, the non-essential first-shell active site residues H244, L257, T259, E260, R290, H351, R386, S389 and S391, along

with second shell active site residues Q242, P245, V293 and Y352, which are all conserved between the *E. coli* and *P. putida* L-aspartate oxidases (**Figures 5.1-2**) were targeted to be substituted by alanine in order to disrupt the activity of those residues and investigate the role of each residue on the activity of the PpLAAO protein, and determine if these roles are consistent with what would be expected from the *E. coli* active site structure. The kinetic constants for H224A, H351A, R290L and R386L mutant forms of the *E. coli* L-AspO have been determined previously by Tedeschi *et al.*[118] and comparison of these mutants and mutants of the same residues in the PpLAAO protein will also show how identical the active sites of the two proteins are.

```
Q88MZ2_PpLAAO      MSQQFQH--DVLVIGSGAAGLSLALNLPSHLRVAVLSKGDLSNGSTFWAQGGVAAVLDNT 58
P10902_L-AspO      MNTLPEHSCDVLIIGSGAAGLSLALRLADQHQVIVLSKGPVTEGSTFYAQGGIAAVFDET 60
                   *.   :*  ***:************.*..: :* ***** :::****:****:***:*:*
                        ¦β1¦¦ β2 ¦  ¦   α1   ¦     ¦β3¦¦β4¦    ¦α2¦           ¦

Q88MZ2_PpLAAO      DTVQSHVEDTLNAGGGLCHEDAVRFTVEHSREAIQWLIEQGVPFTRDEHYSVDDGGFEFH 118
P10902_L-AspO      DSIDSHVEDTLIAGAGICDRHAVEFVASNARSCVQWLIDQGVLFDTHIQPNGEES---YH 117
                   *:::******* **.*:*...**.*...::*..:****:*** *  . : . ::.   :*
                        α3     ¦      ¦        α4        ¦          ¦β5¦

Q88MZ2_PpLAAO      LTREGGHSHRRIIHAADATGAAIFTTLLEQARQRPNIQLLEQRVAVDLITERRLGLPGER 178
P10902_L-AspO      LTREGGHSHRRILHAADATGREVETTLVSKALNHPNIRVLERSNAVDLIVSDKIGLPGTR 177
                   ************:*******  : ***:.:* ::****::**:  *****.. ::**** *
                                          ¦ α5 ¦   ¦β6 ¦¦   β7   ¦α6¦

Q88MZ2_PpLAAO      -CLGAYVLDRNTGEVDTFGARFTVLATGGAAKVYLYTSNPDGACGDGIAMAWRAGCRVAN 237
P10902_L-AspO      RVVGAWVWNRNKETVETCHAKAVVLATGGASKVYQYTTNPDISSGDGIAMAWRAGCRVAN 237
                     :**:* :**.  *:*  *: .*******:*** **:*** :.***************
                   ¦  β8   ¦    ¦ β9 ¦ ¦β10¦    ¦α7¦β11¦ ¦α8¦   ¦  α9  ¦

Q88MZ2_PpLAAO      LEFNQFHPTCLYHPQAKSFLITEALRGEGALLRLPNGERFMPRFDPREELAPRDIVARAI 297
P10902_L-AspO      LEFNQFHPTALYHPQARNFLLTEALRGEGAYLKRPDGTRFMPDFDERGELAPRDIVARAI 297
                   *********.******:.**:********* *: *:* **** ** * ************
                      ¦ β12  ¦           ¦α10¦  ¦β13¦     ¦α11¦  ¦α12¦ ¦    α13

Q88MZ2_PpLAAO      DHEMKRLGVDCVYLDITHKPADFIKSHFPTVYERCLAFGIDITRQPIPVVPAAHYTCGGV 357
P10902_L-AspO      DHEMKRLGADCMFLDISHKPADFIRQHFPMIYEKLLGLGIDLTQEPVPIVPAAHYTCGGV 357
                   ********.**::***:*******:.*** :**: *.:***:*:::*:*:***********
                         ¦    ¦β14¦     ¦ α14¦ ¦  α15  ¦          ¦   β15   ¦¦β16

Q88MZ2_PpLAAO      MVDDCGHTDVPGLYAIGETSFTGLHGANRMASNSLLECFVYGRAAAADIQAHLEQVAMPK 417
P10902_L-AspO      MVDDHGRTDVEGLYAIGEVSYTGLHGANRMASNSLLECLVYGWSAAEDITRRMPYAHDIS 417
                   **** *:*** *******.*:*****************:*** :** **  ::  .   .
                    ¦    ¦β17¦β18¦¦α16¦¦β19¦       ¦        α17      ¦α18¦

Q88MZ2_PpLAAO      ALPGWDASQVTDSDEDVIIAHNWDELRRFMWDYVGIVRTSKRLQRAQHRIRLLLDEIDEF 477
P10902_L-AspO      TLPPWDESRVENPDERVVIQHNWHELRLFMWDYVGIVRTTKRLERALRRITMLQQEIDEY 477
                   :** ** *:* :.** *:* ***.*** ***********:***:** :** :* :****:
                              ¦        α19        ¦¦β20¦ ¦         α20

Q88MZ2_PpLAAO      YSNYKVSRDLIELRNLAQVAELMILSAMQRKESRGLHYTLDYPGMLDEAKDTILNPL--- 534
P10902_L-AspO      YAHFRVSNNLLELRNLVQVAELIVRCAMMRKESRGLHFTLDYPELLTHSGPSILSPGNHY 537
                   *::::**.:*:*****.*****:: .** ********:***** :* .:  :**.*
                   ¦      ¦         α21         ¦

Q88MZ2_PpLAAO      ---
P10902_L-AspO      INR 540
```

Figure 5.1 ClustalW2 alignment of the L-aspartate oxidases from *P. putida* (PpLAAO) and *E. coli* (L-AspO) with positions of α-helix and β-sheet structures in L-AspO. * represents conservation of identical residues, : represents conservation of strongly similar residues and . represents conservation of weakly similar residues. For the L-AspO sequence, FAD-binding domain residues are in red, capping domain residues are in green and helical domain residues are in blue. Shared active site residues are highlighted in yellow.

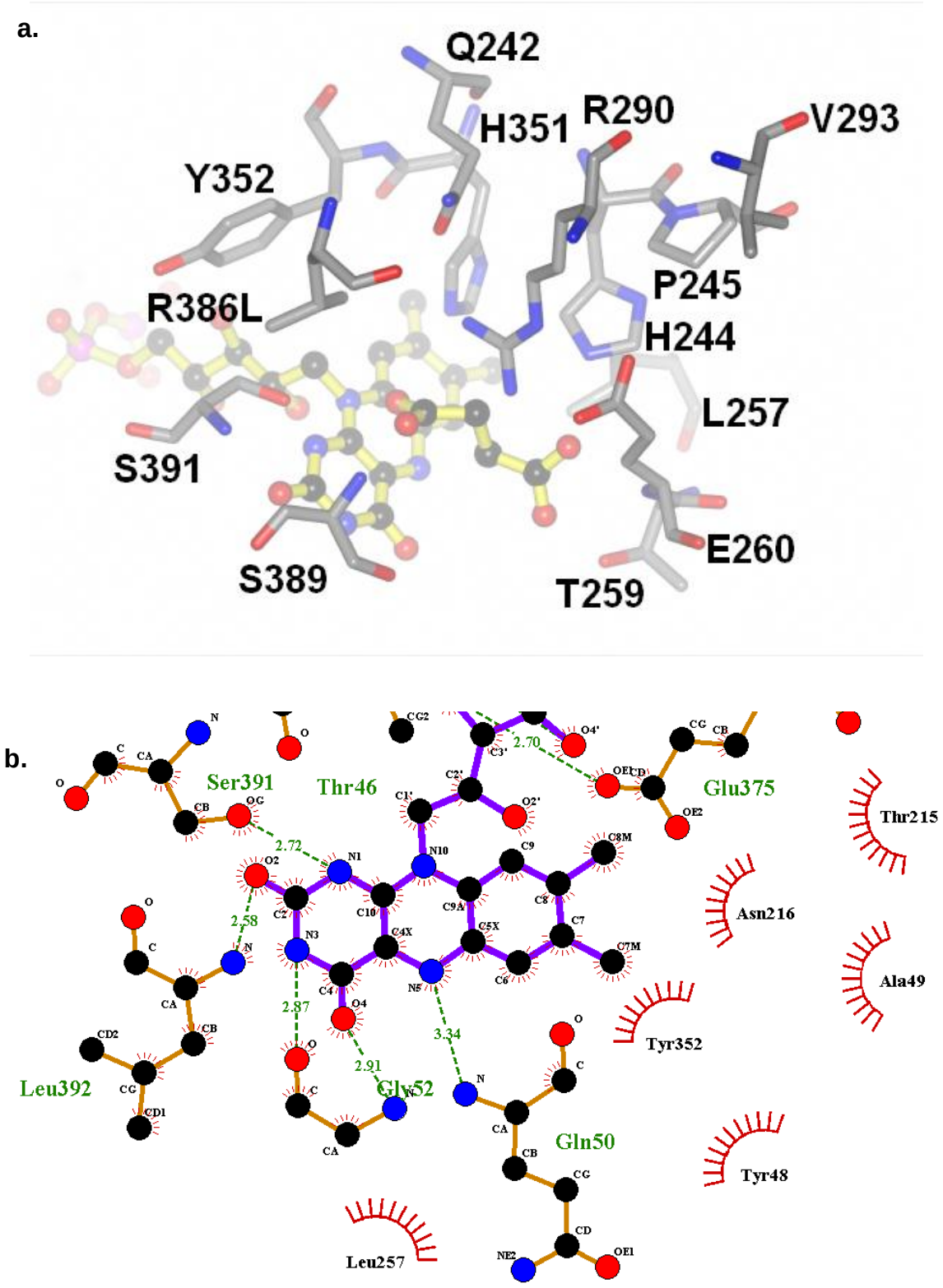

Figure 5.2 Active site structure of the *E. coli* L-AspO solved by Bossi *et al.*.[65] **a.** The thirteen active site residues targeted for mutagenesis. Active site residues in grey, FAD and succinate in yellow. **b.** LigPlot+[67] representation of residues binding to flavin ring of L-AspO. Hydrogen bonds represented by dashed green lines and van der Waals forces represented by red combs. **c.** LigPlot+[67] representation of residues binding succinate in active site of of L-AspO. Hydrogen bonds represented by dashed green lines and van der Waals forces represented by red combs.

c.

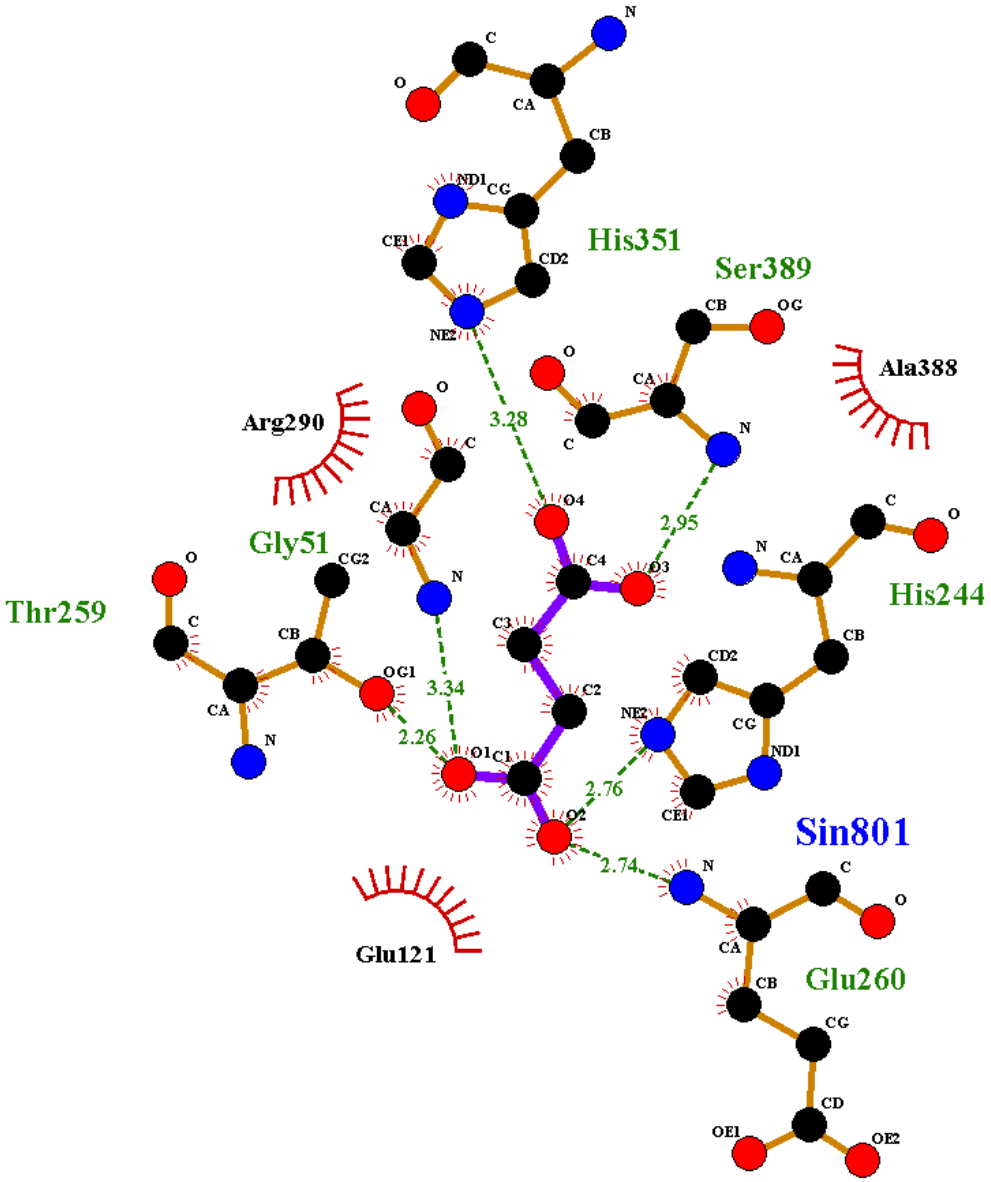

Figure 5.2 Active site structure of the *E. coli* L-AspO solved by Bossi *et al.*.[65] **a.** The thirteen active site residues targeted for mutagenesis. Active site residues in grey, FAD and succinate in yellow. **b.** LigPlot+[67] representation of residues binding to flavin ring of L-AspO. Hydrogen bonds represented by dashed green lines and van der Waals forces represented by red combs. **c.** LigPlot+[67] representation of residues binding succinate in active site of of L-AspO. Hydrogen bonds represented by dashed green lines and van der Waals forces represented by red combs.

5.2 Generation of active site mutants of PpLAAO

To investigate the effect of each of these active site residues on the overall activity and substrate specificity of the PpLAAO enzyme, each active site residue was individually mutated to alanine in order to disrupt any bonding effects of those residues.

The thirteen SDM mutants were produced from the YSBLIC-3C-PpLAAO plasmid using the Stratagene QuikChange method where two complementary, overlapping mutagenic primers are used to form a copy of the entire plasmid ring, and the original wild-type plasmid is digested using *Dpn*I restriction enzyme, which targets the methylated DNA in plasmids that have been purified by Miniprep, but not unmethylated DNA produced by PCR.

The thirteen mutants were produced using Phusion polymerase as in **Section 2.4**. PCR product was treated with *Dpn*I to remove the wild-type plasmid template and was then used to transform electrocompetent *E.coli* Top10 cells or chemically competent *E. coli* BL21-Gold-DE3 cells (**Section 2.4, Table 2.6**). Depending on the number of colonies produced, a number of colonies from each transformation were picked and gene overexpression was induced. Cells were then harvested and the insoluble protein fractions were analysed on 12% SDS-PAGE gel in order to make sure that the gene inserts in the plasmids were actually capable of expressing protein of the correct size before having them sequenced (**Figures 5.3-5.8**).

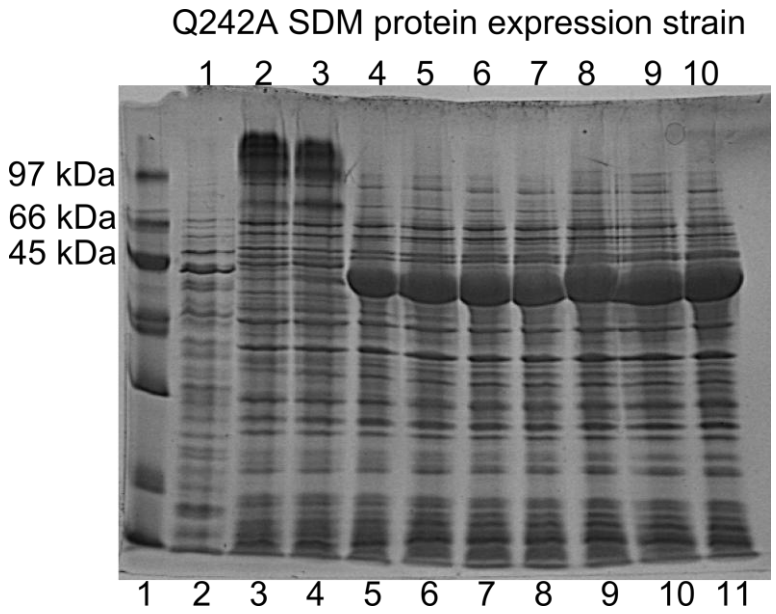

Figure 5.3 SDS-PAGE separation of protein from electrocompetent *E. coli* BL21-DE3 cells transformed with mutated PpLAAO YSBLIC3C plasmids Q242A1-10: Lane 1, BioRad low molecular weight marker; Lane 2-11, insoluble protein fraction from Q242A1-10.

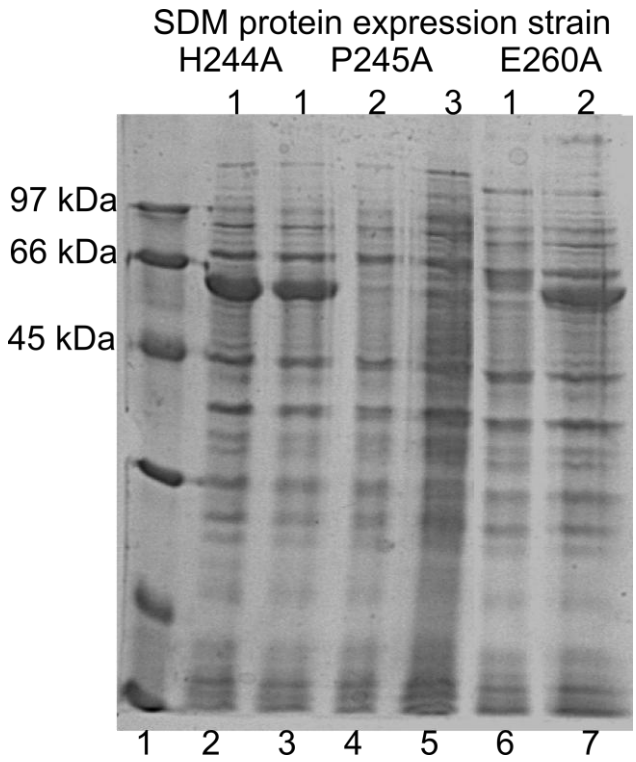

Figure 5.4 SDS-PAGE separation of protein from *E. coli* BL21-Gold-DE3 cells transformed with mutated PpLAAO YSBLIC3C plasmids H244A1, P245A1-3 and E260A1-2. Lane 1, BioRad low molecular weight marker; Lane 2, insoluble protein fraction from H244A1; Lane 3-5, insoluble protein fraction from P245A1-3; Lane 6-7, insoluble protein fraction from E260A1-2.

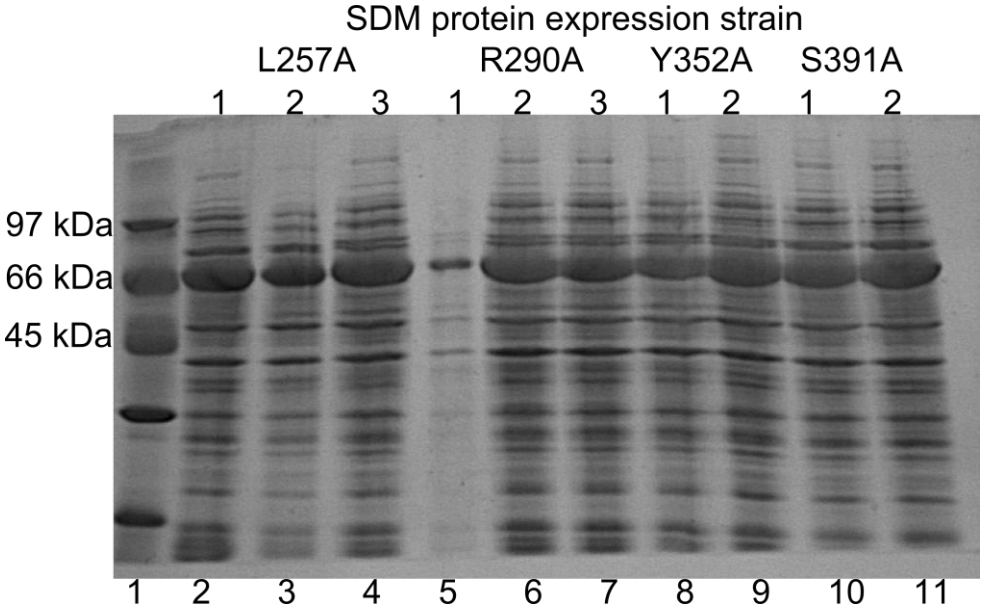

Figure 5.5 SDS-PAGE separation of protein from *E. coli* BL21-Gold-DE3 cells transformed with mutated PpLAAO YSBLIC3C plasmids L257A1-3, R290A1-3, Y352A1-2 and S391A1-2. Lane 1, BioRad low molecular weight marker; Lane 2-4, insoluble protein fraction from L257A1-3; Lane 4-7, insoluble protein fraction from R290A1-3; Lane 8-9, insoluble protein fraction from Y352A1-2; Lane 8-9, insoluble protein fraction from Y352A1-2; Lane 10-11, insoluble protein fraction from S391A1-2.

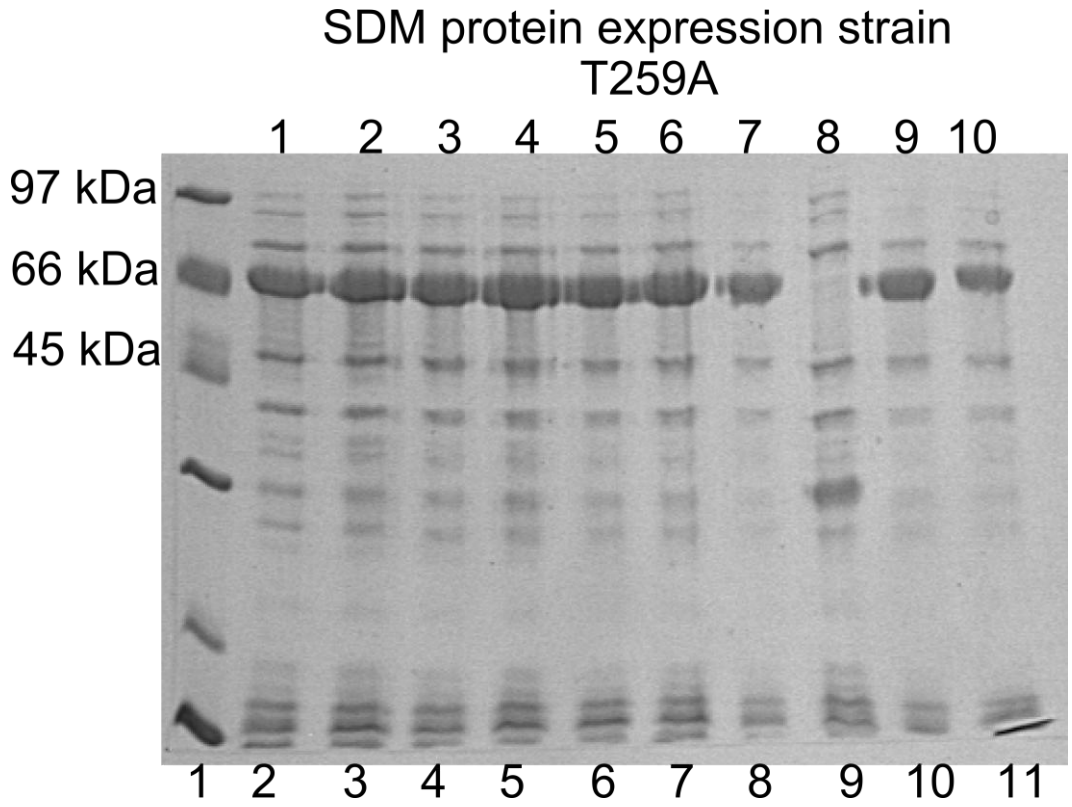

Figure 5.6 SDS-PAGE separation of protein from *E. coli* BL21-Gold-DE3 cells transformed with mutated PpLAAO YSBLIC3C plasmids T259A1-10: Lane 1, BioRad low molecular weight marker; Lane 2-11, insoluble protein fraction from T259A1-10.

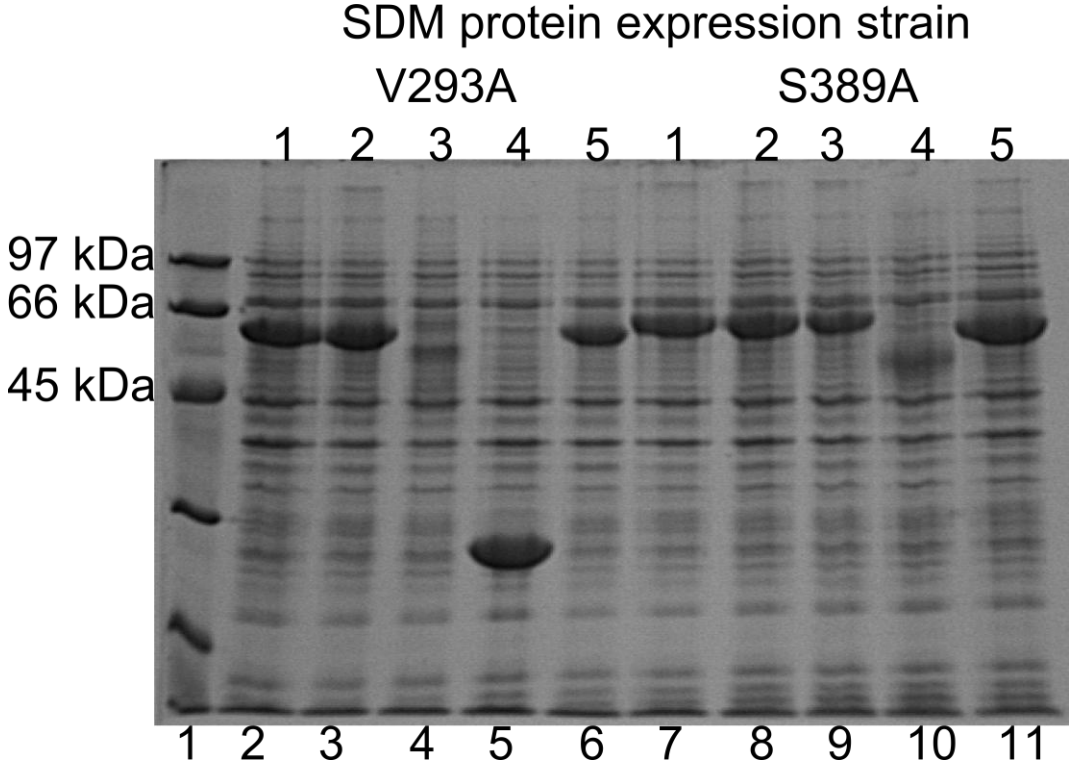

Figure 5.7 SDS-PAGE separation of protein from *E. coli* BL21-Gold-DE3 cells transformed with mutated PpLAAO YSBLIC3C plasmids V293A1-5 and S389A1-5. Lane 1, BioRad low molecular weight marker; Lane 2-6, insoluble protein fraction from V293A1-5; Lane 7-11, insoluble protein fraction from S389A1-5.

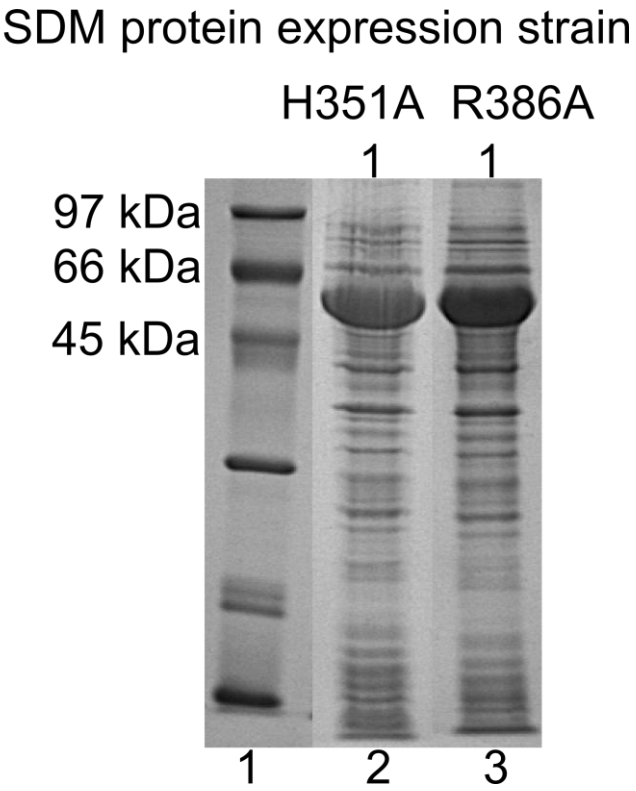

Figure 5.8 SDS-PAGE separation of protein from electrocompetent *E. coli* BL21-DE3 cells transformed with mutated PpLAAO YSBLIC3C plasmids H351A1-2 and R386A1-2. Lane 1, BioRad low molecular weight marker; Lane 2-3, insoluble protein fraction from H351A1-2; Lane 4-5, insoluble protein fraction from R386A1-2.

Based on these results the plasmids from the Q242A1, H244A1, P245A1, L257A1, T259A1, E260A2, R290A2, V293A1, H351A1, Y352A1, R386A1, S389A5 and S391A1 strains were purified by Miniprep and sent for sequencing at the University of York Genomics department (**Section 2.4**). All thirteen of these plasmids had mutated as expected.

5.3 Purification of PpLAAO active site mutants

The wild type and mutated versions of the pET-YSBLIC-3C-PpLAAO plasmids were used to transform *E. coli* BL21-DE3 cells. A 2 L culture was grown and induced for each strain of the pET-YSBLIC-3C-PpLAAO plasmid as in **Section 2.5.1**, these were harvested and the soluble protein subjected to nickel affinity chromatography using a Prepacked HiTrap Chelating HP column followed by gel filtration chromatography using a 120 mL HiLoad 16/60 Superdex 75 column in order to purify the proteins (**Section 2.5.2**).

The E260A mutant did not produce any soluble protein (**Figure 5.9**) and the V293A mutant protein precipitated after the gel filtration chromatography. All the other pET-YSBLIC-3C-PpLAAO proteins were purified (**Figures 5.10-5.20**) with a yield of 15-20 mg from the 2 L culture. As with the wild type protein, the mutants eluted from the column after 52 mL. A calibration by the EMBL (http://www.embl.de/pepcore/pepcore_services/protein_purification/chromatography/hiload16-60_superdex75/ Accessed 17/01/2012) of the 120 mL HiLoad 16/60 Superdex 75 column suggests that the protein size in solution when purified was roughly 116 kDa. As the PpLAAO protein is 59 kDa, this suggests that the proteins are found in a dimeric form in solution.

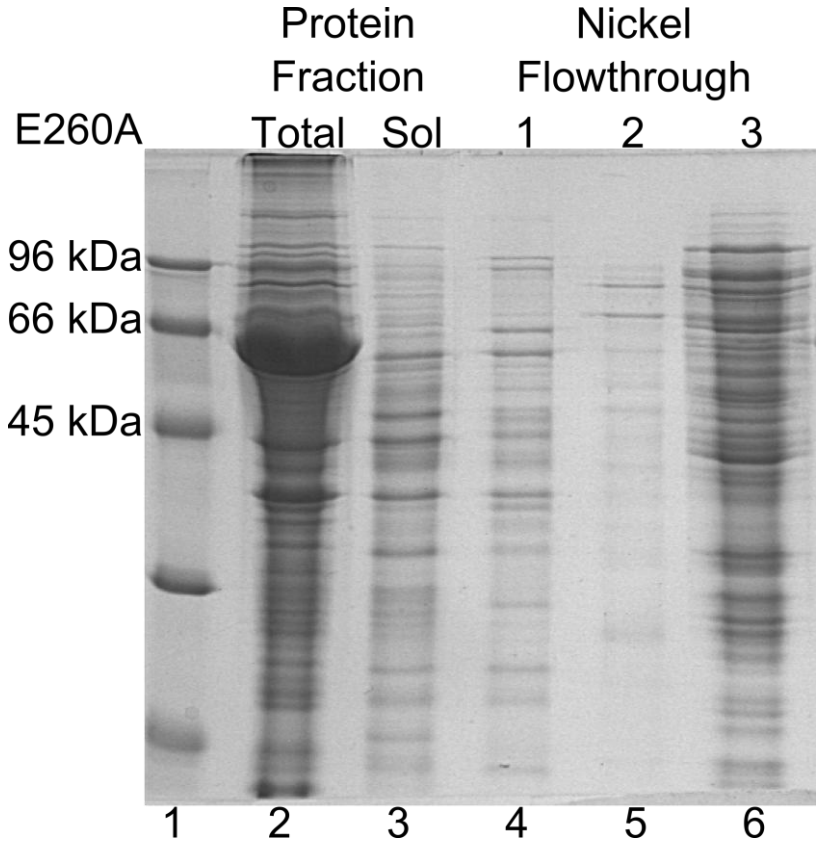

Figure 5.9 SDS-PAGE separation of protein from *E. coli* BL21-DE3 transformed with pET-YSBLIC3C-PpLAAO-E260A subjected to metal affinity based chromatography. Lane 1, low range molecular weight marker; Lane 2, Total protein fraction of sonicated BL21-pET-YSBLIC3C-PpLAAO-E260A induced culture (59 kDa); Lane 3, Soluble fraction of sonicated BL21-pET-YSBLIC3C-PpLAAO-E260A induced culture (59 kDa); Lane 4-6, Protein flow-through from column loading of soluble fraction of sonicated BL21-pET-YSBLIC3C-PpLAAO-E260A induced culture.

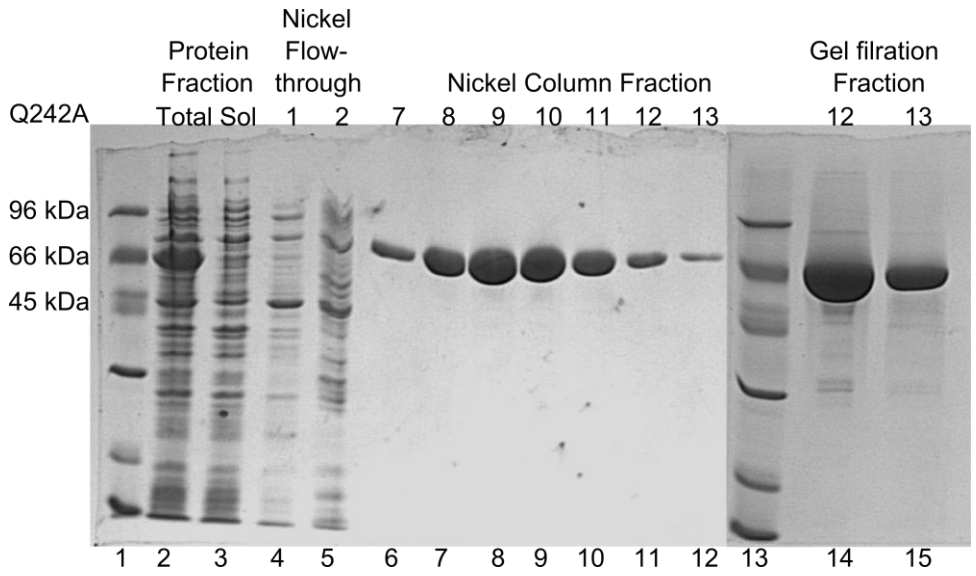

Figure 5.10 SDS-PAGE separation of protein purified from *E. coli* BL21-DE3 transformed with pET-YSBLIC3C-PpLAAO-Q242A using metal affinity based chromatography and gel filtration chromatography. Lane 1, low range molecular weight marker; Lane 2, Soluble fraction of sonicated BL21-pET-YSBLIC3C-PpLAAO-Q242A induced culture (59 kDa); Lane 3-5, Protein flow-through from column loading of soluble fraction of sonicated BL21-pET-YSBLIC3C-PpLAAO-Q242A induced culture; Lane 6-12, protein fractions 7-13 from FPLC imidazole gradient of loaded BL21-pET-YSBLIC3C-PpLAAO-Q242A protein (59 kDa); Lane 13, low range molecular weight marker; Lane 14-15, Gel filtration fractions 12-13 of BL21-pET-YSBLIC3C-PpLAAO-Q242A (59 kDa).

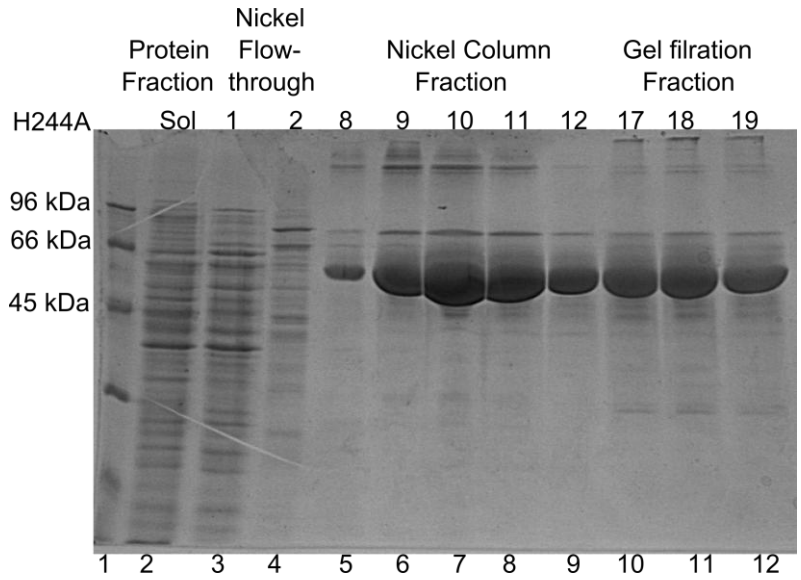

Figure 5.11 SDS-PAGE separation of protein purified from *E. coli* BL21-DE3 transformed with pET-YSBLIC3C-PpLAAO-H244A using metal affinity based chromatography and gel filtration chromatography. Lane 1, low range molecular weight marker; Lane 2, Soluble fraction of sonicated BL21-pET-YSBLIC3C-PpLAAO-H244A induced culture (59 kDa); Lane 3-4, Protein flow-through from column loading of soluble fraction of sonicated BL21-pET-YSBLIC3C-PpLAAO-H244A induced culture; Lane 5-9, protein fractions 8-12 from FPLC imidazole gradient of loaded BL21-pET-YSBLIC3C-PpLAAO-H244A protein (59 kDa); Lane 10-12, Gel filtration fractions 17-19 of BL21-pET-YSBLIC3C-PpLAAO-H244A (59 kDa).

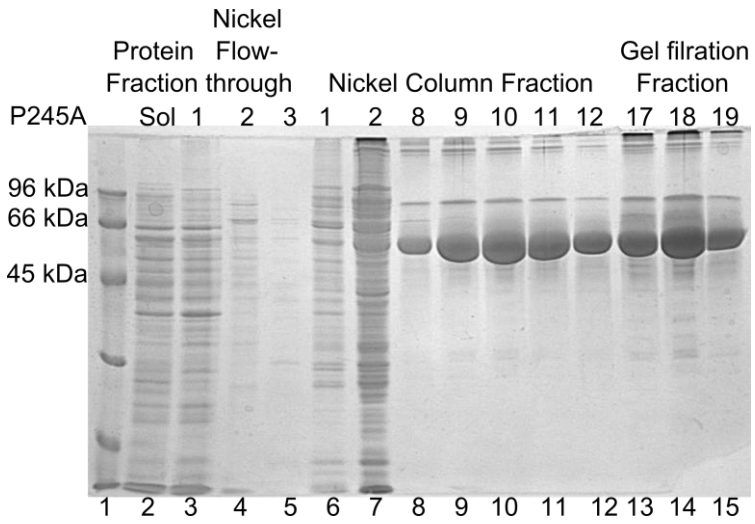

Figure 5.12 SDS-PAGE separation of protein purified from *E. coli* BL21-DE3 transformed with pET-YSBLIC3C-PpLAAO-P245A using metal affinity based chromatography and gel filtration chromatography. Lane 1, low range molecular weight marker; Lane 2, Soluble fraction of sonicated BL21-pET-YSBLIC3C-PpLAAO-P245A induced culture (59 kDa); Lane 3-5, Protein flow-through from column loading of soluble fraction of sonicated BL21-pET-YSBLIC3C-PpLAAO-P245A induced culture; Lane 6-7, protein fractions 1-2 from FPLC imidazole gradient of loaded BL21-pET-YSBLIC3C-PpLAAO-P245A protein (59 kDa); Lane 8-12, protein fractions 8-12 from FPLC imidazole gradient of loaded BL21-pET-YSBLIC3C-PpLAAO-P245A protein (59 kDa); Lane 13-15, Gel filtration fractions 17-19 of BL21-pET-YSBLIC3C-PpLAAO-P245A (59 kDa).

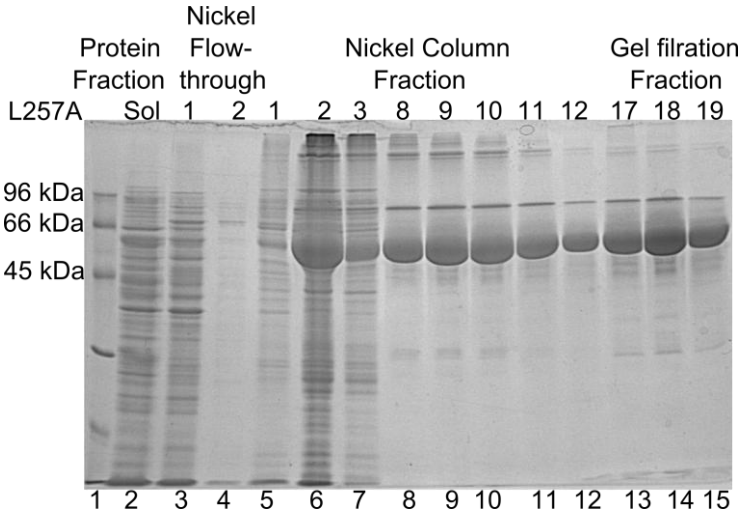

Figure 5.13 SDS-PAGE separation of protein purified from *E. coli* BL21-DE3 transformed with pET-YSBLIC3C-PpLAAO-L257A using metal affinity based chromatography and gel filtration chromatography. Lane 1, low range molecular weight marker; Lane 2, Soluble fraction of sonicated BL21-pET-YSBLIC3C-PpLAAO-L257A induced culture (59 kDa); Lane 3-4, Protein flow-through from column loading of soluble fraction of sonicated BL21-pET-YSBLIC3C-PpLAAO-L257A induced culture; Lane 5-7, protein fractions 1-3 from FPLC imidazole gradient of loaded BL21-pET-YSBLIC3C-PpLAAO-L257A protein (59 kDa); Lane 8-12, protein fractions 8-12 from FPLC imidazole gradient of loaded BL21-pET-YSBLIC3C-PpLAAO-L257A protein (59 kDa); Lane 13-15, Gel filtration fractions 17-19 of BL21-pET-YSBLIC3C-PpLAAO-L257A (59 kDa).

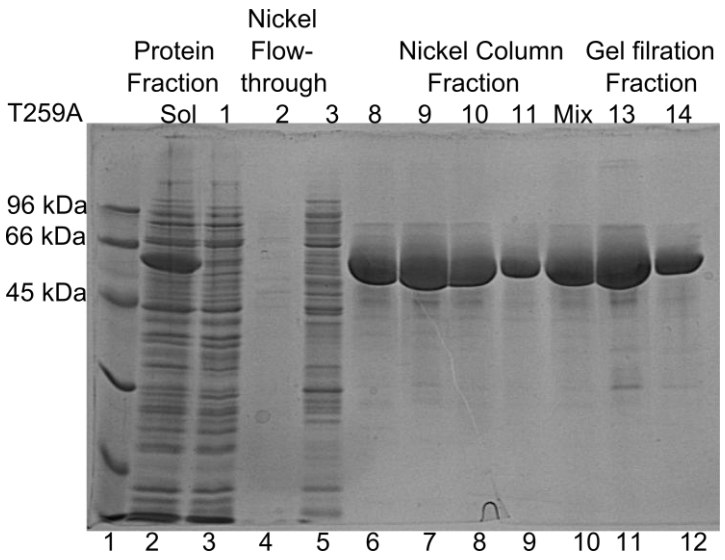

Figure 5.14 SDS-PAGE separation of protein purified from *E. coli* BL21-DE3 transformed with pET-YSBLIC3C-PpLAAO-T259A using metal affinity based chromatography and gel filtration chromatography. Lane 1, low range molecular weight marker; Lane 2, Soluble fraction of sonicated BL21-pET-YSBLIC3C-PpLAAO-T259A induced culture (59 kDa); Lane 3-5, Protein flow-through from column loading of soluble fraction of sonicated BL21-pET-YSBLIC3C-PpLAAO-T259A induced culture; Lane 6-9, protein fractions 8-11 from FPLC imidazole gradient of loaded BL21-pET-YSBLIC3C-PpLAAO-T259A protein (59 kDa); Lane 10, combined fractions from FPLC imidazole gradient of loaded BL21-pET-YSBLIC3C-PpLAAO-T259A protein (59 kDa); Lane 11-12, Gel filtration fractions 13-14 of BL21-pET-YSBLIC3C-PpLAAO-T259A (59 kDa).

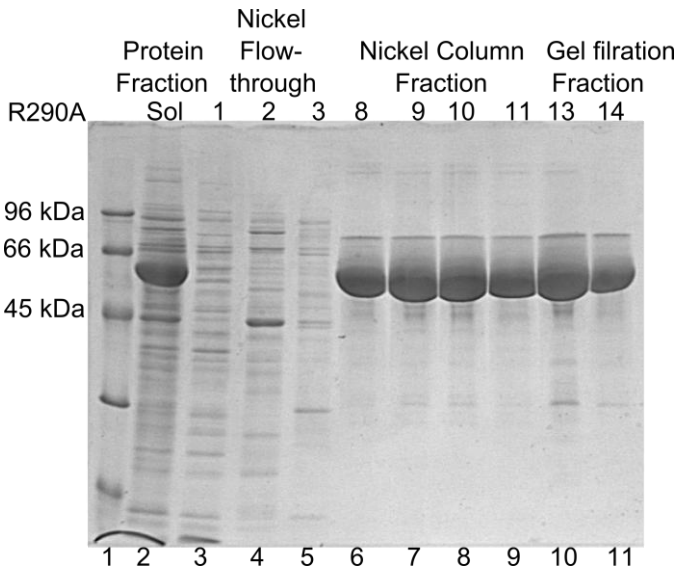

Figure 5.15 SDS-PAGE separation of protein purified from *E. coli* BL21-DE3 transformed with pET-YSBLIC3C-PpLAAO-R290A using metal affinity based chromatography and gel filtration chromatography. Lane 1, low range molecular weight marker; Lane 2, Soluble fraction of sonicated BL21-pET-YSBLIC3C-PpLAAO-R290A induced culture (59 kDa); Lane 3-5, Protein flow-through from column loading of soluble fraction of sonicated BL21-pET-YSBLIC3C-PpLAAO-R290A induced culture; Lane 6-9, protein fractions 8-11 from FPLC imidazole gradient of loaded BL21-pET-YSBLIC3C-PpLAAO-R290A protein (59 kDa); Lane 10-11, Gel filtration fractions 13-14 of BL21-pET-YSBLIC3C-PpLAAO-R290A (59 kDa).

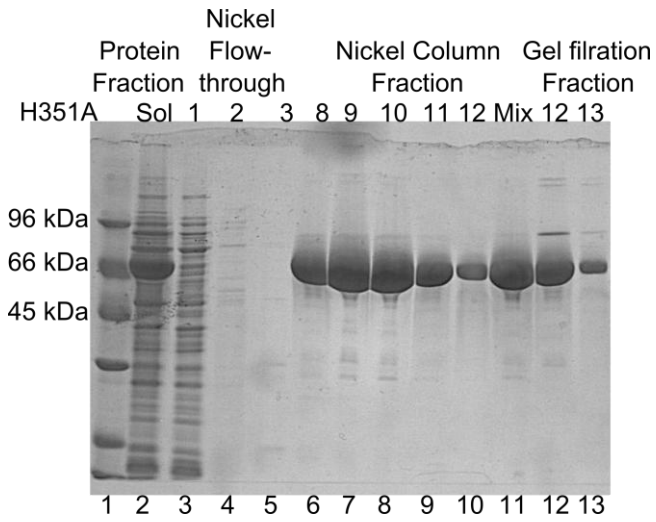

Figure 5.16 SDS-PAGE separation of protein purified from *E. coli* BL21-DE3 transformed with pET-YSBLIC3C-PpLAAO-H351A using metal affinity based chromatography and gel filtration chromatography. Lane 1, low range molecular weight marker; Lane 2, Soluble fraction of sonicated BL21-pET-YSBLIC3C-PpLAAO-H351A induced culture (59 kDa); Lane 3-5, Protein flow-through from column loading of soluble fraction of sonicated BL21-pET-YSBLIC3C-PpLAAO-H351A induced culture; Lane 6-10, protein fractions 8-12 from FPLC imidazole gradient of loaded BL21-pET-YSBLIC3C-PpLAAO-H351A protein (59 kDa); Lane 11, combined fractions from FPLC imidazole gradient of loaded BL21-pET-YSBLIC3C-PpLAAO-H351A protein (59 kDa); Lane 12-13, Gel filtration fractions 12-13 of BL21-pET-YSBLIC3C-PpLAAO-H351A (59 kDa).

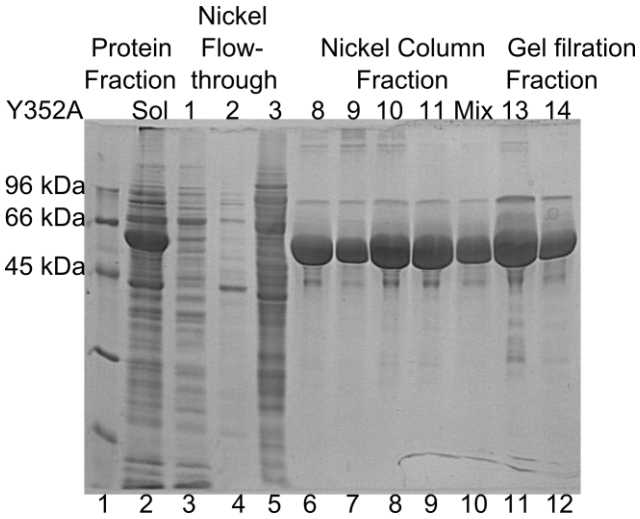

Figure 5.17 SDS-PAGE separation of protein purified from *E. coli* BL21-DE3 transformed with pET-YSBLIC3C-PpLAAO-Y352A using metal affinity based chromatography and gel filtration chromatography. Lane 1, low range molecular weight marker; Lane 2, Soluble fraction of sonicated BL21-pET-YSBLIC3C-PpLAAO-Y352A induced culture (59 kDa); Lane 3-5, Protein flow-through from column loading of soluble fraction of sonicated BL21-pET-YSBLIC3C-PpLAAO-Y352A induced culture; Lane 6-9, protein fractions 8-11 from FPLC imidazole gradient of loaded BL21-pET-YSBLIC3C-PpLAAO-Y352A protein (59 kDa); Lane 10, combined fractions from FPLC imidazole gradient of loaded BL21-pET-YSBLIC3C-PpLAAO-Y352A protein (59 kDa); Lane 11-12, Gel filtration fractions 13-14 of BL21-pET-YSBLIC3C-PpLAAO-Y352A (59 kDa).

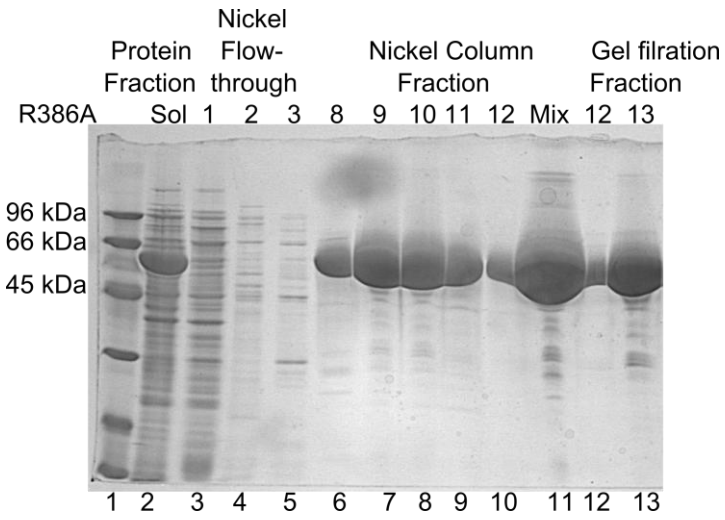

Figure 5.18 SDS-PAGE separation of protein purified from *E. coli* BL21-DE3 transformed with pET-YSBLIC3C-PpLAAO-R386A using metal affinity based chromatography and gel filtration chromatography. Lane 1, low range molecular weight marker; Lane 2, Soluble fraction of sonicated BL21-pET-YSBLIC3C-PpLAAO-R386A induced culture (59 kDa); Lane 3-5, Protein flow-through from column loading of soluble fraction of sonicated BL21-pET-YSBLIC3C-PpLAAO-R386A induced culture; Lane 6-10, protein fractions 8-12 from FPLC imidazole gradient of loaded BL21-pET-YSBLIC3C-PpLAAO-R386A protein (59 kDa); Lane 11, combined fractions from FPLC imidazole gradient of loaded BL21-pET-YSBLIC3C-PpLAAO-R386A protein (59 kDa); Lane 12-13, Gel filtration fractions 12-13 of BL21-pET-YSBLIC3C-PpLAAO-R386A (59 kDa).

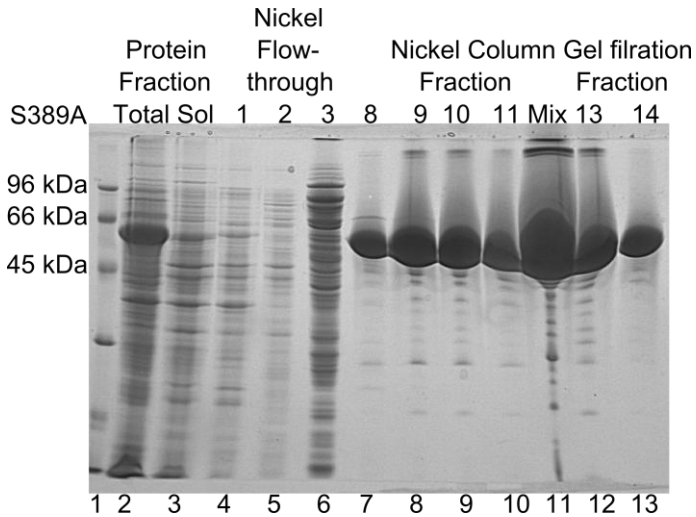

Figure 5.19 SDS-PAGE separation of protein purified from *E. coli* BL21-DE3 transformed with pET-YSBLIC3C-PpLAAO-S389A using metal affinity based chromatography and gel filtration chromatography. Lane 1, low range molecular weight marker; Lane 2-3, Total/Soluble protein from sonicated BL21-pET-YSBLIC3C-PpLAAO-S389A induced culture (59 kDa); Lane 4-6, Protein flow-through from column loading of soluble fraction of sonicated BL21-pET-YSBLIC3C-PpLAAO-S389A induced culture; Lane 7-10, protein fractions 8-11 from FPLC imidazole gradient of loaded BL21-pET-YSBLIC3C-PpLAAO-S389A protein (59 kDa); Lane 11, combined fractions from FPLC imidazole gradient of loaded BL21-pET-YSBLIC3C-PpLAAO-S389A protein (59 kDa); Lane 12-13, Gel filtration fractions 13-14 of BL21-pET-YSBLIC3C-PpLAAO-S389A (59 kDa).

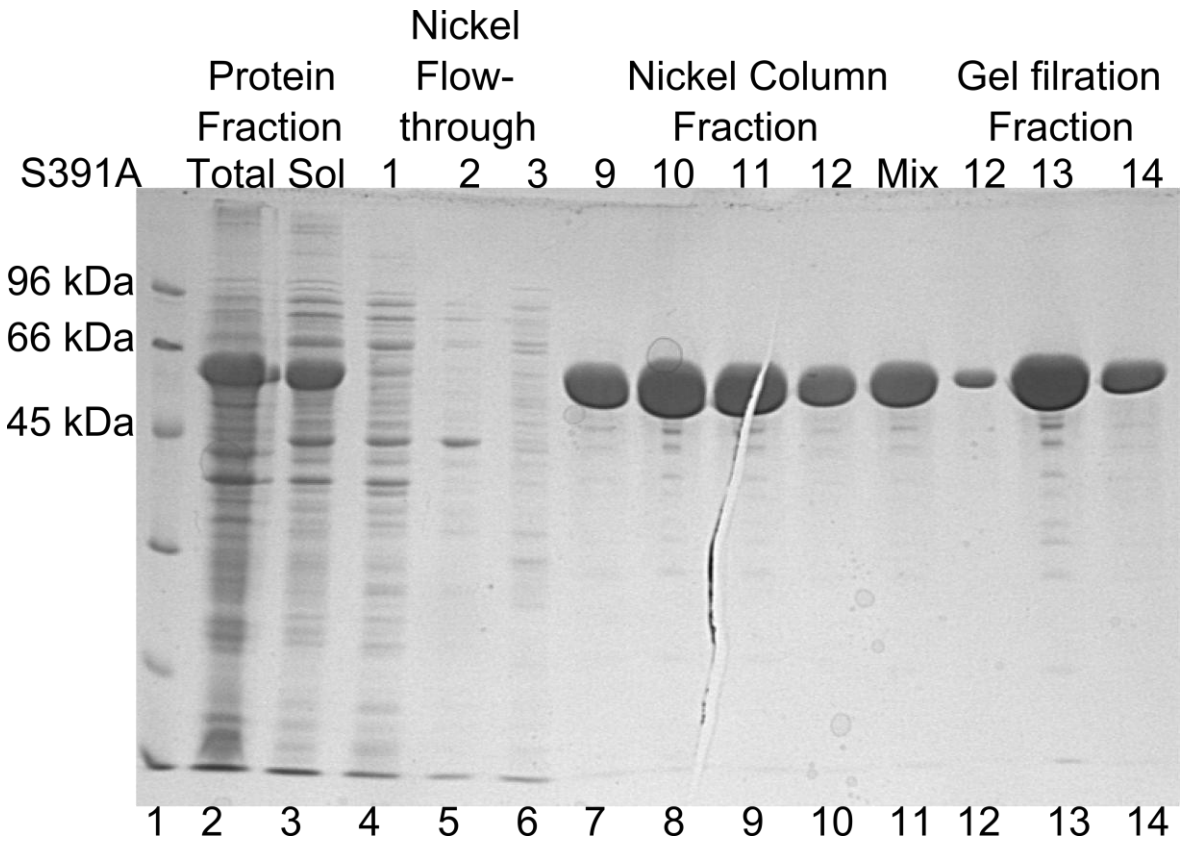

Figure 5.20 SDS-PAGE separation of protein purified from *E. coli* BL21-DE3 transformed with pET-YSBLIC3C-PpLAAO-S391A using metal affinity based chromatography and gel filtration chromatography. Lane 1, low range molecular weight marker; Lane 2-3, Total/Soluble protein from sonicated BL21-pET-YSBLIC3C-PpLAAO-S391A induced culture (59 kDa); Lane 4-6, Protein flow-through from column loading of soluble fraction of sonicated BL21-pET-YSBLIC3C-PpLAAO-S391A induced culture; Lane 7-10, protein fractions 9-12 from FPLC imidazole gradient of loaded BL21-pET-YSBLIC3C-PpLAAO-S391A protein (59 kDa); Lane 11, combined fractions from FPLC imidazole gradient of loaded BL21-pET-YSBLIC3C-PpLAAO-S391A protein (59 kDa); Lane 12-14, Gel filtration fractions 12-14 of BL21-pET-YSBLIC3C-PpLAAO-S391A (59 kDa).

The purified H351A mutant protein solution was clear in colour, whereas the other PpLAAO proteins were yellow due to the presence of the FAD cofactor. This suggests that the H351 residue is involved in the binding of FAD, and that the mutation to alanine has disrupted the binding. This appears to be consistent with the active site structure of the homologous *E. coli* L-AspO (**Figure 5.2a**) and work by Tedeschi *et al.*.[118]

5.4 Activity assay of active site mutants

The kinetic parameters of each of the active site mutants were determined against the wild-type substrates L-aspartate, L-asparagine and L-glutamate by measuring the initial rate activity of each

enzyme against substrate concentrations of 0.781 mM, 1.56 mM, 3.13 mM, 6.25 mM, 12.5 mM, 25.0 mM, 37.5 and 50.0 mM with a final protein concentration of 0.1 mg mL^{-1}, as in **Section 2.5.3**. However, as the wild-type protein only began showing activity against L-glutamate at higher concentration, the kinetic parameters against L-glutamate were determined by measuring the initial rate activities against concentrations of 50 mM, 100 mM, 150 mM, 200 mM, 250 mM, 300 mM, 350 mM, 400 mM and 500 mM L-glutamate.

The R386A mutant was inactive against all the substrates tested. All other mutants showed varying levels of activity against L-aspartate; however none were more efficient than the wild-type protein (**Table 5.1a, Figure 5.21**). The T259A, H351A and Y352A mutants did show activity against L-aspartate, (**Figures 5.22a, b and c**) however as these mutants did not reach V_{max} at the substrate concentration tested, it was not possible to determine the values of K_M and k_{cat} for these mutants, as noted in **Table 5.1a**.

Aside from the wild-type PpLAAO, only the S391A protein showed any activity against L-asparagine, however both the binding and catalytic efficiency had been reduced compared to the wild type protein (**Table 5.1a**) and the potential substrate inhibition seen in the wild-type protein appears to be present in the S391A mutant (**Figure 5.23b**).

The wild type PpLAAO protein also showed activity against L-glutamate, with a K_M of 345 mM and a k_{cat} of 1.65 s^{-1} (**Table 5.1b**). The two mutants that showed activity against L-glutamate, Q242A and S389A, both appeared to have higher binding efficiency (roughly a 50-fold decrease in K_M for Q242A and 35-fold decrease in K_M for S389A). However the catalytic efficiency of these mutants had been decreased roughly ten-fold and five-fold for Q242A and S389A respectively (**Table 5.1b**). Although, in both of these cases, the standard error of the data points is quite high and two data points from each had to be removed as they had negative values (**Figure 5.24b and c**), so the presumed activity may just be due to background noise of the assay.

The effect on the activity that the H244A and H351A mutants have on the activity of PpLAAO is consistent with the effect of the same mutations in the L-AspO protein made by Tedeschi *et al.*[118] as they all resulted in an increase in the K_M of the enzyme against L-aspartate (**Table 5.2**). Mutation of R290 in both cases caused a large loss of activity; however the PpLAAO R290A mutant was not completely inactive unlike the L-AspO R290L mutant. Conversely, the PpLAAO R386A mutant was inactive, unlike the L-AspO R386L mutant, which had a thousand-fold higher K_M against L-aspartate than the wild type L-AspO (**Table 5.2**).

Table 5.1 a. Kinetic parameters of wild-type and active site mutants of PpLAAO protein against L-aspartate and L-asparagine. **b.** Kinetic parameters of wild-type and active site mutants of PpLAAO protein against L-glutamate. Parameters determine using Grafit 7.0 software unless otherwise stated.

a.	L-aspartate			L-asparagine		
Strain	K_M / mM	k_{cat}/ s^{-1}	k_{cat} K_M^{-1}/ M^{-1} s^{-1}	K_M / mM	k_{cat}/ s^{-1}	k_{cat} K_M^{-1}/ M^{-1} s^{-1}
Wild Type	2.263	10.6	4684.04	(0.6166)	(4.5)	(7298.09)
Q242A	63.27	2.28	35.97	No detectable activity		
H244A	75.44	23.69	314.02	No detectable activity		
P245A	158.9[1]	25.62[1]	161.23[1]	No detectable activity		
L257A	599.88	59.28	98.87	No detectable activity		
T259A	Couldn't fit to Michaelis Menten			No detectable activity		
R290A	26.11	0.23	8.84	No detectable activity		
H351A	Couldn't fit to Michaelis Menten			No detectable activity		
Y352A	Couldn't fit to Michaelis Menten			No detectable activity		
R386A	No detectable activity			No detectable activity		
S389A	14.29	7.837	548.43	No detectable activity		
S391A	3.258	2.501	767.65	(5.98)	(0.23)	(39.15)

[1]Parameters determined using GraphPad Plus 5

b.	L-glutamate		
Strain	K_M / mM	k_{cat}/ s^{-1}	k_{cat} K_M^{-1}/ M^{-1} s^{-1}
Wild Type	345.16	1.65	4.77
Q242A	6.77	0.13	18.48
H244A	No detectable activity		
P245A	No detectable activity		
L257A	No detectable activity		
T259A	No detectable activity		
R290A	No detectable activity		
H351A	No detectable activity		
Y352A	No detectable activity		
R386A	No detectable activity		
S389A	9.20	0.24	26.30
S391A	No detectable activity		

Table 5.2 Comparison of the kinetic parameters of mutated forms of the *E. coli* L-AspO made by Tedeschi *et al.*[118] and mutants of the same residues in PpLAAO.

E. coli L-AspO[118]				PpLAAO			
Form	K_M / mM	k_{cat}/ s^{-1}	k_{cat} K_M^{-1}/ M^{-1} s^{-1}	Form	K_M / mM	k_{cat}/ s^{-1}	k_{cat} K_M^{-1}/ M^{-1} s^{-1}
WT	1.6	0.49	306	WT	2.263	10.6	4684.04
H244A	6.1	0.1	16.4	H244A	75.44	23.69	314.02
H351A	9.4	0.0024	0.26	H351A	K_M too high to determine		
R386L	1000	0.0025	0.0025	R386A	Inactive mutant		
R290L	Inactive mutant			R290A	26.11	0.23	8.84

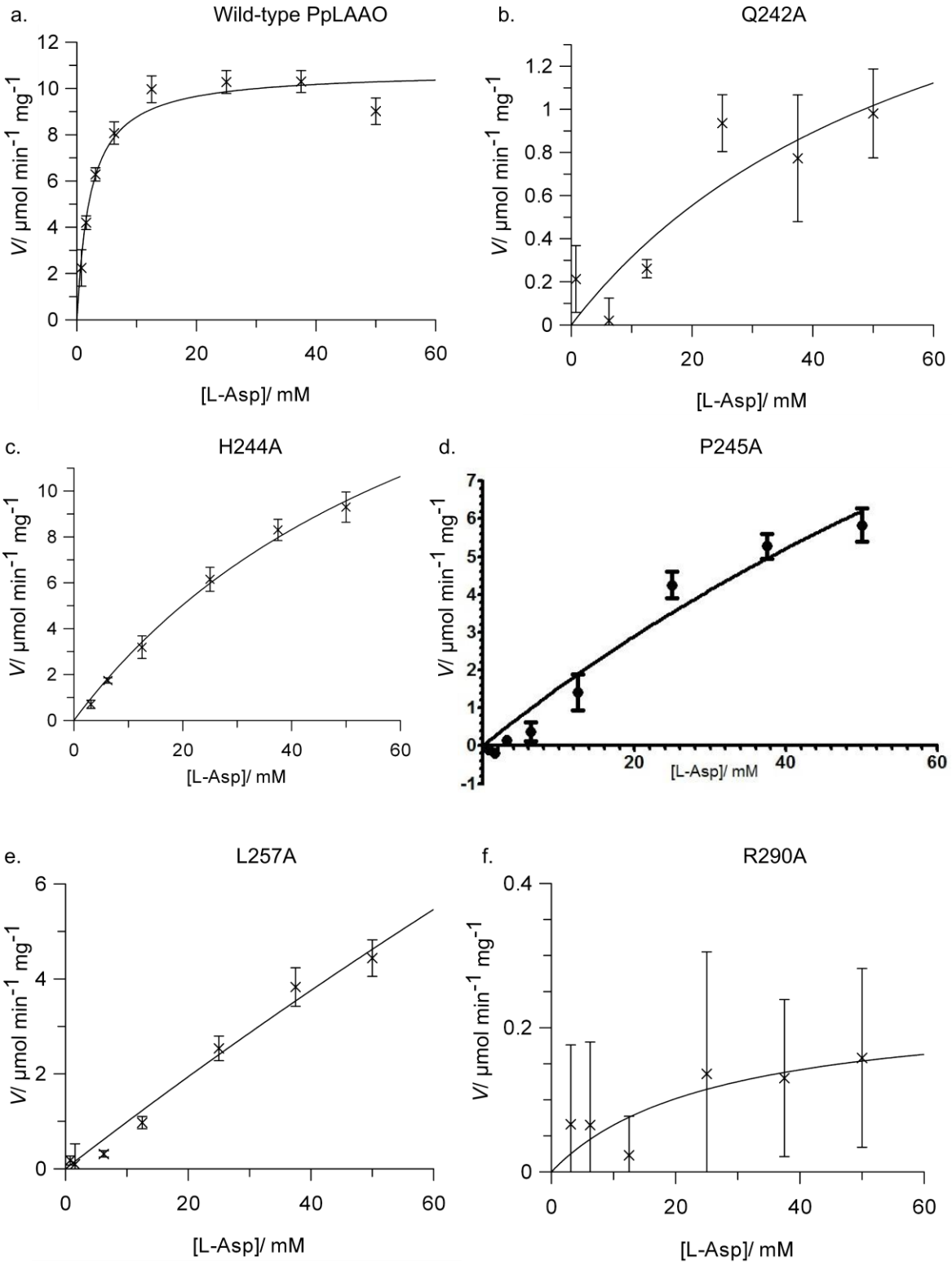

Figure 5.21 Kinetics plots of activity PpLAAO-based proteins against L-aspartate. **a.** Wild type PpLAAO; **b.** Q242A; **c.** H244A; **d.** P245A; **e.** L257A; **f.** R290A; **g.** S389A; **h.** S391A.

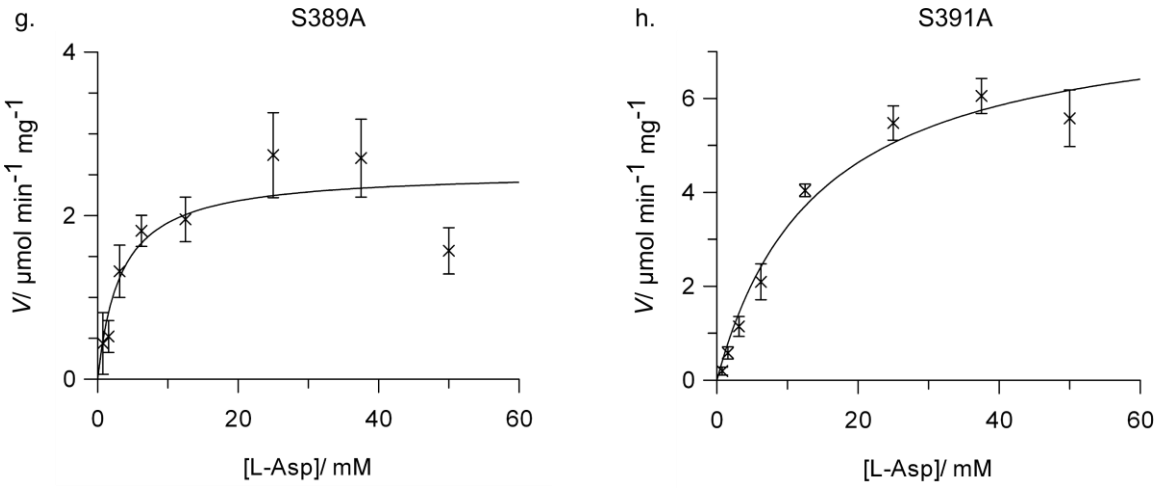

Figure 5.21 Kinetics plots of activity PpLAAO-based proteins against L-aspartate. **a.** Wild type PpLAAO; **b.** Q242A; **c.** H244A; **d.** P245A; **e.** L257A; **f.** R290A; **g.** S389A; **h.** S391A.

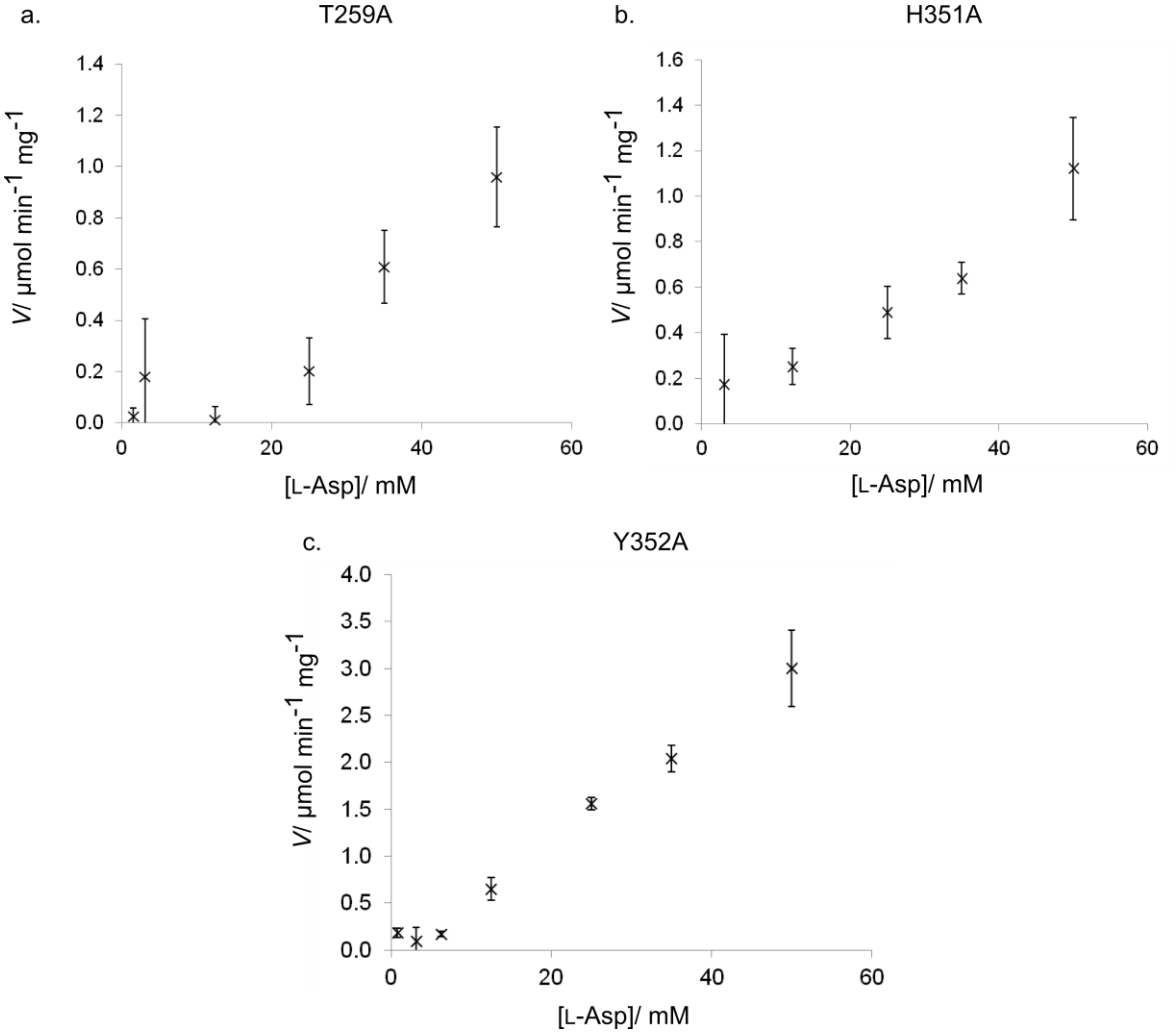

Figure 5.22 Unfitted kinetics data of PpLAAO-based proteins against L-aspartate. **a.** T259A; **b.** H351A; **c.** Y352A.

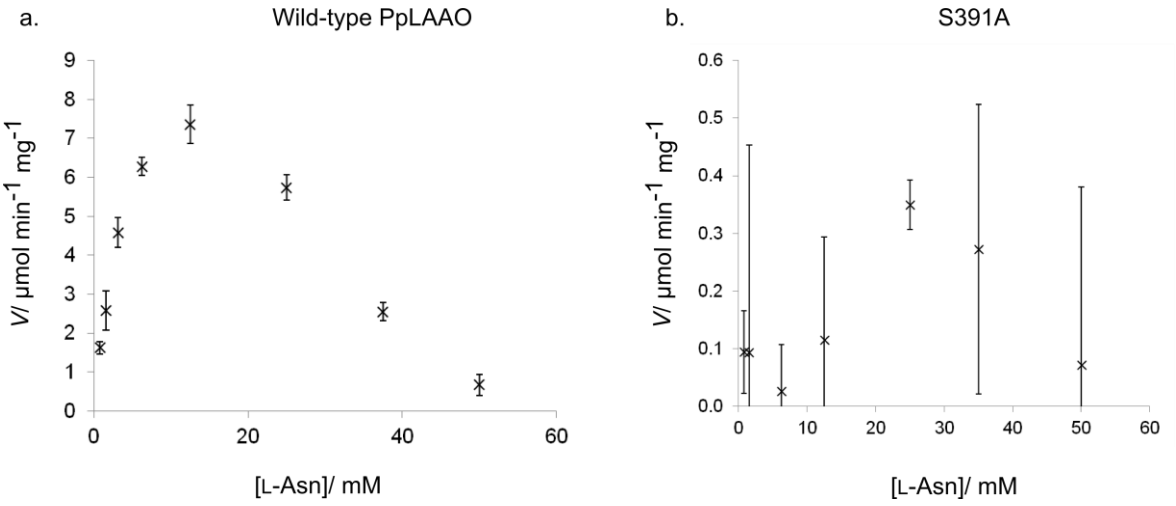

Figure 5.23 Unfitted kinetics data of PpLAAO-based proteins against L-asparagine. **a.** Wild type PpLAAO. **b.** S391A mutant.

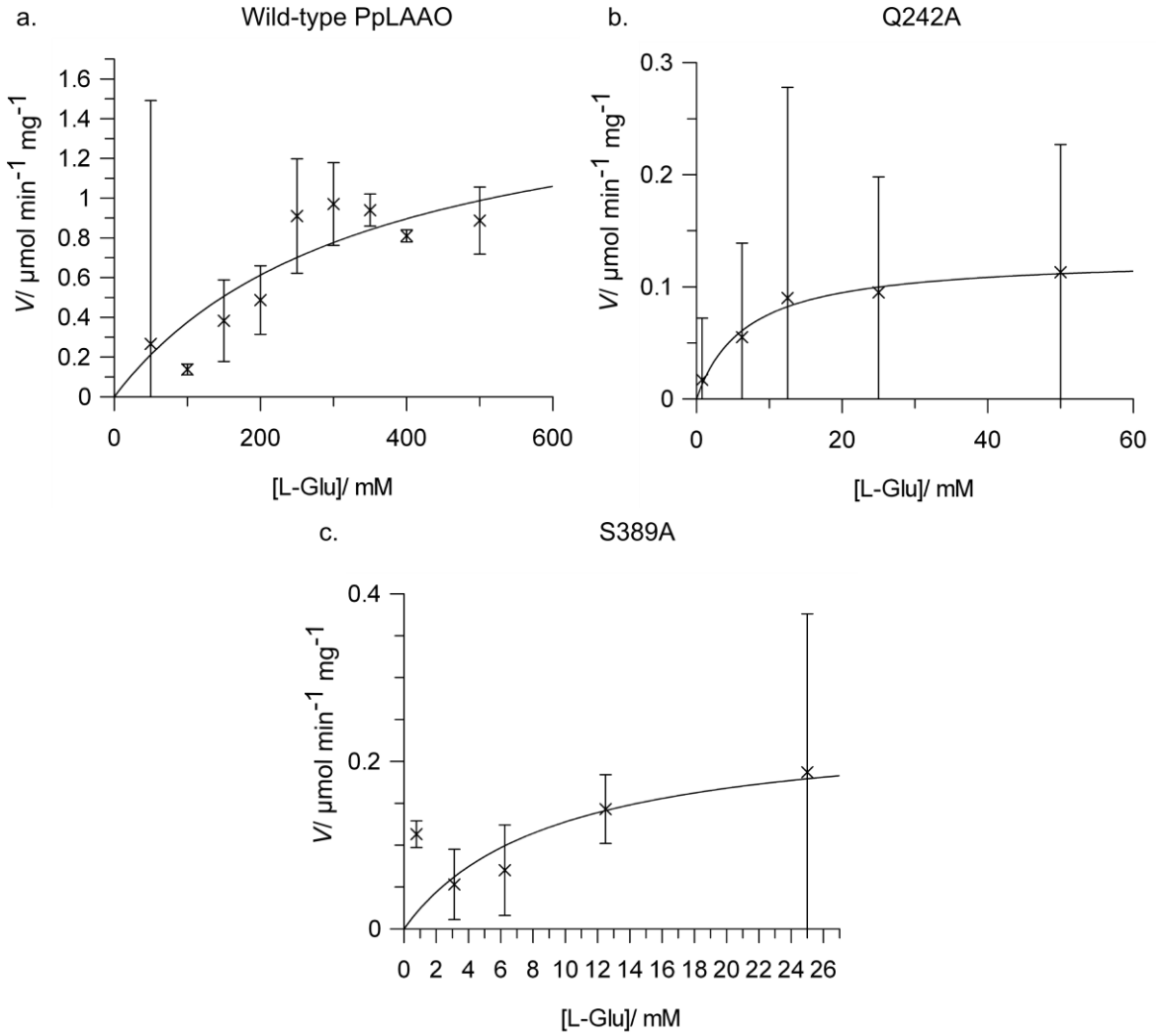

Figure 5.24 Kinetics plots of activity PpLAAO-based proteins against L-glutamate. **a.** Wild type PpLAAO. **b.** Q242A mutant. **c.** S389A mutant.

The activity against target substrates L-homoserine, L-alanine and L-tyrosine was tested in case new activity had been introduced by the mutations; however no activity was observed against these substrates at substrate concentrations up to 50 mM (data not shown).

5.5 Discussion

As the structure of the PpLAAO protein has yet to be solved, the structure of the *E. coli* L-AspO, which has 60% homology and shares conserved active site residues with the PpLAAO protein, was used to form a mutagenesis strategy with the aim of confirming the roles of several active site residues and potentially introducing new substrate specificities into the PpLAAO protein. In compliance with this strategy, thirteen residues either in or near the active site of the *E. coli* L-AspO (Q242, H244, P245, L257, T259, E260, R290, V293, H351, Y352, R386, S389 and S391) were individually mutated into alanine, and these mutated genes were subsequently overexpressed, and protein was purified using the same method used for the wild-type version of PpLAAO.

The E260 residue appears to form hydrogen bonds with two other residues (R263 and R290) in the *E. coli* L-AspO structure.[65] The disruption of these bonds in the E260A mutant appears to have affected the folding of the protein, as the E260A mutant protein was only produced in insoluble form (**Figure 5.9**) and was unable to be purified. The reason for this is unclear, although if the E260 residue was anchoring two arginine side chains in place, the loss of this anchor may have caused the two arginine residues to move into positions that blocked other side chain interactions and resulted in poor folding of the protein.

The V293A mutant could not be purified, as it would spontaneously precipitate after gel filtration chromatography. The reason for this is unclear, as in the *E. coli* L-AspO structure the V293 residue does not appear to form any interactions within its immediate environment. It is possible that the change to the smaller alanine residue allowed the V293A main chain to move more freely than before, causing a loss of protein stability.

The kinetic parameters of the purified wild-type and mutant forms of the PpLAAO protein were determined against L-aspartate, L-asparagine and L-glutamate. The wild type protein showed high activity against L-aspartate, with a K_M of 2.263 mM and a k_{cat}/K_M of 4684 M^{-1} s^{-1}. The activity against L-asparagine was lower, but accurate kinetic parameters were undetermined due to the protein showing substrate inhibition at concentrations above 12.5 mM L-asparagine. The protein also showed very low activity against L-glutamate, with a K_M of 345 mM and a k_{cat}/K_M of 4.77 M^{-1} s^{-1}

Tedeshi *et al*.[118] have previously investigated the effects of the active site residues on the activity of the L-AspO from *E. coli* on L-aspartate by mutating four of the active site residues into; H244A, R290L, H351A and R386L. The results are similar to those found by mutating the PpLAAO protein (**Table 5.2**). In both cases the H244A mutation causes an increase in the K_M against L-aspartate, although it is a larger increase in the PpLAAO protein, as discussed in more detail below. Unlike the *E. coli* L-AspO the H244A mutation appears to cause an increase in k_{cat}, although this may be an inaccurate calculation caused by a lack of data for substrate concentrations higher than 50 mM.

The H351A mutation also causes an increase in the K_M against L-aspartate in both proteins (**Table 5.2,**[118] **Figure 5.21b**), it also reduced catalytic efficiency in the *E. coli* protein, but whether that would be true for the PpLAAO protein is undetermined at this point.

The R386L mutant of the *E. coli* L-AspO protein showed low activity against L-aspartate; however no activity was seen in the R386A mutant of PpLAAO. This may either have been due to the difference between the effects of a leucine side-chain as opposed to an alanine side chain, or it may be that the use of *o*-dianisidine instead of 4-AAP and TBHBA in the activity assay by Tedeshi *et al*.[118] may have allowed them to detect lower levels of activity, as the lowest value k_{cat} that they detected was lower than any of the ones detected for PpLAAO (**Tables 5.1, 5.2**).

Conversely, the PpLAAO R290A mutant showed a low level of activity, whereas the *E. coli* R290L mutant was completely inactive.[118] This difference may be due to the difference in the mutated side chain, so does not necessarily indicate any difference between the *E. coli* L-AspO and the PpLAAO active site structures.

The mutants of the two residues thought to be involved in the binding of the C1 carboxylate of succinate in the *E. coli* L-AspO,[118] H244A and T259A, both show activity against L-aspartate, but with lower binding efficiency compared to the wild-type PpLAAO. The H244 residue is thought to bind the O2 atom of the C1 carboxylate (**Figure 5.2c**), and mutation of this residue to alanine in the *E. coli* L-AspO resulted in a 3.8-fold increase in K_M,[118] whereas in PpLAAO the same mutation has caused a 33-fold increase in K_M (**Table 5.1a**), consistent with the role of the H244 residue in the *E. coli* protein. The T259 residue is thought to bind the O1 atom of the C1 carboxylate (**Figure 5.2c**), and its mutation to alanine in PpLAAO resulted in a greatly decreased binding efficiency, as the initial rate activities did not begin to plateau over the concentrations of L-aspartate tested (**Figure 5.21a**). This mutation is not reported on by Tedeschi *et al.*,[118] but the PpLAAO T259A mutant points towards a role in substrate binding for the T259 residue.

The H351 residue is thought to bind the O4 atom of the C4 carboxylate of the succinate substrate in the *E. coli* L-AspO structure (**Figure 5.2c**).[65] When this residue was mutated to alanine by Tedeschi *et al.* the resulting protein showed activity against L-aspartate that was three orders of magnitude lower than the wild-type activity and a 6.5-fold increase in the dissociation constant for the FAD cofactor compared to the wild-type L-AspO.[118] The PpLAAO H351A mutant also showed poor binding of FAD, as the purified protein was colourless as opposed to the yellow colour of the other purified proteins, and had a lower level of activity than the wild-type protein (**Figure 5.21b**), likely to be due to the loss of the FAD cofactor, although the binding affinity of the protein also appears to be lost in the H351A mutant, as the reactions did not appear to be approaching V_{max} over the substrate concentrations tested (**Figure 5.21b**). This is also consistent with the results of Tedeschi *et al.*[118] who observed a 5.8-fold increase in K_M and a 200-fold decrease in catalytic activity against L-aspartate in the H351A mutant compared to the wild-type *E. coli* L-AspO.

The S389 residue is thought to bind the O3 atom of the C4 carboxylate of the succinate substrate in the *E. coli* L-AspO (**Figure 5.2c**).[65] The PpLAAO S389A mutant showed a 6.3-fold increase in K_M but only a slight reduction in the catalytic activity against L-aspartate (**Table 5.1a**), suggesting that its role is in substrate binding as opposed to catalysis. Against L-glutamate, the S389A mutant showed 38-fold decrease in K_M, but a 6.8-fold decrease in activity compared to the wild-type PpLAAO. The decrease in K_M against L-glutamate could suggest that this residue may be a potential point for saturation mutagenesis when attempting to change substrate specificity, as the increased binding against L-glutamate at the expense of L-aspartate suggests it has a role in substrate specificity.

Of the arginines in the active site, mutation of R386, which is suggested to have a role in binding the α-carboxylate of the actual substrate L-aspartate, gave a mutant with no detectable activity. Mutation of the same residue to leucine in the *E. coli* L-AspO resulted in a mutant with a 196-fold decrease in activity and a 625-fold increase in the K_M for L-aspartate compared to the wild-type form.

Mutation of R290 to alanine, which is thought to have a role in abstracting the proton from the Cα of the L-aspartate substrate in the *E. coli* L-AspO, resulted in a 50-fold decrease in k_{cat} against L-aspartate, although the mutation of the same residue to leucine in the *E. coli* L-AspO resulted in a completely inactive protein.[118] In a related note, the mutation of Q242 side chain, which forms a H-bond with the R290 residue in the L-AspO structure (**Figure 5.2a**),[65] resulted in a mutant with a 30-fold increase in K_M and a 4.6-fold decrease in k_{cat} compared to the wild-type PpLAAO, suggesting that the Q242 residue may have a role in fixing the essential R290 residue in place to

allow for effective proton abstraction. The Q242A mutant also showed increase binding efficiency, but lower catalytic activity against L-glutamate than the wild-type PpLAAO (**Table 5.1b**).

In the *E. coli* L-AspO structure, the S391 residue appears to form H-bonds with the N1 of the FAD flavin ring (**Figure 5.2b**). When mutated to alanine the resulting protein showed a slight reduction in binding efficiency, with a K_M of 3.25 mM compared to the wild-type 2.26 mM, but a 4 fold decrease in catalytic activity (**Table 5.1a**). This suggests that the exact positioning of the flavin ring in conjunction with the positioning of the substrate in the active site is important to the catalytic efficiency of the PpLAAO enzyme, which is consistent with its suggested hydride transfer mechanism.[64] The S391A mutant also showed activity against L-asparagine, although with lower binding efficiency and catalytic efficiency than the wild-type PpLAAO (**Table 5.1a, Figure 5.22**).

The Y352 residue has some van der Waals interactions with the FAD molecule (**Figure 5.2a-b**), as well as forming hydrogen bonds with two residues outside the active site, H382 and E394, shown on the *E. coli* L-AspO structure.[65] When this residue is mutated to alanine, the resulting protein had a reduced binding affinity and catalytic activity against L-aspartate compared to the wild-type PpLAAO (**Figure 5.21c**). This could be due to the loss of the steric interaction with the ribitol chain resulting in a shift of position of the flavin ring, resulting in less efficient proton abstraction from the substrate. Otherwise the loss of the H-bonds to the H382 and E394 residues may result in a shift some of the substrate binding residues, causing a loss of binding affinity.

The remaining two residues P245 and L257, which are both close to the H244 residue that binds the C1 carboxylate of succinate in the *E. coli* L-aspO structure [65] (P245 is adjacent to H244 and L257 sites beneath it (**Figure 5.2a**)), each gave mutants with a greatly increased K_M and increased k_{cat}, which indicates roles in substrate binding which had not been recognised previously.

Overall, this mutagenesis strategy has increased the understanding of the role of the active site residues in PpLAAO and possibly other L-aspartate oxidases. Activity against target substrates L-alanine and L-tyrosine was tested, just in case the changes to the active site had resulted in proteins with activity against different substrates, however no new activity was observed. This is likely to be because the changes to the active site were not large enough to result in a large change in substrate specificity. It may also be because of the hydride transfer mechanism that this protein uses, which requires a specific angle between the substrate and the flavin ring of FAD in order for effective proton abstraction from the substrate, meaning that changes to the active site area a more likely to have a negative effect on overall activity than they would in an enzyme where the positioning of the substrate was not as crucial to the activity of the enzyme. This effect can possibly

be seen with the Q242A and S389A mutants, which both showed better binding efficiency, but far lower catalytic activity against L-glutamate than the wild-type PpLAAO protein.

Chapter 6 CASTing and epPCR of PpLAAO

The site directed mutagenesis (SDM) of the PpLAAO active site residues performed in **Chapter 5** has developed a greater understanding of the roles of the active site residues, with results that are consistent with the active site structure of the *E. coli* L-aspartate oxidase (L-aspO) solved by Bossi *et al*.[65] Now that a highly soluble and active amino acid oxidase (AAO) has been identified, it would be of interest to try and evolve activity towards other amino acid substrates, particularly our targets L-alanine and L-tyrosine.

However, there is a large difference between the side-chains of L-aspartate and those of the target substrates, so one round of directed evolution may not be enough to introduce activity against these two substrates. Because of this the directed evolution libraries will be screened against L-homoserine, as part of a substrate walking approach towards L-alanine (**Figure 6.1**). If any mutants show activity against L-homoserine after one round of directed evolution these could then be used as a basis for evolution of an L-alanine oxidase.

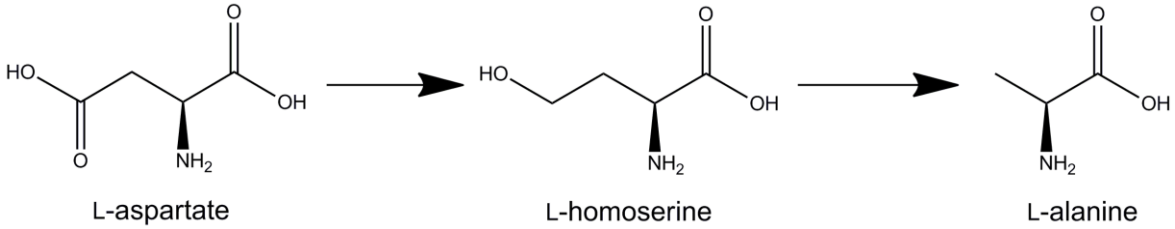

Figure 6.1 Substrate walking from L-aspartate to L-alanine, using L-homoserine as a mid-way point.

As a strategy for this directed evolution, thirteen active site residues from the structure of the *E. coli* L-aspartate oxidase built by Bossi *et al*.[65] (**Section 5.1**) were split into 5 groups as in **Figure 6.2** and **Table 6.1**. Each of these 5 groups contained residues that were sequentially close enough to each other that they were all able to be mutated using one primer set. This would allow for directed evolution using an iterative CASTing approach used by Reetz *et al*,[108] where each group of residues is mutated using site directed saturation mutagenesis (SDSM) and then screened for activity against target substrates, then any strains showing activity are mutated at a different group of residues, and so on.

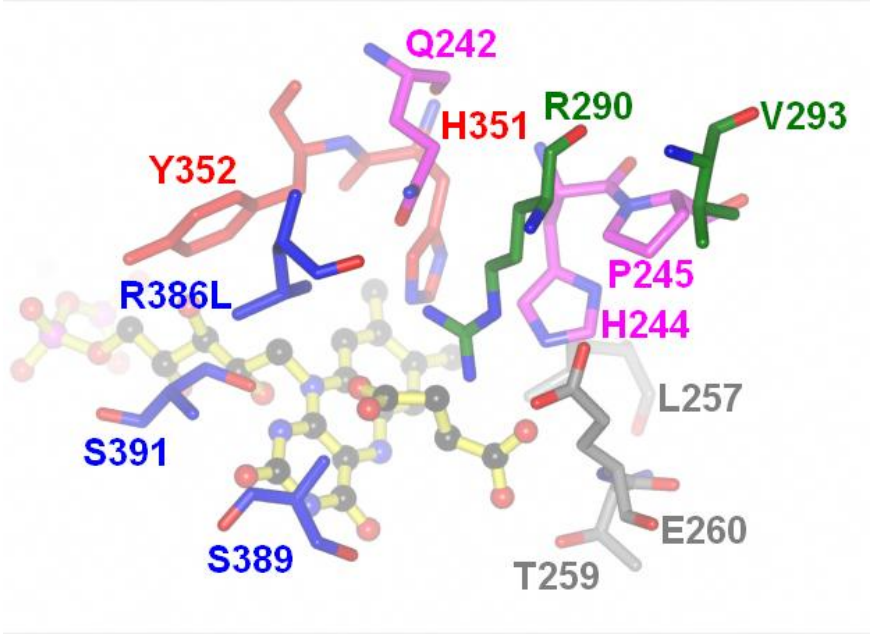

Figure 6.2 Structure of *E. coli* L-aspartate oxidase[65] showing library CASTing designation groups A (red), B (green), C (blue), D (magenta) and E (grey) along with succinate substrate and FAD (yellow).

Table 6.1 CASTing strategy libraries- grouped in order to minimise the distance between amino acids in the DNA sequence for primer design.

Library	Amino acids
A (red)	**H351, Y352**
B (green)	**R290, V293**
C (blue)	**L386, S389, S391**
D (magenta)	**Q242, H244, P245**
E (grey)	**L257, T259, E260**

In order to keep the number of transformants needed to cover at least 95% of all possible combinations of mutations at a low enough number for screening at the lab bench level, the codon degeneracy used for the SDSM reactions was the NDT degeneracy (N: adenine/cytosine/guanine/thymine; D: adenine/guanine/thymine; T: thymine), which forms codons for 12 chemically diverse amino acid side chains (L-phenylalanine, L-leucine, L-isoleucine, L-valine, L-tyrosine, L-histidine, L-asparagine, L-aspartate, L-cysteine, L-arginine, L-serine and glycine).

This was instead of using the standard NNK (K: guanine/thymine) degeneracy, which results in 32 codons for all 20 natural amino acid side chains. As discussed by Reetz *et al.*,[107] using the NDT degeneracy means that 430 transformants need to be screen in a library where 2 residues are mutated in order to cover 95% of all possible mutations, and 5175 transformants are needed for a library with 3 residue mutations. For the NNK degeneracy the numbers of transformants needed are 3066 and 98163 for libraries with 2 and 3 residue mutations respectively.

Although, in most cases, changes in residues that are closer to the active site will have more effect on enzyme activity than mutation in residues further away from the active site, mutating residues throughout the enzyme structure could have a beneficial effect on enzyme activity, as discussed by Morley & Kazlauskas.[109] For this reason the wild type PpLAAO gene sequence was subjected to random mutagenesis using the Stratagene MutaZyme II error prone PCR polymerase, which contains a combination of Stratagene's reduced fidelity MutaZyme I, and a reduced fidelity Taq polymerase to reduce mutational bias between A and T and G and C mutations,[120] resulting in a larger number of possible codon mutations.

6.1 Generation of SDSM CASTing libraries

The SDSM CASTing libraries were produced from the YSBLIC-3C-PpLAAO plasmid using the Stratagene QuikChange method where two complementary, overlapping mutagenic primers are used to form a copy of the entire plasmid ring, and the original wild-type plasmid is digested using *DpnI* restriction enzyme, which targets the methylated DNA in plasmids that have been purified by Miniprep, but not unmethylated DNA produced by PCR.

The PpLAAO CASTing library A was produced using Pfu Turbo HotStart polymerase and primers designed to induce mutations into the sites His351 and Tyr352, with a PCR annealing temperature of 52°C. The PCR reaction was digested with *Dpn*I and then used to transform chemically competent *E.coli* XL10-Gold cells, as in **Section 2.6.1**. Plasmid DNA was purified from six of the resulting colonies, named PNDTA A-F, and the length of the gene insert was checked by PCR amplification using primers that bound to each end of the PpLAAO gene sequence. However the size of the insert appeared to vary between the different plasmids (**Figure 6.3**).

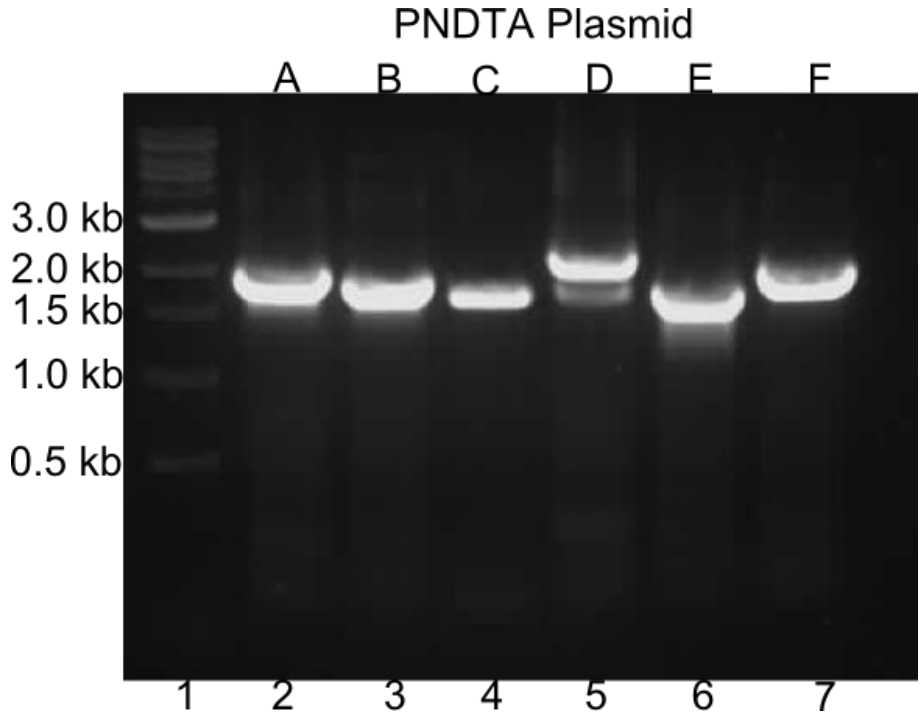

Figure 6.3 1% agarose gel separation of DNA from PCR amplification of plasmid inserts using: Lane 1, 1 kb DNA ladder (0.5 kb, 1 kb, 1.5 kb, 2 kb, 3 kb, 4 kb, 5 kb, 6 kb, 8 kb, 10 kb), Lane 2-7, PCR amplification of insert sequence in pET-YSBLIC3C PNDTAA-F plasmids (Expected- 1605 bp).

PNDTAA-E were sent for sequencing by the York University Genomics department and all five strains had mutations in the expected base pairs (**Table 6.2**). However PNDTAA, PNDTAB and PNDTAD also had 283, 169 and 207 bp (respectively) sections of partial and whole primer insert sequences (**Figure 6.4**), possibly caused by a 9 base pair repeat found on either side of the mutagenic sequence of the primers (**Table 2.3**) which allowed the complementary primers to bind to each other and form chains, which were then incorporated into the new sequence around the primer binding site.

Table 6.2 Summary of changes in mutation site of sequenced PpLAAO mutants (PNDTAA-E)

Plasmid	Nucleotide sequence of mutation site	Amino acid changes from Wild-Type
Wild-type PpLAAO	CATTAC	N/A
PNDTAA	GTTCGT	His351Val, Tyr352Arg
PNDTAB	TATTAT	His351Tyr
PNDTAC	TATCAT	His351Tyr, Tyr352His
PNDTAD	TTTTAT	His351Phe
PNDTAE	CTTGAT	His351Leu, Tyr352Asp

```
WTPpLAAO         ------------------------------------------------------------
PNDTAC           CGGGTTCAATTCCCC-TCTAGAATAATTTTGTTTAACTTTAAGAAGGAGATATACCATGG 59
PNDTAE           -GGGAAAATTTCCCC-TCTAGAATAATTTTGTTTAACTTTAAGAAGGAGATATACCATGG 58
PNDTAB           --GGGCAACATTCCA-TCTAGAATAATTTTGTTTAACTTTAAGAAGGAGATATACCATGG 57
PNDTAD           -GGGCGGAACATTCC-TCTAGAATAATTTTGTTTAACTTTAAGAAGGAGATATACCATGG 58
PNDTAA           --TGCGGGTCATTCCCTCTAGAATAATTTTGTTTAACTTTAAGAAGGAGATATACCATGG 58

WTPpLAAO         ------------------------------------------------------------
PNDTAC           GCAGCAGCCATCATCATCATCATCACAGCAGCGGCCTGGAAGTTCTGTTCCAGGGACCAG 119
PNDTAE           GCAGCAGCCATCATCATCATCATCACAGCAGCGGCCTGGAAGTTCTGTTCCAGGGACCAG 118
PNDTAB           GCAGCAGCCATCATCATCATCATCACAGCAGCGGCCTGGAAGTTCTGTTCCAGGGACCAG 117
PNDTAD           GCAGCAGCCATCATCATCATCATCACAGCAGCGGCCTGGAAGTTCTGTTCCAGGGACCAG 118
PNDTAA           GCAGCAGCCATAAACATCATCATCACAGCAGCGGCCTGGAAGTTCTGTTCCAGGGACCAG 118

WTPpLAAO         --ATGAGCCAACAATTCCAACATGATGTCCTGGTGATCGGCAGCGGTGCCGCCGGTCTCA 58
PNDTAC           CAATGAGCCAACAATTCCAACATGATGTCCTGGTGATCGGCAGCGGTGCCGCCGGTCTCA 179
PNDTAE           CAATGAGCCAACAATTCCAACATGATGTCCTGGTGATCGGCAGCGGTGCCGCCGGTCTCA 178
PNDTAB           CAATGAGCCAACAATTCCAACATGATGTCCTGGTGATCGGCAGCGGTGCCGCCGGTCTCA 177
PNDTAD           CAATGAGCCAACAATTCCAACATGATGTCCTGGTGATCGGCAGCGGTGCCGCCGGTCTCA 178
PNDTAA           CAATGAGCCAACAATTCCAACATGATGTCCTGGTGATCGGCAGCGGTGCCGCCGGTCTCA 178
                   ************************************************************

WTPpLAAO         GCCTGGCACTTAACCTCCCCAGCCACCTTCGCGTTGCCGTATTGAGCAAGGGCGACCTGT 118
PNDTAC           GCCTGGCACTTAACCTCCCCAGCCACCTTCGCGTTGCCGTATTGAGCAAGGGCGACCTGT 239
PNDTAE           GCCTGGCACTTAACCTCCCCAGCCACCTTCGCGTTGCCGTATTGAGCAAGGGCGACCTGT 238
PNDTAB           GCCTGGCACTTAACCTCCCCAGCCACCTTCGCGTTGCCGTATTGAGCAAGGGCGACCTGT 237
PNDTAD           GCCTGGCACTTAACCTCCCCAGCCACCTTCGCGTTGCCGTATTGAGCAAGGGCGACCTGT 238
PNDTAA           GCCTGGCACTTAACCTCCCCAGCCACCTTCGCGTTGCCGTATTGAGCAAGGGCGACCTGT 238
                 ************************************************************

WTPpLAAO         CCAACGGCTCGACCTTCTGGGCCCAGGGCGGCGTCGCTGCAGTGCTGGACAACACCGATA 178
PNDTAC           CCAACGGCTCGACCTTCTGGGCCCAGGGCGGCGTCGCTGCAGTGCTGGACAACACCGATA 299
PNDTAE           CCAACGGCTCGACCTTCTGGGCCCAGGGCGGCGTCGCTGCAGTGCTGGACAACACCGATA 298
PNDTAB           CCAACGGCTCGACCTTCTGGGCCCAGGGCGGCGTCGCTGCAGTGCTGGACAACACCGATA 297
PNDTAD           CCAACGGCTCGACCTTCTGGGCCCAGGGCGGCGTCGCTGCAGTGCTGGACAACACCGATA 298
PNDTAA           CCAACGGCTCGACCTTCTGGGCCCAGGGCGGCGTCGCTGCAGTGCTGGACAACACCGATA 298
                 ************************************************************

WTPpLAAO         CTGTGCAGTCGCATGTCGAGGACACCCTCAATGCCGGCGGCGGGCTGTGCCATGAAGACG 238
PNDTAC           CTGTGCAGTCGCATGTCGAGGACACCCTCAATGCCGGCGGCGGGCTGTGCCATGAAGACG 359
PNDTAE           CTGTGCAGTCGCATGTCGAGGACACCCTCAATGCCGGCGGCGGGCTGTGCCATGAAGACG 358
PNDTAB           CTGTGCAGTCGCATGTCGAGGACACCCTCAATGCCGGCGGCGGGCTGTGCCATGAAGACG 357
PNDTAD           CTGTGCAGTCGCATGTCGAGGACACCCTCAATGCCGGCGGCGGGCTGTGCCATGAAGACG 358
PNDTAA           CTGTGCAGTCGCATGTCGAGGACACCCTCAATGCCGGCGGCGGGCTGTGCCATGAAGACG 358
                 ************************************************************

WTPpLAAO         CAGTGCGCTTTACCGTCGAGCACAGCCGCGAAGCGATCCAATGGCTGATCGAGCAAGGCG 298
PNDTAC           CAGTGCGCTTTACCGTCGAGCACAGCCGCGAAGCGATCCAATGGCTGATCGAGCAAGGCG 419
PNDTAE           CAGTGCGCTTTACCGTCGAGCACAGCCGCGAAGCGATCCAATGGCTGATCGAGCAAGGCG 418
PNDTAB           CAGTGCGCTTTACCGTCGAGCACAGCCGCGAAGCGATCCAATGGCTGATCGAGCAAGGCG 417
PNDTAD           CAGTGCGCTTTACCGTCGAGCACAGCCGCGAAGCGATCCAATGGCTGATCGAGCAAGGCG 418
PNDTAA           CAGTGCGCTTTACCGTCGAGCACAGCCGCGAAGCGATCCAATGGCTGATCGAGCAAGGCG 418
                 ************************************************************

WTPpLAAO         TGCCCTTCACCCGCGATGAGCACTACAGCGTCGACGATGGCGGCTTCGAGTTCCACCTCA 358
PNDTAC           TGCCCTTCACCCGCGATGAGCACTACAGCGTCGACGATGGCGGCTTCGAGTTCCACCTCA 479
PNDTAE           TGCCCTTCACCCGCGATGAGCACTACAGCGTCGACGATGGCGGCTTCGAGTTCCACCTCA 478
PNDTAB           TGCCCTTCACCCGCGATGAGCACTACAGCGTCGACGATGGCGGCTTCGAGTTCCACCTCA 477
PNDTAD           TGCCCTTCACCCGCGATGAGCACTACAGCGTCGACGATGGCGGCTTCGAGTTCCACCTCA 478
PNDTAA           TGCCCTTCACCCGCGATGAGCACTACAGCGTCGACGATGGCGGCTTCGAGTTCCACCTCA 478
                 ************************************************************

WTPpLAAO         CCCGTGAAGGGGGCCATAGCCACCGGCGCATCATCCACGCCGCCGACGCTACCGGCGCGG 418
PNDTAC           CCCGTGAAGGGGGCCATAGCCACCGGCGCATCATCCACGCCGCCGACGCTACCGGCGCGG 539
PNDTAE           CCCGTGAAGGGGGCCATAGCCACCGGCGCATCATCCACGCCGCCGACGCTACCGGCGCGG 538
PNDTAB           CCCGTGAAGGGGGCCATAGCCACCGGCGCATCATCCACGCCGCCGACGCTACCGGCGCGG 537
```

```
PNDTAD          CCCGTGAAGGGGGCCATAGCCACCGGCGCATCATCCACGCCGCCGACGCTACCGGCGCGG 538
PNDTAA          CCCGTGAAGGGGGCCATAGCCACCGGCGCATCATCCACGCCGCCGACGCTACCGGCGCGG 538
                ************************************************************

WTPpLAAO        CAATCTTCACCACGCTGCTGGAACAGGCTCGCCAGCGCCCGAACATCCAGCTGCTGGAGC 478
PNDTAC          CAATCTTCACCACGCTGCTGGAACAGGCTCGCCAGCGCCCGAACATCCAGCTGCTGGAGC 599
PNDTAE          CAATCTTCACCACGCTGCTGGAACAGGCTCGCCAGCGCCCGAACATCCAGCTGCTGGAGC 598
PNDTAB          CAATCTTCACCACGCTGCTGGAACAGGCTCGCCAGCGCCCGAACATCCAGCTGCTGGAGC 597
PNDTAD          CAATCTTCACCACGCTGCTGGAACAGGCTCGCCAGCGCCCGAACATCCAGCTGCTGGAGC 598
PNDTAA          CAATCTTCACCACGCTGCTGGAACAGGCTCGCCAGCGCCCGAACATCCAGCTGCTGGAGC 598
                ************************************************************

WTPpLAAO        AGCGGGTGGCGGTCGACCTGATCACTGAACGCCGCCTGGGCCTGCCCGGCGAACGCTGCC 538
PNDTAC          AGCGGGTGGCGGTCGACCTGATCACTGAACGCCGCCTGGGCCTGCCCGGCGAACGCTGCC 659
PNDTAE          AGCGGGTGGCGGTCGACCTGATCACTGAACGCCGCCTGGGCCTGCCCGGCGAACGCTGCC 658
PNDTAB          AGCGGGTGGCGGTCGACCTGATCACTGAACGCCGCCTGGGCCTGCCCGGCGAACGCTGCC 657
PNDTAD          AGCGGGTGGCGGTCGACCTGATCACTGAACGCCGCCTGGGCCTGCCCGGCGAACGCTGCC 658
PNDTAA          AGCGGGTGGCGGTCGACCTGATCACTGAACGCCGCCTGGGCCTGCCCGGCGAACGCTGCC 658
                ************************************************************

WTPpLAAO        TGGGCGCCTACGTGCTCGACCGCAACACCGGCGAGGTGGACACCTTCGGCGCGCGCTTCA 598
PNDTAC          TGGGCGCCTACGTGCTCGACCGCAACACCGGCGAGGTGGACACCTTCGGCGCGCGCTTCA 719
PNDTAE          TGGGCGCCTACGTGCTCGACCGCAACACCGGCGAGGTGGACACCTTCGGCGCGCGCTTCA 718
PNDTAB          TGGGCGCCTACGTGCTCGACCGCAACACCGGCGAGGTGGACACCTTCGGCGCGCGCTTCA 717
PNDTAD          TGGGCGCCTACGTGCTCGACCGCAACACCGGCGAGGTGGACACCTTCGGCGCGCGCTTCA 718
PNDTAA          TGGGCGCCTACGTGCTCGACCGCAACACCGGCGAGGTGGACACCTTCGGCGCGCGCTTCA 718
                ************************************************************

WTPpLAAO        CCGTGCTGGCCACGGGCGGTGCGGCCAAGGTCTATCTCTACACCAGCAACCCCGATGGTG 658
PNDTAC          CCGTGCTGGCCACGGGCGGTGCGGCCAAGGTCTATCTCTACACCAGCAACCCCGATGGTG 779
PNDTAE          CCGTGCTGGCCACGGGCGGTGCGGCCAAGGTCTATCTCTACACCAGCAACCCCGATGGTG 778
PNDTAB          CCGTGCTGGCCACGGGCGGTGCGGCCAAGGTCTATCTCTACACCAGCAACCCCGATGGTG 777
PNDTAD          CCGTGCTGGCCACGGGCGGTGCGGCCAAGGTCTATCTCTACACCAGCAACCCCGATGGTG 778
PNDTAA          CCGTGCTGGCCACGGGCGGTGCGGCCAAGGTCTATCTCTACACCAGCAACCCCGATGGTG 778
                ************************************************************

WTPpLAAO        CCTGCGGCGACGGTATCGCCATGGCCTGGCGGGCCGGCTGCCGAGTGGCGAACCTGGAAT 718
PNDTAC          CCTGCGGCGACGGTATCGCCATGGCCTGGCGGGCCGGCTGCCGAGTGGCGAACCTGGAAT 839
PNDTAE          CCTGCGGCGACGGTATCGCCATGGCCTGGCGGGCCGGCTGCCGAGTGGCGAACCTGGAAT 838
PNDTAB          CCTGCGGCGACGGTATCGCCATGGCCTGGCGGGCCGGCTGCCGAGTGGCGAACCTGGAAT 837
PNDTAD          CCTGCGGCGACGGTATCGCCATGGCCTGGCGGGCCGGCTGCCGAGTGGCGAACCTGGAAT 838
PNDTAA          CCTGCGGCGACGGTATCGCCATGGCCTGGCGGGCCGGCTGCCGAGTGGCGAACCTGGAAT 838
                ************************************************************

WTPpLAAO        TCAACCAGTTCCACCCGACCTGCCTGTATCACCCACAGGCCAAGAGCTTCCTGATCACCG 778
PNDTAC          TCAACCAGTTCCACCCGACCTGCCTGTATCACCCACAGGCCAAGAGCTTCCTGATCACCG 899
PNDTAE          TCAACCAGTTCCACCCGACCTGCCTGTATCACCCACAGGCCAAGAGCTTCCTGATCACCG 898
PNDTAB          TCAACCAGTTCCACCCGACCTGCCTGTATCACCCACAGGCCAAGAGCTTCCTGATCACCG 897
PNDTAD          TCAACCAGTTCCACCCGACCTGCCTGTATCACCCACAGGCCAAGAGCTTCCTGATCACCG 898
PNDTAA          TCAACCAGTTCCACCCGACCTGCCTGTATCACCCACAGGCCAAGAGCTTCCTGATCACCG 898
                ************************************************************

WTPpLAAO        AAGCCCTGCGCGGCGAGGGCGCCCTGCTGCGCCTGCCCAACGGCGAACGTTTCATGCCAC 838
PNDTAC          AAGCCCTGCGCGGCGAGGGCGCCCTGCTGCGCCTGCCCAACGGCGAACGTTTCATGCCAC 959
PNDTAE          AAGCCCTGCGCGGCGAGGGCGCCCTGCTGCGCCTGCCCAACGGCGAACGTTTCATGCCAC 958
PNDTAB          AAGCCCTGCGCGGCGAGGGCGCCCTGCTGCGCCTGCCCAACGGCGAACGTTTCATGCCAC 957
PNDTAD          AAGCCCTGCGCGGCGAGGGCGCCCTGCTGCGCCTGCCCAACGGCGAACGTTTCATGCCAC 958
PNDTAA          AAGCCCTGCGCGGCGAGGGCGCCCTGCTGCGCCTGCCCAACGGCGAACGTTTCATGCCAC 958
                ************************************************************

WTPpLAAO        GCTTCGACCCACGCGAAGAGCTGGCCCCACGG-------GACA-------TCGTGGCCCG 884
PNDTAC          GCTTCGACCCACGCGAAGAGCTGGCCCCACGG-------GACA-------TCGTGGCCCG 1005
PNDTAE          GCTTCGACCCACGCGAAGAGCTGGCCCCACGG-------GACA-------TCGTGGCCCG 1004
PNDTAB          GCTTCGACCCACGCGAAGAGCTGGCCCCACGG-------GACA-------TCGTGGCCCG 1003
PNDTAD          GCTTCGACCCACGCGAAGAGCTGGCCCCACGG-------GACA-------TCGTGGCCCG 1004
PNDTAA          GCTTCGACCCACGCGAAGAGCTGGACCTGCGGCCGGGGGTGATGGTGGTGCCTGCGGCGCG 1018
                ********************** **  ***       **           * *** **
```

```
WTPpLAAO         CGCCATCGACCACGAGATGAA--GCGC--CTG-GGCG---TGGA----CTGCG------T 926
PNDTAC           CGCCATCGACCACGAGATGAA--GCGC--CTG-GGCG---TGGA----CTGCG------T 1047
PNDTAE           CGCCATCGACCACGAGATGAA--GCGC--CTG-GGCG---TGGA----CTGCG------T 1046
PNDTAB           CGCCATCGACCACGAGATGAA--GCGC--CTG-GGCG---TGGA----CTGCG------T 1045
PNDTAD           CGCCATCGACCACGAGATGAA--GCGCTGCTGCGGCGATTTATA----CTGCGGCGGGGT 1058
PNDTAA           TATTACCTGCGGCGGGGTGAGTGGTGC--CTGCGGCG---TGTATTACCTGCGGCGGGGT 1073
                     * *  *  ** * ***   * **  *** ****   *  *    *****      *

WTPpLAAO         A----------------------TAC---CTG-GAC--ATCACTC-ACAAGC-------- 949
PNDTAC           A----------------------TAC---CTG-GAC--ATCACTC-ACAAGC-------- 1070
PNDTAE           A----------------------TAC---CTG-GAC--ATCACTC-ACAAGC-------- 1069
PNDTAB           A----------------------TAC---CTG-GAC--ATCACTC-ACAAGC-------- 1068
PNDTAD           G----------------------TGGTG-CTGCGGCGAATCATAC-TGCGGCGGGGTG-- 1092
PNDTAA           GATACCCGTCAGCCGATCCCCGGTGGTGCCTGCGGCGTGTATTACCTGCGGCGGGGTGAC 1133
                                       *     *** * *   *    *     **

WTPpLAAO         --------CTGCAG--------AT-TTCATCAAGA--GCCAC-TTCCCCACCGTGTAC-- 987
PNDTAC           --------CTGCAG--------AT-TTCATCAAGA--GCCAC-TTCCCCACCGTGTAC-- 1108
PNDTAE           --------CTGCAG--------AT-TTCATCAAGA--GCCAC-TTCCCCACCGTGTAC-- 1107
PNDTAB           --------CTGCAG--------AT-TTCATCAAGA--GCCAC-TTCCCCACCGTGTAC-- 1106
PNDTAD           GGTGGTG-CTGCGGCGTATCGTAC-TGCGGCGGGGTGGGTGC-TGCGGCGCGTTATACTG 1149
PNDTAA           GGTGGTGCCTGCGGCGGATAATACCTGCGGCGGGGGTGGTGCCTGCGGCGGGTGTTAC-- 1191
                         **** *        *  * *  *  *   *   * * *  *      ***

WTPpLAAO         --GAGCGCTGCCTGGC--CTTTGGCA-TCGATAT-CACCCGTCAGCCGATCCCGGTGGTG 1041
PNDTAC           --GAGCGCTGCCTGGC--CTTTGGCA-TCGATAT-CACCCGTCAGCCGATCCCGGTGGTG 1162
PNDTAE           --GAGCGCTGCCTGGC--CTTTGGCA-TCGATAT-CACCCGTCAGCCGATCCCGGTGGTG 1161
PNDTAB           --GAGCGCTGCCTGGC--CTTTGGCA-TCGATAT-CACCCGTCAGCCGATCCCGGTGGTG 1160
PNDTAD           CGGCGGGGTGATTGGTG-CTGCGGCGGTTAGTAC-TGCG-GCGGGGTGAT--CGGTGGTG 1204
PNDTAA           CTGCGGCG-----GGTGCCTGCGGCGGATTTTACCTGCG-GCGGGGTG----CGGTGGTG 1241
                   * *        **   **  ***      **    *  *   *  *    ********

WTPpLAAO         C------------------------------------------------------------ 1042
PNDTAC           C------------------------------------------------------------ 1163
PNDTAE           C------------------------------------------------------------ 1162
PNDTAB           CTGCGGCGTATCGTACTGCGGCGGGGTGATACTGCGGCGTTTTTTACGTGCGGCGGGTGG 1220
PNDTAD           CG------------------------------------------------------------ 1206
PNDTAA           CC------------------------------------------------------------ 1243
                 *

WTPpLAAO         ------------------------------------------------------------
PNDTAC           ------------------------------------------------------------
PNDTAE           ------------------------------------------------------------
PNDTAB           TGCGTGCGGCGATTTTTACCTGCGGCGGGTGCCTGCGGCGCTTTATACCTGCGGCGGGGT 1280
PNDTAD           ------------------------------------------------------------
PNDTAA           ------------------------------------------------------------

WTPpLAAO         ----------------------------------------------------CTGCGGCGCA 1052
PNDTAC           ----------------------------------------------------CTGCGGCGTA 1173
PNDTAE           ----------------------------------------------------CTGCGGCGCT 1172
PNDTAB           GATGGTGGTGCCTGCGGCGGTTGATACCTGCGGCGGGGTGACGGTGGTGCCTGCGGCGTA 1340
PNDTAD           ------------TGCGGCGCGTTGTACCTGCGGCGGGGTGATGGTGGTGCCTGCGGCGTT 1254
PNDTAA           ------------TGCGGCGTTTGATACCTGCGGCGG-----------TGCCTGCGGCGGT 1280
                                                                 ********

WTPpLAAO         TTACACCTGCGGCGGGGTGATGGTCGACGACTGCGGCCACACCGATGTGCCTGGCTTGTA 1112
PNDTAC           TCATACCTGCGGCGGGGTGATGGTCGACGACTGCGGCCACACCGATGTGCCTGGCTTGTA 1233
PNDTAE           TGATACCTGCGGCGGGGTGATGGTCGACGACTGCGGCCACACCGATGTGCCTGGCTTGTA 1232
PNDTAB           TTATACCTGCGGCGGGGTGATGGTCGACGACTGCGGCCACACCGATGTGCCTGGCTTGTA 1400
PNDTAD           TTATACCTGCGGCGGGGTGATGGTCGACGACTGCGGCCACACCGATGTGCCTGGCTTGTA 1314
PNDTAA           TCGTACCTGCGGCGGGGTGATGGTCGACGACTGCGGCCACACCGATGTGCCTGGCTTGTA 1340
                 *   ************************************************

WTPpLAAO         TGCCATCGGCGAAACCAGTTTCACCGGCCTGCACGGCGCCAACCGCATGGCCAGCAACTC 1172
PNDTAC           TGCCATCGGCGAAACCAGTTTCACCGGCCTGCACGGCGCCAACCGCATGGCCAGCAACTC 1293
PNDTAE           TGCCATCGGCGAAACCAGTTTCACCGGCCTGCACGGCGCCAACCGCATGGCCAGCAACTC 1292
PNDTAB           TGCCATCGGCGAAACCAGTTTCACCGGCCTGCACGGCGCCAACCGCATGGCCAGCAACTC 1460
```

```
PNDTAD          TGCCATCGGCGAAACCAGTTTCACCGGCCTGCACGGCGCCAACCGCATGGCCAGCAACTC 1374
PNDTAA          TGCCATCGGCGAAACCAGTTTCACCGGCCTGCACGGCGCCAACCGCATGGCCAGCAACTC 1400
                ************************************************************

WTPpLAAO        GCTGCTGGAATGTTTTGTGTACGGTCGCGCCGCCGCTGCCGACATCCAGGCGCACCTGGA 1232
PNDTAC          GCTGCTGGAATGTTTTGTGTACGGTCGCGCCGCCGCTGCCGACATCCAGGCGCACCTGGA 1353
PNDTAE          GCTGCTGGAATGTTTTGTGTACGGTCGCGCCGCCGCTGCCGACATCCAGGCGCACCTGGA 1352
PNDTAB          GCTGCTGGAATGTTTTGTGTACGGTCGCGCCGCCGCTGCCGACATCCAGGCGCACCTGGA 1520
PNDTAD          GCTGCTGGAATGTTTTGTGTACGGTCGCGCCGCCGCTGCCGACATCCAGGCGCACCTGGA 1434
PNDTAA          GCTGCTGGAATGTTTTGTGTACGGTCGCGCCGCCGCTGCCGACATCCAGGCGCACCTGGA 1460
                ************************************************************

WTPpLAAO        GCAAGTGGCCATGCCCAAGGCCTTGCCCGGCTGGGACGCCAGCCAGGTGACCGACTCGGA 1292
PNDTAC          GCAAGTGGCCATGCCCAAGGCCTTGCCCGGCTGGGACGCCAGCCAGGTGACCGACTCGGA 1413
PNDTAE          GCAAGTGGCCATGCCCAAGGCCTTGCCCGGCTGGGACGCCAGCCAGGTGACCGACTCGGA 1412
PNDTAB          GCAAGTGGCCATGCCCAAGGCCTTGCCCGGCTGGGACGCCAGCCAGGTGACCGACTCGGA 1580
PNDTAD          GCAAGTGGCCATGCCCAAGGCCTTGCCCGGCTGGGACGCCAGCCAGGTGACCGACTCGGA 1494
PNDTAA          GCAAGTGGCCATGCCCAAGGCCTTGCCCGGCTGGGACGCCAGCCAGGTGACCGACTCGGA 1520
                ************************************************************

WTPpLAAO        CGAGGACGTGATCATTGCGCACAACTGGGACGAACTGCGGCGCTTCATGTGGGACTACGT 1352
PNDTAC          CGAGGACGTGATCATTGCGCACAACTGGGACGAACTGCGGCGCTTCATGTGGGACTACGT 1473
PNDTAE          CGAGGACGTGATCATTGCGCACAACTGGGACGAACTGCGGCGCTTCATGTGGGACTACGT 1472
PNDTAB          CGAGGACGTGATCATTGCGCACAACTGGGACGAACTGCGGCGCTTCATGTGGGACTACGT 1640
PNDTAD          CGAGGACGTGATCATTGCGCACAACTGGGACGAACTGCGGCGCTTCATGTGGGACTACGT 1554
PNDTAA          CGAGGACGTGATCATTGCGCACAACTGGGACGAACTGCGGCGCTTCATGTGGGACTACGT 1580
                ************************************************************

WTPpLAAO        CGGCATCGTGCGCACCAGCAAGCGCCTGCAGCGGGCCCAGCACCGCATTCGCCTGCTGCT 1412
PNDTAC          CGGCATCGTGCGCACCAGCAAGCGCCTGCAGCGGGCCCAGCACCGCATTCGCCTGCTGCT 1533
PNDTAE          CGGCATCGTGCGCACCAGCAAGCGCCTGCAGCGGGCCCAGCACCGCATTCGCCTGCTGCT 1532
PNDTAB          CGGCATCGTGCGCACCAGCAAGCGCCTGCAGCGGGCCCAGCACCGCATTCGCCTGCTGCT 1700
PNDTAD          CGGCATCGTGCGCACCAGCAAGCGCCTGCAGCGGGCCCAGCACCGCATTCGCCTGCTGCT 1614
PNDTAA          CGGCATCGTGCGCACCAGCAAGCGCCTGCAGCGGGCCCAGCACCGCATTCGCCTGCTGCT 1640
                ************************************************************

WTPpLAAO        GGATGAAATCGACGAGTTCTACAGCAACTACAAGGTCAGCCGTGACCTGATCGAGCTGCG 1472
PNDTAC          GGATGAAATCGACGAGTTCTACAGCAACTACAAGGTCAGCCGTGACCTGATCGAGCTGCG 1593
PNDTAE          GGATGAAATCGACGAGTTCTACAGCAACTACAAGGTCAGCCGTGACCTGATCGAGCTGCG 1592
PNDTAB          GGATGAAATCGACGAGTTCTACAGCAACTACAAGGTCAGCCGTGACCTGATCGAGCTGCG 1760
PNDTAD          GGATGAAATCGACGAGTTCTACAGCAACTACAAGGTCAGCCGTGACCTGATCGAGCTGCG 1674
PNDTAA          GGATGAAATCGACGAGTTCTACAGCAACTACAAGGTCAGCCGTGACCTGATCGAGCTGCG 1700
                ************************************************************

WTPpLAAO        CAACCTGGCGCAAGTGGCCGAGCTGATGATCCTGTCAGCCATGCAGCGCAAGGAAAGCCG 1532
PNDTAC          CAACCTGGCGCAAGTGGCCGAGCTGATGATCCTGTCAGCCATGCAGCGCAAGGAAAGCCG 1653
PNDTAE          CAACCTGGCGCAAGTGGCCGAGCTGATGATCCTGTCAGCCATGCAGCGCAAGGAAAGCCG 1652
PNDTAB          CAACCTGGCGCAAGTGGCCGAGCTGATGATCCTGTCAGCCATGCAGCGCAAGGAAAGCCG 1820
PNDTAD          CAACCTGGCGCAAGTGGCCGAGCTGATGATCCTGTCAGCCATGCAGCGCAAGGAAAGCCG 1734
PNDTAA          CAACCTGGCGCAAGTGGCCGAGCTGATGATCCTGTCAGCCATGCAGCGCAAGGAAAGCCG 1760
                ************************************************************

WTPpLAAO        AGGGTTGCATTACACACTGGATTATCCAGGGATGCTGGACGAGGCCAAGGACACCATCCT 1592
PNDTAC          AGGGTTGCATTACACACTGGATTATCCAGGGATGCTGGACGAGGCCAAGGACACCATCCT 1713
PNDTAE          AGGGTTGCATTACACACTGGATTATCCAGGGATGCTGGACGAGGCCAAGGACACCATCCT 1712
PNDTAB          AGGGTTGCATTACACACTGGATTATCCAGGGATGCTGGACGAGGCCAAGGACACCATCCT 1880
PNDTAD          AGGGTTGCATTACACACTGGATTATCCAGGGATGCTGGACGAGGCCAAGGACACCATCCT 1794
PNDTAA          AGGGTTGCATTACACACTGGATTATCCAGGGATGCTGGACGAGGCCAAGGACACCATCCT 1820
                ************************************************************

WTPpLAAO        TAACCCGCTCTGA------------------------------------------------ 1605
PNDTAC          TAACCCGCTCTGACGCGCCTTCTCCTCACATATGGCTAGCATGACTGGTGGACAGCAAAT 1773
PNDTAE          TAACCCGCTCTGACGCGCCTTCTCCTCACATATGGCTAGCATGACTGGTGGACAGCAAAT 1772
PNDTAB          TAACCCGCTCTGACGCGCCTTCTCCTCACATATGGCTAGCATGACTGGTGGACAGCAAAT 1940
PNDTAD          TAACCCGCTCTGACGCGCCTTCTCCTCACATATGGCTAGCATGACTGGTGGACAGCAAAT 1854
PNDTAA          TAACCCGCTCTGACGCGCCTTCTCCTCACATATGGCTAGCATGACTGGTGGACAGCAAAT 1880
                *************
```

```
WTPpLAAO         ------------------------------------------------------------
PNDTAC           GGGTCGCGGATCCGAATTCGAGCTCCGTCGACAAGCTTGCGGCCGCACTCGAGCACCACC 1833
PNDTAE           GGGTCGCGGATCCGAATTCGAGCTCCGTCGACAAGCTTGCGGCCGCACTCGAGCACCACC 1832
PNDTAB           GGGTCGCGGATCCGAATTCGAGCTCCGTCGACAAGCTTGCGGCCGCACTCGAGCACCACC 2000
PNDTAD           GGGTCGCGGATCCGAATTCGAGCTCCGTCGACAAGCTTGCGGCCGCACTCGAGCACCACC 1914
PNDTAA           GGGTCGCGGATCCGAATTCGAGCTCCGTCGACAAGCTTGCGGCCGCACTCGAGCACCACC 1940

WTPpLAAO         ------------------------------------------------------
PNDTAC           ACCACCACCACTGAGATCCGGCTGCTAACAAAGCCCGAAAGGAAGCTAG--GTGGCCC 1889
PNDTAE           ACCACCACCACTGAGATCCGGCTGCTAACAAAGCCCGAAAGGAAGCTAGTGGCGGC-- 1888
PNDTAB           ACCACCACCACTGAGATCCGGCTGCTAACAAAGCCCGAAAG-AAGCTAGTGCT----- 2052
PNDTAD           ACCACCACCACTGAGATCCGGCTGCTAACAAAGCCCGAAAG-AAGCTGA-GTTGCCCC 1970
PNDTAA           ACCACCACCACTGAGATCCGGCTGCTAACAAAGCCCGAAAG-AAGCTA---CTGCCC- 1993
```

Figure 6.4 CLUSTAL 2.0.12 multiple sequence alignment of Wild Type PpLAAO, and PNDTA A-E, insert sequences, with extra oligo sequences in orange text and mutated residues highlighted in yellow.

The PNDTAA-D purified plasmids were also used to transform competent *E.coli* BL21-DE3 cells in order to analyse the protein expression (**Section 2.6.1**). The PNDTAC strain produced protein that was the same size as the wild-type PpLAAO protein (59 kDa), however the PNDTAA strain did not produce any protein and the PNDTAB and PNDTAD strains produced truncated protein that was around 45 kDa in size (**Figure 6.5**), probably due to the extra base pairs causing a stop codon to be formed.

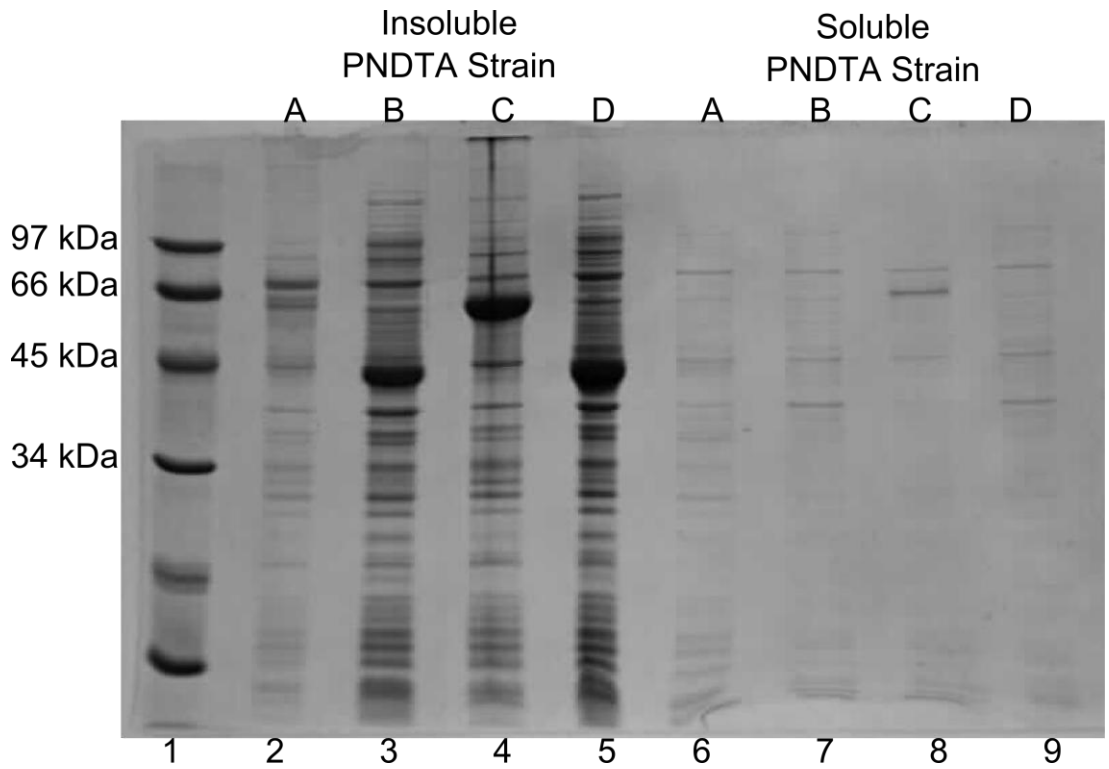

Figure 6.5 SDS-PAGE separation of protein from *E. coli* BL21-DE3 cells transformed with mutated PpLAAO YSBLIC3C plasmids PNDTAA-D: Lane 1, BioRad low molecular weight marker; Lane 2-5, insoluble protein fraction from PNDTAA-D; Lane 6-9, soluble protein fraction from PNDTAA-D.

As the extra insertions were potentially being caused by the primer pairs self annealing, an increase in the annealing temperature of the PCR reaction was attempted. The PCR annealing temperature was optimised using a Eppendorf Mastercycler gradient PCR machine to run the PCR with annealing temperatures of 59.1°C, 61.3°C, 63.5°C, 65.7°C, 67.9°C and 70.5°C. PCR product was visible in all reactions (**Figure 6.6**), so the library was produced with an annealing temperature of 72°C as in **Section 2.6.1**.

The resulting PCR reaction was digested with *Dpn*I and then transformed into *E.coli* BL21-Gold-DE3 competent cells. Nine colonies were picked and protein overexpression was induced as in **Section 2.6.1**. As seven of the nine strains produced proteins that were the expected 59 kDa in size (**Figure 6.7**), ten more transformations were performed, resulting in a total of over 400 colonies. These colonies were pooled together and then Midiprepped to form a pure plasmid library as in **Section 2.6.1**.

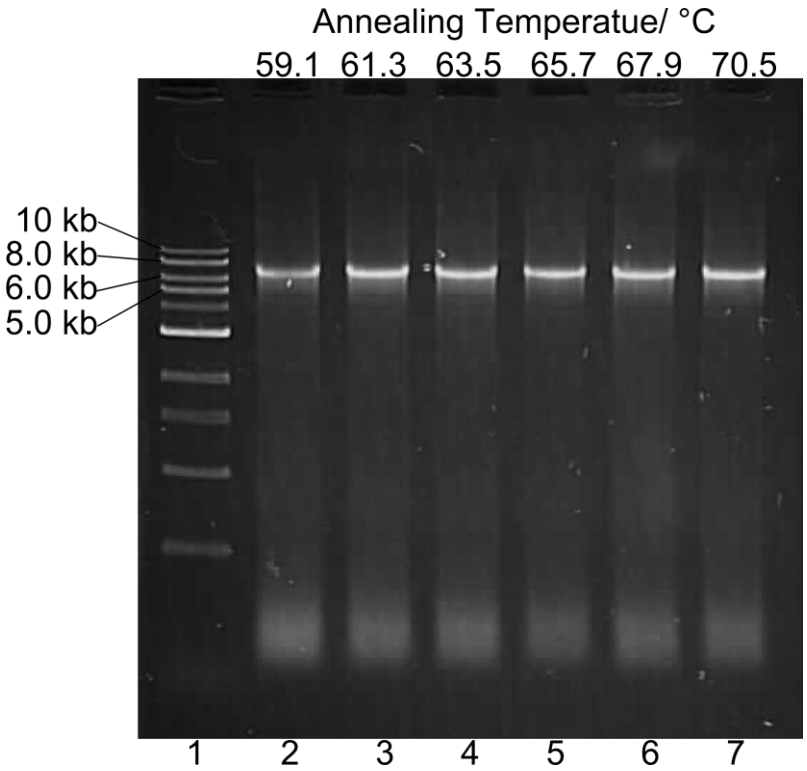

Figure 6.6 1% agarose gel separation of DNA product of SDSM reactions using PNDTA primer set with varying annealing temperatures: Lane 1, 1 kb DNA ladder (0.5 kb, 1 kb, 1.5 kb, 2 kb, 3 kb, 4 kb, 5 kb, 6 kb, 8 kb, 10 kb); Lane 2-7, DNA product of SDSM QuikChange of pET-YSBLIC3C PpLAAO plasmid with annealing temperature of 59- 70°C (6974 bp).

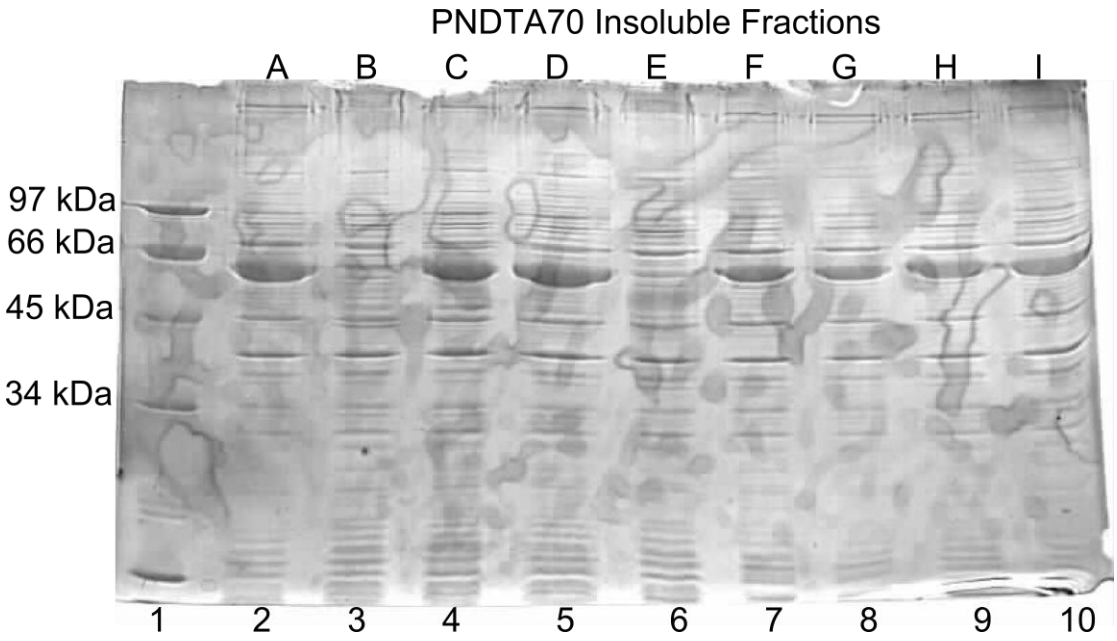

Figure 6.7 SDS-PAGE separation of protein from *E. coli* BL21-Gold-DE3 cells transformed with mutated PpLAAO YSBLIC3C plasmids PNDTA70 A-I: Lane 1, BioRad low molecular weight marker; Lane 2-10, insoluble protein fraction from PNDTA70A-I.

The PpLAAO CASTing library D was produced using Phusion polymerase and a primer set designed to induce mutations in the Gln242, His244 and Pro245 base pairs, as in **Section 2.6.2**. PCR product was treated with *DpnI* to remove the wild-type plasmid template and was then used to transform electrocompetent *E.coli* Top10 cells. Plasmid was purified from five of the resulting colonies, named PNDTD1-5, by Miniprep. The sizes of the gene insert in the purified plasmids were checked using PCR as with the CASTing library A. As the plasmids all appeared to have the same size insert (**Figure 6.8**), the plasmids were sent for sequencing by the York University Genomics department.

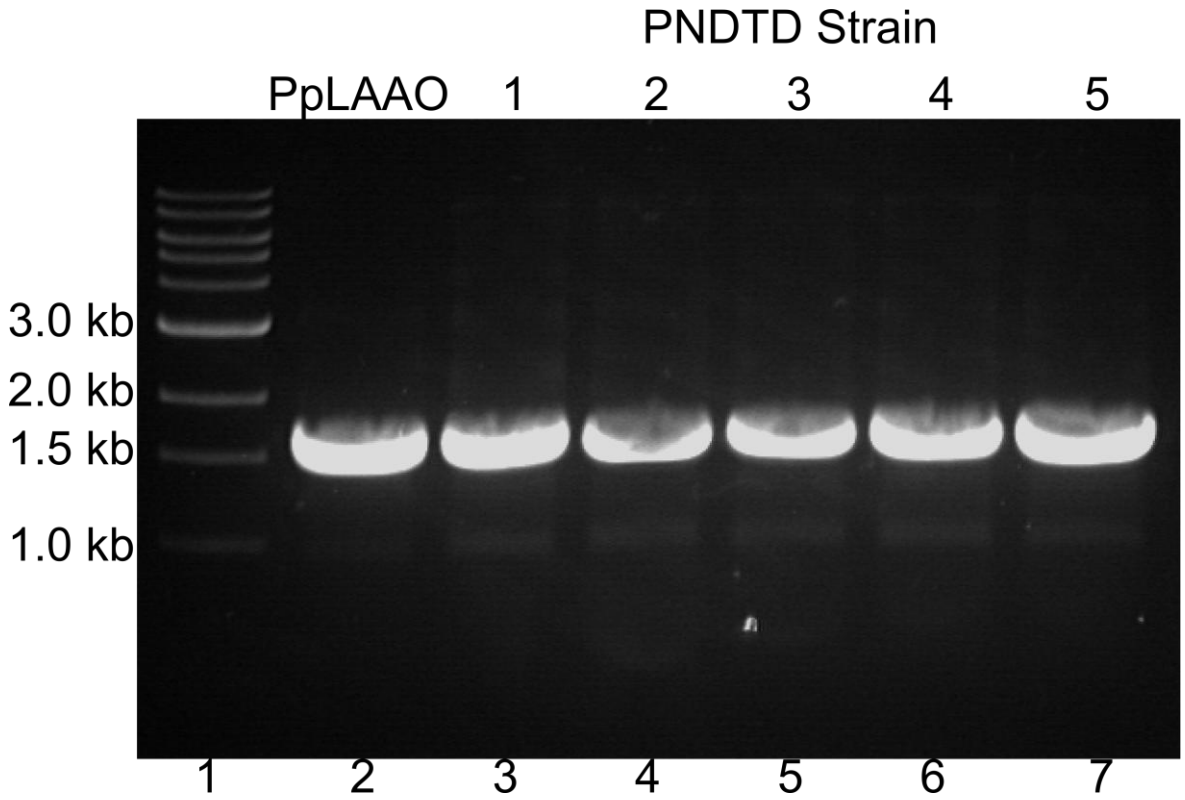

Figure 6.8 1 % agarose gel separation of DNA product of PCR amplification of pET-YSBLIC3C-PNDTD plasmids using PpLAAO-for and PpLAAO-rev primer set to determine gene insert size. Lane 1, 1 kb DNA ladder (0.5 kb, 1 kb, 1.5 kb, 2 kb, 3 kb, 4 kb, 5 kb, 6 kb, 8 kb, 10 kb); Lane 2, DNA amplification of wild type pET-YSBLIC3C-PpLAAO plasmid gene insert, Lane 3-7, DNA amplification of pET-YSBLIC3C-PNDTD1-5 plasmid gene insert.

Plasmids PNDTD2-3 and PNDTD5 had mutated as expected, with only the three target residues showing any mutation (**Table 6.3**). PNDTD1 had mutations at the Gln 242 and His 244 sites but the Pro 245 site (CCG) was unchanged, which should not have been possible under the NDT degeneracy, possibly caused by an error in primer synthesis. All other parts of the protein were as in the wild type. PNDTD4 contained a long primer insert around at primer-binding site, similar to those seen previously when building the PNDTA library.

Table 6.3 Changes to target residues in sequenced PNDTD plasmids

Plasmid ID	Target Nucleotide Sequence	Target Amino Acids
pET-YSBLIC3C-PpLAAO	CAGTTCCACCCG	Gln 242, His 244, Pro 245
pET-YSBLIC3C-PNDTD1	CGTTTCAGCCCG	Arg 242, Ser 244, Pro 245
pET-YSBLIC3C-PNDTD2	GTTTTCAGTGAT	Val 242, Ser 244, Asp 245
pET-YSBLIC3C-PNDTD3	CGTTTCTGTAGT	Arg 242, Cys 244, Ser 245
pET-YSBLIC3C-PNDTD5	ATTTCCATATTA	Iso 242, Iso 244, Leu 245

As most of the colonies appeared to be capable of expressing untruncated mutated protein, transformations were repeated until around 4000 colonies had been produced. These colonies were

scrubbed off the plates and combined, then midi-prepped to form a plasmid library with a concentration of 87 ng μL^{-1}, as in **Section 2.6.2**.

Attempts were made to create the PpLAAO CASTing libraries B, C and E (**Figure 6.1, Table 6.1**) using Pfu Turbo HotStart polymerase and primers sets designed to induce mutations in the Arg 290 and Val 293 positions for library B, the Lys 386, Ser 389 and Ser 391 positions for library C and the Lys 257, Thr 259 and Glu 260 positions for library E. However even when varying the PCR reactions conditions for libraries C and B (**Section 2.6.3**), the reactions failed to produce any visible product that was around the expected 7 kb in size when analysed on agarose gel electrophoresis (**Figure 6.9 a** and **b**) and although the library E did show some product when PCR conditions were varied as in **section 2.6.3** (**Figure 6.9 c**), only 50 colonies were obtained when the digested product was used to transform electrocompetent *E. coli* Top10 cells as in **Section 2.6.4**, whereas around 4000 would be needed to cover 95% of all possible mutation combinations, so a product that would result in a greater number of transformants would be ideal.

Because of this, the reaction conditions were optimised for each library using the Phusion polymerase, as in **Section 2.6.5**. These optimisations resulted in a PCR product that was the expected size for all three of the libraries (**Figure 6.10**). For each library, the condition that resulted in the most visible product on agarose electrophoresis was repeated and digested with *Dpn*I, and levels of product was checked by agarose gel electrophoresis. Unfortunately there appeared to be far less PCR product form the library E reaction after *Dpn*I digestion (**Figure 6.11**).

The library B and library C reactions were used to transform electrocompetent *E. coli* Top10 cells, resulting in 30 colonies from the library B reaction but only 5 from the library C reaction, which was not a good enough transformation efficiency compared to the 4000 colonies needed for 95% coverage of all possible mutation combinations.

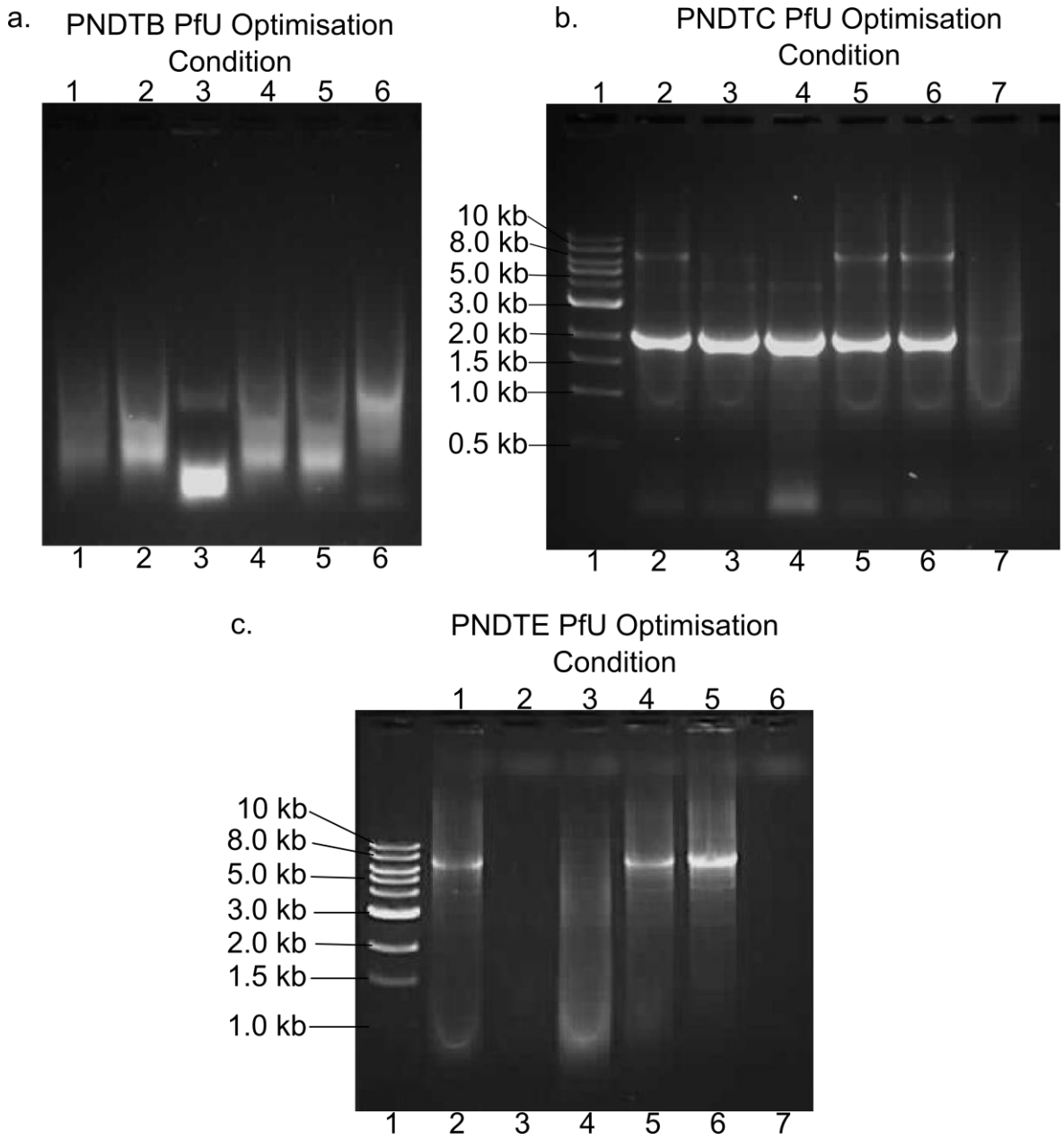

Figure 6.9 1% agarose gel separation of DNA product of SDSM reactions of pET-YSBLIC3C PpLAAO plasmid (6974 bp) using PfU Turbo HotStart polymerase with varying PCR mix conditions. a. SDSM QuikChange using PNDTB primer set. Lane 1-6, DNA product of SDSM using PfU optimisation mix 1-6. b. SDSM QuikChange using PNDTC primer set. Lane 1, 1 kb DNA ladder (0.5 kb, 1 kb, 1.5 kb, 2 kb, 3 kb, 4 kb, 5 kb, 6 kb, 8 kb, 10 kb); Lane 2-7, DNA product of SDSM using PfU optimisation mix 1-6. c. SDSM QuikChange using PNDTE primer set. Lane 1, 1 kb DNA ladder (0.5 kb, 1 kb, 1.5 kb, 2 kb, 3 kb, 4 kb, 5 kb, 6 kb, 8 kb, 10 kb); Lane 2-7, DNA product of SDSM using PfU optimisation mix 1-6.

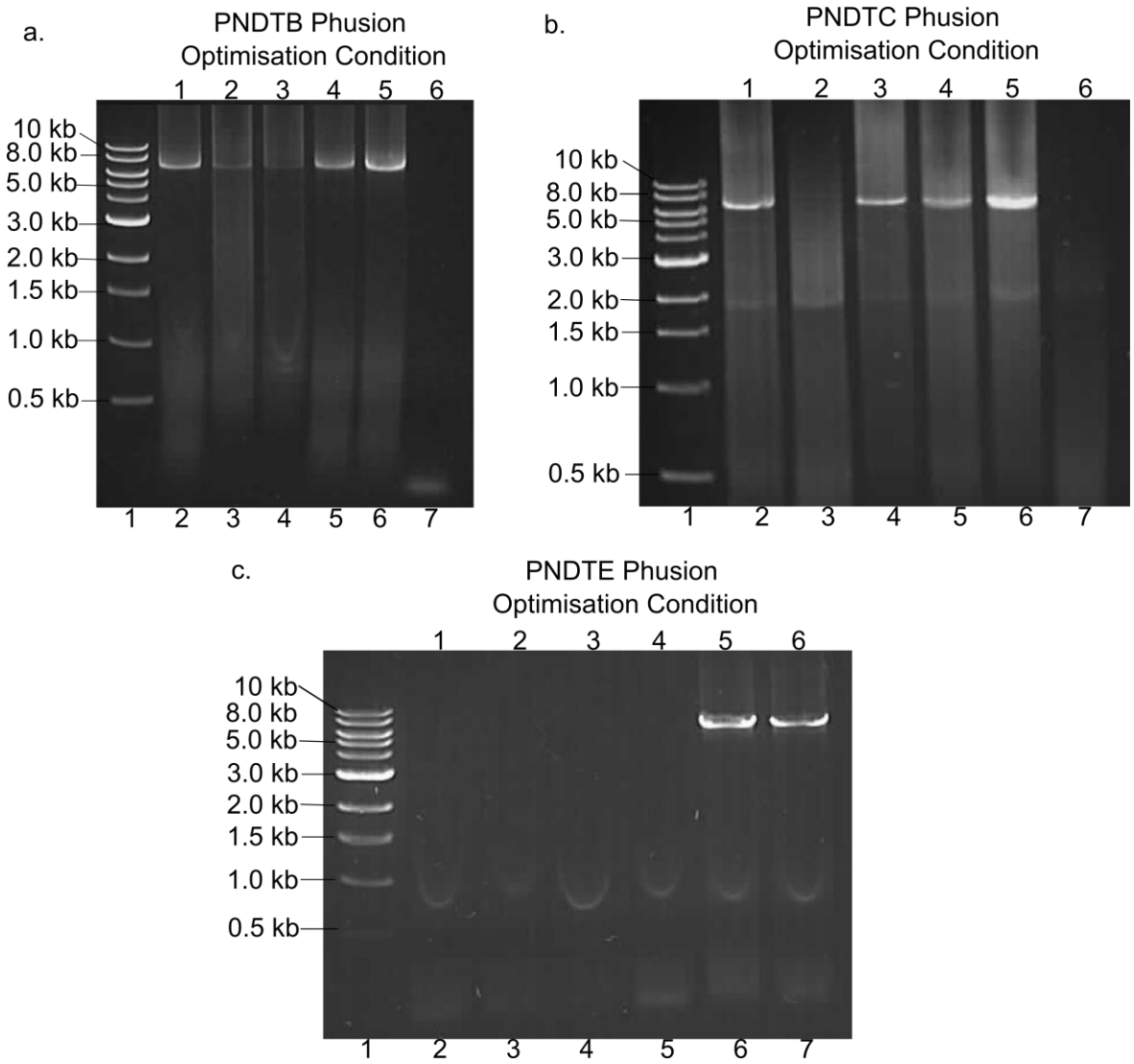

Figure 6.10 1% agarose gel separation of DNA product of SDSM reactions of pET-YSBLIC3C PpLAAO plasmid (6974 bp) using Phusion HotStart polymerase with varying PCR mix conditions. **a.** SDSM QuikChange using PNDTB primer set. Lane 1, 1 kb DNA ladder (0.5 kb, 1 kb, 1.5 kb, 2 kb, 3 kb, 4 kb, 5 kb, 6 kb, 8 kb, 10 kb); Lane 2-7, DNA product of SDSM using Phusion optimisation mix 1-6. **b.** SDSM QuikChange using PNDTC primer set. Lane 1, 1 kb DNA ladder (0.5 kb, 1 kb, 1.5 kb, 2 kb, 3 kb, 4 kb, 5 kb, 6 kb, 8 kb, 10 kb); Lane 2-7, DNA product of SDSM using Phusion optimisation mix 1-6. **c.** SDSM QuikChange using PNDTE primer set. Lane 1, 1 kb DNA ladder (0.5 kb, 1 kb, 1.5 kb, 2 kb, 3 kb, 4 kb, 5 kb, 6 kb, 8 kb, 10 kb); Lane 2-7, DNA product of SDSM using Phusion optimisation mix 1-6.

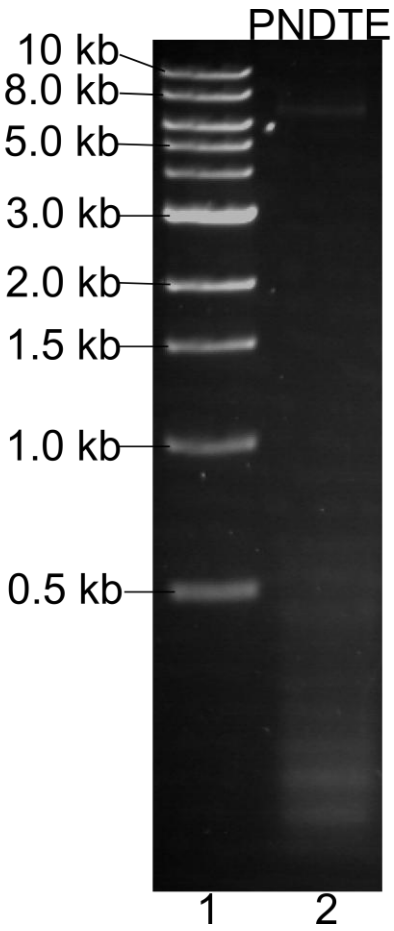

Figure 6.11 1% agarose gel separation of DNA product of SDSM reactions of pET-YSBLIC3C PpLAAO plasmid (6974 bp) using Phusion II HotStart polymerase and PNDTE primer set. Lane 1, 1 kb DNA ladder (0.5 kb, 1 kb, 1.5 kb, 2 kb, 3 kb, 4 kb, 5 kb, 6 kb, 8 kb, 10 kb); Lane 2, DNA product of SDSM using PCR mix C **(Table 2.3)** after digestion with *DpnI*.

Plasmid was purified from four of colonies from the library B transformation and the length of the gene insert was checked using PCR as in **Section 2.6.5**, using the wild-type pET-YSBLIC-3C-PpLAAO plasmid as a positive control. The PCR reaction to check the first plasmid failed to make any visible product. However, two of the remaining three plasmids had gene inserts that were longer than the wild-type plasmid (**Figure 6.12**), suggesting that the primer had been inserted into the new gene sequences, as had happened before with the library A reactions.

As the primer insertions could have been being caused by the polymerase incorporating sub-optimal primer pairings, the library B and C reactions were optimised using KOD HotStart polymerase as it is less efficient at staying bound to DNA than the Phusion polymerase is, due to a dsDNA binding domain that is fused to Phusion polymerases (http://www.finnzymes.com/pcr/phusion_products.html accessed 04/10/12), which may be allowing the Phusion polymerase bind to suboptimal primer pairing

. The optimisations were done as described in **Section 2.6.6** and both resulted in visible product at the expected 7 kb, but also a shorter product around 3 kb long (**Figure 6.13**).

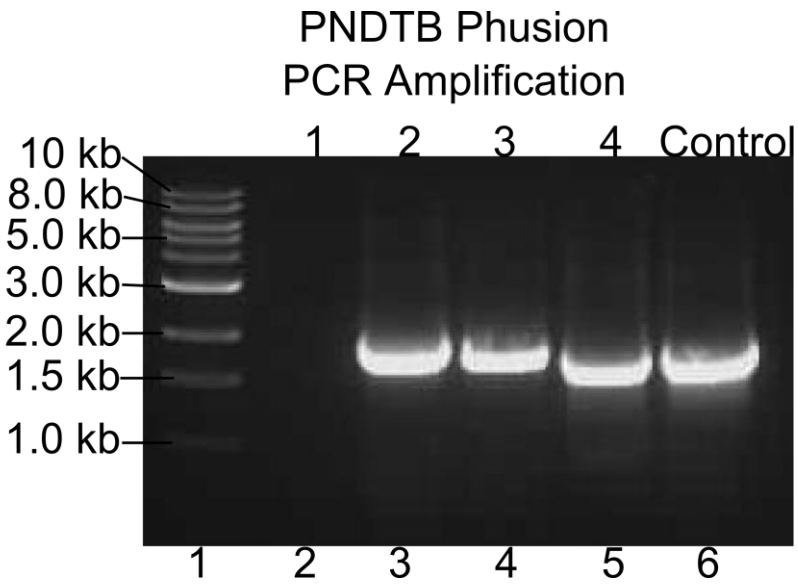

Figure 6.12 1% agarose gel separation of DNA from PCR amplification of plasmid inserts: Lane 1, 1 kb DNA ladder (0.5 kb, 1 kb, 1.5 kb, 2 kb, 3 kb, 4 kb, 5 kb, 6 kb, 8 kb, 10 kb); Lane 2-5, PCR amplification of insert sequence in pET-YSBLIC3C PNDTB Phsuion plasmids 1-4; Lane 6, PCR amplification of insert sequence in pET-YSBLIC3C PpLAAO plasmid (1605 bp).

Reaction condition 1 (**Section 2.6.6, Figure 6.13**) was repeated for both library B and C reactions, and the resulting product was digested using *DpnI* and used to transform electrocompetent *E. coli* Top10 cells. Unfortunately transformation with the library C PCR product did not result in any colonies. The library B product resulted in around 80 colonies, six of which were picked to have their plasmids purified as in **Section 2.6.6**. The length of the gene insert of these plasmids was checked using PCR as in **Section 2.6.6**, along with the wild-type pET-YSBLIC-3C-PpLAAO plasmid as a control.

Unfortunately, four of the six plasmids purified had inserts that were longer than that of the wild-type plasmid (**Figure 6.14**), with plasmids 1 and 2 appearing to have a roughly 2 kb long insert, which was larger than any of the plasmids made using the Phusion polymerase, which had roughly 1.7 kb long inserts at most. (**Figures 6.12, 6.14**).

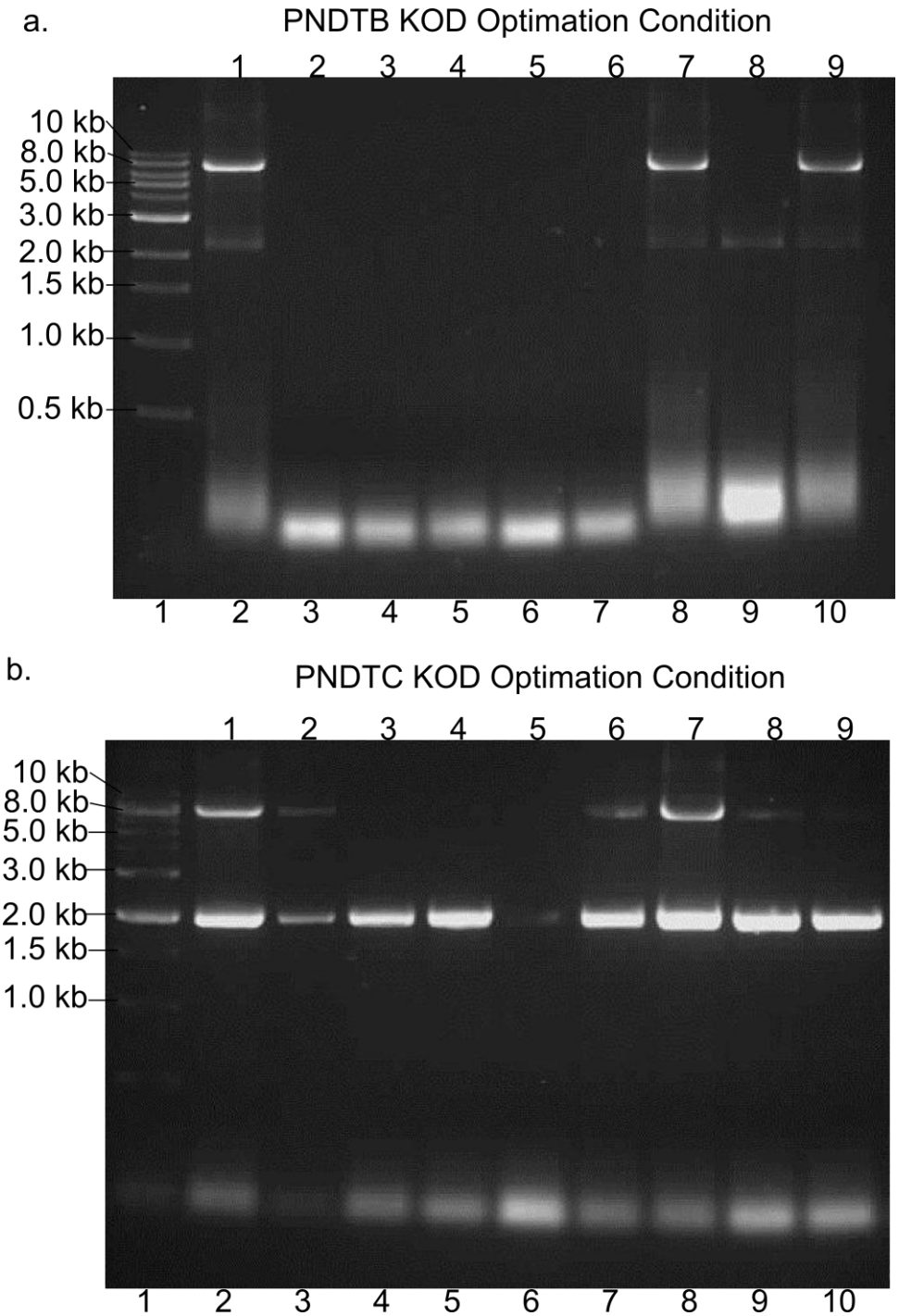

Figure 6.13 1% agarose gel separation of DNA product of SDSM reactions of pET-YSBLIC3C PpLAAO plasmid (6974 bp) using KOD HotStart polymerase with varying PCR mix conditions. **a.** SDSM QuikChange using PNDTB primer set. Lane 1, 1 kb DNA ladder (0.5 kb, 1 kb, 1.5 kb, 2 kb, 3 kb, 4 kb, 5 kb, 6 kb, 8 kb, 10 kb); Lane 2-9, DNA product of SDSM using KOD optimisation mix 1-9. **b.** SDSM QuikChange using PNDTC primer set. Lane 1, 1 kb DNA ladder (0.5kb, 1 kb, 1.5 kb, 2 kb, 3 kb, 4 kb, 5 kb, 6 kb, 8 kb, 10 kb); Lane 2, DNA product of SDSM using KOD optimisation mix 1; Lane 3, Blank lane containing overspill; Lane 4-10, DNA product of SDSM using KOD optimisation mix 3-9.

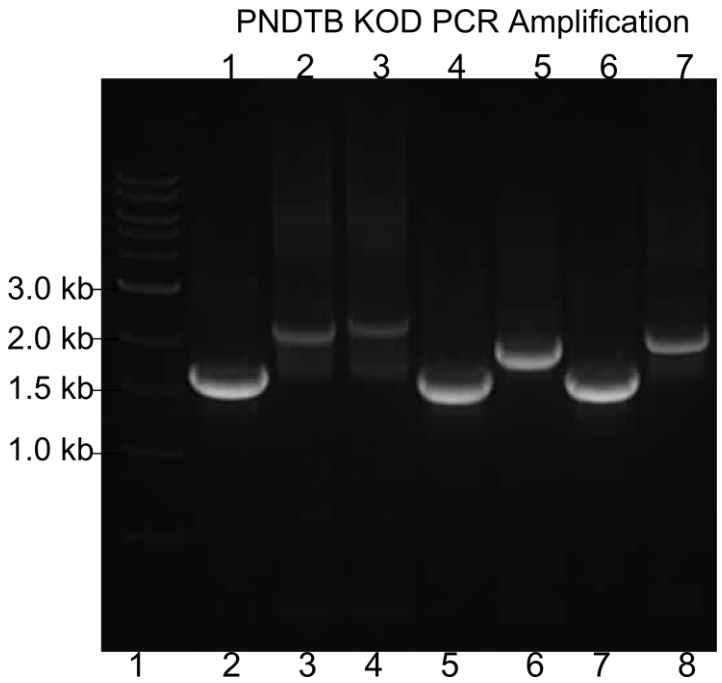

Figure 6.14 1% agarose gel separation of DNA from PCR amplification of plasmid inserts: Lane 1, 1 kb DNA ladder (0.5 kb, 1 kb, 1.5 kb, 2 kb, 3 kb, 4 kb, 5 kb, 6 kb, 8 kb, 10 kb); Lane 2, PCR amplification of insert sequence in pET-YSBLIC3C PpLAAO plasmid (1605 bp); Lane 3-8, PCR amplification of insert sequence in pET-YSBLIC3C PNDTB KOD plasmids 1-6.

6.2 Generation of PpLAAO epPCR library

In order to determine if mutations further away from the active site of the PpLAAO protein could have any effect on the substrate specificity of the enzyme, the pET-YSBLIC-3C-PpLAAO gene sequence was mutated using error prone PCR (epPCR), with a goal of between 2 and 7 mutations per gene sequence. This was done using the GeneMorph® II EZClone domain mutagenesis kit from Stratagene as in **Section 2.7**.

The PpLAAO gene sequence was amplified from the wild-type pET-YSBLIC-3C-PpLAAO plasmid using the error-prone polymerase MutaZyme II. 2.5 µL of the amplified megaprimer product was analysed on 1% agarose gel along with a 2.5 µL of a 20 ng μL^{-1}, 1.1 kb DNA standard provided in the kit. From observing the bands intensity, the megaprimer product was determined to be at least 50 ng μL^{-1} (**Figure 6.15a**), which was enough to necessitate using gel purification to obtain the megaprimer product. After analysis, the remaining epPCR product was run on a 1% agarose gel (**Figure 6.15b**) and the megaprimer band was cut out and purified used Sigma-Aldrich's GenElute Gel Purification kit (**Section 2.7**).

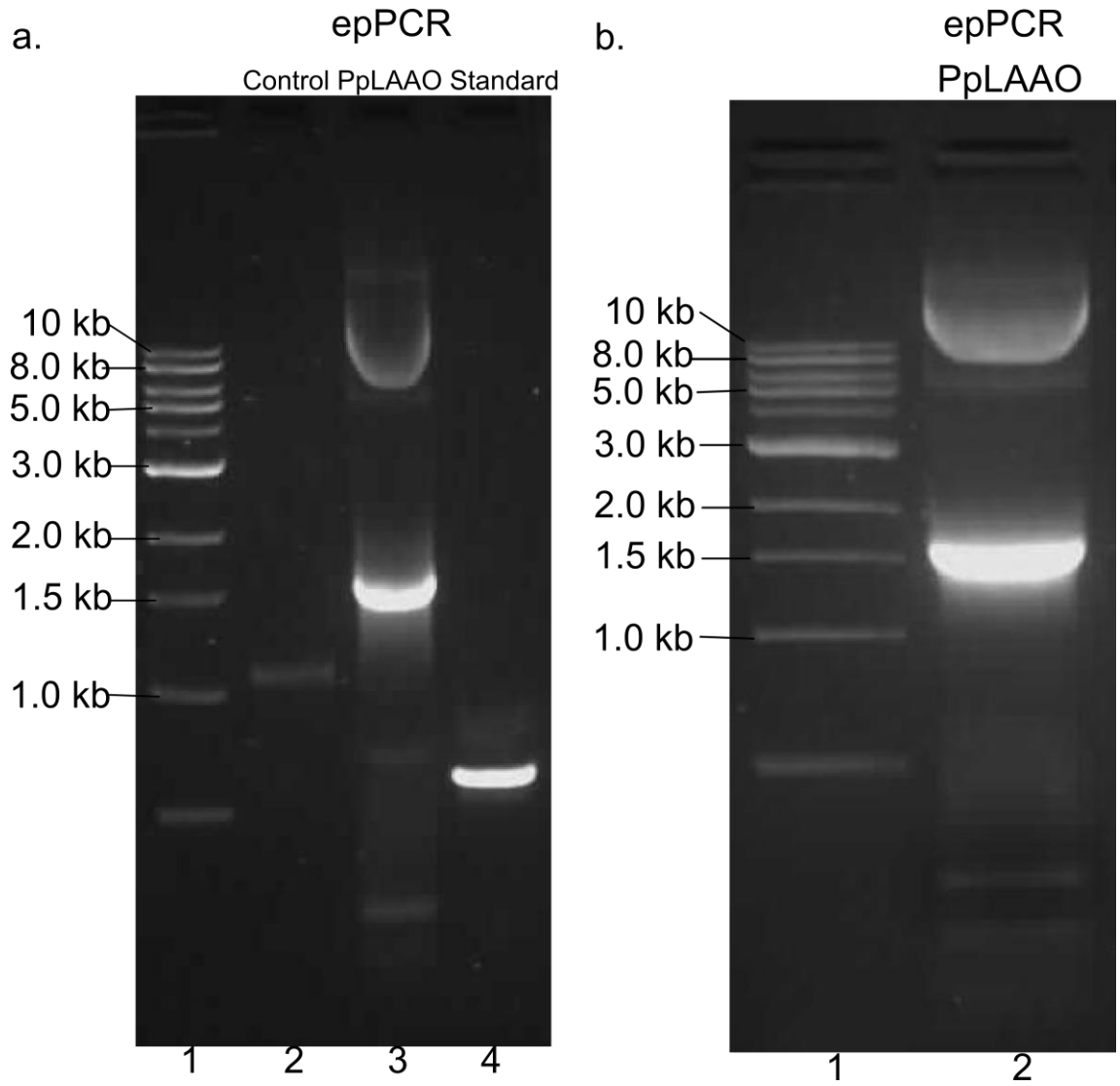

Figure 6.15 1% agarose gel electrophoresis of error-prone PCR products. **a.** 2.5 µL analysis of epPCR product: Lane 1, 1 kb DNA ladder (0.5 kb, 1 kb, 1.5 kb, 2 kb, 3 kb, 4 kb, 5 kb, 6 kb, 8 kb, 10 kb); Lane 2, 20 ng μL^{-1} DNA standard (1.1 kb); Lane 3, 2.5 µL of epPCR amplification of pET-YSBLIC-3C-PpLAAO gene sequence (1605 bp); Lane 4, epPCR amplification of positive control plasmid. **b.** Gel purification of epPCR product: Lane 1, 1 kb DNA ladder (0.5 kb, 1 kb, 1.5 kb, 2 kb, 3 kb, 4 kb, 5 kb, 6 kb, 8 kb, 10 kb); Lane 2, epPCR amplification of pET-YSBLIC-3C-PpLAAO gene sequence (1605 bp).

The mutated megaprimer product was incorporated into the pET-YSBLIC-3C-PpLAAO plasmid using the EZClone reaction mix and Stratagene's QuikChange method. The wild-type plasmid was digested with *DpnI* and the product was used to transform super-competent *E. coli* XL10-Gold cells. This resulted in over 4000 colonies. The colonies were scrubbed off the plates and pooled together, then mini-prepped to form a plasmid library, as in **Section 2.7**.

6.3 Screening of mutagenesis libraries

In order to screen them for activity, the mutagenesis libraries were used to transform competent *E. coli* DE3 cells, which were spread over plates containing 100 µM IPTG to induce gene overexpression. The resulting colonies were then transferred onto filter paper, which was frozen at -80°C overnight to lyse the cells and release the overexpressed protein. The cells were then allowed to soak up a HRP-based assay solution containing the target substrate and 3-diaminobenzidine, which in the presence of H_2O_2 is converted by HRP into an insoluble brown polymer, causing any colonies that produce enzymes with activity against the target substrate turn brown (**Section 2.8.1, Figure 2.4**).

6.3.1 Screening of PpLAAO CASTing library A

The PNDTA library was screened for activity against 20 mM L-aspartate, 1 mM, 2 mM, 4 mM, 10 mM and 20 mM LD-asparagine and 40 mM, 60 mM, 80 mM and 100 mM L-homoserine using the solid-phase HRP assay, as in **Section 2.8.1**, with screens being left to develop in the dark for 4 days.

No activity against L-aspartate was seen in any colonies, which was unsurprising as both the H351A and Y352A mutants showed very little activity against L-aspartate (**Section 5.4**), suggesting that these residues are important to the activity of the PpLAAO enzyme. One colony on the plate with 40 mM L-homoserine and two colonies on the plate with 2 mM LD-asparagine as substrate appeared to be slightly browner in colour than the other colonies on their plates. These colonies were named L-Hse-O, L-Asn-O1 and L-Asn-O2 and were picked and had plasmids purified and gene overexpression induced as in **Section 2.8.2**. The cells were lysed with BugBuster and the soluble fraction was separated by centrifugation, then the concentration of protein in the soluble cell fractions was measured using Bradford reagent as in **Section 2.8.2** (**Table 6.4**).

The activity of the soluble protein fractions was then tested against 20 mM L-aspartate, 20 mM LD-asparagine and 100 mM L-homoserine using the soluble HRP based plate assay as in **Section 2.8.2**, with the rate of change in absorbance and the end point of the assay after 1 hour being measured. Unfortunately no significant activity was seen from any of the soluble protein fractions (**Figure 6.16, Figure 6.17**), with the highest end point absorbance being the L-Hse-O fraction against L-aspartate with an absorbance of 0.0150 (**Figure 6.16**), which is less than 10% of the end-point absorbance of the wild-type PpLAAO soluble fraction against L-aspartate (**Figure 3.18**), suggesting that the brown colour seen in the solid phase assay was a false positive.

Table 6.4 Measured protein concentrations of soluble fractions of *E. coli* BL21-DE3 cells over expressing protein from PNDTA70 plasmids with potential target activity.

Sample Name		Reading 1/ ng mL^{-1}	Reading 2/ ng mL^{-1}	Reading 3/ ng mL^{-1}	Replica Average/ ng mL^{-1}	Sample Average/ ng mL^{-1}	Concentration of undiluted sample/ mg mL^{-1}
L-Hse-O / 1:10 dilution	Replica 1	471	481	480	477	499	4.9
	Replica 2	533	532	543	536		
	Replica 3	483	481	485	483		
LD-Asn-O1/ 1:10 dilution	Replica 1	471	471	489	477	402	4.0
	Replica 2	364	364	372	367		
	Replica 3	357	363	363	361		
LD-Asn-O2 / 1:10 dilution	Replica 1	311	308	314	311	326	3.2
	Replica 2	226	229	238	231		
	Replica 3	437	439	433	436		

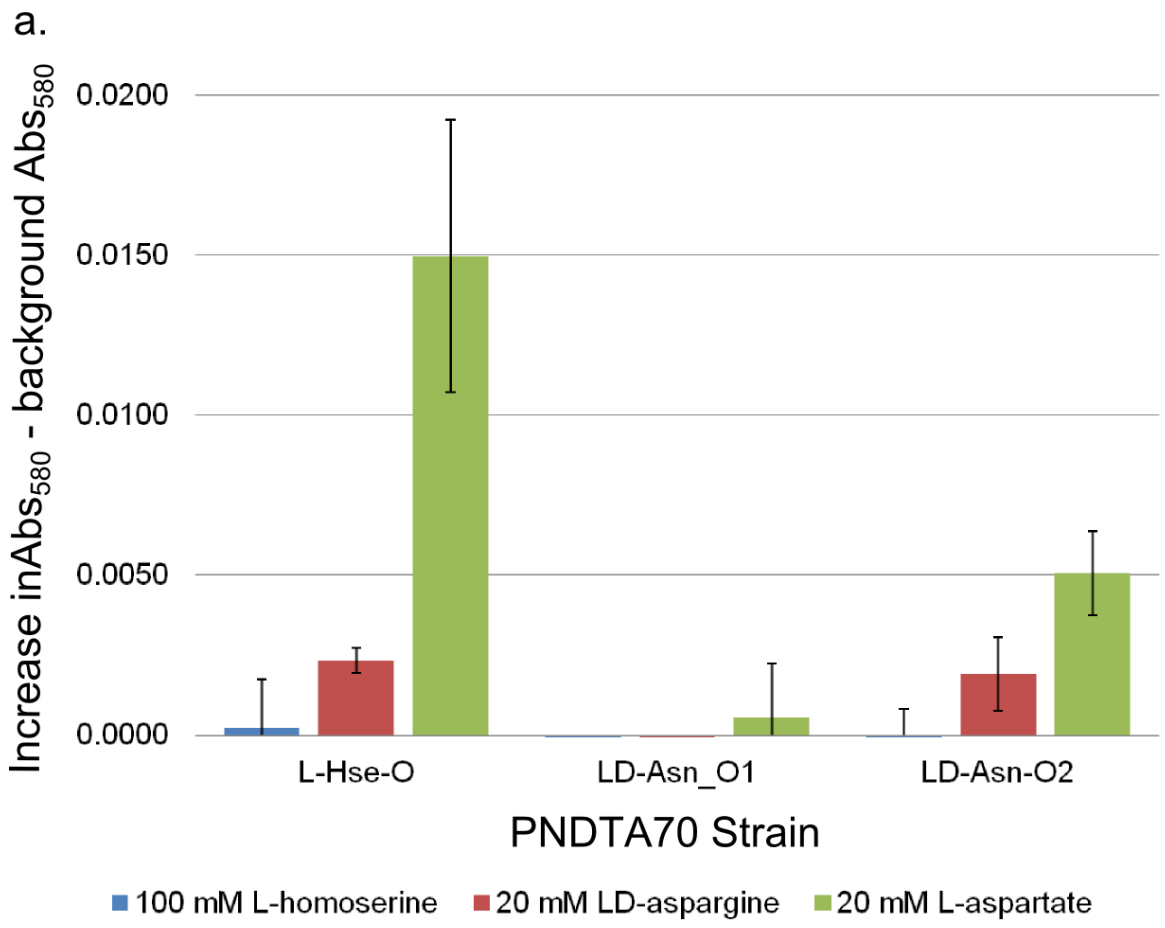

Figure 6.16 Graph of the 1 h end-point activity of L-Hse-O, LD-Asn-O1 and LD-Asn O2 soluble protein fraction against 100 mM L-homoserine (blue), 20 mM LD-asparagine (red) and 20 mM L-aspartate (green).

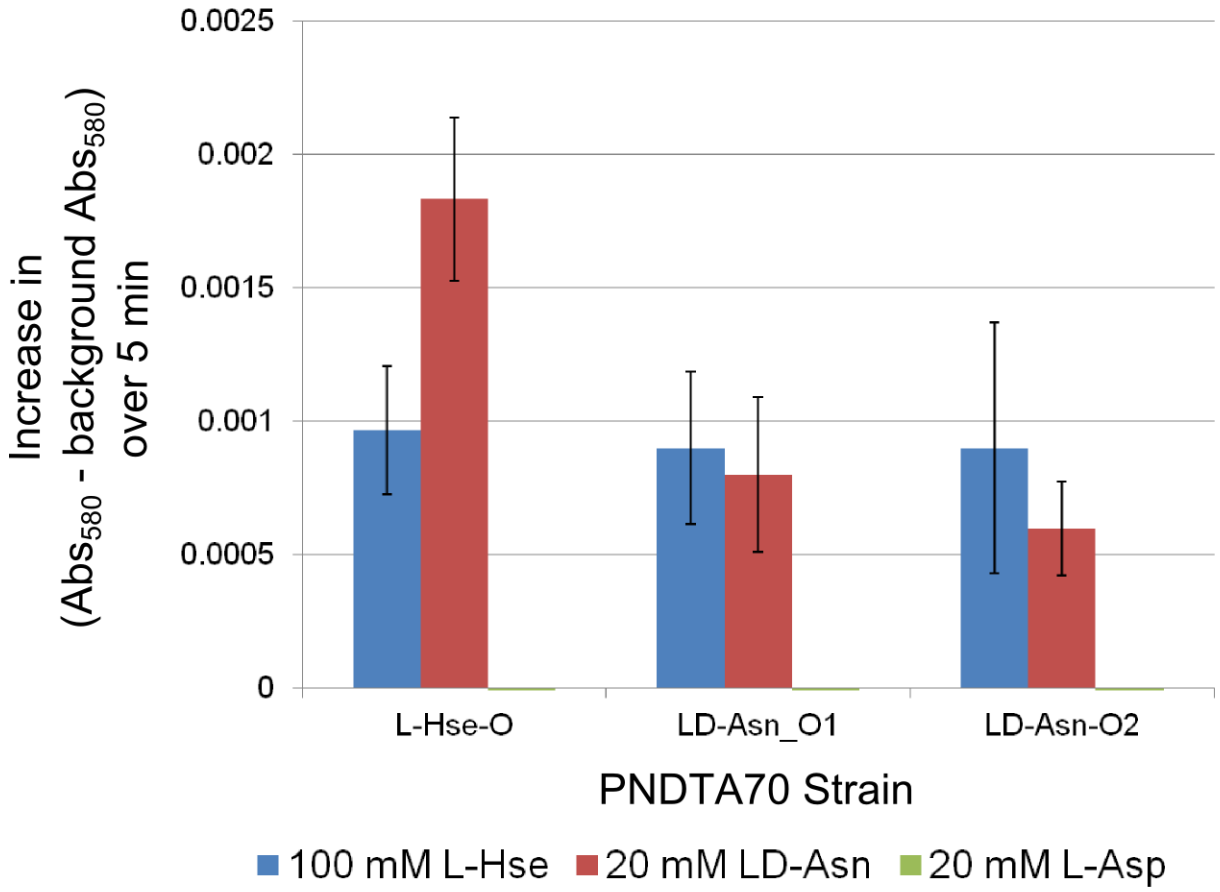

Figure 6.17 Graph of the rate of reaction of L-Hse-O, LD-Asn-O1 and LD-Asn O2 soluble protein fraction against 100 mM L-homoserine (blue), 20 mM LD-asparagine (red) and 20 mM L-aspartate (green) over 5 minutes.

6.3.2 Screening of PpLAAO CASTing library D

The PNDTD plasmid library was screened against 40 mM LD-aspartate, 100 mM L-homoserine, 100 mM L-alanine and 25 mM L-tyrosine using the solid-phase HRP assay, as in **Section 2.8.1**. Several colonies in each screen appeared to show activity against the substrates. Three colonies from the screen against LD-aspartate (**Figure 6.18**), seven colonies from the screen against L-homoserine (**Figure 6.19**), ten colonies from the screen against L-alanine (**Figure 6.20**) and five colonies from the screen against L-tyrosine (**Figure 6.21**) were picked and and had plasmids purified and gene overexpression induced as in **Section 2.8.3**, however the starter cultures for Asp3, H1, H7 and Tyr4 failed to grow.

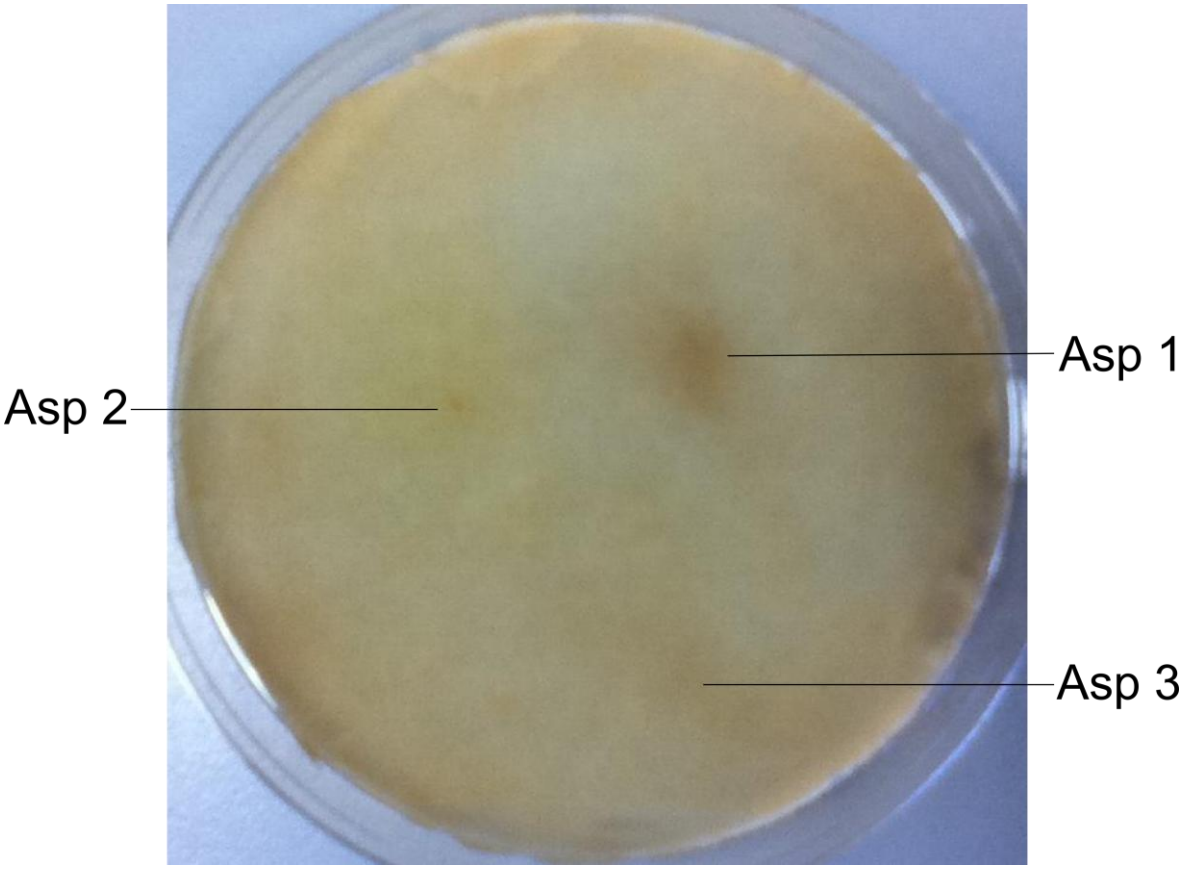

Figure 6.18. Solid phase HRP assay of PNDTD libraries against 40 mM LD-aspartate after 4 days development. Colonies that were picked for protein analysis are labelled.

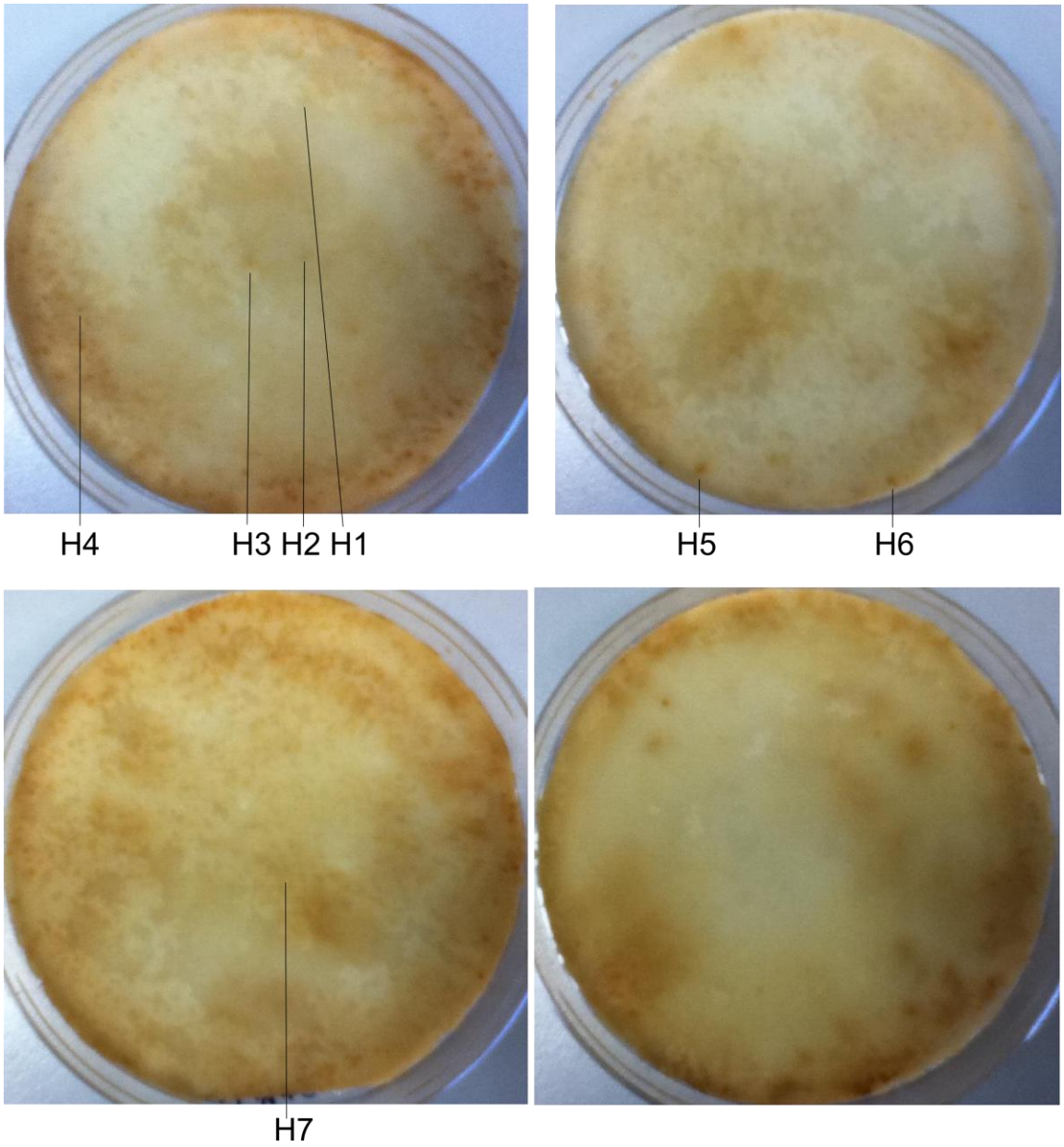

Figure 6.19. Solid phase HRP assay of PNDTD libraries against 100 mM L-homoserine after 4 days development. Colonies that were picked for protein analysis are labelled.

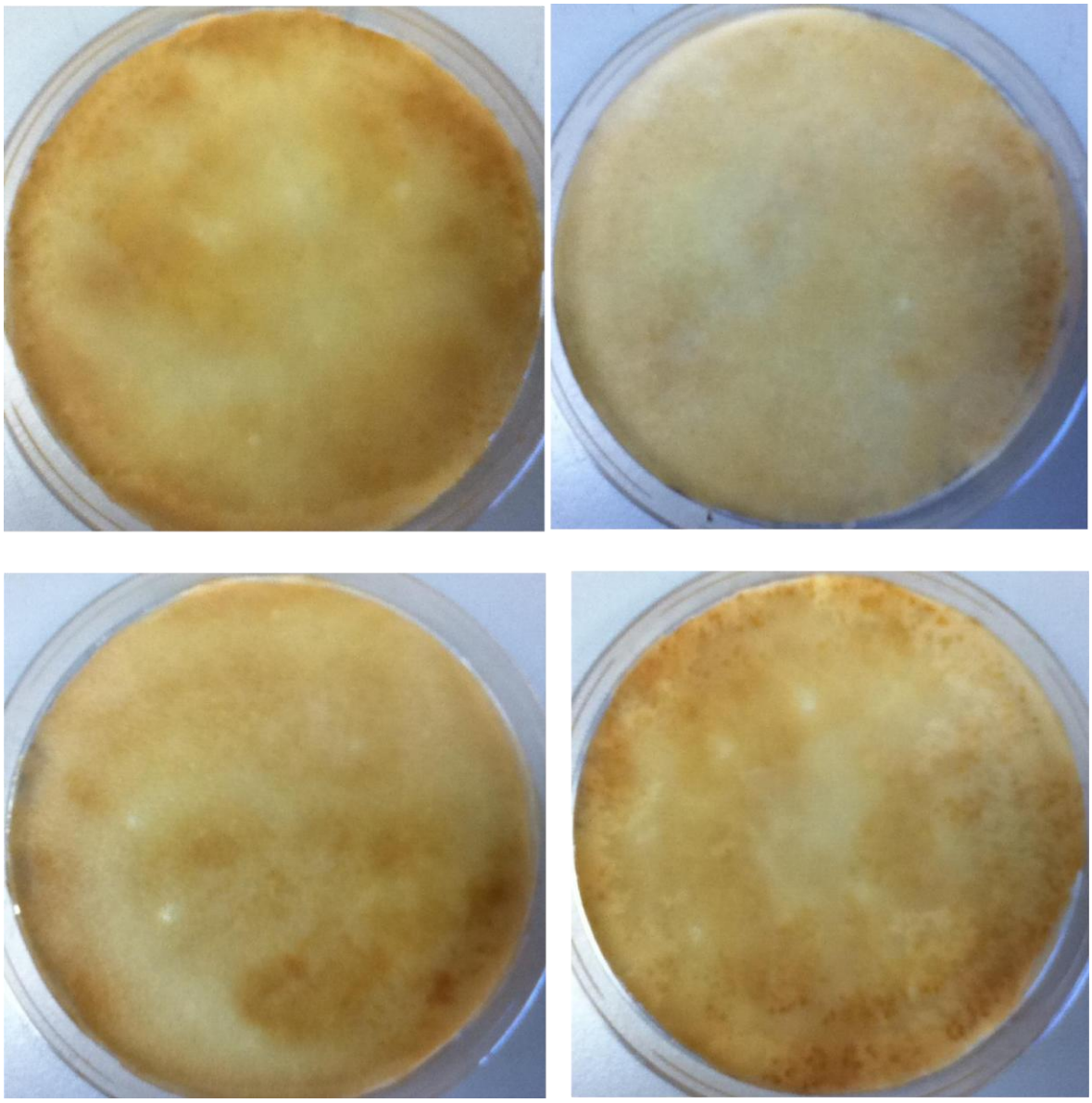

Figure 6.19. Solid phase HRP assay of PNDTD libraries against 100 mM L-homoserine after 4 days development. Colonies that were picked for protein analysis are labelled.

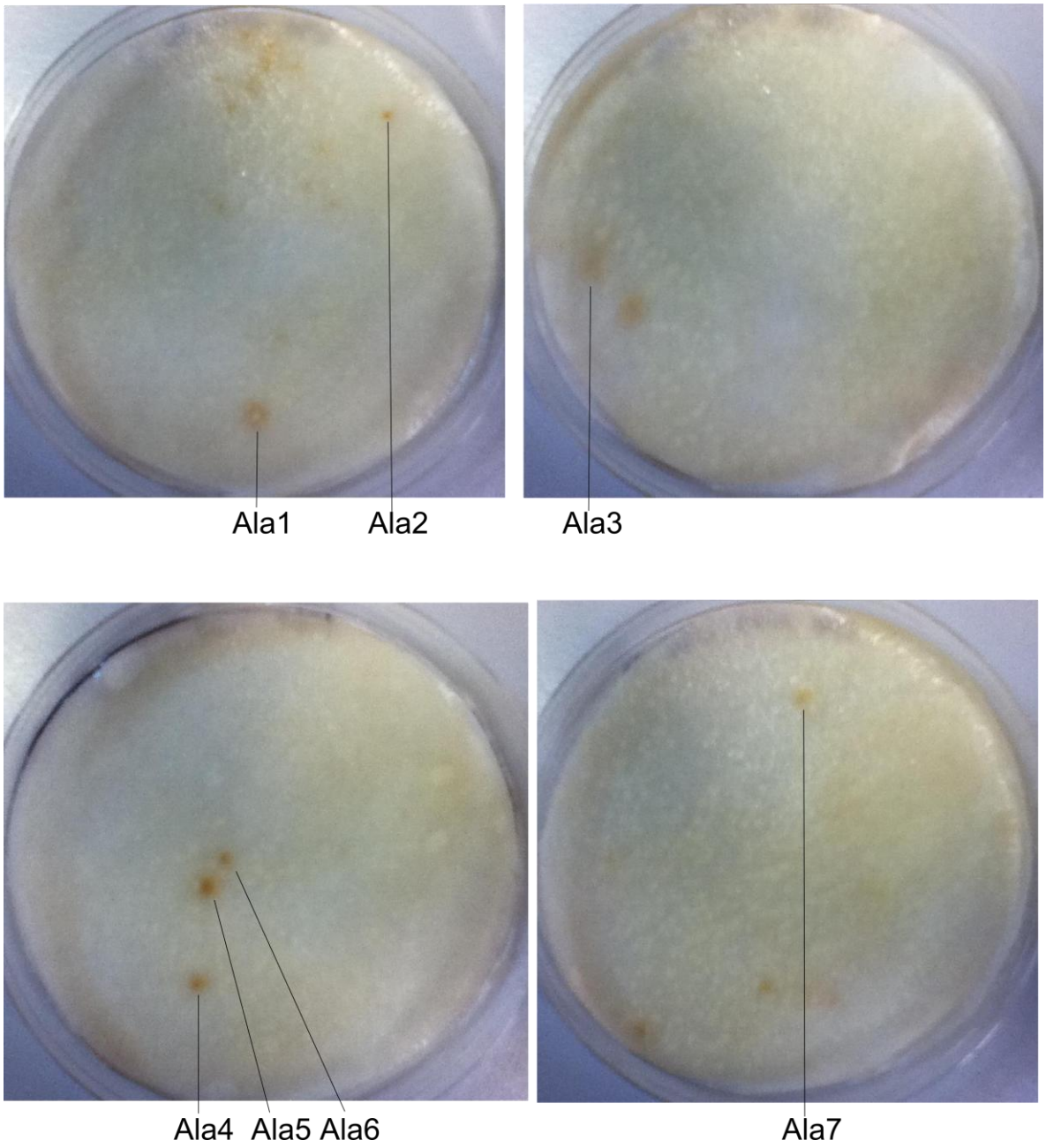

Figure 6.20 Solid phase HRP assay of PNDTD libraries against 100 mM L-alanine after 1 day of development. Colonies that were picked for protein analysis are labelled.

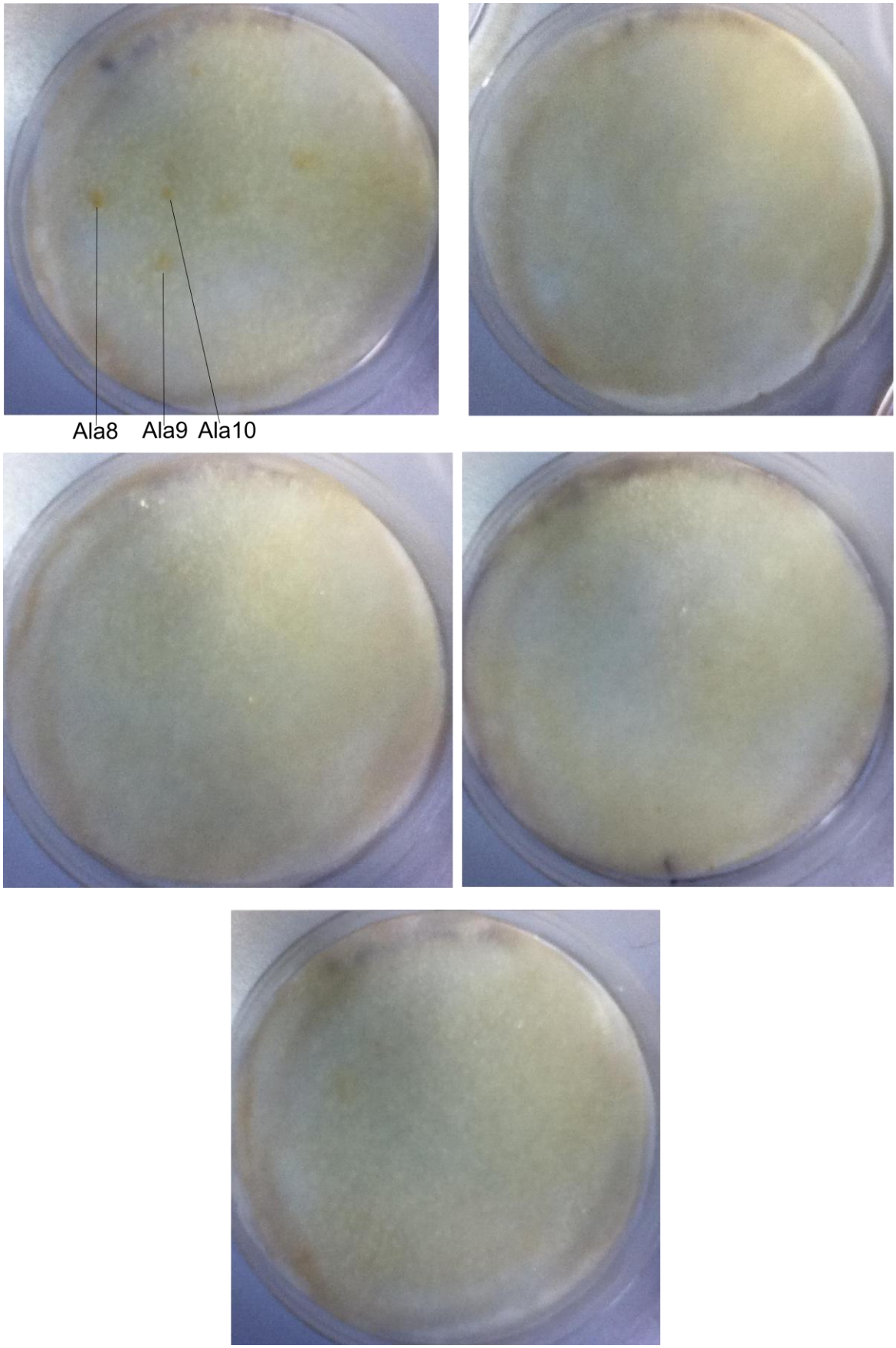

Figure 6.20 Solid phase HRP assay of PNDTD libraries against 100 mM L-alanine after 1 day of development. Colonies that were picked for protein analysis are labelled.

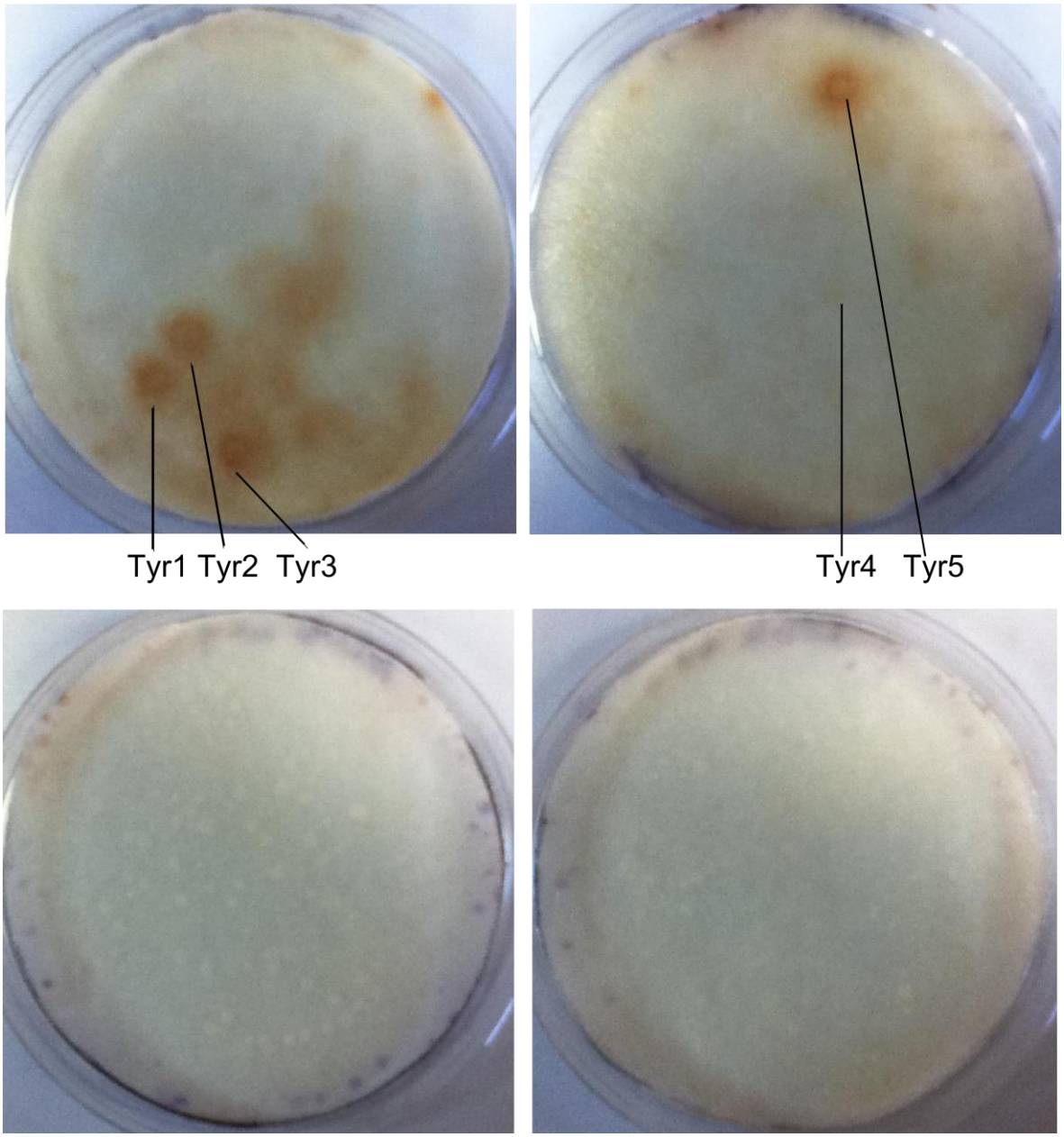

Figure 6.21. Solid phase HRP assay of PNDTD libraries against 25 mM L-tyrosine after 3 days of development. Colonies that were picked for protein analysis are labelled.

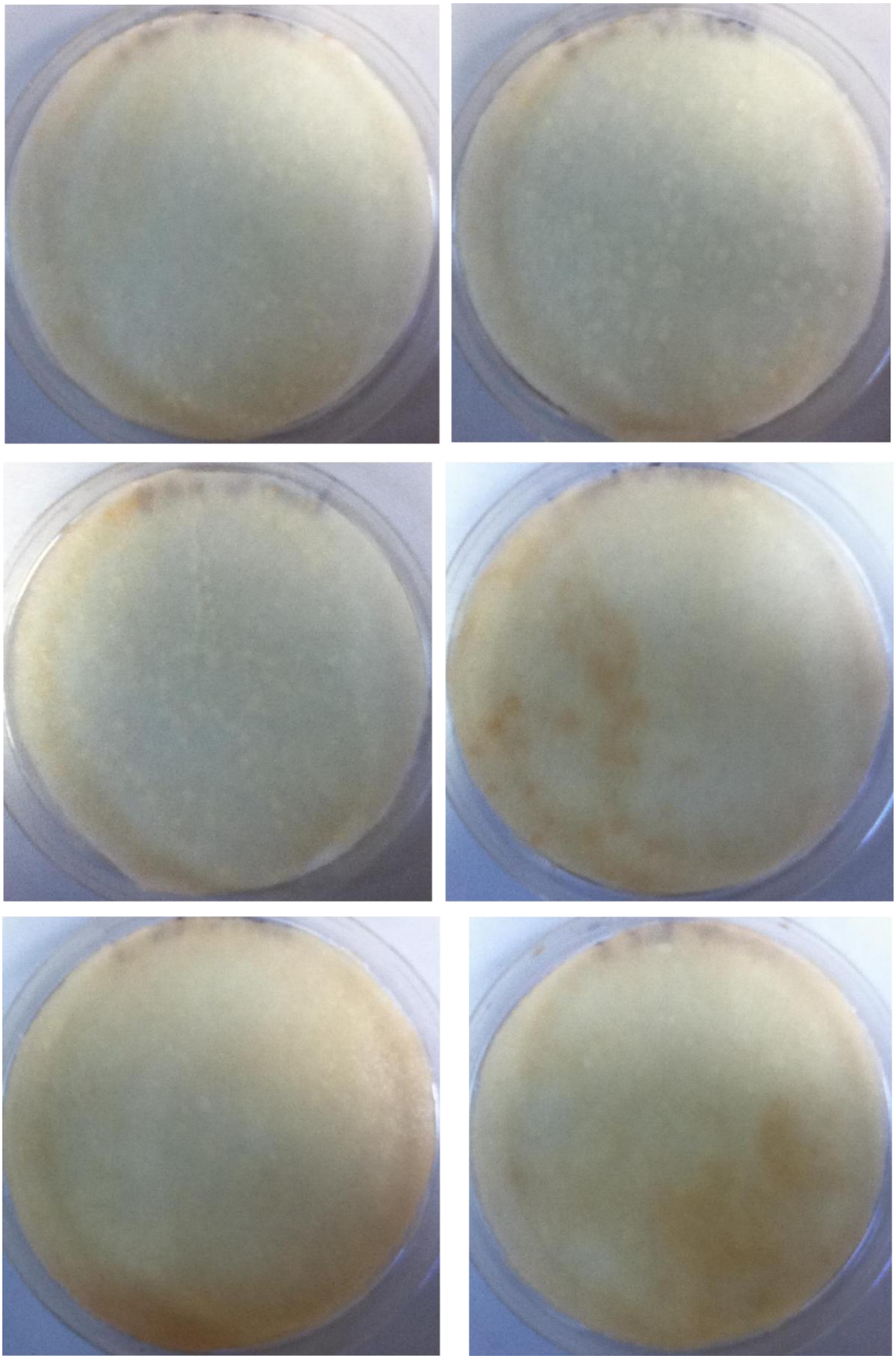

Figure 6.21. Solid phase HRP assay of PNDTD libraries against 25 mM L-tyrosine after 3 days of development. Colonies that were picked for protein analysis are labelled.

The induced cell pellets were lysed by sonication and analysed using 12% SDS-PAGE as in **Section 2.8.3**. Of all the strains only the Ala 3, Ala 5 and Ala 6 strains produced protein of the same size as the wild type PpLAAO protein. Ala 7 and Ala 9 appeared to produce a smaller protein, and the remaining strains failed to produce any proteins (**Figure 6.22**).

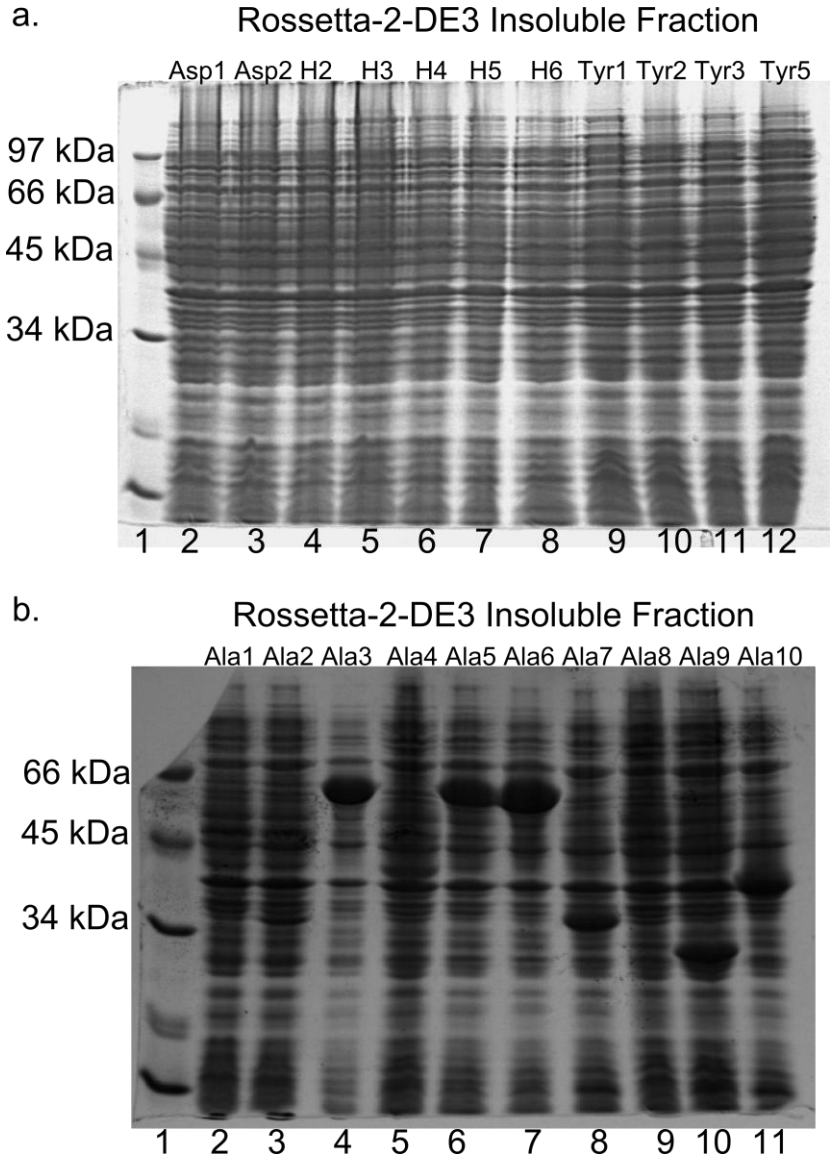

Figure 6.22. 12% SDS-PAGE separation of insoluble protein fractions of hits from the pET-YSBLIC3C-PNDTD library screening. **a.** Lane 1, low range molecular weight marker; Lane 2-3, pET-YSBLIC3C-PNDTD-Asp1-2 insoluble protein fractions; Lane 4-8, pET-YSBLIC3C-PNDTD-H2-6 insoluble protein fractions; Lane 9-12, pET-YSBLIC3C-PNDTD-Tyr1-3 and 5 insoluble protein fractions. **b.** Lane 1, low range molecular weight marker; Lane 2-11, pET-YSBLIC3C-PNDTD-Alal1-10 insoluble protein fractions.

The Ala3, Ala5 and Ala6 plasmids were purified by Miniprep and sent for sequencing, however none of the three had any changes from the wild-type PpLAAO, and further screening using the liquid phase assay showed no noticeable activity against L-alanine.

6.3.3 Screening of PpLAAO error-prone PCR mutants

The PpLAAO epPCR library was screened against 20 mM L-aspartate, 20 mM L-tyrosine, 20 mM L-alanine, 20 mM L-glutamate and 20 mM L-glutamine using the solid-phase HRP assay, as in **Section 2.8.1**. Screens were left to develop in the dark for 1 day. Roughly half of the colonies screened against L-aspartate developed a brown colour; however no colonies in the remaining screens showed any activity.

Five colonies from the screen against L-aspartate (referred to as PPM1-5) were picked and had plasmids purified and gene overexpression induced as in **Section 2.8.4**. Protein expression was analysed using 12% SDS-PAGE. PPM 3 produced a large amount of soluble protein. PPM 1 and 4 produced less soluble protein, PPM 2 produced very little soluble protein and PPM5 produced no soluble protein (**Figure 6.23**).

The purified plasmids were sent for sequencing, however only the pET-YSBLIC-3C-PPM2-4 plasmids sequenced successfully. There were 4 mutations in all and the distance of each mutated residue from the succinate occupying the active site of the *E. coli* L-aspartate oxidase structure solved by Bossi *et al*[65] was determined using the Coot Crystallographic model building software (**Section 2.8.4**).[113]

PPM2 had mutations in two residues, N216K and A504V. N216 is roughly 11.5 Å from the succinate C2 (**Table 6.5**) and is also quite close (3.5 Å) to the flavin part of the FAD molecule, with the mutated form potentially occupying the space that the flavin is in (**Figure 6.24**). This may account for the poor solubility of the protein. A504 is 24.15 Å from the succinate and does not appear to be affecting anything in the active site (**Table 6.5**, **Figure 6.24**), although the mutation could still be causing the enzyme to fold poorly, causing a drop in solubility.

PPM3 had a change in one residue- R121C, which is equivalent to the R120 residue in the *E. coli* L-aspartate oxidase structure. This residue is only 10.6 Å from the active site succinate (**Table 6.5**) and is next to the E121 residue, which is thought to form an ionic interaction with the α-amino group of the L-aspartate substrate in the *E. coli* LASPO.[64]

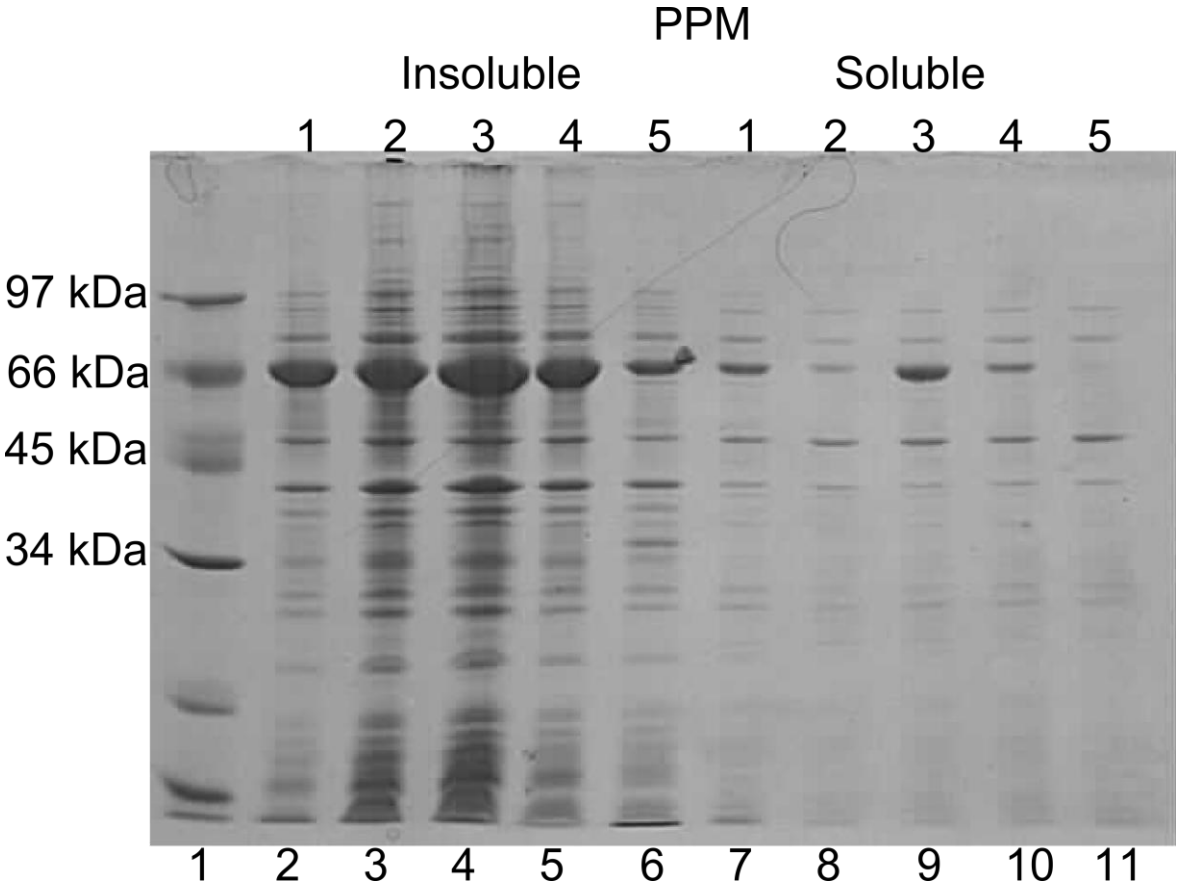

Figure 6.23. 12% SDS-PAGE separation of colonies from *E. coli* BL21-DE3 cells transformed with the error prone PCR products of the pET-YSBLIC3C-PpLAAO plasmid. Lane 1, low range molecular weight marker; Lane 2-6, pET-YSBLIC3C-PPM1-5 insoluble protein fractions; Lane 7-11, pET-YSBLIC3C-PPM1-5 soluble protein fractions.

Table 6.5 Summary of changes to PPM2-4 mutants and distance of affected residues from the succinate occupying the active site in the *E. coli* L-aspartate oxidase structure solved by Bossi *et al.*[65]

Mutant strain	Mutations	Equivalent residue in *E. coli*	Distance from succinate C2 in *E. coli* L-AspO (Å)	Solubility (**Figure 6.21**)	Activity vs. L-Asp
PPM2 (Blue)	N216K	N216	11.3	Low	None
	A504V	A504	24.1		
PPM3 (Red)	R121C	R120	10.6	High	Equivalent to wild type
PPM4 (Magenta)	R491H	R491	27.9	Medium	Lower than wild type

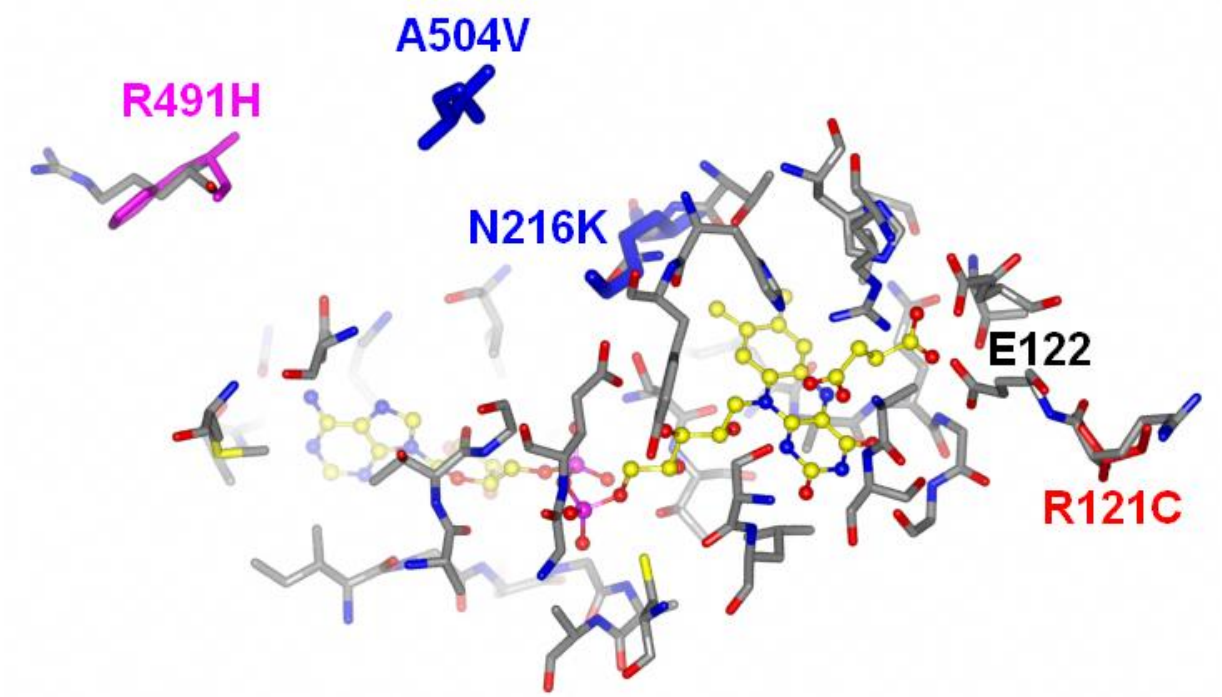

Figure 6.24 PPM2 (Blue), PPM 3 (Red) and PPM 4 (Magenta) mutated residues shown in context of the *E. coli* L-aspartate oxidase active site structure solved by Bossi *et al*.[65] Wild type residues are in grey, FAD and succinate are yellow.

The PPM4 strain had one mutation roughly 28 Å from the active site succinate, R491H. As arginine has a large side chain that is usually involved in several bonding interactions, it is likely that the change to the more compact histidine side chain has affected these bonds and caused the protein to be less soluble.

A quick test of the activity of each of the soluble protein fractions of PPM2-4 against L-aspartate was performed using the soluble HRP-based assay and visual inspection to roughly determine the level of assay development, as in **Section 2.8.4**. The levels of activity were proportional to the solubility of the strains, with PPM2 showing no activity, PPM4 showing lower levels of activity than the wild type protein and PPM3 showing levels of activity equivalent to the wild type PpLAAO soluble protein fraction (**Table 6.5**).

6.4 Conclusions

With the intention of introducing new substrate activities to the PpLAAO protein, particularly L-tyrosine and L-alanine *via* L-homoserine, attempts were made to mutate the PpLAAO gene sequence using an iterative CASTing approach[108] and error-prone PCR (epPCR).

For the iterative CASTing, the thirteen active site residues that were mutated into alanine in **Chapter 5** were split into five groups, each of which contained residues sequentially close enough to be mutated using one primer set. These residues were then mutated in groups using the NDT codon degeneracy, which codes for twelve chemically diverse side chains residues.

Group A contained H351 from the flavin binding domain and Y352, both of which caused a loss of activity when mutated into alanine (**Section 5.4**). A library of around 400 mutated PNDTA colonies was made despite some earlier problems with the mutagenic primers being incorporated into the newly formed plasmids and causing protein truncation. These problems were possibly caused by a 9 bp sequence that was repeated either side of the two residues that were to be mutated (**Table 2.3**) which possibly caused the complementary primers to bind to each other in long chains before being incorporated into the mutagenic primers. In order to discourage this mismatched binding, the annealing temperature was increased to 72°C, which appeared to resolve the problem.

When screened, no activity against L-aspartate was found in any of the PNDTA mutants, and although some colonies appeared to show a small amount of activity against L-asparagine and L-homoserine during the solid-phase screen, no activity could be seen in the liquid phase screen of the induced protein fractions of these strains.

This is not unexpected, as the H351A mutant lost the ability to bind FAD and showed no activity against L-aspartate (**Section 5.3**) and the Y352A mutant had drastically increased K_M against L-aspartate, although as both L-histidine and L-tyrosine were both possible side residues resulting from the NDT degeneracy, there should have been some transformants that had retained the wild-type residues. The lack of this activity shows that not all of the possible mutations had been covered by the PNDTA library. This could be due to chance, as the number of colonies made only guarantees 95% coverage of the all the potential mutations, however it could also mean that the problem with the primer insertions had not been resolved, and that some mutants were inactive due to the protein being truncated or insoluble.

The CASTing group B contained R290 from the capping domain, which showed no activity when mutated into alanine (**Section 5.4**), and V293, which caused a loss of protein stability when mutated into alanine (**Section 5.3**). Attempts to make a PNDTB library were started using PfU Turbo, Phusion and KOD HotStart polymerases. The PfU Turbo polymerase failed to produce any PCR product; however the Phusion and KOD polymerases products both produced a reasonable number of transformants after treatment with *DpnI*. Unfortunately, the transformants from the reactions using both Phusion and KOD polymerases contained plasmids with larger inserts than the

wild-type PpLAAO plasmid, most likely caused by the mutagenic primers being inserted into the newly formed plasmids as was seen in the PNDTA library.

In this case the PNDTB primers do not appear to have a particularly large repeated sequence, however the short sequence GCCC does appear on both sides of the mutagenic sequence of the forward primer, and another CCC sequence is found at the beginning of the forward primer, so these could be causing the primer to form long chains that are then incorporated into the newly formed primers. The longest difference between the PpLAAO wild-type and the PNDTB plasmids appeared to be higher on the plasmids produced using KOD polymerase that those produced using Phusion polymerase (**Figures 6.12, 6.14**) this could be because the higher fidelity Phusion polymerase was not allowing the primers to bind to each other quite as badly as the KOD polymerase was, so the inserted sections weren't able to grow as long as in the products made with KOD polymerase.

The CASTing group C contained R386, S389 and S391, all of which are part of the flavin binding domain of the *E. coli* L-AspO. The mutation of the R386 residue resulted in a loss of activity against L-aspartate. The mutation of S389 caused a slight decrease in catalytic activity and a six-fold increase in the K_M of L-aspartate and the mutation of S391 into alanine caused a slight increase in K_M and a five-fold decrease in the catalytic activity against L-aspartate. Unfortunately, despite attempts to produce a library using PfU Turbo, Phusion and KOD HotStart polymerases, the products of the QuikChange PCR reactions did not result in enough transformants to collect the 4000 transformants needed to ensure 95% coverage of all the potential combinations of mutations of the three targeted residues.

Group D contained Q242 from the flavin binding domain, H244 from the capping domain and P245, all of which resulted in an increase in the K_M of L-aspartate when mutated into alanine residues. Despite there being no obvious repeated or complementary sequences in the PNDTD primer set, some of the PCR products produced using Phusion polymerase still contained inserted primer sequences around the mutation site, however they appeared to be few in number so around 4000 mutated transformants were collected to form the PNDTD library.

This library was the screened against 20 mM L-aspartate, L-alanine, L-homoserine and L-tyrosine. For each substrate there were several colonies that developed positive results for activity against all of these substrates (**Figures 6.18-6.21**). However, when these colonies were grown and the insoluble and soluble protein fractions were analysed on SDS-PAGE, the strains that had shown activity against L-aspartate, L-homoserine and L-tyrosine all failed to produce any protein. Two of the strains that showed activity against L-alanine had produced truncated protein and another four

strains did not produce any protein, however sequencing of the plasmids from the three strains that expressed the correctly sized protein showed that they were expressing the wild-type PpLAAO protein, which did not show any activity detectable against L-alanine.

The reason that these colonies appeared to show activity in the solid phase screen is unclear. There may have been another protein expressed the *E. coli* cells in some cases that was causing a reaction against the targeted substrates, or causing a build-up of H_2O_2 for another reason. It is also possible that these colonies had been exposed to extra oxygen through air bubbles under the filter paper used to soak the colonies in the assay solution, which would cause the reaction buffer to develop more quickly, although care was taken not to allow air bubbles to form when the assay was being carried out.

Group E contained L257, T259 and E260, all from the capping domain of the *E. coli* L-AspO. The mutation of L257 into alanine caused a large increase in the K_M against L-aspartate and the mutation of T259 into alanine resulted in the loss of activity against L-aspartate. The E260A mutant was insoluble when expressed in *E. coli* BL21-DE3 cells. Unfortunately, despite attempts to produce a library using PfU Turbo and Phusion polymerases, the products of the QuikChange PCR reactions did not result in enough transformants to collect the 4000 transformants needed to ensure 95% coverage of all the potential combinations of mutations of the three targeted residues.

As the iterative CASTing approach was being hindered by the issues with primer insertions in the mutated plasmids and difficulty producing enough PCR product to generate large enough numbers of transformants to ensure effective coverage of all possible combinations of mutations for the groups targeting three active site residues, attempts to introduce new substrate activity to the PpLAAO protein using epPCR were started.

The epPCR was setup with a goal of between two and seven base pair substitutions per gene sequence. Over 4000 transformants were collected and used to prepare a plasmid library. When this library was screened roughly half of the colonies screened showed activity against 20 mM L-aspartate; however no colonies showed activity against 20 mM L-tyrosine, L-arginine, L-glutamate or L-glutamine. It is likely that the number of transformants collected for the library was far too low to stand a significant chance of containing a mutant that would show significant activity against a new substrate, however collecting the number of transformants needed (generally between 1,000-1,000,000, but possibly as high as 1,000,000,000)[107] was beyond the scope of what would be practical to do on benchtop without a greater amount of automation available.

Five of the colonies from the screen against L-aspartate were picked and the plasmids were purified and sequenced to determine how effective the mutation had been, however only three of these plasmids (PPM2-4) were sequenced successfully. The PPM2 mutant had mutations in two amino acid residues, N216K and A504V, and had poor solubility and showed no detectable activity against L-aspartate. This lack of activity is consistent with the *E. coli* L-aspartate structure, as the N216 residue is close to the flavin ring of FAD (roughly 3.5 Å) and as lysine is a larger residue than asparagine, the mutation is likely to disrupt the positioning of the flavin ring, which is important to the catalytic activity of the oxidase (**Chapter 5**).[121]

PPM3 had one mutation, R121C, which is equivalent to the R120 residue in the *E. coli* L-AspO structure. Despite it being next to the E122 (E121 in *E. coli*) residue, which is thought to form an ionic interaction with the α-amino group of the L-aspartate substrate,[64] the R121C mutation does not appear to have affected the solubility or the activity of the protein against L-aspartate. This may be due to the fact that the R121 residue side chain extends away from the L-aspartate substrate in the *E. coli* L-AspO structure (**Figure 6.24**).[65]

PPM4 also had one mutation, R491H. The R491 residue is situated away from the active site area, roughly 27 Å from the succinate substrate in the *E. coli* L-AspO structure.[65] The mutant appears to cause a slight drop in solubility and the soluble protein fraction shows less activity than the wild-type PpLAAO protein, however this may be due to the reduction in soluble protein available in the solution as opposed to a reduction in catalytic efficiency. The cause for the lack of solubility is unclear; however it may be due to the replacement of the relatively long and thin arginine side chain with the shorter and wider histidine, which may affect the interactions of the residues around the mutation and cause a disruption in the folding of the protein.

Unfortunately, the attempts to introduce new substrate specificities to the PpLAAO protein using the less labour-intensive CASTing method were hindered by problems caused by unwanted copies of the primer sequences being inserted into the newly generated mutants, causing an unknown proportion of the generated mutants to be inactive. Although the epPCR worked, despite there being fewer mutations per gene sequence than expected (1-2 mutations per gene sequence, as opposed to 2-7), the number of mutants that would have to be generated in order to find one that showed detectable activity against a new substrate would be too large to consider preparing on a benchtop laboratory setup, particularly as the colony screen would be difficult to perform in an automated fashion.

If it was possible to reduce the amount of the primer insertions, the SDSM CASTing method would be a useful way to attempt directed evolution against the PpLAAO protein, and more work would

be useful in determining the cause of the primer insertions. It is possible that the use of DMSO in the PCR reaction to increase the amount of PCR product was also facilitating the poor binding of the primers that was causing them to be incorporated into the mutagenic primers, so attempting to optimize the PCR reaction without using DMSO, possibly by using betaine instead, may be a useful place to start investigating this issue.

Another issue may be that the disruption to the active site caused by mutating several active site residues at one time may knocking out the enzymes activity completely, rather than just changing it. It may be more effective to either use SDSM on one residue at a time, or to target residues further away from the active site in order to fine tune the structure of the enzyme, rather than disrupting it.

Chapter 7 General Discussion

Amino acid oxidases have a variety of roles in Nature and several potential uses as biocatalysts, enzymatic biosensors and potential medical therapies. For use as biocatalysts, it would be useful to find or develop amino acid oxidases with activity against a variety of different amino acids. However, for use in biosensors for amino acids it would be optimal to develop a variety of different amino acid oxidases, each with strong substrate specificity for a different amino acid to minimise the amount of false readings caused by other amino acids in the sample.

Seven target oxidases were selected from the results of a BLAST search using the sequence of the L-amino acid oxidase from *Synechococcus* sp. strain ATCC 27144. These were cloned into the pET-YSBLIC-3C expression vector for expression in *E. coli* expression cell strains and screened against L-amino acid substrates (**Chapter 3**). The L-amino acid oxidase from *Pseudomonas putida* (PpLAAO) was highly soluble, easily purified and showed strong substrate specificity against L-aspartate and L-asparagine, with a very low level of activity against L-glutamate (**Chapter 4**).

A greater understanding of the structure of the active site area of the protein would be beneficial for determining a strategy for directed evolution of the protein using site-directed mutagenesis. However, attempts to solve the structure of the PpLAAO protein by X-ray crystallography were unsuccessful due to the protein appearing to form several different quaternary structures in solution. Because of this the solved structure of a homologous L-aspartate oxidase from *E. coli* (L-AspO) was used to identify potential active site residues of the PpLAAO protein. These active site residues were analysed by alanine scanning in **Chapter 5**, as the residues were each mutated to alanine in turn and the resulting purified protein was assayed for activity against L-aspartate, L-asparagine and L-glutamate.

The results of this mutational analysis were largely consistent with the knowledge of the active site structure of the L-AspO protein. Mutation of residues involved in the binding of the C1 carboxylate (H244 and T259) and the C4 carboxylate (H351 and S389) resulted in an increase in the K_M against L-aspartate. Mutation of P245 and L257 residues, found close to the H244 side chain, also caused a decrease in the binding efficiency of the protein against L-aspartate. Interestingly, the S389A mutant showed higher binding efficiency against L-glutamate than the wild-type protein, although the catalytic activity of the protein was decreased. This may suggest that this residue could be a potential target for site directed mutagenesis when attempting to change substrate specificity.

Mutation of the R290 residue, thought to be involved in abstraction of the α-proton from L-aspartate, caused a decrease in the k_{cat} of the protein against L-aspartate, as did mutation of the Q242 residue, which appears to hold the R290 side chain in place. The S391A mutation also caused a greater decrease in catalytic activity than in binding efficiency, probably because the S391 side chain forms bonds with the flavin ring of FAD, so mutation is likely to cause a disruption in cofactor binding. The binding of FAD was also disrupted by the H351A mutation in both the L-AspO and PpLAAO proteins.

As the PpLAAO protein appeared to be consistent with the active site structure of the L-AspO protein, the L-AspO structure was used to develop an iterative CASTing strategy around the active site residues for the directed evolution of the PpLAAO protein, unfortunately only two of the five initially planned libraries was created, due to problems caused by primer insertions described in **Chapter 6**.

A small scale random mutagenesis attempt was performed using epPCR to introduce mutations into the gene. This library and the successful CASTing libraries were screened for activity against target substrates L-homoserine, L-alanine and L-tyrosine. However, none of the transformants from either mutagenesis attempt showed any novel substrate activity.

The PpLAAO protein could potentially have practical use as part of an enzymatic biosensor for L-aspartate, as current L-aspartate biosensors use a combination of L-glutamate oxidase and an aspartate aminotransferase and require L-glutamate in the sample to be removed prior to use, whereas the PpLAAO protein has very poor activity against L-glutamate.

For future work on this protein, a greater and more conclusive understanding of its structure would be of use. Because of this generating crystals for X-ray diffraction would be useful. As seen in **Chapter 4** it may be possible to force the protein into a single monomer form using protein precipitates like guanidine hydrochloride, therefore a screen of the effects of a variety of precipitates against the purified protein, both in pure form or as part of the crystal screen, may help towards the crystallisation of the PpLAAO protein.

Directed evolution of novel substrate specificity into PpLAAO would also be a priority. A larger scale random mutagenesis library may produce mutants with activity against target substrates, or maybe greater activity against L-asparagine or L-glutamate. Alternatively, production of the CASTing libraries using a different mutagenesis method, such as the In-fusion method developed by Clontech, may result in more reliable libraries without the proportion of truncated mutants found when screening in **Chapter 6**.

Otherwise site-directed saturation mutagenesis could be used to investigate the effects of single active site residues in greater detail. As the S389A mutation appeared to increase the binding efficiency of L-glutamate compared to the wild-type, a library of S389 mutants may also house novel substrate activity, screening of these mutants could also be done using a more sensitive oxidase assay, such as the *o*-dianisidine assay used by Tedeschi *et al*., in order to determine less drastic changes in catalytic activity and substrate binding.

An assay based on using HPLC of the reaction to determine the levels of product produced directly or using fluorescence of the FAD to determine cofactor turnover would have been useful in determining kinetic constants and the optimal temperature and pH of the protein, as they would not be reliant on a separate enzyme that may be affecting the results of the assay.

Other work towards identifying an L-AAO with activity against either L-alanine or L-tyrosine could include cloning more potential L-AAOs in the hope of finding more soluble targets, or using 8M Urea to unfold some of the more insoluble products in order to purify and then refold and investigate them in more detail.

Appendix A *C. glutamicum* as an expression strain

A.1 Introduction

A.1.1 Physiology of *C. glutamicum*

Corynebacterium glutamicum is a non-pathogenic and non-spore-forming[122] member of the *Corynebacterineae*, a Gram-positive group of bacteria that are defined by the presence of mycolic acids in their cell envelope structures. This group also includes the *Mycobacterium* and *Nocardia* genera.[123]

The unique *Corynebacterineae* cell envelope structural organisation is close to that of a Gram-negative bacteria. This cell envelope consists of an arabinogalactan-peptidoglycan polymer, which is covalently linked to an outer lipid layer that mostly contains mycolic acids, which are collectively known as the MAP polymer complex.[123] *C. glutamicum* also has a crystalline single-protein surface layer consisting of hexameric cores of PS2, a 52 kDa protein coded by the *cspB* gene.[124] This PS2 S-layer is anchored to the cell wall by a hydrophobic C-terminal domain and is very resistant to treatment with proteases and detergent,[125] although how much of the cell is covered by the S-layer is dependent on the carbon source and growth conditions of the bacteria.[126]

C. glutamicum, like other *Corynebacterineae* members, has a GC-rich codon content compared to another model bacteria *E. coli* (67% and 51% respectively), and the GC-wobble-position content is much higher in *C. glutamicum* than in *E. coli* (88% and 55% respectively).[127]

A.1.2 History of *C. glutamicum* in the biochemical industry

The first industrial application using the soil bacterium *Corynebacterium glutamicum* was the production of the amino acid L-glutamic acid by fermentation. This process originated in Japan in 1957 after Kinoshita *et al.* discovered that in certain conditions the bacterium could be made to secrete large quantities of L-glutamic acid, which is used as an important food additive and had previously been produced by hydrolysis of soy or other plant proteins.[128]

Later, in the 1970s, random mutagenesis was used to create variant strains of *C. glutamicum* that were capable of efficiently producing L-lysine and L-threonine, and further advances in molecular biology allowed more efficient L-lysine and L-threonine producing strains, as well as strains used to produce other amino acids and vitamins such as diaminopentane.[129]

A.1.3 Use of *C. glutamicum* in protein production and biotransformations

C. glutamicum is considered an attractive microorganism for biocatalysis reactions, due to its high cofactor regeneration rate,[130] as well as the S-layer and mycomembranes of the cell envelope structures, which allows the bacterium to be stable in organic compounds.[123] *C. glutamicum* is also non-pathogenic, has no spore forming abilities and its products can be considered to be food-grade,[128] making it more convenient for use in industry and GMP applications than other, less safe, microorganisms. The GC-rich codon usage compared to *E. coli*[127] may also make it a better producer of proteins from related GC-rich bacteria such as those in the *Nocardia* and *Mycobacterium* genera.[128]

Because of this, there have been many genetic tools and methods developed for *C. glutamicum* transformation and protein production, such as plasmid vectors[131] and methods for the transformation of *C. glutamicum* by electroporation,[132] as it has no natural DNA uptake system.[128] And although *C. glutamicum* is often grown in media containing animal based brain-heart infusion media (BHI),[130, 132] growth and transformations have been shown using LB-media,[133, 134] which is cheaper and more acceptable in industry and GMP applications which discourage the use of animal-based products.

A.1.4 Use of *C. glutamicum* for expression of previous gene targets

As three of the unstudied target gene sequences originally cloned into pET-YSBLIC-3C; the *Anabeana* sp. strain PCC 7120 (AsAAO), the *Bacillus anthracis* Amine Oxidase (BaAO) and the *Nocardia farcinica* oxidoreductase (NfOR); failed to produce soluble protein when expressed in several *E. coli* expression strains (**Chapter 3**), it was thought that expressing the genes in a different expression species, like *C. glutamicum*, may result in more soluble protein production, especially with in the case of NfOR, which is from a genus related to *C. glutamicum*.[123]

To allow for easier cloning procedures, the pEKEx2 shuttle vector[131] was selected as the vector for the target gene sequences, as it is accepted and replicated in both *E. coli* and *C. glutamicum*, allowing for the cloning of the vector to be carried out using high transformation efficiency *E. coli* strains, which were more simple to transform than the *C. glutamicum* strain.

A.2 Results

A.2.1 Attempts to clone AsAAO, BaAO and NfOR sequences into pEK-Ex2 shuttle vector

The pEK-Ex2 *E. coli/ C. glutamicum* shuttle vector was prepared using Miniprep and digested with relevant restriction endonucleases as in **Section A.4.2**. Due to the lack of a ribosome binding site in the pEKEx2 plasmid, amplification primers for the AsAAO, BaAO and NfOR gene sequences were all designed to contain the ribosome binding sequence AAGGAGATATAGAT seven bases upstream of the starting codon ATG, as done by Doo *et al.*.[130] The AsAAO, BaAO and NfOR gene sequences were amplified from the pET-YSBLIC3C-AsAAO, pET-YSBLIC3C-BaAO and pET-YSBLIC3C-NfOR plasmids, respectively, using KOD polymerase as in **Section A.4.3**. Attempts to ligate the amplified gene sequences to the pEK-EX2 shuttle vector were carried out as in **Section A.4.4**. Transformation of *E. coli* Top10 electrocompetent cells with the ligation mixed resulted in 5 colonies from the pEK-Ex2-BaAO reaction and 2 from the pEK-Ex2-NfOR reaction. The pEK-Ex2-AsAAO reaction did not result in any colonies.

Plasmid was purified from each of the colonies using Sigma-Aldrich's GenElute plasmid Miniprep kit, and the size of the gene inserts was checked by PCR as in **Section A.4.4** (**Figure A.1**). Based on the results of this gel, pEK-NfOR-2 and pEK-BaAO-5 were sent for sequencing at the University of York Genomics department. pEK-NfOR-2 had ligated successfully with the correct gene sequence, however the pEK-BaAO-5 plasmid contained a different gene sequence from the BaAO gene.

A.2.2 Transformation and expression of pEKEx2-NfOR plasmid

Following a protocol used by Liebl *et al.*,[132] competent *C.glutamicum* cells were prepared by growth at a low temperature, followed by several washes using ice-cold 10% glycerol as in **Section A.4.5** and both the non recombinant pEKEX2 and the pEKEx2-NfOR plasmid was used to transform these competent cells using electroporation followed by heat shock, as in **Section A.4.6**. Translucent colonies grew after 2-3 days and were then used to innoculate a 5 mL LB culture, which was grown and had gene overexpression induced as in **Section A.4.7**. The induced cells were harvested by centrifugation and sonicated in an attempt to split open the *C. glutamicum* cells and analyse the resulting protein. Soluble and insoluble fractions were analysed using 12% SDS-PAGE, however very little protein was seen in either the insoluble or soluble fractions of the induced cells, and there was no noticeable protein production in the cells transformed with the pEKEx2-NfOR plasmid compared to the cells transformed with non recombinant pEKEx2 plasmid (**Figure A.2**).

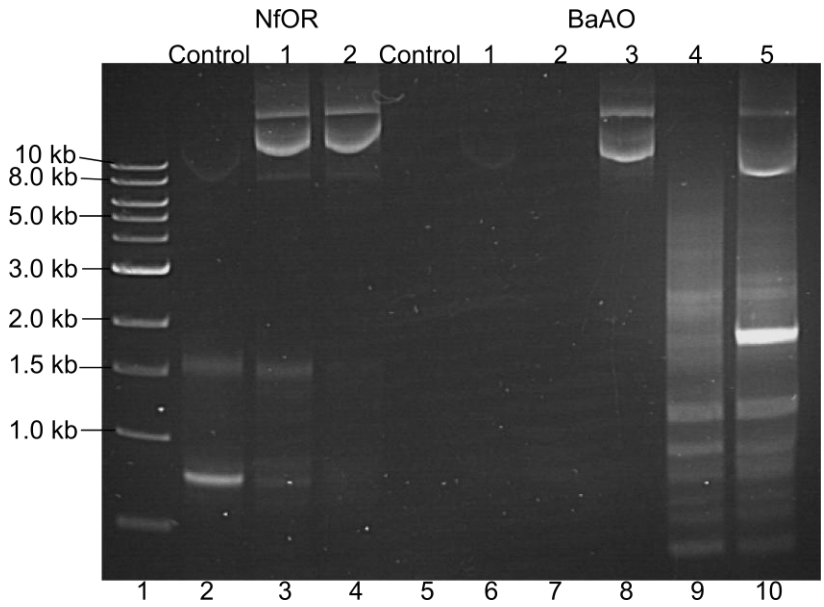

Figure A.1 1% agarose gel separation of DNA from PCR amplification of potential pEKEx2-NfOR and pEKEx2-BaAO plasmid inserts: Lane 1, 1 kb DNA ladder (0.5 kb, 1 kb, 1.5 kb, 2 kb, 3 kb, 4 kb, 5 kb, 6 kb, 8 kb, 10 kb); Lane 2, PCR amplification of pET-YSBLIC-3C-NfOR insert; Lanes 3-4, PCR amplification of pEKEx2-NfOR 1-2 plasmids; Lane 5, PCR amplification of pET-YSBLIC-3C-BaAO insert; Lanes 6-10, PCR amplification of pEKEx2-BaAO-1-5 plasmids.

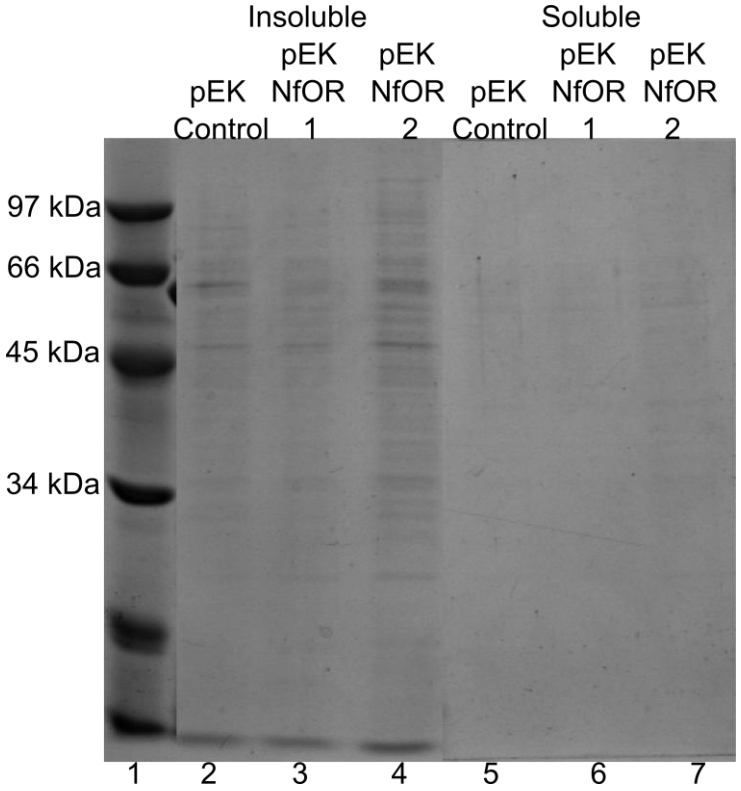

Figure A.2 SDS-PAGE separation of protein from competent *C. glutamicum* ATCC 13032 cells transformed with pEKEx2 plasmid variants: Lane 1, low range molecular weight marker; Lane 2, ATCC 13032-pEKEx2 insoluble fraction; Lanes 3-4, ATCC 13032-pEKEx2-NfOR1-2 insoluble fractions; Lane 5 ATCC 13032-pEKEx2 soluble fraction; Lanes 6-7, ATCC 13032-pEKEx2-NfOR1-2 soluble fractions.

A.3 Discussion

Attempts were made to clone the AsAAO, BaAO and NfOR gene sequences into the pEK-Ex2 shuttle vector for expression in *C. glutamicum*, however, only the NfOR sequence was successfully cloned.

The AsAAO and BaAO gene inserts were amplified sucessfully (data not shown) and the activity of the restriction enzymes had all been checked by performing single enzyme restrictions on the non recombinant pEK-Ex2 plasmid (data not shown), meaning that problems may have been caused by the digestion of the gene insert or during the ligation step. If more time had been available attempts to address these problems would have included using alternative primer designs for the insert PCR amplification and redoing the ligation step with a different batch of ligase and varying plasmid:insert ratios.

Both the non recombinant pEK-Ex2 and the pEK-Ex2 NfOR plasmids were used to transform comptetent *C. glutamicum* cells that had been prepared using a method proposed by Liebl *et al.*.[132] Small translucent colonies took 2-3 days to appear, which was expected based on work by Takano *et al.*.[135] These colonies were picked and gene overexpression was induced in a similar manner to the *E. coli* expression strains, although the time taken for the culture to reach OD_{600} was longer in *C. glutamicum* compared to *E. coli* expression strains (around 5-6 h as opposed to 2-3 h), so the culture was left at 30°C overnight to produce protein, whereas *E. coli* would be left for around 5 h.

Cells were then harvested by centrifugation and sonicated in an attempt to disrupt the *C. glutamicum* cell envelope. However, when analysed on SDS-PAGE there was very little protein found in the insoluble fraction of the sonicated cell cultures, and almost none in the soluble fractions (**Figure A.2**). The lack of protein in the insoluble fractions suggests that there is little cell volume in the cultures, this may either be due to the cells not having had enough time to grow or possibly the *C. glutamicum* being unable to reach higher cell density in LB media.

The lack of soluble protein may just be due to the lack of protein overall, or may suggest that the soniciation was not enough to disrupt the *C. glutamicum* cells. Although Doo *et al.*[130] disrupted their cells using an ultrasonic processor, they were using different growth conditions, which may have affected the variable level of coverage of the protective crystalline protein surface-layer.[126]

Either way, there does not appear to have been any production of the NfOR protein, as both the pEK-Ex2 and pEK-Ex2-NfOR strains have the same protein expression pattern (**Figure A.2**). As the amount of IPTG used to induce gene induction was the same as used successfully by Doo *et*

al.,[130] who were also using the same plasmid vector and ribosomal binding site, it could be possible that the antibiotic selection did not work or *C. glutamicum* was unable to produce the NfOR protein due to another reason (*e.g.* oxidases potentially causing a toxic build-up of H_2O_2 if a compatible substrate is present in the cell cytoplasm.).

If more time had been available to address these issues, transformation and the culture growth could both be repeated with a higher concentration of kanamycin to ensure that the cells had been transformed and the plasmid was being retained during growth. Re-cloning the sequence using a different ribosomal binding site, or potentially a different plasmid vector, could also been have tried. Cloning in a protein that had been expressed successfully in *E. coli*, such as the PpLAAO protein, could also have acted as a useful comparision of how well protein expression was working in the *C. glutamicum* system and cloning in a protein known to be successfully expressed in *C. glutamicum* previously and attempting to overexpress it would determine if the method I was using was suitable for protein expression.

A.4 Materials and Methods

A.4.1 Transformation of electrocompetent *E. coli* with plasmid

Kanamycin sulfate, SOC media and electrocompetent *E. coli* Top10 cells were purchased from Invitrogen. The ingredients for LB-media were purchased from Fisher Scientific and agar was purchased from LAB M Ltd. Electrocompetent *E. coli* Top10 cells were electroporated using a BioRad *E. coli* Pulser.

Electrocompetent *E. coli* Top10 cells were thawed on ice and rapidly mixed with plasmid DNA. Cells were incubated on ice for 1 min and then transferred to an ice-cold 0.2 cm electroporation cuvette. Cells were electroporated at 2.5 kV in the *E. coli* Pulser. Cells were mixed with 950 µL SOC media and then transferred to a fresh 15 mL tube under sterile conditions. Cells were incubated at 37°C with shaking at 180 r.p.m for 90 min. Cells were plated out on pre-warmed LB-agar containing 30 µg mL^{-1} of kanamycin. Colonies were obtained after incubating the agar plates at 37°C overnight.

LB-media (V= 1 L): 10 g tryptone, 5 g yeast extract, 10 g NaCl, H_2O (18.2 Ω·cm)

LB-agar (V= 1 L): 10 g tryptone, 5 g yeast extract, 10 g NaCl, 15 g agar, H_2O (18.2 Ω·cm)

A.4.2 Preparation of pEK-EX2 for cloning

pEK-Ex2 plasmid pellet was provided by Prof. Sun-Yang Park. *BamHI* restriction enzyme, *EcoRI* restriction enzyme, *KpnI* restriction enzyme, 100 x BSA, NEBuffer 1 and NEBuffer 3 were purchased from New England Biolabs. UV-cuvettes for Eppendorf Biophotometer were purchased from Sarstedt.

pEKEx2 plasmid pellet was resuspended in 10 µL of H_2O (18.2 Ω·cm). 1 µL pEKEx2 plasmid was used to transform *E. coli* Top10 electrocompetent cells as in **Section A.4.1**. One colony was used to inoculate 5 mL of LB-media containing 30 µg mL^{-1} kanamycin. This starter culture was grown overnight at 37°C with shaking at 180 r.p.m. Plasmid was purified using Sigma-Aldrich's GenElute Plasmid Miniprep kit. Plasmid concentration was measured using the dsDNA function of an Eppendorf Biophotometer, with an $A_{280\ nm}$ of 1 set equal to 50 µg mL^{-1} DNA.

2 µg of purified pEKEx2 plasmid was digested using the *KpnI*/*BamHI* Restriction mix. 2 µg of purified pEKEx2 plasmid was digested using the *EcoRI*/*BamHI* Restriction mix. Restriction mixes were incubated at 37°C for 3 hours. Restriction digests were separated using 1 % agarose gel electrophoresis, along with a lane of undigested plasmid as a control. Digested gel bands were visualized using an Invitrogen SafeImager system and excised using a scalpel. DNA was purified from the gel bands using Sigma-Aldrich's GenElute Gel Extraction kit. DNA concentration was measured using the dsDNA function of an Eppendorf Biophotometer, with an $A_{280\ nm}$ of 1 set equal to 50 µg mL^{-1} DNA. Digested plasmid was stored at -20°C until needed.

LB-media (V=1 L):	10 g tryptone, 5 g yeast extract, 10 g NaCl, H_2O (18.2 Ω·cm)
KpnI/*BamHI* Restriction mix (v=30 µL):	1 x NEBuffer 1, 1 x BSA, 333.3 U $µL^{-1}$ *KpnI*, 1000 U $µL^{-1}$ *BamHI,* 2 µg DNA
EcoRI/*BamHI* Restriction mix (v=30 µL):	1 x NEBuffer 3, 1 x BSA, 666.7 U $µL^{-1}$ *KpnI*, 666.7 U $µL^{-1}$ *BamHI,* 2 µg DNA

A.4.3 Preparation of gene inserts for cloning into pEKEx2 plasmid

KOD HotStart polymerase kit was purchased from Novagen. YSBLIC3C-AsAAO, YSBLIC3C-BaAO, and YSBLIC3C-NfOR plasmids were prepared previously (**Sections 2.2.1-2.2.4**). *BamHI* restriction enzyme, *EcoRI* restriction enzyme, *KpnI* restriction enzyme, 100 x BSA, NEBuffer 1 and NEBuffer 3 were purchased from New England Biolabs. UV-cuvettes for Eppendorf Biophotometer were purchased from Sarstedt.

AsAAO gene insert was amplified from YSBLIC3C-AsAAO plasmid by PCR using PCR Cycle A (**Table A.1**), PCR mix A (**Table A.2**) and the PekNfOR-for and PekAsAAO-rev primers (**Table A.3**). BaAO gene insert was amplified from YSBLIC3C-BaAO plasmid by PCR using PCR Cycle A (**Table A.1**), PCR mix A (**Table A.2**) and the PekNfOR-for and PekBaAO-rev primers (**Table A.3**). NfOR gene insert was amplified from YSBLIC3C-NfOR plasmid by PCR using PCR Cycle A (**Table A.1**), PCR mix A (**Table A.2**) and the PekNfOR-for and PekNfOR-rev primers (**Table A.3**).

PCR reactions were separated by 1 % agarose gel electrophoresis. Appropriately sized gel bands were visualized using an Invitrogen SafeImager system and excised using a scalpel. DNA was purified from the gel bands using Sigma-Aldrich's GenElute Gel Extraction kit. DNA concentration was measured using the dsDNA function of an Eppendorf Biophotometer, with an A_{280} of 1 set equal to 50 µg mL^{-1} DNA.

Table A.1: Conditions for PCR cycling methods used for the amplification of DNA by PCR.

PCR Cycling	Initial denaturation	Denaturation	Annealing	Extension	Number of Cycles	Final extension
A	95°C, 2 min	95°C, 30 sec	55°C, 30 sec	72°C, 90 sec	30	72°C, 5 min

Table A.2: Composition of PCR mix used for the amplification of DNA by PCR.

PCR mix	V_{total} in µL	$V_{component}$	[Component] in PCR mix
A	50	27 µL H_2O (18.2 Ω·cm) 5 µL 5 x KOD buffer 3 µL 25 mM $MgSO_4$ 5 µL 2 mM (each) dNTPs 1 µL 20 µM forward primer 1 µL 20 µM reverse Primer 1 µL Template DNA 2.5 µL ≥99.5% DMSO 1 µL 1 U $µL^{-1}$ KOD Hot Start DNA polymerase	1 x KOD buffer 1.5 mM $MgSO_4$ 0.2 mM of each dNTP 0.4 µM forward primer 0.4 µM reverse primer 2% (v/v) template DNA 5% DMSO 0.02 U $µL^{-1}$ KOD Hot Start DNA polymerase
B	25	13.75 µL H_2O (18.2 Ω·cm) 2.5 µL 10 x KOD buffer 2.5 µL 2 mM (each) dNTPs 1.5 µL 25 mM $MgSO_4$ 1 µL 10 µM forward primer 1 µL 10 µM reverse primer 1 µL 10 ng $µL^{-1}$ YSBLIC3C-PpLAAO 1.25 µL ≥99.5% DMSO 0.5 µL 1 U $µL^{-1}$ KOD HotStart DNA polymerase	1 x KOD buffer 1.5 mM $MgSO_4$ 0.2 mM of each dNTP 0.4 µM forward primer 0.4 µM reverse primer 2% (v/v) template DNA 5% DMSO 0.02 U $µL^{-1}$ KOD Hot Start DNA polymerase

Table A.3: Sequences of primers used for the amplification of DNA by PCR.

Primer name/ Purification method	Primer sequence
PekAsAAO-rev/ HPSF	TGTGATAAGAATTCTTATTATCGAGGAGCGGTAGAGCCAGCAAAGTGAAT
PekBaAO-rev/ HPSF	TTATCAGAGGTACCTTATCACTTTTCGTTTACTTCATGAGCAACTCGAAT
PekNfOR-for/ HPSF	GCAAGTGTGGATCCAAAGGAGATATAGATATATACCATGGGCAGCAGC
PekNfOR-rev/ HPSF	TCTGATAAGAATTCTTATCACCGGAGGGCGGACGGGCTCGCGGCGTCG
PekSeq-for/ HPSF	ATCATCGGCTCGTATAATGTGTGGAATTGTGAGC
PekSeq-rev/ HPSF	ATTTGATGCCTGGCAGTTCCCTACTCTCG

2 µg of purified BaAO insert was digested using the *KpnI*/*BamHI* Restriction mix. 2 µg of purified AsAAO insert and NfOR insert were both digested using the *EcoRI*/*BamHI* Restriction mix. Restriction mixes were incubated at 37°C for 3 hours. Restriction digests were separated using 1 % agarose gel electrophoresis. Digested gel bands were visualized using an Invitrogen SafeImager system and excised using a scalpel. DNA was purified from the gel bands using Sigma-Aldrich's GenElute Gel Extraction kit. DNA concentration was measured using the dsDNA function of an Eppendorf Biophotometer, with an A_{280} of 1 set equal to 50 µg mL^{-1} DNA. Insert DNA was stored at -20°C until needed.

KpnI/*BamHI* Restriction mix (v= 30 µL): 1 x NEBuffer 1, 1 x BSA, 333.3 U μL^{-1} *KpnI*, 1000 U μL^{-1} *BamHI,* 2 µg DNA

EcoRI/*BamHI* Restriction mix (v= 30 µL): 1 x NEBuffer 3, 1 x BSA, 666.7 U μL^{-1} *KpnI*, 666.7 U μL^{-1} *BamHI,* 2 µg DNA

A.4.4 pEKEx2 ligation

T4 qualified DNA ligase kit was purchased from New England Biolabs. ATP was purchased from Sigma-Aldrich. Ligation mix was incubated using a Techne TC-312 Thermocycler machine.

T4 DNA Ligation mix was prepared using pEK-EX2 plasmid digested with *EcoRI and BamHI* (**Section A.4.2**) and AsAAO insert digested with *EcoRI and BamHI*, (**Section A.4.3**) as well as NfOR insert digested with *EcoRI and BamHI* (**Section A.4.2**). T4 DNA Ligation mix was prepared using pEKEX2 plasmid digested with *KpnI and BamHI* (**Section A.4.2**) and AsAAO insert digested with *KpnI and BamHI,* (**Section A.4.3**). Ligation mix was incubated at 16°C with shaking at 180 r.p.m overnight. Ligation mixes were stored at -20°C until needed.

1 µL of ligation mix was used to transform 75 µL of *E. coli* electrocompetent Top10 Cells as in **Section A.4.1**. This resulted in 5 colonies from the pEK-Ex2-BaAO reaction and 2 colonies from the pEK-Ex2-NfOR reaction. Colonies were each used to inoculate 5 mL of LB-media containing 30 µg mL^{-1} kanamycin. Starter culture was grown overnight at 37°C with shaking at 180 r.p.m. Plasmid was purified using Sigma-Aldrich's GenElute Plasmid Miniprep kit. Plasmid DNA concentration was measured using the dsDNA functions of an Eppendorf Biophotometer.

The gene insert of the purified pEK-Ex2-BaAO plasmids, along with the insert from the YSBLIC3C-BaAO plasmid, were amplified via PCR using PCR cycle A (**Table A.1**), PCR mix B (**Table A.2**) and the PekNfOR-for and PekBaAO-rev primers (**Table A.3**).The gene insert of the purified pEK-Ex2-NfOR plasmids, along with the insert from the YSBLIC3C-NfOR plasmid, were amplified using PCR using PCR cycle A (**Table A.1**), PCR mix B (**Table A.2**) and the PekNfOR-for and PekNfOR-rev primers (**Table A.3**). Products were analysed on 1% agarose electrophoresis gel.

Based on these results, the pEK-Ex2-BaAO5 and pEK-Ex2-NfOR1 plasmids were concentrated to 100-150 ng μl^{-1} and sent for sequencing using the PekSeq-for and PekSeq-rev primers (**Table A.3**) by the York University Genomics group. The sequence chromatograms were analysed with the program Chromas lite, version 2.01 from Technelysium (free software). The pEK-Ex2-NfOR1 plasmid had ligated and contained no undesired mutations, however the pEK-Ex2-BaAO5 plasmid had failed to ligate.

T4 DNA Ligation mix (V= 10 µL):	1 x T4 DNA ligase buffer, 1 mM ATP, 3 µL digested PekEx2 plasmid, 4 µL digested gene inserts, 40 cohesive end units μL^{-1} T4 qualified DNA ligase.
LB-media (V=1 L):	10 g tryptone, 5 g yeast extract, 10 g NaCl, H_2O (18.2 Ω·cm)
EcoRI/*BamHI* Restriction mix (v= 30 µL):	1 x NEBuffer 3, 1 x BSA, 666.7 U μL^{-1} *KpnI*, 666.7 U μL^{-1} *BamHI,* 500 ng DNA

A.4.5 Preparation of competent *C. glutamicum* cells

C. glutamicum ATCC 13032 cells were brought in ampoule form. Ingredients for LB-media and glycerol were purchased from Fisher Scientific and agar was purchased from LAB M Ltd, D-glucose was purchased from Sigma-Aldrich.

1 mL of LB-media was used to resuspend purchased *C. glutamicum* cells. Resuspended cells were used to inoculate LB-agar plates and 100 mL of LB-media. Plates were grown overnight at 30°C and the LB-culture was grown overnight at 30°C with shaking at 180 r.p.m. Both plates and the culture grew. 700 µL of *C. glutamicum* culture was mixed with 300 µL of 50% glycerol and stored at -80°C.

Two colonies of *C. glutamicum* ATCC 13032 were each used to inoculate 10 mL of LB-media containing 2% (v/v) filter-sterilized D-glucose in a 50 mL conical flask. These were grown overnight at 30°C and 180 r.p.m. The next morning 100 mL of LB-media in a 1 L conical flask were inoculated with the overnight culture to an optical density of 0.3 at 600 nm. This culture was then grown at 18°C and 120 r.p.m for 28 h.

The culture was chilled on ice for 10 min before cells were spun down by centrifugation for 10 min at 4,000 *g* in a Harrier 18/80 benchtop centrifuge. The cells were washed with 50 mL of ice-cold 10% (v/v) glycerol four times and were finally resuspended in 0.5 mL of ice-cold 10% (v/v) glycerol. 100 µL aliquots were transferred to ice-cold 1.5 mL Eppendorf tubes and were snap frozen in liquid nitrogen, before storing at -80°C.

LB-media (V= 1 L): 10 g tryptone, 5 g yeast extract, 10 g NaCl, H_2O (18.2 Ω·cm)
LB-agar (V= 1 L): 10 g tryptone, 5 g yeast extract, 10 g NaCl, 15 g agar, H_2O (18.2 Ω·cm)

A.4.6 Transformation of C. glutamicum cells with pEK-Ex2-NfOR plasmid

C. glutamicum ATCC 13032 cells were brought in ampoule form. Ingredients for LB-media were purchased from Fisher Scientific and agar was purchased from LAB M Ltd, D-sorbitol and 0.2 cm gap Electroporation cuvettes were purchased from Sigma-Aldrich. Cells were electroporated in a BioRad Gene Pulser electroporation system with pulse controller.

C. glutamicum was transformed with pEK-Ex2-NfOR plasmid. Non recombinant pEK-Ex2 plasmid and H_2O (18.2 Ω·cm) were also used instead as control reactions.

100 µL of competent *C. glutamicum* ATCC 13032 (**Section A.4.5**) was thawed on ice and 1 µL of plasmid was added and mixed gently with the pipette tip. Cells were transferred to an ice-cold 0.2 cm Electroporation cuvette and tapped firmly on the benchtop to remove any bubbles from the mix.

Cuvettes were wiped with a tissue to remove moisture and then electroporated at 2.5 kV with capacitance of 25 μF and resistance at 200 Ω.
Cells were then added to 1 mL of LB media containing 0.5 M D-sorbitol, which was heatshocked at 46°C for 6 min and then grown at 30°C for 90 min. 200 μL aliquots were then spread on LB agar plates containing 25 μg mL^{-1} kanamycin and 0.5 M D-sorbitol. Plates were grown at 30°C for 3 d.

A.4.7 Gene overexpression of transformed *C. glutamicum* cells

C. glutamicum ATCC 13032 cells were brought in ampoule form. Ingredients for LB-media were purchased from Fisher Scientific. Kanamycin was purchased from Invitrogen and IPTG was purchased from Melford.

One colony of transformed *C. glutamicum* was used to inoculate a 5 mL culture of LB media containing 25 μg mL^{-1} kanamycin; this starter culture was grown overnight at 30°C with shaking at 180 r.p.m. 100 μL of starter culture was then used to inoculate a fresh 5 mL culture of LB media containing 25 μg mL^{-1} kanamycin. This culture was grown at 30°C with shaking at 180 r.p.m until the OD_{600} of the culture was roughly 0.5. Gene overexpression was induced by adding 1 mM IPTG and cells were left to overexpress overnight at 30°C with shaking at 180 r.p.m.

The cells were harvested by centrifugation for 1 min at 16,000 *g* using an Eppendorf 5415 C centrifuge. The supernatant was discarded and the cell pellet was resuspended in 500 μL buffer 1. The cell suspension was sonicated on ice for 30 s at 15 microns. Cell debris was pulled down by spinning at 16,000 *g* for 1 min using an Eppendorf 5415 C centrifuge. The soluble supernatant was separated from the insoluble cell pellet. The cell pellet was then resuspended in 500 μL buffer 1. The soluble and insoluble fractions were analysed by 12.5% SDS-PAGE.

LB-media (V= 1 L): 10 g tryptone, 5 g yeast extract, 10 g NaCl, H_2O (18.2 Ω·cm)

Appendix B Alignment of known and target oxidases

The seven target oxidases expressed in **Chapter 3**, along with the known L-AAO from *Calloselasma rhodostoma* (CrLAAO) and the L-aspartate oxidase from *E. coli* were aligned using the CLUSTAL W2 program from the European Bioinformatics Institute website. (http://www.ebi.ac.uk/Tools/msa/clustalw2/)

```
Q81RW3_BaAO       ---------------------------------------MMQPLTMERMLHIINVGLVKTK 22
P81382_CrLAAO     -----------MNVFFMFSLLFLAALGSCADDRNPLAECFQENDYEEFLEIARNGLKATS 49
Q88MZ2_PpLAAO     -----------MSQQFQH--DVLVIG-------SGAAGLSLALNLPSHLRVAVLSKGDLS 40
P10902_L-AspO     -----------MNTLPEHSCDVLIIG-------SGAAGLSLALRLADQHQVIVLSKGPVT 42
Q8YKW9_AsAAO      MQHREFTGCIHTSCRLPISFIFMFNLNRRQFLLRSTLAIAATVSYDHVQAQKPKSPGTLP 60
P72346_SLAAO      ------------------------MRFSRRRFLQSSLGAAATTGLAGTLAAGGQAQTRST 36
Q5YV66_NfOR       ------------------------------------------------------MVD 3
Q8VPD4_RoLAAO     ---------MAFTRRSFMKGLGATGGAGLAYGAMSTLGLAPSTAAPARTFQPLAAGDLIG 51
O31616_BsGO       ------------------------------------------------------MKR--- 3

Q81RW3_BaAO       N---PKQIIIVGAGISGLVAASLLKEAGHKVTILEANNRIGGRIYTIREP---------- 69
P81382_CrLAAO     N---PKHVVIVGAGMAGLSAAYVLAGAGHQVTVLEASERPGGRVRTYRN---------- 95
Q88MZ2_PpLAAO     N---GSTFWAQGGVAAVLDNTDTVQSHVEDTLNAGGGLCHEDAVRFTVEH---------- 87
P10902_L-AspO     E---GSTFYAQGGIAAVFDETDSIDSHVEDTLIAGAGICDRHAVEFVASN---------- 89
Q8YKW9_AsAAO      KGLPRRKVIVVGAGISGLVAAYELTAVGHDVTLLEASKRIGGRVLTLRGA---------- 110
P72346_SLAAO      PVR-KRSVLVLGAGMAGLTAALSLLRRGHQVTVIEYQNRIGG--RLLSVP---------- 83
Q5YV66_NfOR       R---SVDVVVVGAGIAGLVAARDLVRTGHEVLVLEARDRVGG--RLLNAE---------- 48
Q8VPD4_RoLAAO     KVKGSHSVVVLGGGPAGLCSAFELQKAGYKVTVLEARTRPGGRVWTARGGSEETDLSGET 111
O31616_BsGO       ----HYEAVVIGGGIIGSAIAYYLAKENKNTALFESG-TMGGRTTSAAAG---------- 48
                            *.       :  :     ..

Q81RW3_BaAO       ----FSRGLYFNAGPMRIPDTHKLTLAYIRKFKLPLNLFINKTASDIIYTNNIKKRLSIF 125
P81382_CrLAAO     ----EEAGWYANLGPMRLPEKHRIVREYIRKFDLRLNEFSQENDNAWYFIKNIRKKVGEV 151
Q88MZ2_PpLAAO     ----SREAIQWLIEQGVPFTRDEHYSVDDGGFEFHLTREGGHSHRRIIHAADATGAAIFT 143
P10902_L-AspO     ----ARSCVQWLIDQGVLFDTHIQPNGEES---YHLTREGGHSHRRILHAADATGREVET 142
Q8YKW9_AsAAO      ----FQGEDLLELGAARIPSNHHLTFGYIKHFGLKLSQFAPADG---KYLTIKDGKRLLI 163
P72346_SLAAO      ----LKGGQFSEAGGGHFRANMPYVLSYIRHFKLPLLTLNDGLPR--YLFDGKTADAADL 137
Q5YV66_NfOR       ----LPGGAPIEVGGQWVGPTQHRAMALIHELGLQTFPTHDTGRAIAEIGSSRAEYTGAI 104
Q8VPD4_RoLAAO     QKCTFSEGHFYNVGATRIPQS-HITLDYCRELGVEIQGFGNQNANTFVNYQSDTSLSGQS 170
O31616_BsGO       ----MLGAHAECEERDAFFDFAMHSQRLYKGLGEELYALSGVDIR--QHNGGMFKLAFSE 102

Q81RW3_BaAO       EKNPSILGYPILEREKGKTAEELMLEV----------LEPILNYIKKDPNKNWSIVEKKY 175
P81382_CrLAAO     KKDPGLLKYPVKPSEAGKSAGQLYEES----------LGKVVEELKR---TNCSYILNKY 198
Q88MZ2_PpLAAO     TLLEQARQRPNIQLLEQRVAVDLITERRLGLPGER-CLGAYVLDRNTGEVDTFGARFTVL 202
P10902_L-AspO     TLVSKALNHPNIRVLERSNAVDLIVSDKIGLPGTRRVVGAWVWNRNKETVETCHAKAVVL 202
Q8YKW9_AsAAO      PAKVLFQNQPQIRPQE---------------------------------------------- 179
P72346_SLAAO      SRWPWDLAPQERRVSVASLLNTYLILN--------------GLDTDTVLDANWPDAQAIQ 183
Q5YV66_NfOR       PKLNPLALADVAQAQLRLDRLARRVAR----------TDPWRAERAEALDAQTFDTWLRR 154
Q8VPD4_RoLAAO     VTYRAAKADTFGYMSELLKKATDQGALD-------QVLSREDKDALSEFLSDFGDLSDDG 223
O31616_BsGO       EDVLQLRQMDDLDSVSWYSKEEVLEKE--------------------------------- 129

Q81RW3_BaAO       KAYSLGTFLTEY--YSDGAIDMIGVLLDMEAYMGMSLIEVLREMVFFTSTTKYYEITGGM 233
P81382_CrLAAO     DTYSTKEYLIKEGDLSPGAVDMIGDLLNEDSGYYVSFIESLKHDDIFAYEKRFDEIVDGM 258
Q88MZ2_PpLAAO     ATGGAAKVYLYTSNPDGACGDGIAMAWRAGCRVANLEFNQFHPTCLYHPQAKSFLITEAL 262
P10902_L-AspO     ATGGASKVYQYTTNPDISSGDGIAMAWRAGCRVANLEFNQFHPTALYHPQARNFLLTEAL 262
Q8YKW9_AsAAO      ------------------------------------------------------IQKLTDGF 187
P72346_SLAAO      QLDNLTLSQLIRQVGGSEAFIQLLDAHGGTFTSSSPALGVIPDLAYHFGDQNLFRIQGGN 243
Q5YV66_NfOR       TTYTAAGRSFFRVITEAVFAAGPEDLSALWASCYLGAGGGVDTMIDVAGGAQQDRVVGGT 214
Q8VPD4_RoLAAO     RYLGSSRRGYDSEPGAGLNFGTEKKPFAMQEVIRSGIGRNFSFDFGYDQAMMMFTPVGGM 283
O31616_BsGO       ---------------------------------------------PYASGDIFGASF 141
                                                                          .
```

```
Q81RW3_BaAO        DALPKAFLSQL-NENIFMRYKVEKIIQENSKVMIQVNHEQT--------IERFMVTGDVA 284
P81382_CrLAAO      DKLPTAMYRDI-QDKVHFNAQVIKIQQNDQKVTV-VYETLS--------KETPSVTADYV 308
Q88MZ2_PpLAAO      RGEGALLRLPN-GERFMPRFDPREELAPRDIVARAIDHEMKRLGVDCVYLDITHKPADFI 321
P10902_L-AspO      RGEGAYLKRPD-GTRFMPDFDERGELAPRDIVARAIDHEMKRLGADCMFLDISHKPADFI 321
Q8YKW9_AsAAO       DLLPKAFAQAL-TKEIKLDEPVARIVQTSNGVEVSCLSGQR-------------YLGDYV 233
P72346_SLAAO       DRLPKAMAAAIGSERFILDAPVVAIDQQANRATVTVKDGRT-------------FQGDAI 290
Q5YV66_NfOR        QAIAIALAGEL-GDRVVLGSPVSEVEWDEAGVRVRAGGGTVR--------------ARRA 259
Q8VPD4_RoLAAO      DRIYYAFQDRIGTDNIVFGAEVTSMKNVSEGVTVEYTAGGSK-----------KSITADYA 333
O31616_BsGO        IQDDVHVEPYFVCKAYVKAAKMLGAEIFEHTPVLHVERDGE---------------ALFI 186
                         .                                                .

Q81RW3_BaAO        IVTIPFSALRFVEIQPYNLFSYYKRRAIRELNYIAATKIAIEFKSRFWEKAG-QYGGKSI 343
P81382_CrLAAO      IVCTTSRAVRLIKFNPPLLP--KKAHALRSVHYRSGTKIFLTCTTKFWEDDG-IHGGKST 365
Q88MZ2_PpLAAO      KSHFPTVYERCLAFGIDITR--QPIPVVPAAHYTCGGVMVDDCGHTDVPGLY-AIGETSF 378
P10902_L-AspO      RQHFPMIYEKLLGLGIDLTQ--EPVPIVPAAHYTCGGVMVDDHGRTDVEGLY-AIGEVSY 378
Q8YKW9_AsAAO       LCTVPLTVLNQITFSPELSEE-KKQAAAGGYNYRAATRGFVKFPNRFWEREN-LNGWGFF 291
P72346_SLAAO       ISTIPFTVLPEVAVRPGWSAG--KRRMFAEMEWEQTVKVIAQTRSPVWLAQN-VHGWPMA 347
Q5YV66_NfOR        VVAVPPPLAARIRFSPGLPGD--RDQLVQRMPMGRVVKVNVVYDEPFWRADG-FSGQAVS 316
Q8VPD4_RoLAAO      ICTIPPHLVGRLQNNLPGDVL----TALKAAKPSSSGKLGIEYSRRWWETEDRIYGGASN 389
O31616_BsGO        KTPSGDVWANHVVVASGVWSG----MFFKQLGLNNAFLPVKGECLSVWNDDIPLTKTLYH 242
                             :

Q81RW3_BaAO        TDLP--IRFTYYPSYGIHTPGAATVLASYTWADEALTWDSLPDRERIRYALKNLAEIYG- 400
P81382_CrLAAO      TDLP--SRFIYYPNHNFTN--GVGVIIAYGIGDDANFFQALDFKDCADIVFNDLSLIHQL 421
Q88MZ2_PpLAAO      TGLHGANRMASNSLLECFVYGRAAAADIQAHLEQVAMPKALPGWDASQVTDSDEDVIIAH 438
P10902_L-AspO      TGLHGANRMASNSLLECLVYGWSAAEDITRRMPYAHDISTLPPWDESRVENPDERVVIQH 438
Q8YKW9_AsAAO       DDEE-----LWHTTWDRPE--KTGILHAYLKGEKGLEIDGFEGKTQQQKLLQHWEKILP- 343
P72346_SLAAO       GSDR---PWERVIDITGNEGGGYGNTFFYLNGRNKDAMLARPKSERAQAIVDQFRSDLP- 403
Q5YV66_NfOR        DRRP-----LAVVFDNTPPAGSPGVLVGFLEGRHADACSRMDHPTRRAQVIDDLAGYFG- 370
Q8VPD4_RoLAAO      TDKD---ISQIMFPYDHYNSDRGVVVAYYSSGKRQEAFESLTHRQRLAKAIAEGSEIHG- 445
O31616_BsGO        DHCY--------------IVPRKSGRLVVGATMKPGDWSETPDLGGLESVMKKAKTMLP- 287
                                                                    .

Q81RW3_BaAO        --EIVYSEFVTGTSFSWSKNPYSCGAFTAFEPGQELE------LFPYITSPSGKVHFAG- 451
P81382_CrLAAO      PKKDIQSFCYPSVIQKWSLDKYAMGGITTFTPYQFQH------FSDPLTASQGRIYFAG- 474
Q88MZ2_PpLAAO      NWDELRRFMWDYVGIVRTSKRLQRAQHRIRLLLDEID------EFYSNYKVSRDLIELR- 491
P10902_L-AspO      NWHELRLFMWDYVGIVRTTKRLERALRRITMLQQEID------EYYAHFRVSNNLLELR- 491
Q8YKW9_AsAAO       ---GVSNYSVRSYFHSWTKDIWSKGGWAYPTDEQEKK------LFPELGKSEGKIYFAG- 393
P72346_SLAAO       ---DLFDEVVTLADFAWGEQPWIRGSFGGP-PLGGAW------MIREWTTPEGLIHFAG- 452
Q5YV66_NfOR        ---PRARTPIDYIEKDWADEEYSRGCYGAFTAPGTLTR-----FGHALRPPIGPLHWAGT 422
Q8VPD4_RoLAAO      --EKYTRDISSSFSGSWRRTKYSESAWANWAGSGGSHGGAATPEYEKLLEPVDKIYFAG- 502
O31616_BsGO        ---AIQNMKVDRFWAGLRPGTKDGKPYIGRHPEDSRI-------LFAAGHFRNGILLAPA 337
                                                                      :

Q81RW3_BaAO        EHTTLTHGWMQGAIESGIRVAHEVNEK------------------------ 478
P81382_CrLAAO      EYTAQAHGWIDSTIKSGLRAARDVNLASENPSGIHLSNDNEL--------- 516
Q88MZ2_PpLAAO      NLAQVAELMILSAMQR--KESRGLHYTLDYPGMLDEAKDTILNPL------ 534
P10902_L-AspO      NLVQVAELIVRCAMMR--KESRGLHFTLDYPELLTHSGPSILSPGNHYINR 540
Q8YKW9_AsAAO       EHTSKTRGWLQGALESGLKAAQEIHFAGSTAPR------------------ 426
P72346_SLAAO       DFTTMKSGWVEGAIESGLRAARQIDPGAQPEADTFLRQEQRCN-------- 495
Q5YV66_NfOR        ETATRWAGYIDGAAESGHRTAREIAAALDPRHDAASPSALR---------- 463
Q8VPD4_RoLAAO      DHLSNAIAWQHGALTSARDVVTHIHERVAQEA------------------- 534
O31616_BsGO        TGALISDLIMNKEVNQDWLHAFRIDRKEAVQI------------------- 369
                                   :
```

Figure B.1: ClustalW2 alignment of target oxidases along with two L-AAOs that have known structures, the L-AAO from *C. rhodostoma* (CrLAAO) and the L-aspartate oxidase from *E. coli* (L-AspO). * represents conservation of identical residues, : represents conservation of strongly similar residues and . represents conservation of weakly similar residues. For oxidases with known structures, FAD-binding domain residues are in red, substrate/capping domain residues are in green and helical/dimerisation domain residues are in blue. For the α-helix and β-sheet positions of the L-AspO protein, see **Figure 5.1**.

Bibliography

1. Breuer, M., Ditrich K., Habicher T., Hauer B., Kesseler M., Stürmer R. & Zelinski T. Industrial methods for the production of optically active intermediates. *Angewandte Chemie International Edition, English* **43**, 788–824 (2004).

2. Stephens, T. D., Bunde, C. J. . & Fillmore, B. J. Mechanism of action in thalidomide teratogenesis. *Biochemical Pharmacology* **59**, 1489–1499 (2000).

3. Kusumoto, I. Industrial Production of L-Glutamine. *The Journal of Nutrition* **131**, 2552S–2555S (2001).

4. Hasegawa, H., Shinohara, Y., Akahane, K. & Hashimoto, T. Direct Detection and Evaluation of Conversion of D-Methionine into L-Methionine in Rats by Stable Isotope Methodology. *The Journal of Nutrition* **135**, 2001–2005 (2005).

5. Yagasaki, M. & Hashimoto, S. Synthesis and application of dipeptides; current status and perspectives. *Applied Microbiology and Biotechnology* **81**, 13–22 (2008).

6. Hill, J. B. *et al.* One-pot process for the preparation of .alpha.-L-aspartyl-L-phenylalanine methyl ester from a mixture containing both .alpha. and .beta. isomers thereof, which comprises admixing with said isomeric mixture hydrogen peroxide and an organic acid. (1991).at <http://www.google.com/patents/US5053532>

7. Kim, C. & Shin, C. S. Solvent-free enzymatic synthesis of alitame precursor using eutectic substrate mixtures. *Enzyme and Microbial Technology* **28**, 611–616 (2001).

8. Rozzell, D. & Wagner, F. *Biocatalytic Production of Amino Acids and Derivatives*. (Hanser Publishers: 1992).

9. Chang, C.-Y. & Yang, T.-K. Asymmetric synthesis of ACE inhibitor-Benazepril HCl via a bioreductive reaction. *Tetrahedron: Asymmetry* **14**, 2239–2245 (2003).

10. Ahmad, A. L., Oh, P. C. & Abd Shukor, S. R. Sustainable biocatalytic synthesis of L-homophenylalanine as pharmaceutical drug precursor. *Biotechnology Advances* **27**, 286–296 (2009).

11. Drauz, K. *Enzyme Catalysis in Organic Synthesis*. (John Wiley & Sons: 2012).

12. Liu, B., Wu, Q., Lv, D. & Lin, X. Modulating the synthetase activity of penicillin G acylase in organic media by addition of N-methylimidazole: Using vinyl acetate as activated acyl donor. *Journal of Biotechnology* **153**, 111–115 (2011).

13. Deaguero, A. L., Blum, J. K. & Bommarius, A. S. Improving the Diastereoselectivity of Penicillin G Acylase for Ampicillin Synthesis from Racemic Substrates. *Protein Engineering, Design and Selection* **25**, 135–144 (2012).

14. Brennan, T. M. & Hendrick, M. E. Branched amides of L-aspartyl-d-amino acid dipeptides. (1983).at <http://www.google.com/patents?id=5AY2AAAAEBAJ>

15. Regla, I., Luna H., Pérez, HI., Demare, P., Bustos-Jaimes, I. , V. & Calcagno, ML. Enzymatic resolution of N-acetyl-homophenylalanine with mammalian kidney acetone powders. *Tetrahedron: Asymmetry* **15**, 1285–1288 (2004).

16. Kato, T., Ozaki, T., Tsuzuki, K. & Ohi, N. Practical Synthesis of Novel Cardioprotective Drug, CP-060S. *Organic Process Research & Development* **5**, 122–126 (2000).

17. Vries, T., Wynberg, H., Echten, E., Koek, J., Hoeve, W., Kellogg, R., Broxterman,Q., Minnaard, A., Kaptein, B., Sluis, S., Hulshof, L., & Kooistra J. The Family Approach to the Resolution of Racemates. *Angewandte Chemie International Edition* **37**, 2349–2354 (1998).

18. O'Brien, P. Recent advances in asymmetric synthesis using chiral lithium amide bases. *Journal of the Chemical Society, Perkin Transactions 1* **8**, 1439-1458 (1998)

19. Henderson, K. W., Kerr, W. J. & Moir, J. H. Enantioselective deprotonation reactions using a novel homochiral magnesium amide base. *Chemical Communications* **6**, 479–480 (2000).

20. Adamo, M. F. A., Aggarwal, V. K. & Sage, M. A. Epoxidation of Alkenes by Amine Catalyst Precursors: Implication of Aminium Ion and Radical Cation Intermediates. *Journal of the American Chemical Society* **122**, 8317–8318 (2000).

21. Berger, M., Albrecht, B., Berces, A., Ettmayer, P., Neruda, W. & Woisetschläger, M. S(+)-4-(1-Phenylethylamino)quinazolines as Inhibitors of Human Immunoglobuline E Synthesis: Potency Is Dictated by Stereochemistry and Atomic Point Charges at N-1. *Journal of Medical Chemistry* **44**, 3031–3038 (2001).

22. Schulze, B. & Wubbolts, M. G. Biocatalysis for industrial production of fine chemicals. *Current Opinion in Biotechnology* **10**, 609–615 (1999).

23. Friedrich, A. B. & Antranikian, G. Keratin Degradation by Fervidobacterium pennavorans, a Novel Thermophilic Anaerobic Species of the Order Thermotogales. *Applied Environmental Microbiology* **62**, 2875–2882 (1996).

24. Lucas, C. & Beveridge, J. The analysis of hair keratin. *Biochemical Journal* **34**, 1356–1366 (1940).

25. Riessen, S. & Antranikian, G. Isolation of *Thermoanaerobacter keratinophilus* sp. nov., a novel thermophilic, anaerobic bacterium with keratinolytic activity. *Extremophiles* **5**, 399–408 (2001).

26. Yet, L. Recent Developments in Catalytic Asymmetric Strecker-Type Reactions. *Angewandte Chemie International Edition* **40**, 875–877 (2001).

27. Beller, M. & Eckert, M. Amidocarbonylation—An Efficient Route to Amino Acid Derivatives. *Angewandte Chemie International Edition* **39**, 1010–1027 (2000).

28. Ishitani, H., Komiyama, S., Hasegawa, Y. & Kobayashi, S. Catalytic Asymmetric Strecker Synthesis. Preparation of Enantiomerically Pure α-Amino Acid Derivatives from Aldimines and Tributyltin Cyanide or Achiral Aldehydes, Amines, and Hydrogen Cyanide Using a Chiral Zirconium Catalyst. *Journal of the American Chemical Society* **122**, 762–766 (2000).

29. Hermann, T. Industrial production of amino acids by coryneform bacteria. *Journal of Biotechnology* **104**, 155–172 (2003).

30. Okamoto, K., Kino, K. & Ikeda, M. Hyperproduction of L-Threonine by an *Escherichia coli* Mutant with Impaired L-Threonine Uptake. *Bioscience, Biotechnology, and Biochemistry* **61**, 1877–1882 (1997).

31. Masuda, M., Takamatsu, S., Nishimura, N., Komatsubara, S. & Tosa, T. Improvement of Nitrogen Supply for L-Threonine Production by a Recombinant Strain of *Serratia marcescens*. *Applied Biochemistry and Biotechnology* **37**, 255–265 (1992).

32. Faurie, R. & Thommel, J. *Microbial Production of L-Amino Acids*. (Springer: 2003).

33. Lee, M.-H., Lee H.-W., Park J.-H., Ahn J.-O., Jung J.-K. & Hwang Y.-I. Improved L-threonine production of Escherichia coli mutant by optimization of culture conditions. *Journal of Bioscience and Bioengineering* **101**, 127–130 (2006).

34. Backman, K. O'Connor, M.J., Maruya, A., Rudd, E., McKay, D., Balakrishnan, R., Radjai, M., DiPasquantonio, V., Shoda, D., Hatch, R. & Venkatasubramanian, K. Genetic Engineering of Metabolic Pathways Applied to the Production of Phenylalanine. *Annals of the New York Academy of Sciences* **589**, 16–24 (2006).

35. Taylor, P., Grinter, N., McCarthy, S., Pantaleone, D., Ton, J., Yoshida, R. & Fotheringham, I. D-Phenylalanine Biosynthesis Using Escherichia Coli: Creation of a New Metabolic Pathway. *Applied Biocatalysis in Specialty Chemicals and Pharmaceuticals* **Chapter 5**, 65–75 (2001).

36. Singh, S., Gogoi, B. K. & Bezbaruah, R. L. Racemic resolution of some DL-amino acids using *Aspergillus fumigatus* L-amino acid oxidase. *Current Microbiology* **63**, 94–99 (2011).

37. Weiner, B., Poelarends, G. J., Janssen, D. B. & Feringa, B. L. Biocatalytic Enantioselective Synthesis of *N*-Substituted Aspartic Acids by Aspartate Ammonia Lyase. *Chemistry - A European Journal* **14**, 10094–10100 (2008).

38. Yamada, S., Nabe, K., Izuo, N., Nakamichi, K. & Chibata, I. Production of L-Phenylalanine from Trans-Cinnamic Acid with Rhodotorula Glutinis Containing L-Phenylalanine Ammonia-Lyase Activity. *Applied Environmental Microbiology* **42**, 773–778 (1981).

39. Fusee, M. C. & Weber, J. E. Immobilization by Polyurethane of Pseudomonas dacunhae Cells Containing L-Aspartate β-Decarboxylase Activity and Application to L-Alanine Production. *Applied and Environmental Microbiology* **48**, 694–698 (1984).

40. Tosa, T., Senuma, M., Nakagawa, Y. & Morimoto, T. Industrial Application of Microbial Sensors for Bioprocess Control. *Annals of the New York Academy of Sciences* **672**, 184–194 (1992).

41. Wichmann, R., Wandrey, C., Bückmann, A. F. & Kula, M.-R. Continuous enzymatic transformation in an enzyme membrane reactor with simultaneous NAD(H) regeneration. *Biotechnology and Bioengineering* **67**, 791–804 (2000).

42. Bommarius, A. S. Schwarm, M., Stingl, K., Kottenhahn, M., Huthmacher, K. & Drauz, K. Synthesis and use of enantiomerically pure tert-leucine. *Tetrahedron: Asymmetry* **6**, 2851–2888 (1995).

43. Wegman, M. A., Janssen, M. H. A., van Rantwijk, F. & Sheldon, R. A. Towards Biocatalytic Synthesis of β-Lactam Antibiotics. *Advanced Synthesis & Catalysis* **343**, 559–576 (2001).

44. Müller, U. Assema, F., Gunsior, M., Orf, S., Kremer, S., Schipper, D., Wagemans, A., Townsend, A., Sonke, T., Bovenberg, R. & Wubbolts, M. Metabolic engineering of the E. coli L-phenylalanine pathway for the production of D-phenylglycine (D-Phg). *Metabolic Engineering* **8**, 196–208 (2006).

45. Yang, B., Liu, Z., Deng, B., Zeng, Y., Hu, J., Li, W. & Hu, Z. Isolation and genetic improvement of Pseudomonas sp. strain HUT-78, capable of enzymatic production of L-cysteine from DL-2-amino-Δ2-thiazoline-4-carboxylic acid. *The Journal of General and Applied Microbiology* **57**, 379–386 (2011).

46. Wöltinger, J., Karau, A., Leuchtenberger, W. & Drauz, K. Membrane Reactors at Degussa. *Technology Transfer in Biotechnology* **92**, 289–316 (2005).

47. Asano, Y. & Lübbehüsen, T. L. Enzymes acting on peptides containing d-amino acid. *Journal of Bioscience and Bioengineering* **89**, 295–306 (2000).

48. Komeda, H. & Asano, Y. A novel d-stereoselective amino acid amidase from Brevibacterium iodinum: Gene cloning, expression and characterization. *Enzyme and Microbial Technology* **43**, 276–283 (2008).

49. Moser, R. & Matthews, C. Hydrolysis of aminoacetonitrile: Peptide formation. *Cellular and Molecular Life Sciences* **24**, 658–659 (1968).

50. Khoronenkova, S. V. & Tishkov, V. I. D-amino acid oxidase: physiological role and applications. *Biochemistry (Moscow)* **73**, 1511–1518 (2008).

51. Fitzpatrick, P. F. Oxidation of Amines by Flavoproteins. *The Archives of Biochemistry and Biophysics* **493**, 13–25 (2010).

52. Pilone, M. S. D-Amino acid oxidase: new findings. *Cellular and Molecular Life Sciences* **57**, 1732–1747 (2000).

53. Jimbo, M., Nakanishi, F., Sakai, R., Muramoto, K. & Kamiya, H. Characterization of L-amino acid oxidase and antimicrobial activity of aplysianin A, a sea hare-derived antitumor-antimicrobial protein. *Fisheries Science* **69**, 1240–1246 (2003).

54. Faust, A., Niefind, K., Hummel, W. & Schomburg, D. The structure of a bacterial L-amino acid oxidase from Rhodococcus opacus gives new evidence for the hydride mechanism for dehydrogenation. *Journal of Molecular Biology* **367**, 234–248 (2007).

55. Yu, Z. & Qiao, H. Advances in Non-snake Venom L-Amino Acid Oxidase. *Applied Biochemistry and Biotechnology* **167**, 1–13 (2012).

56. Geueke, B. & Hummel, W. A new bacterial L-amino acid oxidase with a broad substrate specificity: purification and characterization. *Enzyme and Microbial Technology* **31**, 77–87 (2002).

57. Dym, O. & Eisenberg, D. Sequence-structure analysis of FAD-containing proteins. *Protein Science* **10**, 1712–1728 (2001).

58. Edmondson, D. E., Binda, C. & Mattevi, A. Structural insights into the mechanism of amine oxidation by monoamine oxidases A and B. *The Archives of Biochemistry and Biophysics* **464**, 269–276 (2007).

59. Mizutani, H., Miyahara, I., Hirotsu, K., Nishina, Y., Shiga, K., Setoyama, C. & Miura, R. Three-dimensional structure of porcine kidney D-amino acid oxidase at 3.0 A resolution. *Journal of Biochemistry* **120**, 14–17 (1996).

60. Umhau, S., Pollegioni, L., Molla, G., Diederichs, K., Welte, W., Pilone, M. S. & Ghisla, S. The x-ray structure of D-amino acid oxidase at very high resolution identifies the chemical mechanism of flavin-dependent substrate dehydrogenation. *Proceedings of the National Academy of Sciences United States of America* **97**, 12463–12468 (2000).

61. Li, M., Binda, C., Mattevi, A. & Edmondson, D. E. Functional role of the 'aromatic cage' in human monoamine oxidase B: structures and catalytic properties of Tyr435 mutant proteins. *Biochemistry* **45**, 4775–4784 (2006).

62. Atkin, K. E. *et al.* The structure of monoamine oxidase from Aspergillus niger provides a molecular context for improvements in activity obtained by directed evolution. *Journal of Molecular Biology* **384**, 1218–1231 (2008).

63. Moustafa, I. M., Foster, S., Lyubimov, A. Y. & Vrielink, A. Crystal structure of L-AAO from *Calloselasma rhodostoma* with an L-phenylalanine substrate: insights into structure and mechanism. *Journal of Molecular Biology* **364**, 991–1002 (2006).

64. Tedeschi, G., Nonnis, S., Strumbo, B., Cruciani, G., Carosati, E. & Negri, A. On the catalytic role of the active site residue E121 of *E. coli* L-aspartate oxidase. *Biochimie* **92**, 1335–1342 (2010).

65. Bossi, R. T., Negri, A., Tedeschi, G. & Mattevi, A. Structure of FAD-bound L-aspartate oxidase: insight into substrate specificity and catalysis. *Biochemistry* **41**, 3018–3024 (2002).

66. Guillén Schlippe,, Y. V. & Hedstrom, L. A twisted base? The role of arginine in enzyme-catalyzed proton abstractions. *The Archives of Biochemistry and Biophysics* **433**, 266–278 (2005).

67. Laskowski R A, Swindells M B (2011). LigPlot+: multiple ligand-protein interaction diagrams for drug discovery. *J. Chem. Inf. Model.*, **51**, 2778-2786

68. Abe, H., Yoshikawa, N., Sarower, M. G. & Okada, S. Physiological Function and Metabolism of Free D-Alanine in Aquatic Animals. *Biological and Pharmaceutical Bulletin* **28**, 1571–1577 (2005).

69. Verrall, L., Burnet, P., Betts, J. & Harrison, P. The neurobiology of D-amino acid oxidase (DAO) and its involvement in schizophrenia. *Molecular Psychiatry* **15**, 122–137 (2010).

70. Fisher, G. H., D'Aniello, A., Vetere, A., Padula, L., Cusano, G. P. & Man, E. H. Free D-aspartate and D-alanine in normal and Alzheimer brain. *Brain Research Bulletin* **26**, 983–985 (1991).

71. Fisher, G., Lorenzo, N., Abe, H., Fujita, E., Frey, W. H., Emory, C., Di Fiore, M. M. & D' Aniello, A. Free D- and L-amino acids in ventricular cerebrospinal fluid from Alzheimer and normal subjects. *Amino Acids* **15**, 263–269 (1998).

72. Furuchi, T. & Homma, H. Free D-aspartate in mammals. *Biological and Pharmaceutical Bulletin* **28**, 1566–1570 (2005).

73. D'Aniello, G., Tolino, A., D'Aniello, A., Errico, F., Fisher, G. H. & Di Fiore, M. M. The Role of D-Aspartic Acid and *N*-Methyl-D-Aspartic Acid in the Regulation of Prolactin Release. *Endocrinology* **141**, 3862–3870 (2000).

74. D'Aniello, A., Di Cosmo, A., Di Cristo, C., Annunziato, L., Petrucelli, L. & Fisher, G. Involvement of D-Aspartic acid in the synthesis of testosterone in rat testes. *Life Sciences* **59**, 97–104 (1996).

75. D'aniello, A., Di Fiore, M. M., Fisher, G. H., Milone, A., Seleni, A., D'Aniello, S., Perna, A. F. & Ingrosso, D. Occurrence of D-Aspartic Acid and N-Methyl-D-Aspartic Acid in Rat Neuroendocrine Tissues and Their Role in the Modulation of Luteinizing Hormone and Growth Hormone Release. *FASEB Journal* **14**, 699–714 (2000).

76. Wang, Y.-X., Gong, N., Xin, Y.-F., Hao, B., Zhou, X.-J. & Pang, C. C. Biological implications of oxidation and unidirectional chiral inversion of D-amino acids. *Current Drug Metabolism* **13**, 321–331 (2012).

77. Stasyk, T., Lutsik-Kordovsky, M., Wernstedt, C., Antonyuk, V., Klyuchivska, O., Souchelnytskyi, S., Hellman, U. & Stoika, R. A new highly toxic protein isolated from the death cap Amanita phalloides is an L-amino acid oxidase. *FEBS Journal* **277**, 1260–1269 (2010).

78. Tong, H., Chen, W., Shi, W., Qi, F. & Dong, X. SO-LAAO, a Novel L-Amino Acid Oxidase That Enables *Streptococcus Oligofermentans* To Outcompete *Streptococcus Mutans* by Generating H_2O_2 from Peptone. *Journal of Bacteriology* **190**, 4716–4721 (2008).

79. Chen, W. M., Lin, C. Y., Chen, C. A., Wang, J. T. & Sheu, S. Y. Involvement of an L-amino acid oxidase in the activity of the marine bacterium *Pseudoalteromonas flavipulchra* against methicillin-resistant *Staphylococcus aureus*. *Enzyme and Microbial Technology* **47**, 52–58 (2010).

80. Nagaoka, K., Aoki, F., Hayashi, M., Muroi, Y., Sakurai, T., Itoh, K., Ikawa, M., Okabe, M., Imakawa, K. & Sakai, S. L-Amino Acid Oxidase Plays a Crucial Role in Host Defense in the Mammary Glands. *FASEB J* **23**, 2514–2520 (2009).

81. Nuutinen, J. T., Marttinen, E., Soliymani, R., Hildén, K. & Timonen, S. L-Amino Acid Oxidase of the Fungus *Hebeloma Cylindrosporum* Displays Substrate Preference Towards Glutamate. *Microbiology* **158**, 272–283 (2012).

82. Marinoni, I., Nonnis, S., Monteferrante, C., Heathcote, P., Härtig, E., Böttger, L. H., Trautwein, A. X., Negri, A., Albertini, A. M. & Tedeschi, G. Characterization of L-aspartate oxidase and quinolinate synthase from Bacillus subtilis. *FEBS Journal* **275**, 5090–5107 (2008).

83. Boulland, M.-L., Marquet, J., Molinier-Frenkel, V., Möller, P., Guiter, C., Lasoudris, F., Copie-Bergman, C., Baia, M., Gaulard, P., Leroy, K. & Castellano, F. Human IL4I1 is a secreted L-phenylalanine oxidase expressed by mature dendritic cells that inhibits T-lymphocyte proliferation. *Blood* **110**, 220–227 (2007).

84. Wcisło, M., Compagnone, D. & Trojanowicz, M. Enantioselective screen-printed amperometric biosensor for the determination of D-amino acids. *Bioelectrochemistry* **71**, 91–98 (2007).

85. Pernot, P., Mothet, J. P., Schuvailo, O., Soldatkin, A., Pollegioni, L., Pilone, M., Adeline, M. T., Cespuglio, R. & Marinesco, S. Characterization of a Yeast d-Amino Acid Oxidase Microbiosensor for D-Serine Detection in the Central Nervous System. *Analytical Chemistry* **80**, 1589–1597 (2008).

86. Fang, J., Deng, D., Nakamura, H., Akuta, T., Qin, H., Iyer, A. K., Greish, K. & Maeda, H. Oxystress inducing antitumor therapeutics via tumor-targeted delivery of PEG-conjugated D-amino acid oxidase. *Internation Journal of Cancer* **122**, 1135–1144 (2008).

87. Rosini, E., Pollegioni, L., Ghisla, S., Orru, R. & Molla, G. Optimization of D-amino acid oxidase for low substrate concentrations – towards a cancer enzyme therapy. *FEBS Journal* **276**, 4921–4932 (2009).

88. García-García, M., Martínez-Martínez, I., Sánchez-Ferrer, Á. & García-Carmona, F. Production of the Apoptotic Cellular Mediator 4-Methylthio-2-oxobutyric Acid by Using an Enzymatic Stirred Tank Reactor with in Situ Product Removal. *Biotechnology Progress* **24**, 187–191 (2008).

89. Tian, F., Gourine, A. V., Huckstepp, R. T. R. & Dale, N. A microelectrode biosensor for real time monitoring of L-glutamate release. *Analytica Chimica Acta* **645**, 86–91 (2009).

90. Janasek, D. & Spohn, U. A chemiluminometric FIA procedure for the enzymatic determination of L-aspartate. *Sensors and Actuators B: Chemical* **74**, 163–167 (2001).

91. Stefan-van Staden, R.-I., Nejem, R. M., van Staden, J. F. & Aboul-Enein, H. Y. Amperometric biosensor based on diamond paste for the enantioanalysis of L-lysine. *Biosens Bioelectron* **35**, 439–442 (2012).

92. Lukasheva, E. V. & Berezov, T. T. L-lysine α-oxidase: physicochemical and biological properties. *Biochemistry (Moscow)*. **67**, 1152–1158 (2002).

93. Moynihan, K., Elion, G. B., Pegram, C., Reist, C. J., Wellner, D., Bigner, D. D., Griffith, O. W. & Friedman, H. S. L-Amino acid oxidase (LOX) modulation of melphalan activity against intracranial glioma. *Cancer Chemotherapy and Pharmacology* **39**, 179–186 (1996).

94. Claiborne, A. & Fridovich, I. Chemical and enzymic intermediates in the peroxidation of o-dianisidine by horseradish peroxidase. 1. Spectral properties of the products of dianisidine oxidation. *Biochemistry* **18**, 2324–2329 (1979).

95. Shoaf, C. R., Isselbacher, K. J. & Heizer, W. D. Rapid colorimetric assay for intestinal peptide hydrolases. *Analytical Biochemistry* **61**, 72–85 (1974).

96. Isobe, K., Fukuda, N. & Nagasawa, S. Analysis of selective production of N^{α}-benzyloxycarbonyl-L-aminoadipate-δ-semialdehyde and N^{α}-benzyloxycarbonyl-L-aminoadipic acid by Rhodococcus sp. AIU Z-35-1. *Journal of Bioscience and Bioengineering* **105**, 152–156 (2008).

97. Carr, R., Alexeeva, M., Enright, A., Eve, T. S., Dawson, M. J. & Turner, N. J. Directed Evolution of an Amine Oxidase Possessing both Broad Substrate Specificity and High Enantioselectivity. *Angewandte Chemie International Edition* **42**, 4807–4810 (2003).

98. Carr, R., Alexeeva, M., Dawson, M. J., Gotor-Fernándezm V., Humphrey, C. E., Turner, N. J. Directed Evolution of an Amine Oxidase for the Preparative Deracemisation of Cyclic Secondary Amines. *ChemBioChem* **6**, 637–639 (2005).

99. Dunsmore, C. J., Carr, R., Fleming, T. & Turner, N. J. A Chemo-Enzymatic Route to Enantiomerically Pure Cyclic Tertiary Amines. *Journal of the American Chemical Society* **128**, 2224–2225 (2006).

100. Gau, A. E., Heindl, A., Nodop, A., Kahmann, U. & Pistorius, E. K. L-amino acid oxidases with specificity for basic L-amino acids in cyanobacteria. *Zeitschrift für Naturforschung, C, Journal of Biosciences* **62**, 273–284 (2007).

101. Nishiya, Y. & Imanaka, T. Purification and characterization of a novel glycine oxidase from Bacillus subtilis. *FEBS Letters* **438**, 263–266 (1998).

102. Mörtl, M., Diederichs, K., Welte, W., Molla, G., Motteran, L., Andriolo, G., Pilone, M. S., Pollegioni, L. Structure-function correlation in glycine oxidase from Bacillus subtilis. *Journal of Biological Chemistry* **279**, 29718–29727 (2004).

103. Jamil, F., Afza Gardner, Q.-A., Bashir, Q., Rashid, N. & Akhtar, M. Mechanistic and Stereochemical Studies of Glycine Oxidase from Bacillus subtilis Strain R5. *Biochemistry* **49**, 7377–7383 (2010).

104. Kaneko, T., Nakamura, Y., Wolk, C. P., Kuritz, T., Sasamoto, S., Watanabe, A., Iriguchi, M., Ishikawa, A., Kawashima, K., Kimura, T., Kishida, Y., Kohara, M., Matsumoto, M., Matsuno, A., Muraki, A., Nakazaki, N., Shimpo, S., Sugimoto, M., Takazawa, M., Yamada, M., Yasuda, M. & Tabata, S. Complete genomic sequence of the filamentous nitrogen-fixing cyanobacterium Anabaena sp. strain PCC 7120. *DNA Research* **8**, 205–213; 227–253 (2001).

105. Ishikawa, J., Yamashita. A., Mikami, Y., Hoshino, Y., Kurita, H., Hotta, K., Shiba, T. & Hattori, M. The Complete Genomic Sequence of Nocardia Farcinica IFM 10152. *PNAS* **101**, 14925–14930 (2004).

106. Read, T. D. *et al.* The genome sequence of Bacillus anthracis Ames and comparison to closely related bacteria. *Nature* **423**, 81–86 (2003).

107. Reetz, M.T., Kahakeaw, D. & Lohmer, R. Addressing the numbers problem in directed evolution. *Chembiochem* **9**, 1797-1804 (2008).

108. Reetz, M.T., Wang, L.-W. & Bocola, M. Directed evolution of enantioselective enzymes: iterative cycles of CASTing for probing protein-sequence space. *Angewandte Chemie International Edition* **45**, 1236-1241 (2006).

109. Morley, K.L. & Kazlauskas, R.J. Improving enzyme properties: when are closer mutations better? *Trends In Biotechnology* **23**, 231-237 (2005).

110. Laemmli, U.K. Cleavage of structural proteins during the assembly of the head of bacteriophage T4. *Nature* **227**, 680-685 (1970).

111. Studier, F.W. Protein production by auto-induction in high-density shaking cultures. *Protein Expression and Purification* **41**, 207-234 (2005).

112. Lindwall, G., Chau, M.-F., Gardner, S.R. & Kohlstaedt, L.A. A sparse matrix approach to the solubilization of overexpressed proteins. *Protein Engineering* **13**, 67-71 (2000).

113. Emsley, P. & Cowtan, K. Coot: model building tools for molecular graphics *Acta Crystallographica Section D- Biological Crystallography* **60**, 2126-2132 (2004)

114. Fogg, M. J. & Wilkinson, A. J. Higher-throughput approaches to crystallization and crystal structure determination. *Biochemical Society Transactions* **36**, 771–775 (2008).

115. Golovanov, A.P., Hautbergue, G.M., Wilson, S.A. & Lian, L.-Y. A simple method for improving protein solubility and long-term stability. *Journal Of The American Chemical Society* **126**, 8933-8939 (2004).

116. Weickert, M.J., Doherty, D.H., Best, E.A. & Olins, P.O. Optimization of heterologous protein production in Escherichia coli. *Current Opinion in Biotechnology* **7**, 494-499 (1996).

117. Hildebrand, F., Meyer, A. & Eyre-Walker, A. Evidence of Selection upon Genomic GC-Content in Bacteria. *PLoS Genetics* **6**, (2010).

118. Tedeschi, G., Ronchi, S., Simonic, T., Treu, C., Mattevi, A. and Negri, A. (2001) Probing the Active Site of L-aspartate oxidase by Site-Directed Mutagenesis: Role of Basic Residues in Fumarate Reduction. *Biochemistry*, **40**, 4738-4744.

119. Mortarino, M., Negri, A., Tedeschi, G., Simonic, T., Duga, S., Gassen, H. G. & Ronchi, S. L-aspartate oxidase from Escherichia coli. I. Characterization of coenzyme binding and product inhibition. *European Journal of Biochemistry* **239**, 418–426 (1996).

120. Stratagene GeneMorph® II EXClone domain mutagenesis kit instruction manual, Revision B, catalogue #200552.

121. Bacchella, L., Lina, C., Todone, F., Negri, A., Tedeschi, G., Ronchi, S. & Mattevi, A. Crystallization of L-aspartate oxidase, the first enzyme in the bacterial de novo biosynthesis of NAD. *Acta Crystallographica Section D: Biological Crystallography* **55**, 549-551 (1999).

122. Mateos, L. M., Ordóñez, E., Letek, M. & Gil, J. A. Corynebacterium glutamicum as a model bacterium for the bioremediation of arsenic. *International Microbiology* **9**, 207–215 (2010).

123. Bayan, N., Houssin, C., Chami, M. & Leblon, G. Mycomembrane and S-layer: two important structures of Corynebacterium glutamicum cell envelope with promising biotechnology applications. *Journal of Biotechnology* **104**, 55–67 (2003).

124. Scheuring, S., Stahlberg, H., Chami, M., Houssin, C., Rigaud, J.L. & Engel, A. Charting and unzipping the surface layer of Corynebacterium glutamicum with the atomic force microscope. *Molecular Microbiology* **44**, 675–684 (2002).

125. Chami, M., Bayan, N., Peyret, J.L., Gulik-Krzywicki, T., Leblon, G. & Shechter, E. The S-layer protein of Corynebacterium glutamicum is anchored to the cell wall by its C-terminal hydrophobic domain. *Molecular Microbiology* **23**, 483–492 (1997).

126. Soual-Hoebeke, E., de Sousa-D'Auria, C., Chami, M., Baucher, M.F., Guyonvarch, A., Bayan, N., Salim, K. & Leblon, G. S-Layer Protein Production by Corynebacterium Strains Is Dependent on the Carbon Source. *Microbiology* **145**, 3399–3408 (1999).

127. Sanli, G., Blaber, S. I. & Blaber, M. Reduction of wobble-position GC bases in Corynebacteria genes and enhancement of PCR and heterologous expression. *Journal of Molecular Microbiology and Biotechnology* **3**, 123–126 (2001).

128. Vertès, A. A., Inui, M. & Yukawa, H. Manipulating Corynebacteria, from Individual Genes to Chromosomes. *Applied Environmental Microbiology* **71**, 7633–7642 (2005).

129. Kind, S., Jeong, W. K., Schröder, H. & Wittmann, C. Systems-wide metabolic pathway engineering in Corynebacterium glutamicum for bio-based production of diaminopentane. *Metabolic Engineering* **12**, 341–351 (2010).

130. Doo, E.-H., Lee, W.-H., Seo, H.-S., Seo, J.-H. & Park, J.-B. Productivity of cyclohexanone oxidation of the recombinant Corynebacterium glutamicum expressing chnB of Acinetobacter calcoaceticus. *Journal of Biotechnology* **142**, 164–169 (2009).

131. Eikmanns, B. J., Kleinertz, E., Liebl, W. & Sahm, H. A family of Corynebacterium glutamicum/Escherichia coli shuttle vectors for cloning, controlled gene expression, and promoter probing. *Gene* **102**, 93–98 (1991).

132. Liebl, W., Bayerl, A., Schein, B., Stillner, U. & Schleifer, K. H. High efficiency electroporation of intact Corynebacterium glutamicum cells. *FEMS Microbiology Letters* **65**, 299–303 (1989).

133. Haynes, J. A. & Britz, M. L. The Effect of Growth Conditions of Corynebacterium Glutamicum on the Transformation Frequency Obtained by Electroporation. *Journal of General Microbiology* **136**, 255–263 (1990).

134. Park, J.-U., Jo J.-H., Kim Y.-J., Chung S.-S., Lee J.-H. & Lee H.-H. Construction of heat-inducible expression vector of *Corynebacterium glutamicum* and *C. ammoniagenes*: fusion of lambda operator with promoters isolated from C. ammoniagenes. *Journal of Microbiology and Biotechnology* **18**, 639–647 (2008).

135. Takano, H., Shimizu A., Shibosawa R., Sasaki R., Iwagaki S., Minagawa O., Yamanaka K., Miwa K., Beppu T. & Ueda K. Characterization of developmental colony formation in Corynebacterium glutamicum. *Applied Microbiology and Biotechnology* **81**, 127–134 (2008).